PROTEOMICS IN VIRAL DISEASE

A Thesis Submitted to the Board of the Faculty of Biological Sciences,
University of Oxford.
In partial fulfilment of the requirements for the degree of Doctor of Philosophy

Bevin Gangadharan

Exeter College

Oxford

Trinity Term 2006

Glycobiology Institute
Department of Biochemistry
University of Oxford

PROTEOMICS IN VIRAL DISEASE

Bevin Gangadharan, Exeter College, D. Phil. Thesis, Trinity Term 2006

Abstract

The separation, identification, and characterisation of the proteins present in a tissue or biological sample is called 'proteomics'. This technique can be used for example to identify biomarkers and investigate signalling pathways. Increasingly, proteomics is being applied to the analysis of virus related samples; here two such examples are described.

Presently there is no reliable non-invasive way of assessing liver fibrosis. Here a novel 2D-PAGE based proteomics study was used to identify potential fibrosis biomarkers. Serum from patients with varying degrees of hepatic scarring induced by infection with the hepatitis C virus (HCV) was analysed. Several proteins associated with liver scarring and/or viral infection were identified. The most prominent changes were observed when comparing serum samples from cirrhotic patients with healthy controls: Expression of inter-α-trypsin inhibitor heavy chain H4 fragments, α1 antichymotrypsin, apolipoprotein L1 (Apo L1), prealbumin and albumin was decreased in cirrhotic serum, whereas CD5 antigen like protein (CD5L) and β2 glycoprotein I (β2GPI) increased. In general, α2 macroglobulin (a2M) and immunoglobulin components increased with hepatic fibrosis whereas haptoglobin and complement components (C3, C4 and factor H-related protein 1) decreased. Novel proteins associated with HCV-induced fibrosis include the inter-α-trypsin inhibitor heavy chain H4 fragments, complement factor H-related protein 1, CD5L, Apo L1, β2GPI and the increase in thiolester cleaved products of a2M. The relationship between these changes is discussed.

One of the accessory genes of the HIV viral genome encodes for the Nef protein. Nef is present in lipid rafts and increases viral replication within infected host cells by binding to a guanine nucleotide exchange factor, Vav. This leads to activation of a GTPase, Cdc42, however, the signalling pathway is poorly understood. 2D-PAGE based proteomics was used to identify differentially expressed raft-associated proteins by comparing T cells in the presence and absence of Nef. A ubiquitin conjugating enzyme UbcH7, which acts in conjugation with c-Cbl, was absent from the rafts of Nef-transfected cells. Vav ubiquitination was also absent from these rafts. In collaboration with Dr. Alison Simmons and Prof. Andrew McMichael the absence of UbcH7 in rafts was found to be caused by βPix forming a ternary complex with c-Cbl and activated Cdc42. Vav ubiquitination was restored and viral replication was diminished when βPix was knocked down providing a new candidate target for inhibiting HIV replication.

This thesis demonstrates the use of proteomics in providing novel information for virus related samples. This influential technology benefits in both biomarker discovery to aid clinicians with early diagnosis of diseased individuals and in the elucidation of novel signalling pathways in infected cells to provide new candidate targets.

ACKNOWLEDGEMENTS

I would especially like to thank my supervisor, Dr. Nicole Zitzmann, for her continual assistance throughout my D. Phil and also Prof. Raymond Dwek for his support. I would like to acknowledge all members of the Oxford GlycoProteomics and Virology groups for their support especially Dr. Robin Antrobus and Dr. Sripadi Prabhakar for identifying all the proteins mentioned and Dr. Ángel García-Alonso, Dr. María Pardo-Pérez, and Dave Chittenden for their assistance with various practical aspects. I am extremely thankful to David Giles for casting all the gels for my projects and everyone for assisting me with writing this thesis especially Dr. Jo O'Leary. I am also grateful to Dr. Narayan Ramamurthy who sat next to me for most of my thesis writing and encouraged me to progress and complete this thesis.

I would like to thank Dr. Pauline Rudd and everyone in her group who collaborated with our group in the glycan-related projects, especially Dr. Louise Royle, Yun-Gon Kim and Simon Fry for explaining to me the whole glycan analysis process.

I am grateful to Dr. Alison Simmons, Dr. Paul Klenerman and United Therapeutics Corporation for supplying us with samples for the projects and also to John Northfield for showing me the cytokine analysis procedure on the serum samples.

I would like to thank the Oxford Glycobiology Institute, the Medical Research Council and Oxford GlycoSciences for financially supporting me. I would also like to acknowledge everyone in the Oxford Glycobiology Institute and Department of Biochemistry for all their support during my D. Phil.

Finally I would like to express thanks to all my family members for their support over the last few years – my brother Shibu, my sister in-law Silpa, my father and my mother. I would especially like to thank my adorable 2 year old baby niece, Alina. Her company during the later stages of my D. Phil has helped in relieving stressful times when my experiments did not work and in particular during thesis writing.

TABLE OF CONTENTS

ABBREVIATIONS

2D-PAGE	two dimensional polyacrylamide gel electrophoresis
a2M	α2 macroglobulin
aa	amino acid
ACE	angiotensin converting enzyme
ADP	adenosine diphosphate
AIDA	Advanced Image Data Analyser
AIDS	acquired immunodeficiency syndrome
ALP	alkaline phosphatase
ALT	alanine aminotransferase
Apo A1	apolipoprotein A1
Apo A2	apolipoprotein A2
Apo L1	apolipoprotein L1
APS	ammonium persulphate
ARF6	ADP ribosylation factor 6
ASB 14	amidosulphobetaine 14
AST	aspartate aminotransferase
ATCC	American Type Culture Collection
ATP	adenosine triphosphate
β2GPI	β2 glycoprotein I
BCA	bicinchoninic acid
BPG	1,3-bisphosphoglycerate
βPix	PAK interacting exchange factor
BSA	bovine serum albumin
C3	complement C3
C4	complement C4
CA	capsid
CD5L	CD5 antigen-like protein
CH	complement factor H
CHAPS	3-([3-Cholamidopropyl]dimethylammonio)-1-propanesulphonate
CTGF	connective tissue growth factor
DC-SIGN	dendritic cell-specific intercellular adhesion molecule-3-grabbing nonintegrin
DMSO	dimethyl sulphoxide
dTDP	thymidine diphosphate
dTMP	thymidine monophosphate
DTT	dithiothreitol
ECM	extracellular matrix
EDTA	ethylene diamine tetra-acetate
EGFP	enhanced green fluorescent protein
ELISA	enzyme-linked immunosorbent assay
ER	endoplasmic reticulum
ExPASy	Expert Protein Analysis System
FACS	fluorescence-activated cell sorter

*.flt	graphics filter files
G2A	glycine to alanine mutation
GA3P	glyceraldehyde 3-phosphate
GDP	guanosine diphosphate
GEF	guanine nucleotide exchange factor
GGT	gamma glutamyl transpeptidase
GlcNAc	*N*-acetylglucosamine
GM1	ganglioside lipid raft marker
GnT-III	*N*-acetylglucosaminyltransferase III
GP73	Golgi protein 73
GPI	glycosylphosphatidylinositol
GST	glutathione-S-transferase
GTP	guanosine triphosphate
h	hour(s)
H&E	haematoxylin & eosin
HAI	Histology Activity Index
HBsAg	hepatitis B surface antigen
HBV	hepatitis B virus
HCC	hepatocellular carcinoma
HCl	hydrochloric acid
HCV	hepatitis C virus
HDL	high-density lipoprotein
HGF	hepatocyte growth factor
HIV	human immunodeficiency virus
HMWK	high molecular weight kininogen
HPLC	high performance liquid chromatography
HSC	hepatic stellate cells
ICAT	isotope coded affinity tag
IEF	isoelectric focusing
IgA	immunoglobulin A
IgG	immunoglobulin G
IgM	immunoglobulin M
IL-6	interleukin 6
IL-8	interleukin 8
IL-10	interleukin 10
IN	integrase
INFα	interferon alpha
IPG	immobilised pH gradient
IRES	internal ribosome entry site
iTRAQ	isobaric tagging for relative and absolute quantitation
IU	international units
kDa	kilodaltons
LC	liquid chromatography
LDH-A	lactate dehydrogenase-A isoform
LDL	low-density lipoprotein
LDS	lauryl alcohol sulphate, lithium salt

LFT	liver function test
LIMS	laboratory information management system
L-SIGN	liver/lymph node-specific intercellular adhesion molecule-3-grabbing integrin
MA	matrix
MALDI-Tof	matrix assisted laser desorption / ionisation-time of flight
MCI	molecular cluster index
Melanie II	Medical ELectrophoresis ANalysis Interactive Expert II
MHC-1	major histocompatibility complex 1
min	minute(s)
MMP	matrix metalloproteinase
MOPS	3-(*N*-morpholino) propane sulphonic acid
mRNA	messenger RNA
MS	mass spectrometry
MWCO	molecular weight cut-off
MWt	molecular weight
NAD^+	nicotinamide adenine dinucleotide (oxidised form)
NADH	nicotinamide adenine dinucleotide (reduced form)
NC	nucleocapsid
NDSB	non-detergent sulphobetaines
ng	nanogram
NH_4HCO_3	ammonium bicarbonate
NL	non-linear
NMT	*N*-myristoyltransferase
NS	non-silencing
NS2	HCV non-structural protein 2
NS3	HCV non-structural protein 3
NS4A	HCV non-structural protein 4A
NS4B	HCV non-structural protein 4B
NS5A	HCV non-structural protein 5A
NS5B	HCV non-structural protein 5B
ORF	open reading frame
p7	HCV ion channel-forming protein
PAI-1	plasminogen activator inhibitor-1
PAK	p21-activated kinase
PCR	polymerase chain reaction
PD	pull-down
PDA	piperazine diacrylamide
PDB	p21 binding domain
PDGF	platelet derived growth factor
pg	picogram
Pi	inorganic phosphate
pI	isoelectric point
PI3K	phosphatidylinositol 3-kinase
PIIIP	procollagen III peptide
PMSF	phenylmethylsulphonyl fluoride

PON1	paraoxonase/arylesterase 1
PR	protease
QC	quality control
RBC	red blood cell
RBP	retinol binding protein
RNA	ribonucleic acid
RT	reverse transcriptase
s	second(s)
SARS	severe acute respiratory syndrome
SDS	sodium dodecyl sulphate
SDS-PAGE	sodium dodecyl sulphate polyacrylamide gel electrophoresis
SELDI	surface-enhanced laser desorption / ionisation
SIC	spreading initiation centre
SILAC	stable isotope labelling by amino acids in cell culture
siRNA	small interfering RNA
SIV	simian immunodeficiency virus
SR-BI	scavenger receptor class B type I
TBP	tributyl phosphine
TCA	trichloroacetic acid
TEMED	*N*,*N*,*N'*,*N'*– tetramethylethylenediamine
TGF-β1	transforming growth factor-beta 1
*.tif	tagged image file format
TIMP	tissue inhibitor of metalloproteinases
TNFα	tumour necrosis factor alpha
tPA	tissue-type plasminogen activator
tsg	TNF-stimulated gene
TSG	protein encoded by *tsg* gene
UbcH7	ubiquitin-conjugating enzyme E2
UTI	urinary trypsin inhibitor
VLDL	very low-density lipoprotein
v/v	volume/volume
WCL	whole cell lysate
WT	wild-type
w/w	weight/weight
w/v	weight/volume
YKL-40	Chondrex
ZAG	zinc-α2-glycoprotein

CHAPTER 1

Introduction

1.1 Proteomics

The term 'proteome' was first used by Wasinger *et al.*, 1995 and means the total protein complement expressed by a genome. The separation, identification, and characterisation of the proteins present in a tissue or biological sample is called 'proteomics'.

Proteins have many functions within the cell including regulation of genes, relaying signals within and between cells, and driving metabolic processes. Perturbing such activities may lead to pharmacological, toxicological or disease events. Proteins involved in these events can be identified by comparing protein expression in healthy and diseased individuals or in control and drug treated individuals. Identification of proteins with altered expression profiles may allow investigation of new targets for the development of drugs, help with disease diagnosis, and may further understanding of mechanisms of drug action or toxicity.

The study and exploitation of genetic sequence information is referred to as genomics. Functional genomics, which investigates the relationship between the pattern of gene activity and disease, is a major new area of interest following the completion of the Human Genome Project (Greenhalgh, 2005). However, on the whole, disease processes manifest themselves not at the level of genes, but at the protein level. Whilst aberrant gene activity may lead to disease states, there is a poor correlation between the level of gene transcription and the relative levels of active proteins within the tissue (Petricoin and Liotta, 2003). Therefore, relating gene expression to pathology is difficult at the level of mRNA. In addition, post-

translational modifications and gene splicing add complexity to protein expression patterns. This means that a gene sequence does not determine the complete structure and function of proteins.

Proteomics allows identification of key proteins implicated in disease, cell signalling, metabolic processes, etc. In combination with genomics studies, proteomics provides an alternative approach to target characterisation, identification of biomarkers and development of therapeutics.

1.2 Techniques used in proteomics

Proteins can be separated exclusively by size using sodium dodecyl sulphate polyacrylamide gel electrophoresis (SDS-PAGE). Two dimensional polyacrylamide gel electrophoresis (2D-PAGE) is a key method for resolving complex mixtures of proteins. Proteins are separated first according to their charge (or isoelectric point, pI), in a process known as isoelectric focusing (IEF), and then on the basis of size by SDS-PAGE. This results in a two dimensional array of spots. Thousands of proteins can be separated in this way yielding information such as apparent pI and molecular weight for each protein.

2D-PAGE was first introduced 30 years ago (Klose, 1975; O'Farrell, 1975). In these early experiments separation in the first dimension was carried out in carrier ampholyte-containing polyacrylamide gels cast in narrow tubes. There were a number of inherent disadvantages to this technique. Sample separation was highly sensitive to the presence of salts and other impurities, there were quantitative inconsistencies with different carrier ampholyte lots leading to reduced

reproducibility of separation, and the pH gradient tended to drift towards the cathode over time affecting reproducibility, particularly in the basic area of the gel. A more robust method, immobilised pH gradient isoelectric focusing (IPG-IEF), was developed whereby pH gradients are immobilised into the acrylamide first dimension gel (Bjellqvist *et al.*, 1982). For additional robustness and ease of handling, gels are cast onto a plastic film backing. Many of the problems associated with carrier ampholytes and tube gels (e.g. gradient drift and difficulties in gel handling) are overcome with this technology. These IPG strips also facilitate increased protein loading.

For the first dimension IEF step, the protein sample must be completely solubilised, disaggregated, denatured, and reduced. To achieve this, samples are prepared in a mixture of detergents, chaotropes and reducing agents. Typically this includes urea, which solubilises and unfolds most proteins to their fully random coil conformation, with all ionisable groups exposed to solution. This may be combined with thiourea which further improves solubilisation, particularly of membrane proteins (Rabilloud, 1998). Neutral or zwitterionic detergents such as Triton X-100 (non-ionic; O'Farrell, 1975), Amidosulphobetaine 14 [ASB 14] (zwitterionic; Chevallet *et al.*, 1998), 3-([3-Cholamidopropyl]dimethylammonio)-1-propanesulphonate [CHAPS] (zwitterionic; Perdew *et al.*, 1983) are included to aid solubilisation and to prevent aggregation through hydrophobic interactions. More recently, zwitterionic non-detergent sulphobetaines (NDSB) have also been used to limit protein aggregation and aid solubilisation. The reducing agent dithiothreitol (DTT) is most commonly used to break any disulphide bonds and

allows proteins to unfold completely. Tributyl phosphine (TBP), which improves protein solubility during isoelectric focusing resulting in shorter run times and increased resolution (Herbert *et al.*, 1998), has been used as a reducing agent more recently. TBP is non-ionic and thus does not migrate in the IPG, therefore maintaining reducing conditions during the course of IEF. The addition of carrier ampholytes helps to stabilise the gradient producing more uniform conductivity across the pH gradient without disturbing IEF or affecting the shape of the gradient. Carrier ampholytes improve separations, particularly with high sample loads, and enhance protein solubility by minimising protein aggregation due to charge-charge interactions.

The second dimension is most commonly run using the vertical format with the Tris-Glycine running buffer system described by Laemmli, 1970. This buffer system separates proteins at high pH, which confers the advantage of minimal protein aggregation and clean separation even at relatively heavy protein loads. IPG strips must be equilibrated prior to application onto the second dimension gel. The strip is usually conditioned in a viscous buffer to reduce the effects of electroendoosmosis. This is usually achieved using urea and glycerol, where the latter has the added benefit of improving transfer of proteins from the first to the second dimension (Gorg *et al.*, 1985). The equilibration solution is buffered with Tris-HCl to maintain the strip in a pH range suitable for electrophoresis and the presence of DTT preserves the fully reduced state of denatured, unalkylated proteins. Most importantly, SDS is also included to denature proteins and form negatively charged SDS-protein complexes where the negative charge is directly

proportional to the mass of the protein. Thus, electrophoresis of proteins through a sieving gel in the presence of SDS separates proteins on the basis of molecular mass.

Once separated, proteins are visualised by staining. There are many detection methods used to visualise protein spots on gels, each with their advantages and disadvantages. Silver staining is a highly sensitive non-radioactive method (1 ng detection limit). The chemistry underpinning silver staining was first applied to protein staining in the 1970s (Kerenyi and Gallyas, 1972). Studies show that silver staining is up to 100 times more sensitive than Coomassie Blue stain and allows the detection of proteins that could previously only be detected by autoradiography. There are a number of key disadvantages associated with silver stain including limited linearity of staining (Peats, 1984); high background, usually formed during development; and significant batch to batch variability because the staining procedure is a complex, multi-step process using numerous reagents for which quality is critical. Furthermore, many methods use formaldehyde in the fixation step or glutaraldehyde in the sensitiser, that can interfere with mass spectrometric analysis. Whilst omission of these reagents overcomes this problem, sensitivity is compromised (Shevchenko *et al.*, 1996).

Coomassie staining, although 50- to 100-fold less sensitive than silver staining, is a relatively simple method and more quantitative than silver staining (Meyer and Lamberts, 1965). Colloidal staining methods are recommended, because they show the highest sensitivity, down to 100 ng/protein spot (Neuhoff *et al.*, 1985).

Relatively recently several fluorescent stains have been developed for protein detection that, in general, are very reproducible and more compatible with mass spectrometry than Coomassie or silver stains. The linear dynamic range of these fluorescent stains extends over at least three orders of magnitude, far exceeding those of Coomassie and silver stains. With regard to sensitivity, these fluorescent stains are generally far superior to Coomassie and comparable to silver staining (White *et al.*, 2004). The first and probably most successful commercially available fluorescent stain recommended for 2D-PAGE is SYPRO® Ruby (Berggren *et al.*, 1999). This dye, comprising ruthenium as part of an organic complex that interacts non-covalently with proteins, has a sensitivity as low as 250 pg. More recently other fluorescent stains have been introduced including the Flamingo™ (Bio-Rad; detection limit of 250 pg) and Lightening Fast/Deep Purple stains (FLUOROtechnics/GE Healthcare; detection limit 100 pg) (Mackintosh *et al.*, 2003).

Once stained, the gels are imaged digitally for comparative image analysis to pinpoint protein spots of interest, i.e. those which are up- or down-regulated in response to treatment or which are subjected to post-translational modification. Processing of images remains a major bottleneck in the process and currently substantial manual intervention is required with all available processing software. Many vendors are trying to circumvent this issue and researchers are concentrating on ways to improve spot detection that will primarily remove operator subjectivity (Cutler *et al.*, 2003).

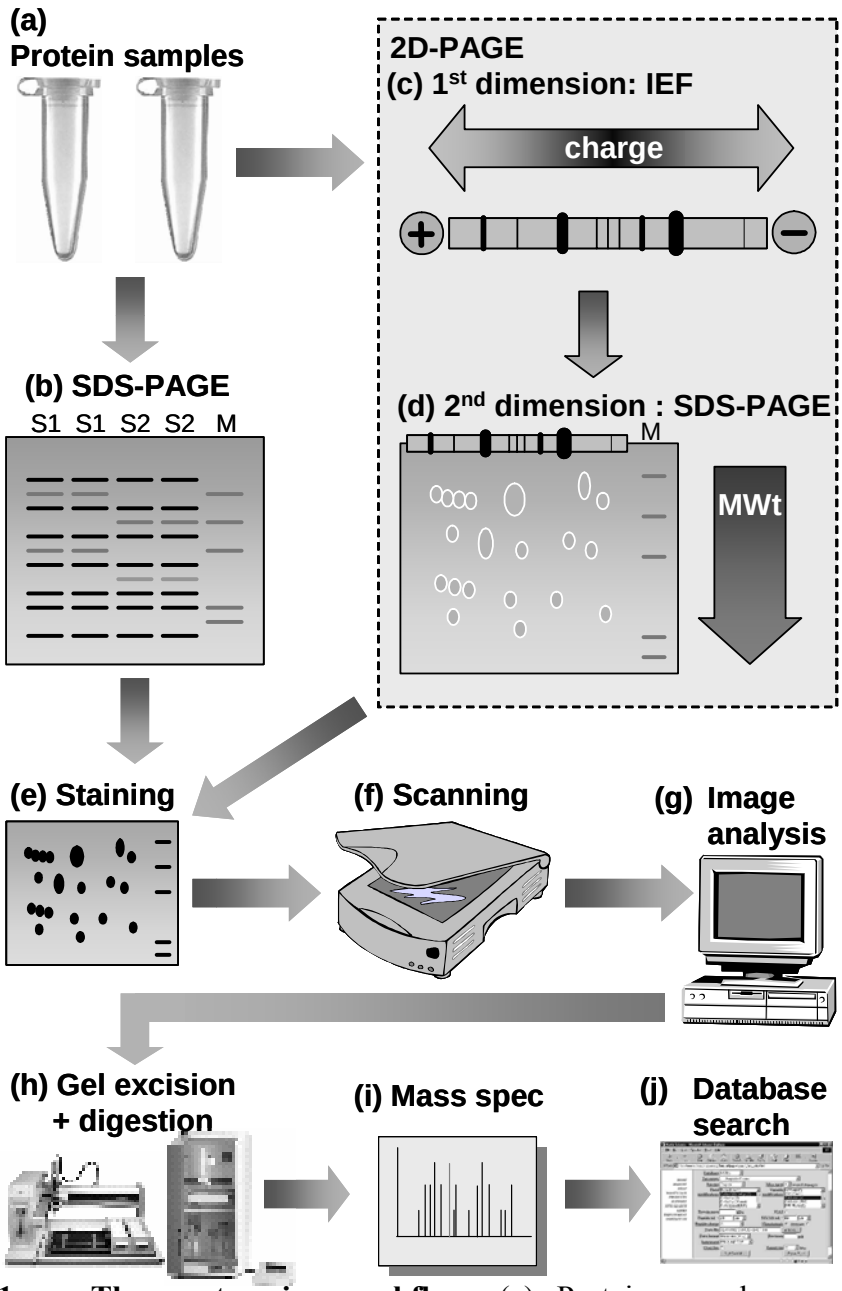

Figure 1 The proteomics workflow. (a) Protein samples are initially denatured, solubilised and reduced. (b) Samples can be analysed by SDS-PAGE where proteins are separated by size. Alternatively proteins can be separated by high resolution 2D-PAGE (c and d). In 2D-PAGE, proteins are firstly separated by (c) charge using isoelectric focusing followed by (d) SDS-PAGE to separate proteins by molecular weight. The proteins on the gel are then (e) stained, (f) scanned and (g) analysed using computer-aided software to identify differences in band/spot intensity. (h) Spots/bands of interest are excised from the gel and digested with the enzyme trypsin. (i) The resulting peptides are analysed by nanospray MS/MS and finally (j) the data generated by mass spectrometry are put into a search engine to identify the proteins of interest.

Protein gel spots of interest can be excised manually or by using an automated robot. The gel spots are then enzymically digested *in situ*, usually with trypsin, again either manually or using a robot. The masses of the peptides generated can be determined by matrix assisted laser desorption / ionisation-time of flight mass spectrometry (MALDI-Tof MS), which enables rapid analysis of peptides and proteins (Courchesne and Patterson, 1999). The 'mass fingerprint' obtained with this technique is compared with theoretical digests of proteins in primary sequence databases to identify the protein. For structural analysis and more stringent searching of databases, nanospray ionisation MS/MS can be used to generate mass and sequence information (Griffiths, 2000). This technique has the advantage of allowing structural elucidation of modified peptides in complex digests (Shevchenko *et al.*, 1996). Liquid chromatography (LC) coupled to tandem mass spectrometry, LC-MS/MS, is a powerful technique for the analysis of peptides and proteins and can be applied to complex in-solution digests for proteome analysis (Aebersold and Mann, 2003). This technique coupled with stable isotope labelling provides a powerful approach to quantitative proteomics. Various labelling methods are available including isotope coded affinity tag, ICAT (Gygi *et al.*, 1999); stable isotope labelling by amino acids in cell culture, SILAC (Ong *et al.*, 2002); and isobaric tagging for relative and absolute quantitation, iTRAQ (Ross *et al.*, 2004). Searching of protein sequence databases with mass spectrometry data and the use of bioinformatic tools are the final steps in the proteomics workflow (Figure 1).

1.3 Proteomics in viral disease

Increasingly proteomics is being applied to the analysis of virus-related samples. Proteomics has aided virology in numerous ways from identifying unknown plant viruses (Potato virus X; Cooper *et al.*, 2003) to understanding further viruses responsible for outbreaks within the human population (e.g. SARS; Jiang *et al.*, 2005).

Proteomics has proved to be beneficial in the elucidation of serological biomarkers for various diseased states including viral diseases (Jacobs *et al.*, 2005). For the study described herein, this influential technology has been used to identify novel serum markers of virally induced liver fibrosis (Chapter 2). There is currently no reliable non-invasive method for assessing liver fibrosis and alternatives to liver biopsy are required. To date, no other gel-based proteomics studies to identify biomarkers for hepatic fibrosis have been published.

Proteomics is also highly advantageous in analysing changes in protein regulation and phosphorylation in signalling pathways within cells including the examination of aberrant signalling that may be observed in virally infected cells (Pelech, 2004). The Human Immunodeficiency Virus (HIV) viral genome contains an accessory protein, Nef, that increases viral replication through changes in signalling processes within infected host cells (Das and Jameel, 2005). Nef is present in lipid rafts and viral replication is increased when Nef binds to a guanine nucleotide exchange factor leading to the activation of a GTPase (Fackler *et al.*, 1999). There is a need to understand further this signalling pathway since the initial events facilitating this GTPase activation are unknown. The study

described herein uses proteomics to help unravel this unknown signalling pathway (Chapter 3). Knowledge of this complete pathway may aid in the understanding of HIV replication thereby providing new candidate targets for inhibiting HIV replication.

CHAPTER 2

Proteomics of serum from Hepatitis C Virus infected individuals

2.1 Introduction

Chronic hepatic disease damages the liver; the resulting wound-healing process can lead to liver fibrosis and the subsequent development of cirrhosis. One of the leading causes of hepatic fibrosis and cirrhosis is infection with the Hepatitis C virus (HCV). HCV is a major human pathogen infecting more than 200 million individuals (Libra *et al.*, 2005), approximately 3% of the world's population. At least 85% of those infected become chronic carriers and are at severe risk of developing liver fibrosis and cirrhosis. Of the patients with cirrhosis, 30-50% develop hepatocellular carcinoma (HCC) (Giannini and Brechot, 2003). Needle liver biopsy is the primary tool for the diagnosis and assessment of fibrosis yet there are a number of well-documented limitations and disadvantages to this technique. Non-invasive diagnostic methods have been proposed as alternatives or adjuncts to biopsies. Here, using proteomics, serum from patients with varying levels of HCV-induced hepatic scarring are compared to identify potential biomarkers for liver fibrosis.

LIVER FIBROSIS

2.1.1 Normal liver physiology

The liver is a solid organ situated in the right upper quadrant of the abdomen. It receives approximately 75% of its blood supply via the hepatic portal vein from the small intestine, stomach, pancreas and spleen and the remaining 25% from the hepatic artery (Berne and Levy, 1998). Most of the liver volume is occupied by liver cells (hepatocytes), which are arranged in plates one cell thick, bordering

vascular structures called sinusoids through which blood from both the portal vein and hepatic artery mixes and flows. Branches of the portal vein pass in between lobules in the liver and terminate in the sinusoids (Figure 2). These sinusoids are distensible vascular channels lined with highly fenestrated endothelial cells and are encircled by hepatocytes with microvilli on their surface that are thought to be important for normal physiological processes. As blood flows through these sinusoids, plasma is filtered into the space between these endothelial cells and the surrounding hepatocytes (the space of Disse) and provides the major fraction of the body's lymph (Figure 3a). The blood flowing through these sinusoids empties into central veins of lobules throughout the liver which coalesce into the hepatic vein (Underwood, 1996).

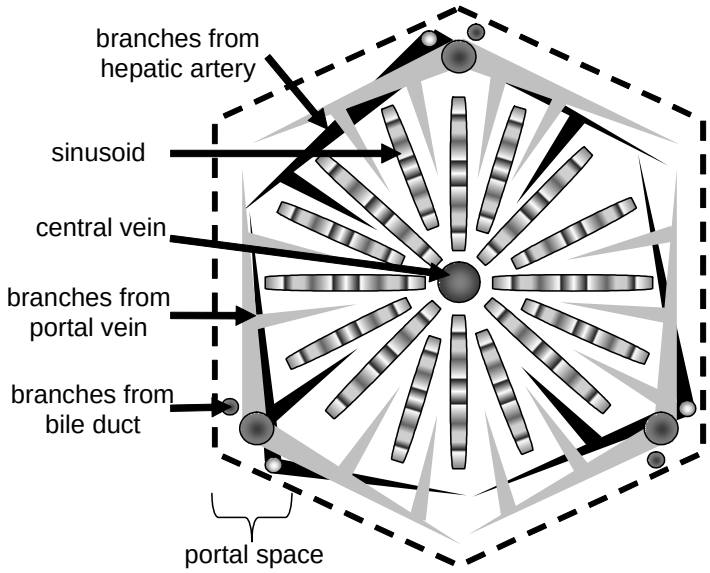

Figure 2 Simplified diagrammatic representation of a normal liver lobule. Blood from the hepatic portal vein and hepatic artery enters into branches within these lobules before passing through the sinusoids and finally emptying into the central veins that combine to form the hepatic vein. Adapted from Underwood, 1996.

Within the space of Disse are hepatic stellate (star shaped) cells (HSC). The ratio of HSCs to hepatocytes in the normal liver is approximately 1:20. In the normal liver HSCs are the main storage sites of vitamin A. HSCs produce and degrade extracellular matrix (ECM) proteins in both the normal and fibrotic liver; they may also be involved in hepatic regeneration both in the normal liver and in response to hepatic injury (MacSween *et al.*, 2002). HSCs are the key source of ECM components including collagens, non-collagen glycoproteins, growth factors, glycosaminoglycans and proteoglycans (Schuppan *et al.*, 2001). Activation of the HSCs (Section 2.1.2) causes an imbalance between the production and degradation of ECM proteins that results in fibrous tissue (fibrosis) being deposited in the liver.

2.1.2 Liver fibrosis

Hepatic fibrosis is a wound healing response characterised by the excessive accumulation of scar tissue (i.e. ECM) in the liver. The replacement of normal structural elements of tissues with excessive amounts of non-functional scar tissue is seen in various diseases including liver fibrosis, cirrhosis, atherosclerosis, Crohn's disease and keloid scars in skin (Diegelmann and Evans, 2004). All forms of wound healing share similar biology. Briefly, wound healing is directed by growth factors / cytokines; collagen is deposited in the ECM; transforming growth factor-beta 1 (TGF-β1) mediates ECM production; TGF-β1 decreases the secretion of proteases responsible for the breakdown of the ECM and stimulates tissue inhibitor of metalloproteinases (TIMP) (Diegelmann and Evans, 2004).

In liver fibrosis several morphological changes are observed in the hepatic architecture (Figure 3b). Kupffer cells (liver macrophages) in the blood pass through the hepatic sinusoids and become activated by adverse stimuli such as viruses or toxins. Cytokines including TGF-β1, interleukin-6 (IL-6) and tumour necrosis factor alpha (TNFα), released from the Kupffer cells activate the HSCs, resulting in hepatic scarring. Hepatocyte microvilli and endothelial fenestrae disappear thereby decreasing transport of lipoproteins and chylomicron remnants across the sinusoidal wall (MacSween *et al.*, 2002).

Collagens, in particular the fibril forming collagens (types I and III) and the sheet-forming basement membrane collagen (type IV), are the primary components of the excessive ECM production in hepatic fibrosis. Expression of these collagens can increase by up to 10-fold in cirrhosis (Schuppan *et al.*, 2001). Other ECM components, including laminin (a glycoprotein basement membrane linker); hyaluronan (a polymer of dimeric glucuronic acid and glucosamine that forms proteoglycan aggregates in the ECM); elastin (a coiled and cross linked glycoprotein forming elastic fibres); and fibronectin (a fibrous glycoprotein which interacts with collagen), also increase (MacSween *et al.*, 2002).

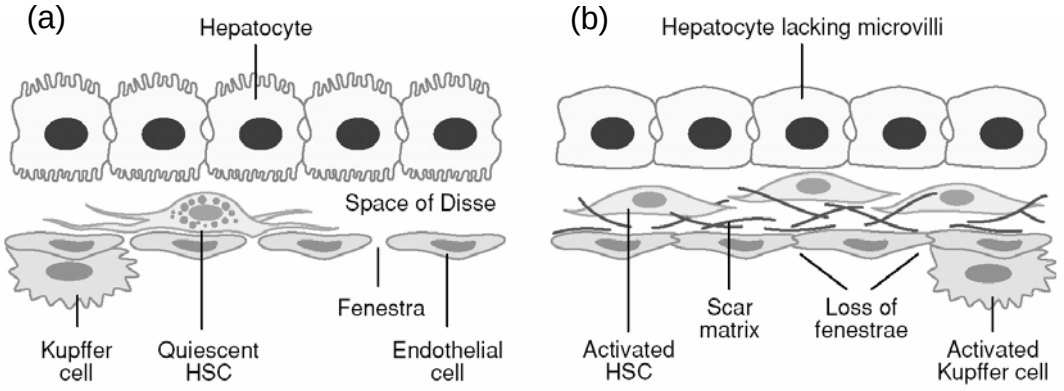

Figure 3 Morphological changes in hepatic architecture in liver fibrosis (a) *Normal liver*: Kupffer cells are located in the sinusoids and HSCs are perisinusoidal. Hepatocyte microvilli are important for the normal physiological function of the cells. Fenestrae of the sinusoidal endothelial cells allow passage of lipoproteins and chylomicron remnants (b) *Hepatic fibrosis*: Changes in both cellular responses and ECM composition. Activation of HSCs leads to the scar accumulation. Loss of endothelial fenestrae decreases transport across the sinusoidal wall leading to deterioration of hepatic function. Activation of Kupffer cells accompanies liver injury and contributes to HSC activation. Adapted from Bataller and Brenner, 2005.

In the early stages of liver fibrosis, the liver tries to balance fibrogenesis by initiating fibrolysis. Fibrolysis, the removal of excess ECM, is achieved by two families of proteolytic enzymes, the collagenases and, most importantly, matrix metalloproteinases (MMPs). MMPs are released from HSCs during early activation and are themselves activated by the serine protease, plasmin. However, the liver may be unsuccessful in balancing ECM levels and repeated injury to the liver (e.g. from toxins, hepatic viruses) results in fibrogenesis prevailing over fibrolysis. As a result, ECM production increases and the secretion and activity of MMPs decreases. In the later stages of fibrosis, the HSCs become fully activated

leading to the synthesis and release of TIMPs. TGF-β1, the most prominent profibrogenic cytokine, directly activates TIMPs and through a downstream process, decreases the levels of plasmin thereby decreasing MMP activation. Furthermore, TGF-β1 activates HSCs to synthesise more ECM.

Activated Kupffer cells also produce platelet derived growth factor (PDGF), which maintains HSCs in their activated state. In addition to TGF-β1, the cytokines IL-8 and IL-10 are secreted from HSCs which activate neighbouring HSCs. Hepatocytes damaged from fibrosis release reactive oxygen species and fibrogenic mediators which further activate HSCs (MacSween *et al.*, 2002).

HSCs also secrete angiotensin II which activates adjacent HSCs. Angiotensin II is part of the renin-angiotensin system and is a vasoconstrictor that increases blood pressure. This system involves the kidney enzyme, renin, which acts on liver synthesised angiotensinogen to form angiotensin I and an enzyme in the lung, angiotensin converting enzyme (ACE) converts angiotensin I to angiotensin II. In a similar way to TIMPs, angiotensin II can stimulate ECM synthesis and inhibit ECM degradation (Bataller and Brenner, 2005).

Chronic HCV infection is one cause of liver fibrosis (Section 2.1.4), other adverse stimuli include alcohol abuse, haemochromatosis, Wilson's disease, alpha1-antitrypsin deficiency, glycogen storage diseases and hepatitis B virus (HBV) infection (Section 2.1.3). In most patients, progression from fibrosis to cirrhosis usually occurs after an interval of 15 – 20 years (Berenguer *et al.*, 2003).

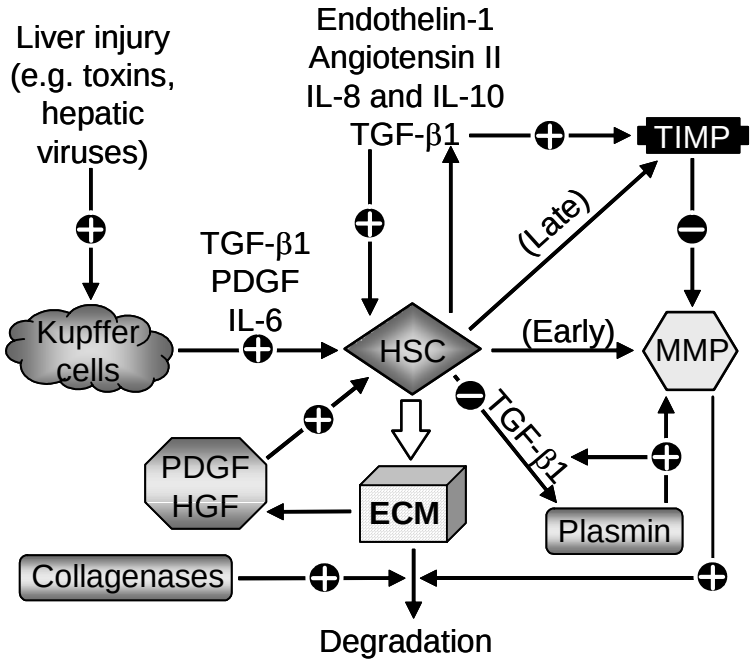

Figure 4 A summary of the mechanism of ECM production in hepatic fibrosis. Cytokines and growth factors are produced from Kupffer cells upon hepatic injury which activate hepatic stellate cells (HSCs) leading to extracellular matrix (ECM) accumulation. In the early stages of liver fibrosis, HSCs release matrix metalloproteinases (MMPs) which degrade excess ECM and are themselves activated by plasmin. Repeated hepatic injury results in fibrogenesis prevailing over fibrolysis and fully activated HSCs produce tissue inhibitors of MMPs (TIMPS). HSCs themselves secrete cytokines and other factors which activate neighbouring HSCs. The main profibrogenic cytokine, TGF-β1 is synthesised from both Kupffer cells and HSCs which activates neighbouring HSCs, TIMPs and decreases plasmin thereby decreasing MMP activation and ECM degradation.

Hepatic cirrhosis is the most severe form of liver scarring and, unlike hepatic fibrosis, is generally considered to be irreversible and nodular (Wolf, 2005). Cirrhosis is the cause of over 6000 deaths every year in the UK and approximately 27,000 in the USA, making it the ninth leading cause of death (MacSween *et al.*, 2002). Cirrhosis is a major risk factor for hepatocellular carcinoma (HCC),

particularly in HCV-infected patients (Naoumov *et al.*, 1997). At this stage of liver cancer, the only curative approach is liver transplantation (Dalgic *et al.*, 2005). In the case of virally induced liver cancer, hepatic scarring and HCC can recur after transplantation. Clearly it is imperative to diagnose fibrosis in the early stages of reversible liver scarring so that irreversible cirrhosis can be prevented.

2.1.3 Non-viral hepatic fibrosis

HCV infection is a major cause of hepatic fibrosis (Section 2.1.4). Other, non-viral causes of hepatic fibrosis include:

a. alcoholic fibrosis. The oxidative metabolite of alcohol, acetaldehyde, is thought to activate HSCs and increases collagen synthesis. Acetaldehyde can also damage cell membranes, initiate lipid peroxidation and activate Kupffer cells to produce TGF-β1, all factors that can further activate HSCs (Siegmund and Brenner, 2005; Purohit and Brenner, 2006).

b. haemochromatosis, a rare genetic disorder that results in the over abundance of iron in body tissues including the liver. There is a strong correlation between the levels of iron in the liver and the degree of hepatic fibrosis. Unlike other liver diseases, haemochromatosis does not display necrosis or inflammation. The exact mechanism by which iron overload causes fibrosis is unclear but cytokine expression in haemochromatosis appears to resemble that of inflammatory HCV infection suggesting that this condition maybe associated to some

extent with a sub-morphological inflammatory process (Bridle *et al.*, 2003).

c. Wilson's disease, an inherited disorder primarily caused by an excess of copper in body tissues, particularly the central nervous system and liver, resulting in brain and hepatic damage, respectively. Again, the precise mechanism by which copper overload causes fibrosis is unknown but it is believed that some cytokines of liver inflammation are copper-dependent, some of which may stimulate TGF-β1 (Brewer, 2003).

d. α1-antitrypsin deficiency, which can cause chronic hepatic fibrosis in neonates or in late childhood. In this condition, α1-antitrypsin is misfolded and accumulates in the endoplasmic reticulum (ER) and Golgi. The misfolded protein is re-routed for lysosomal degradation and this change in intracellular traffic appears to culminate in liver cell necrosis and fibrosis (Moustafellos *et al.*, 2000).

Liver fibrosis has also been observed, although rarely, in patients with glycogen storage disease type III. This disease is characterised by an accumulation of abnormal glycogen in the liver and muscle, however it is unclear how this triggers hepatic fibrosis (Siciliano *et al.*, 2000).

2.1.4 HCV-induced fibrosis

Hepatitis C, a contagious disease of the liver caused by HCV, is the major cause of non-A, non-B hepatitis (NANBH) (Alter, 1999). The virus belongs to the Hepacivirus genus of the *Flaviviridae* family (Lauer and Walker, 2001). HCV, a spherical, enveloped, positive, single-stranded RNA virus approximately 50 nm in diameter consists of a 5' non-coding region, a single open reading frame (ORF) and a 3' non-coding region. The single ORF, approximately 9500 nucleotides in length, encodes a single polyprotein of about 3000 amino acids (Purcell, 1997). This polyprotein is processed by cellular and virally-encoded proteases to yield eleven mature proteins. There are three structural proteins (C, core; E1 & E2, envelope proteins), six non-structural proteins (NS2, NS3, NS4A, NS4B, NS5A, NS5B) and a transmembrane, ion channel-forming protein, p7 (Voisset and Dubuisson, 2004; Pavlović *et al.*, 2003). The NS proteins include enzymes required for protein processing (NS2 and NS3 are proteases) and viral replication (NS5B is an RNA-dependent RNA polymerase). In addition, the F protein (frame shift protein) is encoded by the open reading frame overlapping the core gene in the HCV genome (Lindenbach and Rice, 2005) but its function is unknown. The organisation of the HCV RNA genome is shown in Figure 5.

Six major HCV genotypes (1-6), and more than 100 subtypes (a, b, etc), have been described (Geller, 2002). The major genotypes differ in their geographical distribution: genotypes 1, 2, 3 are observed worldwide; genotype 4 appears to be a Pan-African type; genotype 5 is the principal genotype in South Africa; genotype 6 is principally found in Asia (Nguyen and Keeffe, 2005).

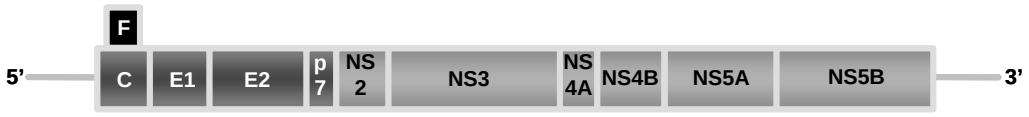

Figure 5 The HCV RNA genome. Simplified genome structure which encodes a single polyprotein that is cleaved into 11 polypeptides including structural and non-structural proteins. C, core; E1/E2, envelope glycoproteins; p7, ion channel forming protein; NS3/NS4A/NS4B/NS5A/NS5B, non-structural proteins. Adapted from Lindenbach and Rice, 2005.

Acute HCV infection is rarely symptomatic with persistent infection developing in 43–86% of the cases (Mondelli *et al.*, 2005). Serological tests are available to non-invasively diagnose patients infected with HCV. Individuals infected with the virus produce Hepatitis C antibodies that can be detected using immunometric assays (Ren *et al.*, 2005; Gretch, 1997) or the HCV RNA can be detected using polymerase chain reaction (PCR) (Beuselinck *et al.*, 2005; Gretch, 1997). At least 85% of those infected with HCV become chronic carriers, putting 170 million patients at risk of developing liver cirrhosis and hepatocellular carcinoma. Presently, the only reasonably reliable treatment for HCV infection is pegylated interferon alpha (INFα) either alone or in combination with the guanosine analogue ribavirin (Di Bisceglie and Hoofnagle, 2002; McHutchison and Poynard, 1999). However, this treatment yields sustained response rates of just 54-56 % and research is ongoing to develop new HCV therapeutics.

HCV and HBV can lead to liver fibrosis where scarring is thought to be induced by perturbations in lipid metabolism (Schuppan *et al.*, 2003; Yi *et al.*,

2003). These viruses are thought to stimulate TGF-β1 release in chronic viral hepatitis leading to excess synthesis and deposition of ECM. HBV can cause liver fibrosis by increasing lipid peroxidation and the virus has been shown to down-regulate selenoprotein P, an extracellular glycoprotein which has antioxidant properties and protects cells against lipid peroxidation (Yi *et al.*, 2003). HCV is also thought to increase lipid peroxidation but also induces other disorders in lipid metabolism, as described below, although the mechanism of action is largely unknown.

Several cell surface molecules have been proposed as receptor candidates to mediate cell entry of HCV. These include the scavenger receptor class B type I (SR-BI), the low-density lipoprotein receptors (LDL receptors), CD81 and L-SIGN, the liver homologue of DC-SIGN (Scarselli *et al.*, 2002; Agnello *et al.*, 1999; Pileri *et al.*, 1998; Gardner *et al.*, 2003). Once hepatocytes are infected, HCV core is believed to lead to disorder in lipid metabolism in fibrosis (Schuppan *et al.*, 2003) and is thought to play a role in the development of hepatic steatosis, lipid accumulation in the liver (Moriya *et al.*, 1997). This steatosis alters the composition of the liver matrix upsetting the balance between ECM synthesis and degradation which appears to ultimately lead to hepatic fibrosis (Tilg and Diehl, 2000).

Triglyceride transfer proteins are major regulators of the assembly and secretion of very low-density lipoproteins (VLDL) and both are carriers of cholesterol and triglycerides. The HCV core protein inhibits triglyceride transfer proteins thereby decreasing synthesis and transport of VLDL resulting in possible

decreases in intracellular cholesterol and triglyceride clearance (Perlemuter *et al.*, 2002). The exact mechanism is unknown. Although HCV core protein does not associate with either of these carrier proteins, it is hypothesised that it may interact with lipids. In this way, lipid mobilisation by triglyceride transfer proteins would be prevented, ultimately resulting in deranged lipid metabolism. HCV core also increases lipid peroxidation, again by an unknown mechanism (Perlemuter *et al.*, 2002). Increased lipid peroxidation can activate HSCs resulting in liver fibrosis (Poli, 2000). In addition to the derangement in lipid metabolism caused by HCV core, HCV core itself is thought to lead to the induction of the profibrotic cytokine TGF-β1 by an unknown mechanism. Both HCV core and TGF-β1 up-regulate HSC synthesised connective tissue growth factor (CTGF) which is shown to play a role as a mediator of ECM production in hepatic fibrosis (Shin *et al.*, 2005; Rachfal and Brigstock, 2003).

There is some evidence that the HCV non-structural proteins may contribute to liver fibrosis. Incubation of activated HSCs with HCV core and NS3 has been shown to increase reactive oxygen species, which in the same way as lipid peroxidation, can further activate HSCs for ECM production. Whilst infection of HSCs with core appears mainly to result in HSC activation, NS3-NS5 increase TGF-β1 secretion and the expression of procollagen α1 which is involved in ECM production (Bataller *et al.*, 2004). The mechanism by which NS3 interacts with HSCs is unclear since the receptors for non-structural proteins are unknown.

2.1.5 Biopsy and histological analysis

Currently a needle biopsy is the gold standard for assessing the severity of hepatic fibrosis (Mardini and Record, 2005). Histological analysis of these biopsies can reveal signs of architectural damage, give an indication of the extent of fibrosis and enable assessment of liver fibrosis before and/or during therapy. The degree of necrosis, inflammation and fibrosis can be determined using various stains. Haematoxylin & eosin (H&E) stains for the nucleus and cytoplasm, respectively, give an indication of cell morphology; α-smooth muscle actin highlights activated HSCs; Masson's trichrome and Sirius Red stains for collagen in the ECM to determine the extent of fibrosis (Jiang *et al.*, 2004; Russo *et al.*, 2005; Borges *et al.*, 2005).

Figure 2 shows a simplified representation of a normal liver lobule. Histological analysis of these lobules is imperative for diagnosing the extent of fibrosis. In mild fibrosis, accumulation of ECM around the portal areas, portal fibrosis, is observed. In more moderate fibrosis, the fibrous ECM can join between a number of portal areas (portal to portal bridging) or in more severe cases join between the portal tracts and central vein (portal to central bridging) (Fischer *et al.*, 1996). The histological examination of this bridging fibrosis is essential for fibrosis scoring.

Although needle biopsies are commonly used to determine fibrosis scores (see Section 2.1.6), this method has several disadvantages. Firstly, the invasive procedure can cause severe discomfort, the procedure is expensive and not without risk (Cadranel and Mathurin, 2002). Puncturing of the lung or gallbladder

is a major risk and as many as 40% of patients experience severe pains and in rare cases death can occur (Thampanitchawong and Piratvisuth, 1999). Secondly, the rate of false-negatives from liver biopsy is 15-20% (Cadranel and Mathurin, 2002). Sampling error mostly occurs when small biopsies (less than 10 mm) are analysed. Liver scarring may not be homogenous throughout the liver and since a biopsy specimen represents only 1/50,000th of the total liver mass, it may not reflect the true extent of fibrosis (Guido and Rugge, 2004). A biopsy in excess of 10 mm in length increases the reliability of fibrosis assessment but even so fibrosis may be underestimated and cirrhosis missed in some patients. In addition to sampling errors there may be interobserver variability when histological biopsy specimens are examined. There is therefore an urgent need for a reliable, non-invasive, serological assessment of hepatic fibrosis.

2.1.6 Fibrosis scoring

Several systems have been developed using semi-quantitative scoring classifications to delineate the degree of hepatic fibrosis based on histological analysis of biopsy specimens (Okafor and Ojo, 2004). The most commonly used are the Knodell, METAVIR and Ishak scoring systems.

The Knodell scoring system was first developed in the early 1980s when little was known about liver fibrosis and uses a simple scale to allow for clear separation of mild from extensive fibrosis (Knodell *et al.*, 1981). This uses three scoring systems for necroinflammation and one for fibrosis that together are used to determine the Histology Activity Index (HAI). The Knodell fibrosis scoring system uses a discontinuous scale from 0 to 4: 0 = No fibrosis; 1 = Portal fibrosis;

3 = Bridging fibrosis; 4 = Cirrhosis; forcing a rating to be low (0-1) or high (3-4). This is a very crude classification system since all types of bridging fibrosis, no matter how many bridges, is given a score of 3, and cirrhosis, whether early or late, is assigned a score of 4. The reproducibility of this scoring index is poor with occasional difficulties distinguishing between stages 1 and 3. In addition, its discontinuous scale complicates statistical analysis in clinical trials. The main disadvantage of this inflammation/fibrosis HAI index is that the sum of all four parameters does not distinguish the inflammation in hepatitis from remodelling with fibrosis (Brunt, 2000).

In the mid 1990s, a simple yet more comprehensive histological evaluation of HCV fibrosis, now universally referred to as the METAVIR scoring system, was proposed (Bedossa and Poynard, 1996). The continuous METAVIR scoring system has been shown to be more reproducible than the Knodell system (Brunt, 2000). In this case, a fibrosis score of 2 represents few bridges whereas a score of 3 signifies extensive bridging but both early and late cirrhosis have the same score of 4.

The Ishak classification was devised around the same time as the METAVIR scale and is a modification of the HAI scoring system (Ishak *et al.*, 1995). The fibrosis scores between the Ishak, METAVIR and Knodell scoring systems can, to some extent, be interconverted (Table 1). With the Ishak scale, the degree of fibrosis is scored continuously using a more favourable wider scale from 0 to 6 (Table 2). This broader range enables clinicians to diagnose the exact extent of liver scarring and also permits a better assessment of the effect of therapy on

Ishak	Knodell	METAVIR
0	0	0
1	0-1	0-1
2	1	1
2-3	1-3	1-2
3	1-3	2
4	3	3
5	3-4	3-4
6	4	4

Table 1 Conversion between the three main fibrosis scoring systems. The Ishak, Knodell and METAVIR fibrosis scoring systems are most commonly used to assess hepatic scarring. Although the numerical values for the fibrosis stages varies among these systems, they can be interconverted to some extent. Adapted from Poynard *et al.*, 2004a.

fibrosis. In a similar way to the original HAI scoring system, the Ishak score also takes into account a necroinflammatory score based on 4 parameters: (A) interface hepatitis; (B) confluent necrosis; (C) focal lobular necrosis; (D) portal inflammation. Parameters A, C and D are assigned scores from 0-4 and parameter B has a score range from 0-6 so the maximum possible score for this modified HAI grading is 18.

Changes in liver architecture	Score
No fibrosis	0
Fibrous expansion of some portal areas	1
Fibrous expansion of most portal areas	2
As in score 2 but with occasional portal to portal bridging	3
As in score 2 but with marked bridging as well as portal-central	4
As in score 4 but with occasional nodules (incomplete cirrhosis)	5
Cirrhosis	6

Table 2 The seven point Ishak scoring system. This continuous scoring system uses a more favourable wider scale allowing clinicians to more accurately establish the degree of hepatic scarring. Adapted from Ishak *et al.*, 1995.

2.1.7 Serological tests for liver disease

Routine liver function tests (LFTs) of blood samples may show an elevation of liver enzymes and changes in other analytes in hepatitis and fibrosis / cirrhosis. Table 3 details the commonly used analytes.

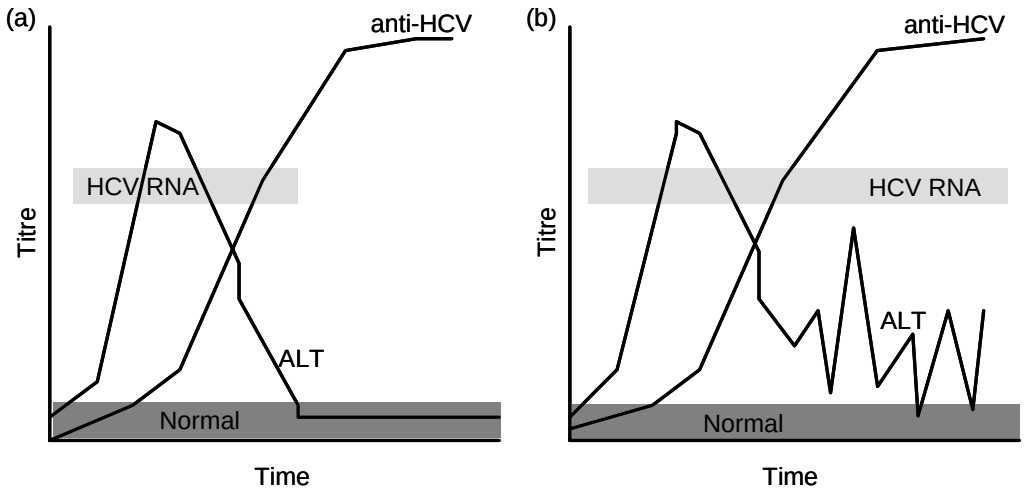

Figure 6 Biochemical, serological and virological profiles of HCV infection
(a) Self-limiting HCV infection where the virus is cleared by the immune system. When HCV RNA is cleared, ALT levels drop to normal levels.
(b) Chronically evolving acute HCV where the virus persists. When anti-HCV antibodies begin to peak, ALT levels can change erratically and also enter the normal reference range.
Adapted from Mondelli *et al.*, 2005

Analyte [normal concentration range]	Relationship to liver disease
Alanine aminotransferase (ALT) [0-45 IU/l]	- cytosolic enzyme elevated in all types of hepatitis - viral-mediated hepatocyte damage results in leakage of ALT - normal levels may be observed in fibrosis, cirrhosis or HCC due to hepatocyte apoptosis leading to less ALT synthesis (Bacon, 2002; Puoti, 2003) - no correlation with HCV RNA & changes erratically in chronic HCV (Figure 6)
Alkaline phosphatase (ALP) [30-120 IU/l]	- originates from liver & bone - increased in many liver diseases including cirrhosis and HCC but also in non-liver diseases, e.g bone disorders (Burlina and Bugiardini, 1978)
Bilirubin [2-17 μmol/l]	- results from haem breakdown - secretion of conjugated bilirubin into bile is impaired in liver diseases (e.g. viral hepatitis) resulting in its presence in urine - unconjugated bilirubin elevated in blood due to increased production, defect in hepatic uptake or conjugation but poor indicator of cirrhosis since only slightly increased or normal (Owens *et al.*, 1977) - decreased bilirubin clearance in cirrhosis where biliary excretion & conjugation are impaired - serum bilirubin is a reasonable marker for cirrhosis
Albumin [40-60 g/l]	- major serum protein synthesised by the liver - rough indicator of liver disease where decreased levels indicate compromised hepatic synthetic function - normal in chronic liver disease & decreases only for severe hepatic damage / inflammation (e.g. advanced hepatitis, cirrhosis or hepatocellular necrosis) (Ljubimova *et al.*, 1997) - albumin and platelet count can be used to predict prognosis of death in patients with HCV-induced cirrhosis
Aspartate aminotransferase (AST) [0-35 IU/l]	- mitochondrial & cytosolic enzyme - not very specific since found in other organs - elevated in liver inflammation and necrosis - viral-mediated hepatocyte damage results in leakage of AST - normal or only slightly elevated levels in fibrosis/cirrhosis
Gamma glutamyl transpeptidase (GGT) [0-30 IU/l]	- located in hepatocytes & biliary epithelial cells - elevated in users of liver toxic substances like alcohol with or without cirrhosis (Pol *et al.*, 1990) - elevated in HCV infection where it follows hepatic fibrosis or cirrhosis (Hwang *et al.*, 2000) - mechanism unknown but synthesis may be elevated as an adaptive response (Silva *et al.*, 2004) - not specific & elevated in other diseases (pancreatic/renal failure & diabetes)

Table 3 Commonly used LFTs and their relationship to hepatic disease. LFTs are routinely measured in hospitals to assess hepatic function. In general, these tests give a reasonable indication of liver inflammation but inadequately correlate with hepatic scarring. The square parentheses show the normal reference range of the analytes. All information displayed is based on the report by Limdi and Hyde, 2003 unless stated otherwise.

2.1.8 Non-invasive tests for assessing liver fibrosis

Some researchers claim that there are a small number of serum proteins already fairly well established as surrogate markers for liver fibrosis which correlate to some degree with the hepatic fibrogenic process. Some of these markers are shown in Table 4.

Presently the most reliable serological assessment of liver fibrosis uses a panel of five markers called the FibroTest which was established in 2001 by the MULTIVIRC group in France (Imbert-Bismut *et al.*, 2001). This test includes the following biomarkers: a2M, haptoglobin, apolipoprotein A1 (Apo A1), GGT and bilirubin. This cocktail of markers has already been shown to correlate with liver fibrosis – both acute phase proteins, a2M and haptoglobin, have been established as fibrosis markers for approximately 30 years (Hiramatsu *et al.*, 1976), the LFTs (GGT and bilirubin) have been used to assess hepatic function in hospitals for decades (Stanosek *et al.*, 1965) and liver synthesised Apo A1 has already been shown by the same group to correlate with liver scarring due to its binding with the fibronectin in the ECM (Paradis *et al.*, 1996b). In the same way as HAI scoring systems, this group also has created a test for assessing necroinflammation called the ActiTest which uses the same five markers but with ALT for hepatic function as an additional test (Halfon *et al.*, 2002). Although all six of these markers have already been described for hepatic fibrosis and liver disease, the combination of these several markers greatly improves scarring assessment and is superior to other serological fibrosis tests with the best correlation with biopsy

Fibrosis marker	General comments and reliability of marker
Collagen type IV	- increases with increased hepatic scarring - only useful for HCC or cirrhosis and unreliable for early stages of fibrosis (Hong *et al.*, 1995, Castera *et al.*, 2000)
Procollagen III peptide (PIIIP)	- aminoterminal peptide of procollagen III - secreted into circulation during conversion of type III procollagen to type III collagen giving a rough indication of collagen synthesis - collagen III increases mostly in early fibrosis but overall collagen I is predominantly produced by HSCs (MacSween *et al.*, 2002) - reliable for methotrexate-induced liver fibrosis [methotrexate is a drug for psoriasis but liver fibrosis is a side effect (Chalmers *et al.*, 2005)] - unreliable for other origins of hepatic fibrosis, e.g normal PIIIP levels in haemochromatosis where severe liver fibrosis and cirrhosis are present (Colombo *et al.*, 1983; Colombo *et al.*, 1985) - in viral hepatitis, PIIIP is more related to necroinflammation than ECM deposition (Surrenti *et al.*, 1987) - poor diagnostic value in HCV-induced fibrosis (Gabrielli *et al.*, 1997) - increases in other forms of scarring (e.g. skin fibrosis from burns patients) (Ulrich *et al.*, 2002)
Hyaluronan	- non-collagenous glycoprotein in ECM secreted into circulation - glycosaminoglycan composed of repeating glucoronic acid dimeric units and *N*-acetyl glucosamine - synthesised and secreted from HSCs during fibrogenesis - fibrosis or cirrhosis patients can have same or lower levels than healthy controls (Pares *et al.*, 1996; Patel *et al.*, 2003; Leroy *et al.*, 2004) - can increase with food ingestion (Wong and Gibson, 1998) and change significantly depending on age (Wong *et al.*, 1998) - in HBV-induced fibrosis, levels in patients with an Ishak score of 3 were inaccurately higher than in patients with a score of 4 (Montazeri *et al.*, 2005) - unreliable marker with limited value in predicting histological changes over a treatment regime in HCV patients (Patel *et al.*, 2003)
Laminin	- ECM glycoprotein synthesised and secreted into the circulation from HSCs - unreliable marker even for cirrhosis (Gonzalez Reimers *et al.*, 1996) - fibrosis patients can have similar or lower levels than healthy controls (Castera *et al.*, 2000; Santos *et al.*, 2005)
YKL-40 (Chondrex)	- human cartilage glycoprotein expressed in liver & thought to be involved in tissue remodelling - member of chitinase family and is a lectin which binds to heparin and chitin - increases with hepatic scarring & more reliable than hyaluronan (Zheng *et al.*, 2005) - unreliable since fibrosis patients can have similar or decreased levels compared to healthy controls (Johansen *et al.*, 2000)
MMP-2 TIMP-1	- increase with fibrosis but with low correlation (Kasahara *et al.*, 1997) - also increase in other forms of scarring e.g. skin (Ulrich *et al.*, 2003) - TIMPs are less informative than PIIIP, laminin and collagen type IV for fibrosis (Tsutsumi *et al.*, 1996).
Prothrombin time	- prothrombin is a clotting factor in plasma - plasma clotting time (prothrombin time) is measured for clotting disorders - decreases with increased hepatic scarring and is favourable due to its low cost (Cadranel and Mathurin, 2002) - significant overlap in prothrombin time for intermediate grades of liver fibrosis but more reliable than three LFTs: AST, ALT and GGT (Qiu *et al.*, 2004)
Platelet count	- platelets are enucleated cells which control bleeding (haemostasis) by coagulating blood and play a role in wound healing (García *et al.*, 2004a)

	- as with activated Kuppfer cells, they release PDGF which contributes to repair processing by activating fibroblasts leading to scarring - platelet count and age of the patient can help in diagnosing cirrhosis but is unreliable for the lower stages of fibrosis (Poynard and Bedossa, 1997; Myers *et al.*, 2003) - combination with AST and ALT levels helps but sensitivity is too low to replace liver biopsy (Park *et al.*, 2004)
α2 macroglobulin (a2M)	- acute phase glycoproteins (i.e. circulatory proteins that change by > 25% in response to inflammation (Gabay and Kushner, 1999)) - synthesis stimulated by inflammatory cytokines (e.g. IL-6, TGF-β1 and TNFα) from Kupffer cells in fibrosis which activates HSCs (Gabay and Kushner, 1999)
Haptoglobin	- usually both a2M and haptoglobin increase in inflammation, e.g. pancreatitis (Quilliot *et al.*, 2001; Griesbacher *et al.*, 2003) but in hepatic disease (e.g. steatosis, cirrhosis, hepatitis, HCC) only a2M increases and haptoglobin decreases (Meliconi *et al.*, 1988) - a2M and haptoglobin correlate reasonably well with fibrosis and have been used to for > 30 years (Hiramatsu *et al.*, 1976)
FibroTest	- a panel of five markers: a2M, haptoglobin, apolipoprotein A1 (Apo A1), GGT and bilirubin (Imbert-Bismut *et al.*, 2001) - only moderate correlation with fibrosis and considerable overlap between the intermediate stages of fibrosis being effective at eliminating biopsy in about a quarter of patients (Rossi *et al.*, 2003) - does not predict presence / absence of fibrosis or reduce need for biopsy - varies between analysers leading to significant fibrosis being missed (Rosenthal-Allieri *et al.*, 2005; Thuluvath and Krok, 2005)
Glycan analysis	- analysis of serum '*N*-glycome' revealed GlycoCirrhoTest biomarker which differentiates fibrosis patients from both controls and cirrhotic patients - galactosylation decreases and modification of serum *N*-glycans with a bisecting *N*-acetylglucosamine (GlcNAc) residue increases in cirrhosis (Callewaert *et al.*, 2004) - GlcNAc modification caused by *N*-acetylglucosaminyltransferase III (GnT-III) which is elevated in serum for HBV-induced cirrhosis and HCC (Shim *et al.*, 2004) - GlycoCirrhoTest only reliable as a cirrhosis marker since there is overlap between the intermediate fibrosis stages (Callewaert *et al.*, 2004) - MALDI-Tof MS analysis of serum *N*-glycans from patients with hepatic cirrhosis revealed increase in bisecting GlcNAc residue, increase in core fucosylation and presence of agalactosylated neutral glycans but the value of these glycan markers over various degrees of fibrosis has yet to be assessed (Morelle *et al.*, 2006)

Table 4 Common serological biomarkers for assessing hepatic fibrosis and cirrhosis. In general, these biomarkers show overlap for the intermediate fibrosis stages and only appear to show some reliablity for diagnosing cirrhosis. Therefore, there is still an urgent need to develop and validate a reliable non-invasive assay to accurately reflect the full spectrum of fibrosis stages

scoring (Poynard *et al.*, 2004b). Since their initial study, this group has published several papers claiming that their method of assessing the degree of hepatic fibrosis can decrease the need for liver biopsies but do not completely eliminate the requirements of the invasive procedure. Another group has evaluated the FibroTest showing only moderate correlation with fibrosis and considerable overlap between the intermediate stages of fibrosis being effective at eliminating biopsy in only 26% of patients (Rossi *et al.*, 2003). This group found that FibroTest could not accurately predict either the presence or absence of fibrosis and could not reliably be used to reduce the need for liver biopsy. Others have also found that this test has variability between different analytical analysers with discrepancies for a2M and to a lesser extent Apo A1 leading to significant fibrosis being missed (Rosenthal-Allieri *et al.*, 2005; Thuluvath and Krok, 2005). Despite these disadvantages, the FibroTest presently remains the best group of fibrosis biomarkers. Soon serum biomarkers may become standard clinical practice for patients with hepatic fibrosis, but current studies show that FibroTest, along with the presently discovered markers, do not eliminate the need for biopsy (Thuluvath and Krok, 2005).

Non-invasive assessment of liver fibrosis does not necessarily need to be performed from serological analysis and studies have been carried out by other means. Since fibrosis alters the architecture of the liver near the portal, central and sinusoidal areas (Figures 2 and 3), the hepatic haemodynamics are affected. Researchers have therefore claimed that the velocity of blood flowing throughout the liver may aid in assessing the extent of hepatic scarring. The blood velocity

can be determined by means of high-frequency sound waves to bounce off flowing blood in vessels using a technique called ultrasonography. Increased portal bridging is observed with increasing fibrosis leading to increased portal resistance and pressure (portal hypertension) with slower blood flow. The ratio of hepatic artery to portal vein velocity therefore increases with fibrosis and studies claim that a ratio greater than or equal to 3.5 can help in diagnosing cirrhosis (Hirata *et al.*, 2001). However, results show that up to 31% of patients with a ratio above this threshold had only moderate fibrosis and that therefore this test is an unreliable method for diagnosing cirrhosis. The unreliability of this technique has also been emphasised by others who have shown that 63% of biopsy-proven cirrhotic cases were unnoticed by ultrasonography (Ong and Tan, 2003).

A recent study has employed a non-invasive technique called transient elastography which also uses ultrasonography but also applies low frequency elastic waves whose propagation velocity through the liver is dependent on hepatic elasticity (Sandrin *et al.*, 2003). Liver stiffness is related to the degree of scarring and hepatic elasticity has been shown to increase with fibrosis stage due to the increased presence of elastin and other ECM components (Yeh *et al.*, 2002). A more recent prospective study of this transient elastography test, more commonly referred to as FibroScan, shows some overlap between the intermediate stages of fibrosis and therefore this test faces the same issues as all other suggested fibrosis markers (Foucher *et al.*, 2006). Another disadvantage of the FibroScan test is that it is highly operator dependent and does not reliably differentiate hepatic steatosis from fibrosis (Bataller and Brenner, 2005).

However, FibroScan holds much promise with similar or possibly better performance than FibroTest in HCV patients (Castera *et al.*, 2005; Colletta *et al.*, 2005; Castera *et al.*, 2006).

In addition to protein markers, studies are now being carried out on serum glycans to evaluate liver fibrosis. FibroTest has been combined with GlycoCirrhoTest described in Table 4. The combination of these tests showed 75% sensitivity and 100% specificity for cirrhosis and therefore liver biopsy may become unnecessary only for patients who are positive for this combination test. However, they state that a further and larger study is required to fully validate their results (Callewaert *et al.*, 2004). Others state that these glycan markers do not additionally contribute as a fibrosis biomarker compared to the previously identified protein markers and incorrectly display positive results for non-liver autoimmune diseases (Paradis, 2005).

Many of the serum markers already described for liver fibrosis, only appear to be useful in diagnosing cirrhosis where the scarring is so severe that the liver architecture is essentially irreversibly damaged. Therefore, there is still an urgent need to develop and validate a reliable non-invasive assay to accurately reflect the full spectrum of fibrosis stages (and preferably also inflammation) in hepatic fibrosis. Ideally a serum marker is required to reliably diagnose the early stages of fibrosis where the liver architecture can be reversibly corrected using anti-fibrotic drugs (Section 2.1.10).

2.1.9 Proteomics in hepatitis

Proteomics has been applied to the analysis of viral hepatitis in several ways. Most studies have been carried out on virally-induced HCC following the pioneering 2D-PAGE proteome characterisation of the HCC cell line (Seow *et al.*, 2000). Proteome analysis of liver tissue has helped to reveal differential changes in liver enzymes between normal, cirrhotic and HCC patients. However, since this aberrant change in liver enzymes is not reflected in serum, these markers are only useful for biopsy specimens (Lim *et al.*, 2002). These initial studies were followed by the 2D-PAGE comparison of HBV- and HCV-associated HCC, again with most differences observed in liver enzymes (Kim *et al.*, 2003). More recently, non-gel-based quantitative proteomic ICAT labelling has been applied to identify 261 differentially regulated proteins in HCC which has helped in understanding the mechanism of this liver cancer as well as potential drug targets for treatment (Li *et al.*, 2004). Similarly, the carcinogenesis of HCV-related HCC is now better understood from gel-based proteomics (Yokoyama *et al.*, 2004).

The first suggestion that proteomics could be beneficial for serum biomarker discovery in viral hepatic disease was made by researchers in a joint collaboration between the Thomas Jefferson University, Oxford Glycobiology Institute and Fox Chase Cancer Centre (Steel *et al.*, 2001). Since this review, the same groups released the first extensive 2D-PAGE analysis of serum from patients with HBV-induced HCC and successfully elucidated two potential serological markers for this cancer: an isoform of Apo A1 and a fragment of Complement C3, both of which were decreased in HCC (Steel *et al.*, 2003a). These groups also observed

that woodchucks with HCC have higher levels of core α-1,6-linked fucose and the analysis of fucosylated proteins led to the discovery that Golgi protein 73 (GP73) is hyperfucosylated and increased in expression in HCC (Block *et al.*, 2005). The use of GP73 was later combined with other established HCC markers, α-fetoprotein and des-γ carboxyprothrombin, along with surface-enhanced laser desorption / ionisation (SELDI) to diagnose HCV-related cirrhosis (Schwegler *et al.*, 2005).

Glycoprotein analysis has been shown to be of particular interest in the analysis of serum from HBV-related chronic hepatitis and HCC. De-*N*-glycosylation of serum glycoproteins prior to 2D-PAGE analysis simplified the serum proteome and enhanced the resolution of many polypeptides allowing the determination of two potential serum markers: pre-serum amyloid P, which was present in the serum of patients with HBV-related chronic hepatitis and healthy controls but absent in HBV-induced HCC; and also a ceruloplasmin fragment which was absent in the serum of healthy controls but present in HBV-related chronic hepatitis and HCC (Comunale *et al.*, 2004). More recently, glycan analysis of total serum has revealed that core fucosylation increases with the development of HCC. This hyperfucosylation was observed on 19 different glycoproteins including a2M, GP73 and IgG (Comunale *et al.*, 2006).

Inflammatory biomarkers have also been identified by both proteomics and glycan analysis. In HBV-induced hepatitis, 2D-PAGE has revealed many changes including a decrease in haptoglobin and alterations in spot profile to both Apo A1 and α1-antitrypsin (He *et al.*, 2003). Also it has long been known that in liver

cirrhosis and many inflammatory diseases, including hepatitis, the level of the carbohydrate antigen, sialyl Lewix X, in plasma increases (Sunayama *et al.*, 1993). The markers determined from both of these approaches appear to correlate well with necroinflammatory scores.

Early proteomics based approaches to identify a cirrhosis biomarker were carried out on the serum of rats with chemically induced cirrhosis. A marker was identified using SELDI to determine the molecular weight of the differentially expressed protein followed by MALDI-Tof MS analysis. The identified cirrhosis biomarker was histidine-rich glycoprotein, but a glycoprotein of this family has not been discovered in serum from human patients with cirrhosis (Xu *et al.*, 2004). 2D-PAGE analysis of rat livers with chemically induced cirrhosis has helped to identify liver enzymes related with hepatic scarring: decrease of enzymes involved in β-oxidation and an increase in proteins for lipid peroxidation (Low *et al.*, 2004).

To date, the only proteomics assessment for the different stages of liver fibrosis with human serum samples was performed using SELDI. Considerable overlap was observed for the intermediate stages of HBV-related fibrosis indicating that this was an unreliable proteomics approach to investigate the extent of hepatic scarring (Poon *et al.*, 2005). More recently changes in the serum proteome of HCV-induced cirrhosis developing into HCC has been evaluated using SELDI leading to the discovery of an elevation of κ and λ immunoglobulin light chains in HCC (Ward *et al.*, 2006). The disadvantage of SELDI is ion suppression and quantification of individual proteins for complex samples like serum (Seibert *et*

al., 2004). Others have analysed 2D-PAGE changes in serum glycoproteins for alcohol induced cirrhosis where the glycosylation patterns were changed in haptoglobin, α1-antitrypsin and transferrin compared to healthy controls. However the same changes were observed in alcoholics without any liver disease. Also the protein expression of haptoglobin and spots of albumin were found to be decreased in the serum samples from patients with alcoholic-induced cirrhosis (Gravel *et al.*, 1996).

2.1.10 Anti-fibrotic therapies

Many drugs have been shown to prevent fibrosis progression in rodents but their effectiveness in humans has not been proven. This is largely because, in the absence of reliable non-invasive tests, liver biopsies would be required to accurately assess the efficacy of these drugs over the course of the treatment (Bataller and Brenner, 2005). This indicates the urgent need for reliable non-invasive markers for hepatic fibrosis in drug discovery.

The onset of liver scarring usually involves inflammation which promotes liver fibrosis progression. As a result, anti-inflammatory drugs, e.g. corticosteroids, have been used for fibrosis patients (Czaja and Carpenter, 2004). Another approach is to inhibit HSC activation which has been carried out with antioxidants such as vitamin E, phosphatidylcholine and silymarin (Di Sario *et al.*, 2005). Researchers have also targeted collagen in rodents to decrease fibrosis: the inhibition of collagen synthesis has effectively been performed using prolyl-4-hydroxylase inhibitors and halofuginone and collagen degradation has been

accomplished using MMPs (Shimizu, 2001; Gnainsky *et al.*, 2004; Siller-Lopez *et al.*, 2004). The efficacy of these collagen-related drugs in humans is unknown. Other suggested targets for anti-fibrotic strategies include the disruption of TGF-β1 synthesis and inhibition of endothein-1 receptors which appear to be successful in rodents but again their effect in humans is unknown (Gressner *et al.*, 2002; Cho *et al.*, 2000).

Inhibitors of the renin-angiotensin system appear to be the most promising drugs for liver fibrosis although they have yet to be tested in humans. Inhibitors of this system are widely used as anti-fibrotic agents and appear to be safe for renal and cardiac fibrosis (Bataller and Brenner, 2005). Preliminary studies on HCV-induced scarring show a decrease in fibrosis progression but these trials are still ongoing and these inhibitors have not been accepted yet in clinical practice (Rimola, 2003).

All of these anti-fibrotic approaches possess little benefit for the essentially irreversible scarring in cirrhosis and ideally should be administered in the early stages of fibrosis. Therefore it is imperative that a reliable procedure, preferably non-invasive, is available to accurately diagnose mild fibrosis in time so that these anti-fibrotic methods can successfully be applied to prevent further progression with scarring.

2.1.11 Aims of the chapter

The serum markers already described for hepatic scarring (Section 2.1.8) are helpful in aiding the diagnosis of liver fibrosis. However, all appear to have

significant overlap for the intermediate stages of fibrosis and therefore biopsy remains as the most reliable option. The serological biomarkers already described were determined by predicting which proteins could be secreted into serum based on the architectural damage caused to the liver during scarring. However, given the limitations of these markers, efforts are required to identify serum components that may be differentially expressed in disease. A recent review on liver fibrosis specifically highlighted proteomics as one of the most appropriate techniques for assisting fibrosis biomarker discovery (Bataller and Brenner, 2005). For the study described herein, the first of its kind, 2D-PAGE based proteomics has been used to identify serum biomarkers of fibrosis by analysing varying stages of HCV-induced hepatic fibrosis and cirrhosis alongside healthy controls.

2.2 Materials and Methods

2.2.1 Materials

Bicinchoninic acid (BCA) reagent, copper (II) sulphate pentahydrate, tributyl phosphine, 3-[(3- cholamidopropyl)dimethylammonio]-1-propanesulphonate (CHAPS), iodoacetamide, bovine serum albumin (BSA) and Glu-fibrinogen were purchased from Sigma (Dorset, UK). Bromophenol blue, sodium dodecyl sulphate (SDS), ammonium bicarbonate and sodium thiosulphate were provided by Fluka (Buchs SG, Switzerland). HPLC grade water, absolute ethanol, hydrochloric acid (HCl), glycine, butan-2-ol and 2% dimethyldichlorosilane in octamethylcyclotetrasiloxane (Repelcote) were purchased from BDH (Dorset, UK). Acrylamide and carrier ampholytes (SERVALYT®) were purchased from SERVA (Heidelberg, Germany). 2-Amino-2-(hydroxymethyl)-1,3-propanediol (Tris), agarose, and sequencing grade bovine trypsin were supplied by Roche (East Sussex, UK). Dimethylbenzylammonium propane sulphonate (non-detergent sulphobetaine-256 – NDSB-256) was purchased from Calbiochem, Merck Biosciences (Nottingham, UK). Thiourea, glycerol and chloroform were provided by Fisher Scientific (Leicestershire, UK). Acetic acid and acetonitrile were purchased from Riedel-de Haën (Seelze, Germany). Formic acid was provided by ROMIL (Cambridge, UK). Unstained ProSieve® molecular weight protein standards were from Cambrex (Berkshire, UK). Steritop 0.22 μm filters and Milli Q / Elix systems for producing Milli Q water were purchased from Millipore (Watford, UK). 10 well Bis-Tris-HCl gels, LDS sample buffer, NuPAGE® reducing agent, 3-(*N*-morpholino) propane sulphonic acid (MOPS) Running

Buffer, NuPAGE® Antioxidant, PowerEase® power supply, NOVEX Xcell SureLock™ Mini-Cell system and the equipment and reagents for the ZOOM IEF fractionator (ZOOM urea, ZOOM CHAPS, ZOOM thiourea, ZOOM pH 3-10 Carrier ampholytes, 50X Novex IEF Anode buffer, 10X Novex IEF Cathode buffer) were all supplied by Invitrogen (Paisley, UK). Urea, dithiothreitol (DTT), γ-methacryloxy-propyl-trimethoxysilane (Bind-Silane), dry strip cover mineral oil, Immobiline® IPG DryStrips, electrode wicks and the electrophoresis equipment for running the first dimension (reswelling tray, Multiphor II, EPS 3500XL power supply) were all from GE Healthcare (Buckinghamshire, UK). *N,N,N',N'*– tetramethylethylenediamine (TEMED), piperazine diacrylamide (PDA), ammonium persulphate (APS) and the PowerPac 1000 power pack were purchased from Bio-Rad (Hertfordshire, UK). The casting tank, gel casting machine, second dimension running tanks, staining tanks, OGT 1238 fluorescent dye, Apollo linear fluorescence scanner, robotic gel excisor, Rosetta software and the LIMS system were provided by Oxford GlycoSciences (Abingdon, UK). Melanie II image analysis software (release 2.3) was from Bio-Rad / The Melanie Group (Geneva, Switzerland) but was customised by Oxford GlycoSciences. Advanced Image Data Analyser (AIDA) software was supplied by Raytest (Straubenhardt, Germany). Techclean hydroentangled cellulose/polyester c-fold wipes were provided by Techspray (Bedford, UK). Decon90 was supplied by Decon (East Sussex, UK). The Coomassie Plus protein assay kit was purchased from Pierce (Northumberland, UK). The E-833 power supplies for running the second dimension tanks were from Consort (Turnhout, Belgium). LAS1000Pro

Intelligent Dark Box II CCD camera was purchased from Fuji (Düsseldorf, Germany). The RTE-101 recycling thermostatic water bath was purchased from Thermo NESLAB (Newington, NH, USA). The Savant SpeedVac® and vacuum vaporiser were purchased from Thermo Electron (Hampshire, UK). The POLARstar Galaxy plate reader (firmware version 4.30-0) and associated FLUOstar software (software version 4.30-0) were from BMG Labtechnologies GmbH (Offenburg, Germany). Non-skirted 96 well 200 µl PCR plates were purchased from ABgene® (Surrey, UK). The automated DigestPro workstation was provided by ABiMED (Langenfeld, Germany). Inkjet acetate sheets were supplied by Lyreco (Shropshire, UK). The glass plates for the gel cassette were supplied by Soham Scientific (Cambridgeshire, UK). The Class II cabinets were from Walker (Derbyshire, UK). The CapLC™ HPLC, MassLynx software version 4.0 and the Q-Tof mass spectrometer were purchased from Waters (Hertfordshire, UK). The C18 PepMap analytical column was purchased from LC packings (CA, USA). The Mascot Daemon search engine (version 1.8) was provided by Matrix Science (London UK).

2.2.2 Samples for analysis: Liver fibrosis and cirrhosis study

Normal healthy control and HCV infected human serum samples were taken from patients within the Oxford Radcliffe Hospitals NHS Trust (in collaboration with Dr. Paul Klenerman, Peter Medawar Building for Pathogen Research, University of Oxford; Ethical Approval number corec 98-137) and the University

College London Hospitals NHS Trust (via Dr. Nikolai Naoumov, Institute of Hepatology, University College London).

All samples were screened to be negative for Hepatitis B. Details of the age, gender, alanine aminotransferase (ALT) levels, HCV genotype, Ishak fibrosis score, inflammatory score and biopsy date for all patients are shown in Table A1 in the Appendix. All patients were not on treatment. Patients in each of the following categories were analysed (the numbers in parentheses indicate the Ishak fibrosis score):

4 x Normal healthy controls	(0)
4 x Mild fibrosis	(1)
3 x Moderate fibrosis	(3)
4 x Cirrhosis	(6)

2.2.3 Estimation of protein concentration

2.2.3.1 Bicinchoninic acid (BCA) protein assay

Protein concentration of samples was determined using the BCA assay method of Smith *et al.*, 1985. The assay was carried out using 96 well flat bottomed plates. The protein determination reagent was prepared using one part copper (II) sulphate pentahydrate to 50 parts BCA solution. 200 µl of this working reagent was mixed with 10 µl of sample in each well. A 6 point linear standard curve was established (in duplicate) with 0, 0.2, 0.4, 0.6, 0.8 and 1.0 mg/ml BSA.

The plate was incubated for 30 min at 37 °C and the absorbances were read at 560 nm on a POLARstar Galaxy plate reader using the FLUOstar Galaxy

software. The concentrations of the samples were determined from the linear standard curve using in-house developed software.

2.2.3.2 Coomassie Plus protein assay

The Coomassie Plus protein assay was carried out using 96 well flat bottomed plates. 300 µl of the ready-made working reagent was added to 10 µl of standards and samples. A broad range 11 point non-linear standard curve was established (in duplicate) with 0, 12.5, 25, 50, 100, 200, 400, 600, 800, 1000 and 1500 µg/ml BSA. The absorbances were read immediately at 600 nm on a POLARstar Galaxy plate reader using the FLUOstar Galaxy software. The concentrations of the samples were determined from the standard curve using in-house developed software.

2.2.4 Two dimensional polyacrylamide gel electrophoresis (2D-PAGE)

2D-PAGE was performed essentially as described by Gorg and Weiss, 1999. Sample preparation, electrophoresis, staining, scanning and spot excision were carried out in category I; class 100,000 Clean Room conditions.

2.2.4.1 Immobilised pH Gradient-Isoelectric focusing (IPG-IEF)

Serum samples were prepared in 9.8 M urea, 4% (w/v) CHAPS to ensure total denaturation of HCV infected samples and to allow accurate protein quantification using the BCA assay (Section 2.2.3.1) since major interfering substances where

absent in this buffer composition. Samples were diluted further to give a final concentration of 5 M urea, 2 M thiourea, 4% (w/v) CHAPS, 65 mM DTT, 2 mM TBP, 150 mM NDSB-256, and 0.0012% (w/v) bromophenol blue to act as a tracking dye during IEF. For pH 3-10 NL (non-linear) IPG strips, the protein solution was vortex mixed with 0.45% (v/v) pH 2-4 carrier ampholytes, 0.45% (v/v) pH 9-11 carrier ampholytes and 0.9% (v/v) pH 3-10 carrier ampholytes and incubated at room temperature for 1 h to ensure complete denaturation and solubilisation. Samples were spun at 16,000 g for 15 min. 375 µl of supernatant (containing 500 µg serum) was carefully pipetted into separate lanes of a reswelling tray. Immobiline® IPG DryStrips (18 cm, 3 mm wide, pH 3-10 NL) were placed face down onto the protein-containing samples in each lane of the reswelling tray and overlaid with 2 ml of dry strip cover mineral oil. Rehydration was performed for 20 h at room temperature.

After rehydration, the strips were briefly drained of excess mineral oil and transferred to the Multiphor II with the gel facing upwards. Electrode wicks 2 cm in length were soaked with 100 µl HPLC grade water and blotted to ensure that they were damp but not excessively wet. These damp wicks were placed on either end of the IPG strips. Electrode bars were fixed onto the wicks at either end of the IPG strips and mineral oil was poured into the sample tray until the strips were immersed. The wicks were prodded gently using tweezers to remove air bubbles and ensure good contact with the IPG gel. IEF was carried out at 300 V for 2 h and then 3500 V up to 75 kVh according to Sanchez *et al.*, 1997 using an EPS 3500XL power supply. For all stages of the process, the current limit was set to 10

mA for 12 gels, and the power limit to 5 W. The temperature was maintained at 17 °C using an RTE-101 recycling thermostatic water bath.

2.2.4.2 Gel casting

Large format, ~1 mm thick, 20 cm(w) x 18 cm(h), SDS-PAGE gradient gels (9–16%T, 2.67%C) were prepared in-house. Glass plates for the gel cassettes were cleaned on both sides with 1% (v/v) Decon90 solution using a sponge and rinsed with Milli Q water before being allowed to dry. The plates were treated so that the gel was covalently bound to one of the glass plates in the gel cassette. The gel plates that were to be bound to the gel were wiped on one side with ethanol before attaching a barcode label (for tracking) and then wiped with ethanol on the other side. The plates that were not to be bound to the gel were only wiped with ethanol on the side to be coated. All polishing and wiping steps were carried out using a cellulose wipe. These treatments were performed inside a Class II cabinet to be free from contamination and to protect the user. The plates which were used for attaching to the gel were treated with one 2 ml application and a separate 1 ml application of 0.4% (v/v) Bind-Silane in ethanol and then left for at least 1 h to cure before rinsing with Milli Q water. These Bind-Silane treated plates were allowed to dry for at least 1 h and then polished with ethanol using a cellulose wipe. The glass plates to be used on the other side of the cassette were treated with 1 ml of undiluted Repelcote to reduce adhesion of the gel to this plate and allowed to dry for 15 min followed by three slow passes over the plate with a heat gun to seal the Repelcote to the plate. The plates were then allowed to stand for 10

min to cool before being polished firstly with Milli Q water and then ethanol, using separate cellulose wipes for each polishing. Alternating Repelcote and Bind-Silane treated plates separated by 1 mm spacers on either side were then loaded into a casting tank. A total of 13 cassettes were placed in the casting tank and each one was separated using an inkjet acetate sheet with the rough side facing the bind plate.

The formulation of polyacrylamide used was essentially equivalent to that used by Hochstrasser *et al.*, 1988. Acrylamide solutions were vacuum filtered using a 0.22 μm Steritop filter and all gel casting solutions were degassed in a sonicating water bath before use. The acrylamide solution for the high percentage gel matrix was made with 1.067% (w/w) PDA in 40% (w/v) acrylamide. This solution was diluted 4-fold in Milli Q water to give the acrylamide solution for the low percentage gel matrix. 1.2 and 3.2% (w/v) APS solutions in 0.5% (w/v) sodium thiosulphate and 0.6 and 1.4% (v/v) TEMED solutions in Milli Q water were prepared. These six solutions along with approximately 1.9 M Tris HCl (pH 8.8) were placed onto a peristaltic pump driven gradient gel casting machine connected to the casting tank stacked with gel cassettes. The concentration of this Tris buffer was dependent on the calibration parameters of the casting machine on the day of casting. The more concentrated acrylamide, APS and TEMED solutions were used to establish the high percentage acrylamide end of the gel and the less concentrated for the low percentage end. The caster established a 9–16%T, 2.67%C gradient for all the gels in the casting tank. Each gel was overlaid with water saturated isobutanol and allowed to set for 5 h after which the isobutanol

was poured off and replaced with Milli Q water in order to help displace the isobutanol and was repeated after 10 min. Having finished rinsing the gels, they were then covered in 1.9 M Tris HCl (pH 8.8) and allowed to stand overnight before the gel cassettes were separated and cleaned. A quality control (QC) was performed on one of the gels by splitting the gel cassette apart and examining firstly by eye, the condition of the top edge of the gel to determine how level the gel was, and secondly, by examining the binding quality of the acrylamide gel onto the Bind-Silane treated glass plate. This was achieved by scraping the gel off the plate to check the binding. If the QC was acceptable, the remaining batch of 12 gels were covered with 375 mM Tris (pH 8.8) and finally stored at 4 °C and used within three weeks.

2.2.4.3 SDS-PAGE

Immediately post IEF, the IPG strips were incubated in 2 ml of reducing equilibration solution (4 M urea, 2 M thiourea, 50 mM Tris HCl (pH 6.8), 30% (v/v) glycerol, 2% (w/v) SDS, 130 mM DTT, 0.002% (w/v) bromophenol blue) for 15 min at 20 °C. The strips were drained of equilibration solution and overlaid onto the second dimension gels and sealed in place with 90 °C, 0.5% (w/v) agarose in 25 mM Tris, 192 mM glycine, 0.1% (w/v) SDS (reservoir buffer). The flat end of a spatula was used to aid placement of the IPG strip. Once the agarose had set, second dimension electrophoresis was carried out.

The reservoir buffer of Laemmli (Laemmli, 1970) was used for all large format gels. Electrophoresis was carried out in an electrophoresis tank similar to that

described by Amess and Tolkovsky, 1995. The current was set at 20 mA per gel for 1 h, followed by 40 mA per gel for approximately 4 h. The power limit was set to 150 W for a tank containing 6 gels and the voltage limit was set to 600 V throughout the run. The temperature was maintained at 10 °C using a recycling thermostatic water bath. Electrophoresis was terminated once the bromophenol blue tracking dye had reached the bottom of the gel.

2.2.5 SDS-PAGE of mini gels

For small format SDS-PAGE gels, 10 well 4-12% (w/v) NuPAGE® Bis-Tris-HCl (buffered at pH 6.4) gels were used. Samples were vortex mixed with NuPAGE® LDS sample buffer and NuPAGE® reducing agent according to the manufacturer's guidelines and heated for 10 min at 70 °C. The samples were vortex mixed briefly and spun at 16,000 g for 5 min before loading. Typically 10 μg in 10-20 μl was loaded per lane. Lanes without samples were filled with equivalent volumes of sample buffer to ensure even protein migration between lanes.

Gels were fixed into a NOVEX Xcell SureLock™ Mini-Cell system. The inner chamber was filled with 200 ml 0.25% (v/v) NuPAGE® Antioxidant in NuPAGE® MOPS SDS Running Buffer. The outer chamber was filled with NuPAGE® MOPS SDS Running Buffer. Electrophoresis was performed using a PowerEase® power supply at 200 V, 120 mA until the dye front had reached the bottom of the gel (~ 50 min). Unstained ProSieve® molecular weight protein standards were run alongside the samples for molecular weight estimation.

2.2.6 Total protein staining

Gels were removed from the running tanks and the plastic spacers on either side of the gel cassette were displaced to allow opening of the glass plates. The IPG strip and the overlay agarose were discarded. Prior to fixing, the gels were briefly washed in Milli Q water to remove running buffer. Staining of small format gels was performed in small sandwich boxes with 50 ml of each solution. Large format gels were stained in specially built staining tanks with 6 litres of each solution for a set of 12 gels.

Firstly, the proteins on the gels were fixed in 40% (v/v) ethanol, 10% (v/v) acetic acid overnight. The gels were then incubated in Priming Solution (7.5% (v/v) acetic acid, 0.05% (w/v) SDS) for 30 min. OGT 1238, a proprietary fluorescent dye based on the structure of (aminostyry1)pyridinium dyes (Hassner *et al.*, 1984), was used to stain the gels. The stock solution of this dye (2 mg/ml in dimethyl sulphoxide, DMSO) was prepared in 7.5% (v/v) acetic acid to give a final concentration of 1.2 mg/l. The gels were incubated in this staining solution for approximately 4.5 h in the dark. To decrease background fluorescence the gels were washed in deionised water for 5 min post-staining followed by a further wash in 50% (v/v) ethanol for 5 min.

2.2.7 Image analysis

2.2.7.1 Scanning

Large format 2D-PAGE gels stained with OGT 1238 dye were imaged (16-bit monochrome fluorescent images, 200 μm resolution) with a 488 nm Apollo linear

fluorescence scanner. Gels were scanned in Tagged Image File format (*.tif) onto a shared server and were automatically cropped and converted into graphics filter files (*.flt) for image analysis.

Scanned gels were sealed in plastic bags and stored at 4 °C with approximately 10 ml 40% (v/v) ethanol, 10% (v/v) acetic acid until required for excising protein spots.

Mini gels stained with OGT 1238 dye were imaged as 8-bit monochrome images on a LAS1000Pro CCD camera. Prior to capturing images the parameters were set to chemiluminescence/fluorescence and the CCD camera was cooled to -25 °C. The gel was placed onto an ethanol-cleaned glass plate and inserted onto level 3 of the imaging tray. Images were acquired over different exposure times (typically between 0.5 to 2 min) until the optimum image was produced.

Densitometric analyses of small format gels was carried out using AIDA software and images were exported in *.tif format. Densitometric data were saved as a text document on the AIDA software and then automatically converted to Microsoft Excel format for further analysis.

2.2.7.2 Differential image analysis

Differential image analysis was carried out essentially as described by García *et al.*, 2004b. Scanned images of all 2D-PAGE gels were analysed with a custom version of the Medical ELectrophoresis ANalysis Interactive Expert II (Melanie II) software. All gels were internally calibrated for pI and molecular weight using the *E. coli* proteome as a standard (Tonella *et al.*, 1998), typically using 10-15

calibrated landmarks on each gel. This allowed the software to warp the gels so that they superimposed each other to aid with image analysis.

A set algorithm for this software programme was used to detect protein spots on all 2D-PAGE gels. A synthetic image was created for all gels within the same group and the spots were detected using the same parameters. The spot features of these synthetic images were manually edited to remove artefacts that were incorrectly detected and not suitable for image analysis. Spot boundaries that were not correctly split were also edited. Once these synthetic gels had been successfully curated, each of the original gel images were curated in a similar manner using the edited synthetic gel as a template. Feature shapes were not edited on the original gels unless spot splitting was required.

The most representative original gel among all the gels included in the image analysis was chosen as the primary master. Features in all other gels were paired to this primary master gel and any features present in other gels but not the primary master were also added/reclustered so that all valid features were included in the analysis. Finally a synthetic composite master image was created which represented all the features from all the original gel images in the study. These were grouped together into linked sets or 'clusters' and given a unique identifying index called the molecular cluster index (MCI).

Differentially expressed features were determined using the Rosetta™ software. Typically four gels from one set were compared with four gels from another set (e.g. four control gels vs. four cirrhotic gels). The optical density of each feature was determined by summing pixels within the feature boundary and

the volume was determined by integrating this optical density over the area of the feature. All statistical calculations performed by Rosetta™ were based on the percentage volume of the features, i.e. (feature volume / total volume of all features over the image) x 100. Changes in protein expression were determined as a ratio of averaged percentage feature volumes. The parameters on Rosetta™ were set with a 75% feature presence threshold i.e. three of the four gels in the set must have a feature present to be considered a valid change. For the three moderate fibrosis serum gels, the feature presence threshold was set at 66% i.e. two of the three gels must have a feature present. Only differentially expressed changes that were 2-fold or more different were considered to be significant and were visually analysed on a Proteograph. The MCIs which recorded a Rank Sum p-value ≤ 0.05 were selected as statistically significant changes with 95% confidence. As an additional check, all features displayed as differentially expressed by Rosetta™ were validated further by visualising the features across all gels in a montage format on the Melanie II software.

2.2.8 Spot excision

For all small format SDS-PAGE gels, bands were manually excised with a clean scalpel. Gels stained with OGT 1238 stain were visualised on a Dark Reader light box in a dark room to aid manual excision of bands.

For large format 2D-PAGE gels, the co-ordinates of each differentially expressed protein feature were determined on the Melanie II software. Based on these co-ordinates a list of commands (called a cutfile) were generated that were

sent to a software-driven robot gel excisor. The software programmed x,y movements of the robot arms and directed a cutting head to cut and remove features. To avoid contamination between spots, a new cutter tip was used on the cutting head for each gel feature. The robot excised gel features by shearing and aspirating actions and the cutter tips with the isolated gel pieces were ejected into separate wells of a 96 well reaction plate with laser made holes on the bottom. The cutter tips were removed and the gel pieces were dried in a SpeedVac® for 1-2 h prior to automated in-gel digestion (Section 2.2.10.2).

2.2.9 Laboratory information management systems (LIMS) software

All samples, gels, gel batches, cast batches and cutfiles were given codes that were logged into a LIMS system with full details about the samples including sample type, concentration and sample load. The barcode numbers, pI range and lot numbers of IPG strips were also added to the LIMS database. Each 2D-PAGE gel was provided with a unique number given on an attached barcode. Barcode scanners were available on the Apollo scanner and spot excisor for identifying the gels. These barcode numbers were entered into the LIMS database so that the progression of the 2D-PAGE process could be monitored.

2.2.10 Protein identification

2.2.10.1 Manual in-gel digestion

For mini gels, the protein bands of interest were carefully excised from the gel using a scalpel and finely sliced into small pieces for manual digestion. All steps

were carried out at room temperature unless otherwise stated. For all steps where buffer was added to the gel pieces the samples were agitated on a shaker. The gel pieces were dried for 1-2 h in a Savant SpeedVac® linked to a vacuum vaporiser and then washed three times with 50 µl 20 mM ammonium bicarbonate (NH_4HCO_3) for 20 min. The supernatant was removed and the proteins in the gel were reduced with a minimal volume of 10 mM DTT in 20 mM NH_4HCO_3 for 45 min. The DTT solution was removed and free thiols were alkylated with a similar volume of 50 mM iodoacetamide in 20 mM NH_4HCO_3 with samples incubated in the dark for 20 min. Prior to trypsinisation the gels were dehydrated with 50 µl 20 mM NH_4HCO_3 in 50% (v/v) acetonitrile for 20 min. The supernatant was removed and dehydrated further with 100% acetonitrile for 20 min until the gel pieces turned white. The gel pieces were then dried completely in a SpeedVac® for 1 h. The dried pieces were covered with a minimal volume of 20 mM NH_4HCO_3 containing 10 ng/µl bovine trypsin. After 5 min, the excess trypsin solution was removed and 10 µl 20 mM NH_4HCO_3 was added. The gel pieces were incubated overnight in a 37 °C oven (12-15 h).

Post digestion, any residual solution was removed and placed in a new tube. The peptides in the gel were extracted three times with 50 µl 5% (v/v) formic acid, 50% (v/v) acetonitrile for 20 min and the extracts were pooled together with the residual digestion solution. The pooled extracts were dried down completely in a SpeedVac® and the peptides were reconstituted with 6-7 µl 0.1% (v/v) formic acid. Samples were vortex mixed briefly, shaken for 20 min and then sonicated for 2 min to aid the peptides to dissolve.

2.2.10.2 Automated in-gel digestion

All steps were carried out in an automated DigestPro workstation at room temperature unless stated otherwise. Solutions were added to the gel pieces using needles and removed through the laser made holes on the bottom of the plate by applying nitrogen pressure as described by Houthaeve *et al.*, 1997. Gels were washed with 50 µl acetonitrile and 50 µl 50 mM NH_4HCO_3 for 15 min. The supernatant was removed and the gels were dehydrated with 100 µl acetonitrile for 10 min. The acetonitrile was removed and the proteins in the gel were reduced with 30 µl 10 mM DTT in 25 mM NH_4HCO_3 for 10 min at 60 °C. Once the samples had cooled (20 min) the supernatant was removed and the gel proteins were alkylated with 30 µl 50 mM iodoacetamide in 25 mM NH_4HCO_3 for 15 min. The iodoacetamide solution was removed and the gel pieces were washed with 50 µl 50 mM NH_4HCO_3 for 15 min before dehydrating the gels twice with 50 µl acetonitrile for 15 min. The acetonitrile was removed and the workstation was paused for 10 min to allow drying.

18 ng/µl bovine trypsin was kept inside the automated robot in its inactive form by storing in acidic conditions (10% (v/v) acetonitrile, 1 mM HCl). The trypsin was activated by diluting it 2-fold with 25 mM NH_4HCO_3. 15 µl of this 9 ng/µl trypsin solution was added to each gel piece and left for 10 min to allow gel swelling. Gel pieces were incubated at 37 °C for 2 h after which 10 µl water was added to compensate for any water loss. The gel pieces were then incubated at 37 °C for a further 2 h.

10 µl 25 mM NH_4HCO_3 was added to each gel piece and incubated for 10 min. To dehydrate the gel, 20 µl acetonitrile was added and left for 10 min. The supernatant was transferred to a 96 well collection plate and 20 µl 10% (v/v) formic acid was added to the gels and left for 10 min to extract the peptides. The supernatant was added to the collection plate and the gels were dehydrated with 30 µl acetonitrile for 15 min. This supernatant was also added to the collection plate. The pooled extracts were dried completely in a SpeedVac® and the peptides were reconstituted by dissolving in 6.5 µl 0.1% (v/v) formic acid.

2.2.10.3 Mass spectrometric analysis

Mass spectrometric analysis was carried out using a Q-Tof 1 mass spectrometer coupled to a CapLC configured with a 300 µm id/ 5 mm C18 precolumn and a 75 µm id/25 cm C18 PepMap analytical column. Tryptic peptides were eluted to the mass spectrometer using a 45 min 5-95% (v/v) acetonitrile gradient containing 0.1% (v/v) formic acid at a flow rate of 200 nl/min. Spectra were acquired using the MassLynx software version 4.0 in an automatic data dependent fashion with a 1 s survey scan followed by three 1 s MS/MS scans of the most intense ions. The selected precursor ions were excluded from further analysis for 2 min. Processed spectra were searched against the Swiss-Prot database (release 47.5 of 19-Jul-2005: 188477 entries) using the Mascot Daemon search engine (Perkins *et al.*, 1999). Searches were restricted to the human taxonomy allowing carbamidomethyl cysteine as a fixed modification and oxidised methionine as a potential variable modification.

2.2.11 In-solution isoelectric focusing

Serum samples were diluted 5-fold in 9.8 M urea, 4% (w/v) CHAPS to ensure total denaturation of HCV infected samples. Samples were diluted further to give a total protein concentration of 298.5 μg/ml and a final sample buffer concentration of 5 M ZOOM urea, 2 M ZOOM thiourea, 4% (w/v) ZOOM CHAPS, 65 mM DTT, 2 mM TBP, 150 mM NDSB-256, 1.8% (v/v) pH 3-10 ZOOM carrier ampholytes and 0.002% (w/v) bromophenol blue to act as a tracking dye during IEF.

In-solution IEF was carried out according to the method by Tang and Speicher, 2005 using an IEF fractionator. The IEF fractionator was assembled according to the manufacturer's recommendations using pre-washed fraction chambers with the following pH ranges: pH 3-4.6; pH 4.6-5.4; pH 5.4-6.2; pH 6.2-7; pH 7-10. The anode buffer was prepared with 7 M ZOOM urea, 2 M ZOOM thiourea and 8.25X Novex IEF Anode buffer (pH 3.0). The cathode buffer was prepared with 7 M ZOOM urea, 2 M ZOOM thiourea and 1X Novex IEF Cathode buffer (pH 10.4). Anode and cathode buffers (17.5 ml each) were loaded into the respective electrode reservoirs of the IEF fractionator. The caps for the five fraction chambers were removed and 670 μl of the serum sample prepared in sample buffer was pipetted into each chamber. The chamber caps were replaced and fractionation was performed with a PowerPac 1000 power pack using 100 V for 20 min, 200 V for 80 min and 600 V for 80 min with a current limit set at 2 mA and a power limit set at 2 W.

The caps for the five fraction chambers were removed and the solutions in each chamber were collected into fresh tubes. The concentrations of each fraction were determined by Coomassie Plus protein assay as described in Section 2.2.3.2.

Detergents and salts were removed from the samples by chloroform–methanol precipitation (Wessel and Flugge, 1984) using the same approach as Schulenberg and Patton, 2004 for precipitating proteins from IEF fractionator sample buffer prior to SDS-PAGE. To each of the five 670 µl recovered pH fractions, 2.68 ml methanol was added, vortex mixed and spun at 14,000g for 10 s. 670 µl chloroform was added to each tube, vortex mixed and spun at 14,000g for 10 s. 2.01 ml Milli Q water was added, vortex mixed and spun at 14,000g for 1 min. The top aqueous layer was carefully aspirated off and discarded. 2.01 ml methanol was added, vortex mixed and spun at 14,000g for 2 min. The top methanol layer was carefully aspirated off and discarded. The protein pellet was dried completely in a SpeedVac and then redissolved in 50 µl IEF sample buffer (as shown in Section 2.2.4.1). After vortex mixing and sonicating the samples, a Coomassie Plus protein assay was performed again as described in Section 2.2.3.2. Samples were then analysed by SDS-PAGE using the method outlined in Section 2.2.5.

2.3 Results and Discussion

2.3.1 Liver fibrosis study: an overview

Although liver biopsy is currently the most reliable way of assessing hepatic fibrosis, this invasive approach has several associated complications including pain, haemorrhage and occasionally death. Furthermore, as fibrosis may not be homogenous throughout the liver, a biopsy specimen may not represent the true extent of liver scarring. Consequently, many researchers have assessed non-invasive serological methods using ECM-related proteins, inflammatory proteins and/or LFTs already used routinely in hospitals. Although these markers, which are expected to change in liver fibrosis, are useful tools, some unreliability exists particularly for the intermediate stages of fibrosis. Rather than predicting which proteins could be differentially expressed in fibrosis, a more favourable approach for identifying serological biomarkers in disease is to use proteomics. Here a 2D-PAGE proteomics approach to identify biomarkers by analysing multiple samples over a range of HCV-induced fibrosis stages including normal healthy controls is described.

2.3.2 Clinical data for fibrosis study

The clinical data provided is shown in Table A1. The presence of HCV RNA was determined by PCR for all infected patients (viral titres were not provided). This method, considered to be the gold standard for diagnosing HCV infection, is more reliable than immunoassay based methods (Gretch, 1997).

2.3.2.1 Correlation between fibrosis and necroinflammatory scores

In addition to controls (0), three varying stages of fibrosis were investigated; mild fibrosis (1), moderate fibrosis (3) and cirrhosis (6); the numbers in parentheses indicate the Ishak fibrosis score (Table A1). Four individuals were analysed for each fibrosis stage with the exception of moderate fibrosis where the clinician was able to only acquire serum samples from three patients. No patients within this fibrosis study were on interferon or ribavirin therapy.

The Ishak modified HAI scoring system, which is significantly more reliable than other available scoring methods, was used to determine both the fibrosis and necroinflammatory scores. From the necroinflammatory data provided (for 6 of the 11 diseased patients), all the Ishak HAI scores were ≤4, indicating minor necroinflammation. There appears to be no correlation between the extent of fibrosis and necroinflammation based on the data provided for mild and moderate fibrosis which is consistent with previous studies (Brunt, 2000).

2.3.2.2 LFTs in fibrosis and hepatic inflammation

ALT levels, ranging from 21-142 IU/l, were provided for 8 of the 15 individuals. The normal reference range for ALT is 0-45 IU/l (Limdi and Hyde, 2003). There appears to be no correlation between the extent of fibrosis and blood ALT concentration; some patients within the mild and moderate fibrosis category showed ALT levels within the normal reference range indicating that ALT is an unreliable marker for liver fibrosis. It is known that ALT can fluctuate erratically during the late stages of chronically evolving HCV infection and cirrhotic ALT

levels may overlap with those of normal controls (Figure 6). It has been shown that patients with the higher levels of ALT could have a higher chance of progressing from fibrosis to cirrhosis, or cirrhosis to HCC (Tarao *et al.*, 1999). In a similar way, patients with persistently normal or low ALT levels often do not progress to HCC (Tarao *et al.*, 2004). Although ALT is usually associated with liver inflammation, no correlation with necroinflammatory scores was observed here. Again, this was as expected as at least a third of all HCV infected patients have levels of ALT within the normal reference range despite biopsy analysis indicating the presence of liver inflammation (Haber *et al.*, 1995).

It would have been interesting to look at other LFTs, in particular GGT and bilirubin, as these both have been shown to correlate reasonably well with fibrosis stage in the serological FibroTest analysis (Imbert-Bismut *et al.*, 2001; Table 3). AST levels, along with the already provided ALT concentrations, may have also been useful since a AST:ALT ratio greater than 1 has previously been shown to be a reasonable predictor of cirrhosis (Williams and Hoofnagle, 1988; Park *et al.*, 2000).

2.3.2.3 Variables between patients

One issue with the statistical analysis of the samples in this study is that only three serum samples were analysed for moderate fibrosis whereas four samples were considered for all other stages. Since drugs may affect the expression of serum proteins, all fibrosis and cirrhosis patients in this study were not on any form of therapy. It was challenging for the clinician to acquire samples from

patients who were not on any form of treatment as antiviral therapy is normally given immediately to HCV positive patients. For this reason, we were only able to analyse three serum samples from patients with moderate fibrosis.

Due to the difficulties in obtaining multiple HCV-induced fibrosis samples from patients who were not on any form of HCV therapy, it was not possible to keep other factors constant while only the fibrosis stage varied. From the details provided by the clinician, patients varied in sex, age (from 33-77 years) and HCV genotype (although most had genotype 1). It was also not possible for the clinician to accurately record whether these patients were in the postprandial or fasting state, which would certainly change the expression of various serum proteins. Fasting has been shown to increase cholesterol, triglycerides, LDL, VLDL, apolipoprotein B, and decrease HDL and apolipoprotein E (Markel *et al.*, 1985; Savendahl and Underwood, 1999). We believe that these variables do not compromise the results since, should the potential biomarkers in this study be used to monitor fibrosis score in patients, these variables would not be controlled. In addition to this, a fibrosis biomarker should ideally be able to be applied to a wide range of patients with differences in all these factors. The analysis of several serum samples for each fibrosis stage helps to reduce the issues with these variables.

2.3.3 Total protein as an indicator for chronic inflammation

Prior to electrophoresis analysis, the total protein concentration of each serum sample was determined by the BCA assay. The normal reference range for total serum protein is 60-83 mg/ml (Sidhaye, 2005). Occasionally total protein analysis is carried out along with LFTs and values outside the normal reference range may help to reflect nutritional state, kidney disease and liver disease (Hayden and van Heyningen, 2001). Elevated levels of total serum protein may give a crude indication of the extent of chronic inflammation and therefore are expected to correlate with the degree of hepatitis (Sidhaye, 2005). However, this test is not considered to contribute to clinical management and is therefore not usually included in the panel of LFTs (Watts *et al.*, 2000). Here, the total protein assay results revealed no correlation with either the Ishak fibrosis or necroinflammatory scores (Table A1). Responders to interferon and ribavirin treatment show a decrease in both fibrosis and hepatic inflammation (Anatol *et al.*, 2005). In one particular patient who responded to antiviral treatment with an iminosugar where viral titre decreased, total serum protein levels declined (data not shown) suggesting that total protein is a reasonably reliable indicator for monitoring inflammation in individuals. In this case, termination of antiviral therapy led to a subsequent increase in total protein suggesting that liver inflammation became worse and this correlated with an increased viral titre as well as development of HCC. Analysis of further serum samples can help to establish if total protein is useful in assessing liver inflammation progression within individuals.

2.3.4 2D-PAGE analysis of serum from patients with liver scarring

To identify biomarkers for different stages of HCV-induced fibrosis, serum samples from the 15 individuals detailed in Table A1 were analysed in a 2D-PAGE-based proteomics study. 500 μg of each of the serum samples were separated by 2D-PAGE (3-10 NL; 9-16% PAGE gradient). Differential image analysis was carried out to compare gels for controls with each of the three stages of liver scarring: mild fibrosis, moderate fibrosis and cirrhosis. Figure 7 shows synthetic gel images for each of the three stages of hepatic scarring investigated. These images are representative of all the features in the differential analysis; original gel images for all samples are shown in the Appendix, Figure A1. A total of 53 differerentially expressed features were excised, digested with trypsin, analysed by LC-MS/MS, and identified using the SwissProt database. 83 differentially expressed proteins were identified and are listed, with details of their theoretical molecular weight, pI, and function in Table A2. Table 5 shows a summary of selected differentially expressed proteins that have been classified according to their function. Further information about the proteins, including amino acid sequence and sites of glycosylation, was derived from the ExPASy database (http://www.expasy.ch/).

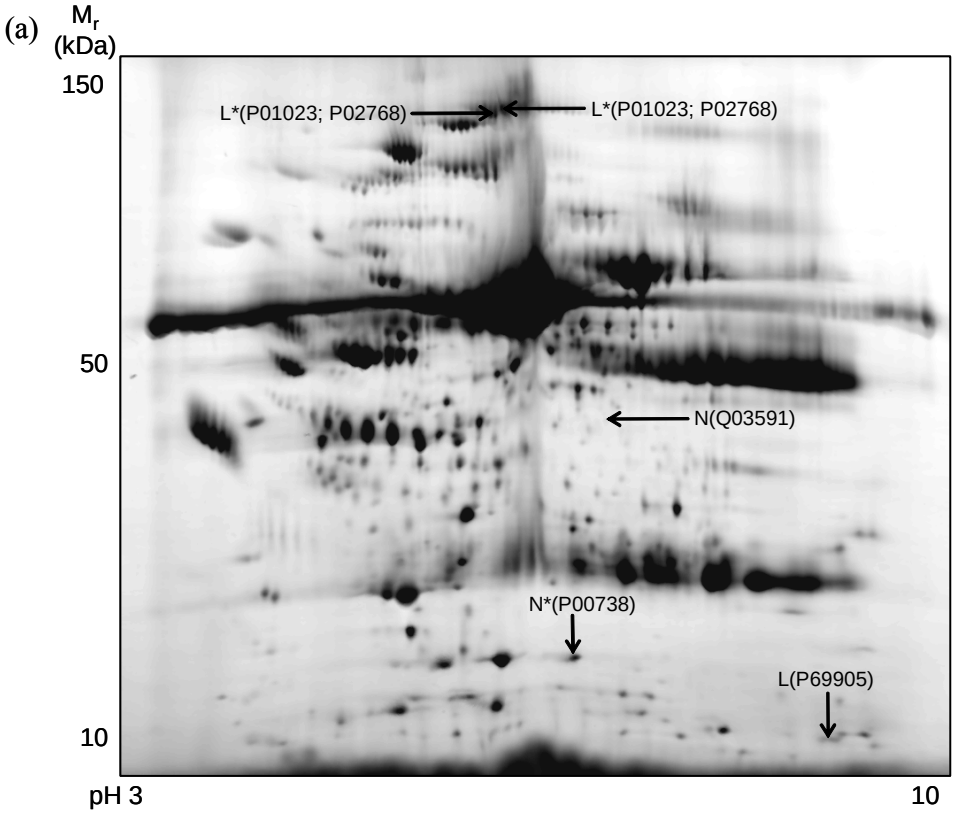
(a)
M_r (kDa)
150
50
10
pH 3
10
L*(P01023; P02768)
L*(P01023; P02768)
N(Q03591)
N*(P00738)
L(P69905)

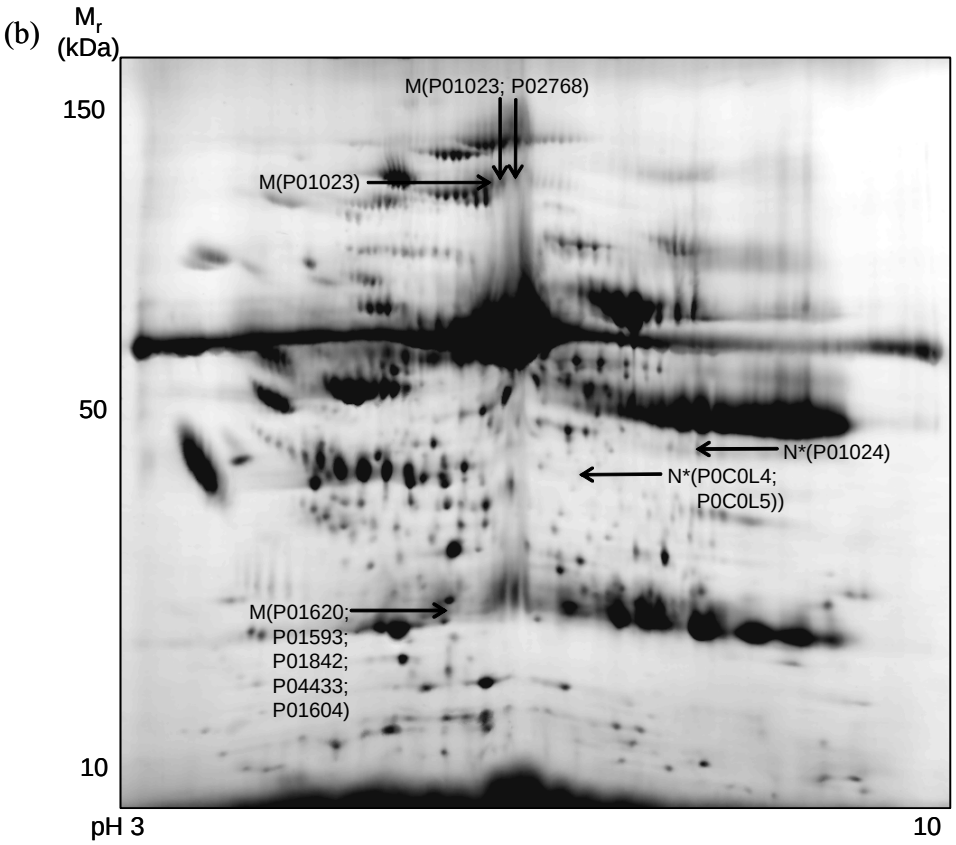
(b)
M_r (kDa)
150
50
10
pH 3
10
M(P01023; P02768)
M(P01023)
N*(P01024)
N*(P0C0L4; P0C0L5))
M(P01620; P01593; P01842; P04433; P01604)

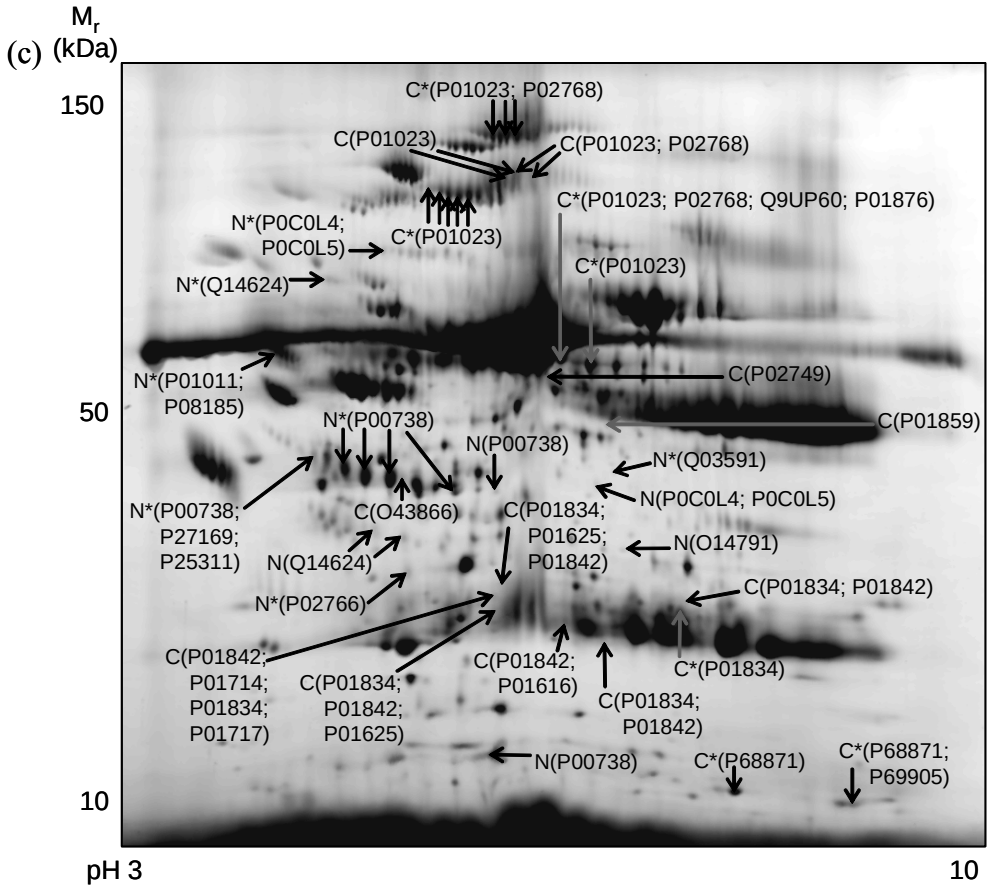

Figure 7 Synthetic 2D-PAGE images representing all protein spots present in serum samples from healthy controls versus the different stages of hepatic scarring. Gels were stained with the fluorescent dye OGT 1238. Images for all four control gels were merged with all the gels for each stage of hepatic scarring using the customised Melanie software to create the synthetic gels shown. (a) Control versus mild fibrosis; (b) Control versus moderate fibrosis; (c) Control versus cirrhosis. Differentially expressed features along with their Swiss-Prot accession numbers are highlighted.

N, features present only in serum from healthy controls

L, features present only in serum from mild fibrosis patients

M, features present only in serum from moderate fibrosis patients

C, features present only in serum from cirrhosis patients

, features present in serum from both control and heptic scarring but expressed to a higher extent in asterisked stage of hepatic scarring (e.g. L for mild, M* for moderate, C* for cirrhosis) or control (N*)

For complete gel figures, see Appendix (Figure A1)

Classification	Protein Name	Changes in relation to controls			Protein function
		Mild	Moderate	Cirrhosis	
Plasmin associated	α2 macroglobulin	↑	⇑	↑⇑	Inhibits plasmin
	Inter-α-trypsin inhibitor heavy chain H4	–	–	↓⇓	Can be cleaved by kallikrein (leads to plasmin activation)
Decreased due to compromise in hepatic synthetic function	Albumin	–	–	↓	Liver synthesised protein, most abundant protein of serum
	Prealbumin (Transthyretin)	–	–	↓	Liver synthesised protein; carries vitamin A
	Complement C3, C4 and factor H-related protein 1	⇓	↓	↓⇓	Liver synthesised protein; involved in complement cascade
Hepatocyte growth factor (HGF) related	α1 antichymotrypsin	–	–	↓	HGF decreases α1 antichymotrypsin
	Haptoglobin	↓	↓	↓⇓	HGF decreases haptoglobin synthesis
Lipid metabolism	Apolipoprotein L1	–	–	⇓	Levels correlate with triglycerides and cholesterol
	β2 glycoprotein I	–	–	⇑	Binds to chylomicrons and high-density lipoproteins
	Paraoxonase / arylesterase 1	–	–	↓	Degrades oxidised lipids in lipoproteins and cells
	Zinc-α2-glycoprotein	–	–	↓	Stimulates lipolysis in adipocytes
Immune system related	CD5 antigen-like	–	–	⇑	Possible immune system regulation role; IgM related
	IgA1 + IgG2 heavy chain & Ig light chain regions	–	↑	↑⇑	Immunoglobulin fragments

Table 5 Summary of selected differentially expressed proteins identified in serum samples of healthy controls versus the different stages of hepatic scarring

Proteins shown were differentially expressed by 2-fold or more when comparing serum gels from healthy controls with the different stages of hepatic fibrosis

⇑, present only in serum from hepatic scarring patients

↑, present in serum from both control and hepatic scarring patients but expressed to a higher extent in hepatic scarring

–, no significant change

↓, present in serum from both control and hepatic scarring patients but expressed to a higher extent in control serum

⇓, present only in serum from healthy controls

2.3.5 Increase of CD5L in cirrhotic patients may be related to viral load

CD5 antigen-like protein (CD5L) was observed in cirrhotic serum samples but appeared to be absent from healthy controls (Figure 8). It was observed at 41 kDa, pI 5.3 which is consistent with its theoretical molecular weight and pI (38 kDa, pI 5.3). Since CD5L was identified in close proximity to the highly intense features of the haptoglobin β-chain, it was difficult to determine if CD5L was genuinely absent in the serum samples from healthy controls. To confirm the absence of CD5L in healthy controls, pooled control serum was depleted of four major abundant proteins (albumin, IgG, transferrin and haptoglobin) using an in-house developed immunoprecipitation method which works on the basis of the kit described by Khundmiri *et al.*, 2003. The absence of haptoglobin in this depleted sample resulted in better representation of this region of the gel and analysis confirmed that CD5L is absent from serum of healthy controls (Figure 8c).

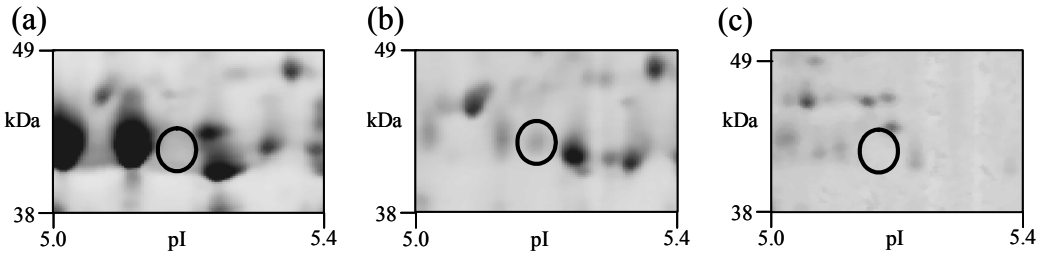

Figure 8 CD5L increases in serum from cirrhotic patients. In each case a magnified region of the gel is shown with the relative position of CD5L circled. Representative serum gel images are shown for (a) healthy controls, (b) cirrhosis patients, and (c) control serum depleted of high abundant proteins

CD5L is a member of the scavenger receptor cysteine-rich superfamily, which also includes T and B cell antigens CD5 and CD6, that are associated with regulation of the immune system (Tissot *et al.*, 2002). CD5L was first identified by 2D-PAGE based proteomics and found to be associated with IgM (Tissot *et al.*, 1994). Several researchers have shown that serum levels of anti-HCV core IgM may be useful in the diagnosis of HCV infection particularly for active viral replication (Tabone *et al.*, 1997; Sagnelli *et al.*, 2005). Using 2D-PAGE based proteomics, CD5L was identified as an IgM-associated protein in the serum cryoprecipitate of a HCV-infected patient (Damoc *et al.*, 2003); this is the only reported association of HCV with CD5L to date. Abnormal plasma globulins (IgM/IgG) that precipitate when serum is cooled (cryoprecipitation) are one of the most important extrahepatic manifestations of chronic HCV infection where the virus induces B cell proliferation (Garini *et al.*, 2005).

CD5+ B cells are significantly increased in proliferation in chronic HCV infection and this expanded CD5+ B cell population may reflect the attempt by the immune system to protect against the development of progressive liver disease (Curry *et al.*, 2000). Knodell HAI index and HCV viral load have been shown to positively correlate with CD5+ B cell expansion (Zuckerman *et al.*, 2002). A follow up study showed that the CD5+ B cell expansion decreased with interferon and ribavirin antiviral therapy, correlating with a reduction in HCV RNA load. However, in non-responders to therapy the CD5+ B cell expansion was not significantly changed and was similar to healthy controls. Other studies suggest that CD5+ B cell lymphoproliferation may correlate with other HCV antiviral

therapies (Zuckerman *et al.*, 2003). CD5+ B cell lymphoproliferation has also been examined in HBV infected individuals (Zuckerman *et al.*, 2002). In general, levels of CD5+ B cells are highest in HCV patients, followed by HBV patients, with lower levels in healthy control patients. In the study described herein, viral titres were not provided by the clinician, therefore no correlation between the observed increased expression of CD5L and viral titre can be made. Higher HCV RNA levels may have been present in the cirrhotic patients, the only samples in which CD5L was detected. However, there is a poor correlation between viral load and fibrosis score and others have shown that there is no difference in HCV RNA in patients with chronic hepatitis, cirrhosis or HCC (Agha *et al.*, 1999; Nousbaum *et al.*, 1995).

There is no reported association between CD5L and liver fibrosis. It is probable that the observed increased levels of CD5L in cirrhotic patients in this study are associated with HCV infection rather than liver cirrhosis. This could be confirmed by checking for the absence of CD5L in serum samples from patients with non-virally induced cirrhosis (e.g. alcoholic). Other studies have shown that another member of the scavenger receptor cysteine-rich family, 90K/MAC-2BP, is a useful tumour marker for analysing the progression of cirrhosis to HCC in HCV infected patients (Correale *et al.*, 1999). However, this glycoprotein was not found to correlate with liver compromise but with the levels of anti-HCV antibodies suggesting that, as proposed for CD5L, this is a marker for HCV-infection rather than development of fibrosis/cirrhosis.

2.3.6 Decrease in inter-α-trypsin inhibitor heavy chain H4 may be related to the reduction in plasmin-mediated ECM degradation

Expression of inter-α-trypsin inhibitor heavy chain H4, a glycoprotein synthesised in the liver, was found to be greater in the control samples than in those from patients with cirrhosis. The protein was differentially expressed in three areas of the gels: two spots at approximately 35 kDa were absent in the cirrhotic gels but present in healthy controls and in samples from patients with intermediate stages of fibrosis; one smear at approximately 84 kDa was decreased in expression in cirrhotic serum samples compared with healthy controls (Figure 9).

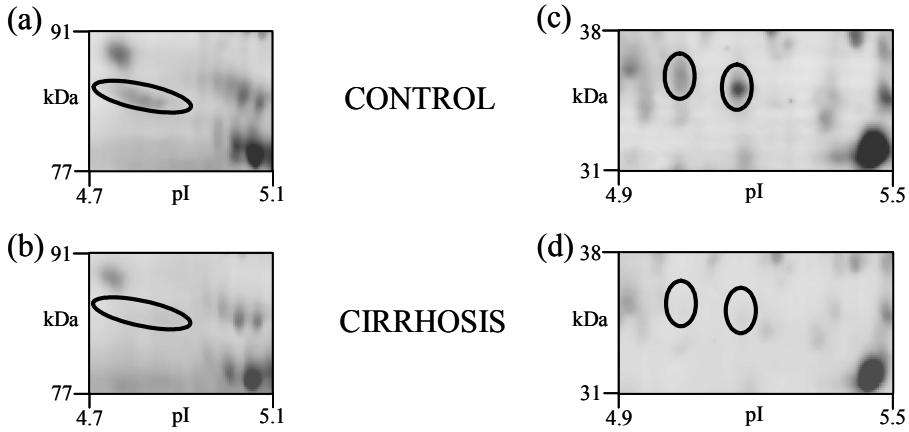

Figure 9 Apparent absence of cleaved inter-α-trypsin inhibitor in serum from cirrhosis patients. The inhibitor is cleaved by kallikrein into 35 and 70 kDa fragments. (a) and (b) the *N*-glycosylated form of the larger 70 kDa fragment found at 84 kDa. (c) and (d) the smaller 35 kDa fragment. Control samples are shown in (a) and (c); cirrhosis samples are shown in (b) and (d). Zoomed images from representative gels are shown in each case.

The inter-α inhibitor proteins are a family of serine protease inhibitors thought to be associated with inflammation and wound healing (Josic *et al.*, 2006). They usually consist of heavy and light chains; the heavy chain of some inter-α inhibitor proteins have been shown to interact with hyaluronan which may stabilise the ECM (Bost *et al.*, 1998). The heavy chain of inter-α-trypsin inhibitor H4, identified in the proteomics study herein, has never been described in hepatic fibrosis. It may be associated with hyaluronan and possibly ECM stabilisation.

Inter-α-trypsin inhibitor proteins may possess acute phase and anti-inflammatory roles since they form complexes with TSG proteins which are encoded by TNF-stimulated genes (*tsg*), an association that enhances plasmin inhibition (Wisniewski *et al.*, 1996). Inter-α-trypsin inhibitor proteins can increase the plasma clearance of plasmin and the enzyme which breaks down elastin, elastase (Pratt *et al.*, 1987), both of which contribute to ECM degradation. The trypsin inhibitor achieves this by acting as a shuttle to transfer these fibrolytic proteinases to other proteinase inhibitors, e.g. α2 macroglobulin (a2M), for clearance.

To our knowledge the inter-α-trypsin inhibitor identified in this proteomics study, inter-α-trypsin inhibitor heavy chain H4, has never been described in hepatic cirrhosis. Here, decreased expression of inter-α-trypsin inhibitor heavy chain H4 has been observed in cirrhotic patients. This inhibitor is cleaved proteolytically by kallikrein into 35 and 70 kDa fragments (Nishimura *et al.*, 1995). The two lower molecular weight spots observed on the gels for the control patients account for the 35 kDa fragment; all peptides identified by mass

spectrometry for both of these spots correspond to this fragment (Figure 10). The higher molecular weight smear observed at approximately 84 kDa is a glycosylated form of the 70 kDa fragment, as confirmed by the identification of peptide sequences (Figure 10). This fragment contains four *N*-glycosylation sites (at aa 81, 207, 517 and 577) and the smear shape is consistent with that seen for glycoprotein trains. It was encouraging to observe decreased expression of both fragments of this glycoprotein in cirrhosis, indicating that the observed changes are significant.

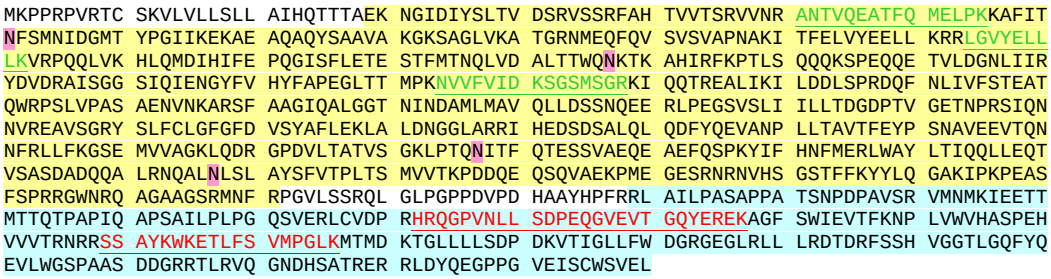

Figure 10 Cleavage of inter-α-trypsin inhibitor heavy chain H4 by kallikrein. The precursor of this inhibitor is 930 aa long and the 35 and 70 kDa fragments span aa 689-930 and aa 29-661, respectively. The full length sequence of the precursor is shown and identified peptides are underlined. The 35 kDa chain is shaded in blue and peptides identified for the spots at 35 kDa are shown in red. The 70 kDa chain is shaded in yellow with peptides identified for the smear at 84 kDa in green. Potential *N*-glycosylation sites are shaded in pink.

The decreased levels of the 35 and 70 kDa fragments may suggest that kallikrein is decreased in cirrhosis and therefore inter-α-trypsin inhibitor heavy chain remains in its uncleaved form. In this case elevated levels of the uncleaved protein would be expected in the serum of patients with cirrhosis. Uncleaved

inter-α-trypsin inhibitor has a molecular weight of 105 kDa and pI 6.5. However, it was not possible to detect this protein by image analysis as the more highly abundant protein plasminogen runs in the same relative position and it is therefore likely that the presence of any uncleaved inter-α-trypsin inhibitor would be masked. Secondly, proteins are usually poorly represented in this high molecular weight region of the gel since they are not well transferred onto the second dimension gel matrix from the IEF strip (Oh-Ishi and Maeda, 2002). Since inter-α-trypsin inhibitor proteins have been shown to inhibit plasmin and elastase (Pratt *et al.*, 1987), the suggested decreased cleavage of inter-α-trypsin inhibitor heavy chain H4 in cirrhosis may result in a more effective inhibitor against these enzymes thereby decreasing ECM degradation.

Whilst inter-α-trypsin inhibitor heavy chain H4 has not been reported previously in hepatic scarring, it has long been known that plasma kallikrein is reduced in liver cirrhosis and is involved in fibrolytic processes in the liver (Faciullacci *et al.*, 1976). The protease usually acts on high molecular weight kininogen (HMWK) in serum to form the vasodilator bradykinin. Bradykinin has been shown to stimulate tissue-type plasminogen activator (tPA), a protease that proteolytically activates plasminogen to plasmin. tPA is also activated by ACE inhibition (Nagaoka *et al.*, 2003), offering an additional explanation for the use of inhibitors of the renin-angiotensin system in the treatment of hepatic fibrosis (see Section 2.1.10). Plasmin activates MMPs for ECM degradation in the initial stages of hepatic scarring but later this step is overridden by the increased activation of TIMPs (see Section 2.1.2). Thus decreased levels of kallikrein in

cirrhosis decrease bradykinin formation resulting in reduced stimulation of hepatic tPA and therefore decreased formation of plasmin. Consequently activation of MMPs is reduced, thereby decreasing ECM degradation. Also, activated HSCs synthesise plasminogen activator inhibitor-1 (PAI-1); this synthesis is stimulated by TGF-β1. The increased levels of PAI-1 in liver fibrosis inhibit tPA which decreases plasmin activity and ultimately further reduces ECM breakdown (Nagaoka *et al.*, 2003).

Expression of another liver synthesised inter-α-trypsin inhibitor, urinary trypsin inhibitor (UTI), with a molecular weight of approximately 25 kDa also decreases with hepatic cirrhosis (Lin *et al.*, 2004). This protein is excreted by the kidneys and urinary levels of this inhibitor correlate well with plasma levels. Levels of this protein decrease in hepatitis patients but most significantly in those with liver cirrhosis. Interestingly, although the levels of this inter-α-trypsin inhibitor decrease in HCC as well, it does not decrease to the same extent as in hepatic cirrhosis (Lin *et al.*, 2004).

Further tests are required to validate if inter-α-trypsin inhibitor heavy chain H4 could be a reliable marker for liver cirrhosis and whether it is superior to the smaller 25 kDa inter-α-trypsin inhibitor already described.

2.3.7 Thiolester cleavage of α2 macroglobulin may increase with hepatic fibrosis

Differential image analysis clearly revealed that serum levels of the acute phase protein α2 macroglobulin (a2M) increase with the development of hepatic fibrosis (Figure 11). a2M is a 161 kDa protein (1474 aa precursor) with a pI of 6.0 synthesised by both hepatocytes and activated HSCs (Naveau *et al.*, 1994; Kawser *et al.*, 1998). A number of gel features were identified as a2M with molecular weights of 135-141 kDa, 111-123 kDa, 61-62 kDa (Figure 11). These molecular weight ranges were determined by the Melanie II image analysis software based on calibrated landmarks. However, calibrated landmarks were not available for proteins greater than 100 kDa and therefore some of these ranges may be inaccurate.

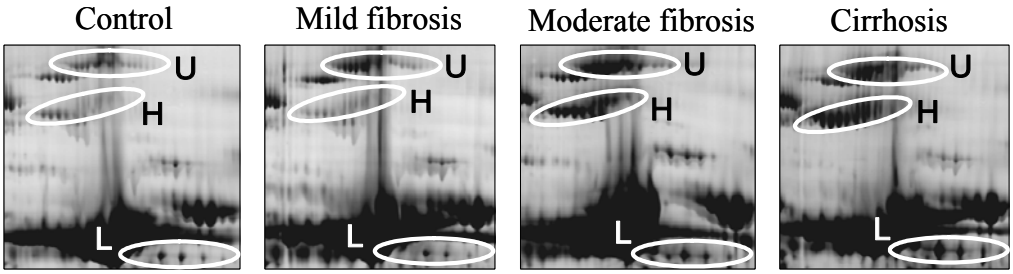

Figure 11 Thiolester cleavage of α2 macroglobulin. Represenative gel images of serum from healthy individuals (control), mild fibrosis pateints, moderate fibrosis pateints and cirrhosis pateints. U = Uncleaved a2M; H = high molecular weight fragment from thiolester cleavage; L = low molecular weight fragment from thiolester cleavage. Close up gel images are shown in each case encompassing the region where all fragments were found to be differentially expressed.

The protein trains which appeared in the 135-141 kDa region had a pI of 5.6-5.7 and contained peptides spanning from aa 72 to 1397 (Figure 12a). This sequence of peptides has a calculated mass of 147 kDa and it is possible that the full-length sequence is present in these spots. Uncleaved a2M contains 8 *N*-linked glycosylation sites and the spot trains observed for these spots on the gel indicates that the protein is glycosylated. Therefore the molecular weight of the sample determined from the gel should be higher than the theoretical mass calculated from the peptide sequences. The decreased apparent molecular mass of the sample indicates that calibration of molecular weight for extremely large proteins is unreliable unless suitable calibrated landmarks are also applied to these regions. Negatively charged glycans, e.g. sialic acids, may account for spots being observed below pH 6.0.

The protein trains which appeared in the 111-123 kDa region of the gel had a pI range of 5.4-5.8 and contained peptides spanning from aa 72 to 912, suggesting cleavage of the C-terminal end of a2M (Figure 12b). Since the identified peptides precede a thiolester site (at aa 971-975), it is probable that the protein was cleaved at this position resulting in this high molecular weight fragment. Such a cleavage would result in a protein with a theoretical molecular weight of 107 kDa and a pI of 5.8. The charge is consistent with the migration on the gel. The train of protein spots is indicative of glycosylation that may account for the slightly higher molecular weight seen on the gel. a2M has six *N*-glycosylation sites preceding the thiolester site (at aa 55, 70, 247, 396, 410 and 869). Again negatively charged glycans may account for the spots observed below pI 5.8.

The protein trains which appeared in the 61-62 kDa region had a pI range of 5.9-6.0 and contained peptides spanning from aa 1004 to 1467, corresponding to the C-terminal end of the protein, after the thiolester cleavage site (Figure 12b). Cleavage at the thiolester site would result in a protein with a theoretical molecular weight of 55 kDa and a pI of 6.6, in reasonable agreement with the experimental data. There are two potential *N*-glycosylation sites within the sequence of this low molecular weight fragment (at aa 991 and 1424) which, if occupied, would account for the differences between the experimental and theoretical data.

With respect to healthy control serum, the 61-62 kDa thiolester cleaved C-terminal end of a2M was found to change by more than 2-fold in percentage spot volume only in cirrhotic serum. The 111-123 kDa thiolester cleaved N-terminal end of a2M changed by more than 2-fold mostly in cirrhotic serum and with fewer glycoforms in serum from moderate fibrosis patients. Uncleaved a2M changed by more than 2-fold in all stages of fibrosis with the number of glycoforms increasing with hepatic scarring. Together these data suggest that not only does a2M expression increase with liver fibrosis but cleavage at the thiolester site may also increase. To our knowledge this is the first suggestion that thiolester cleavage of a2M increases with hepatic fibrosis. Therefore, assaying for all three a2M chains (i.e. uncleaved and the N- & C-terminal thiolester cleaved products) may provide a more valuable indication for the stage of liver fibrosis.

(a)

MGKNKLLHPS LVLLLLVLLP TDASVSGKPQ YMVLVPSLLH TETTEKGCVL LSYLNETVTV SASLESVRGN RSLFTDLEAE
NDVLHCVAFA VPKSSSNEEV MFLTVQVKGP TQEFKKRTTV MVKNEDSLVF VQTDKSIYKP GQTVKFRVVS MDENFHPLNE
LIPLVYIQDP KGNRIAQWQS FQLEGGLKQF SFPLSSEPFQ GSYKVVVQKK SGGRTEHPFT VEEFVLPKFE VQVTVPKIIT
ILEEEMNVSV CGLYTYGKPV PGHVTVSICR KYSDASDCHG EDSQAFCEKF SGQLNSHGCF YQQVKTKVFQ LKRKEYEMKL
HTEAQIQEEG TVVELTGRQS SEITRTITKL SFVKVDSHFR QGIPFFGQVR LVDGKGVPIP NKVIFIRGNE ANYYSNATTD
EHGLVQFSIN TTNVMGTSLT VRVNYKDRSP CYGYQWVSEE HEEAHHTAYL VFSPSKSFVH LEPMSHELPC GHTQTVQAHY
ILNGGTLLGL KKLSFYYLIM AKGGIVRTGT HGLLVKQEDM KGHFSISIPV KSDIAPVARL LIYAVLPTGD VIGDSAKYDV
ENCLANKVDL SFSPSQSLPA SHAHLRVTAA PQSVCALRAV DQSVLLMKPD AELSASSVYN LLPEKDLTGF PGPLNDQDDE
DCINRHNVYI NGITYTPVSS TNEKDMYSFL EDMGLKAFTN SKIRKPKMCP QLQQYEMHGP EGLRVGFYES DVMGRGHARL
VHVEEPHTET VRKYFPETWI WDLVVVNSAG VAEVGVTVPD TITEWKAGAF CLSEDAGLGI SSTASLRAFQ PFFVELTMPY
SVIRGEAFTL KATVLNYLPK CIRVSVQLEA SPAFLAVPVE KEQAPHCICA NGRQTVSWAV TPKSLGNVNF TVSAEALESQ
ELCGTEVPSV PEHGRKDTVI KPLLVEPEGL EKETTFNSLL CPSGGEVSEE LSLKLPPNVV EESARASVSV LGDILGSAMQ
NTQNLLQMPY GCGEQNMVLF APNIYVLDYL NETQQLTPEV KSKAIGYLNT GYQRQLNYKH YDGSYSTFGE RYGRNQGNTW
LTAFVLKTFA QARAYIFIDE AHITQALIWL SQRQKDNGCF RSSGSLLNNA IKGGVEDEVT LSAYITIALL EIPLTVTHPV
VRNALFCLES AWKTAQEGDH GSHVYTKALL AYAFALAGNQ DKRKEVLKSL NEEAVKKDNS VHWERPQKPK APVGHFYEPQ
APSAEVEMTS YVLLAYLTAQ PAPTSEDLTS ATNIVKWITK QQNAQGGFSS TQDTVVALHA LSKYGAATFT RTGKAAQVTI
QSSGTFSSKF QVDNNNRLLL QQVSLPELPG EYSMKVTGEG CVYLQTSLKY NILPEKEEFP FALGVQTLPQ TCDEPKAHTS
FQISLSVSYT GSRSASNMAI VDVKMVSGFI PLKPTVKMLE RSNHVSRTEV SSNHVLIYLD KVSNQTLSLF FTVLQDVPVR
DLKPAIVKVY DYYETDEFAI AEYNAPCSKD LGNA

(b)

MGKNKLLHPS LVLLLLVLLP TDASVSGKPQ YMVLVPSLLH TETTEKGCVL LSYLNETVTV SASLESVRGN RSLFTDLEAE
NDVLHCVAFA VPKSSSNEEV MFLTVQVKGP TQEFKKRTTV MVKNEDSLVF VQTDKSIYKP GQTVKFRVVS MDENFHPLNE
LIPLVYIQDP KGNRIAQWQS FQLEGGLKQF SFPLSSEPFQ GSYKVVVQKK SGGRTEHPFT VEEFVLPKFE VQVTVPKIIT
ILEEEMNVSV CGLYTYGKPV PGHVTVSICR KYSDASDCHG EDSQAFCEKF SGQLNSHGCF YQQVKTKVFQ LKRKEYEMKL
HTEAQIQEEG TVVELTGRQS SEITRTITKL SFVKVDSHFR QGIPFFGQVR LVDGKGVPIP NKVIFIRGNE ANYYSNATTD
EHGLVQFSIN TTNVMGTSLT VRVNYKDRSP CYGYQWVSEE HEEAHHTAYL VFSPSKSFVH LEPMSHELPC GHTQTVQAHY
ILNGGTLLGL KKLSFYYLIM AKGGIVRTGT HGLLVKQEDM KGHFSISIPV KSDIAPVARL LIYAVLPTGD VIGDSAKYDV
ENCLANKVDL SFSPSQSLPA SHAHLRVTAA PQSVCALRAV DQSVLLMKPD AELSASSVYN LLPEKDLTGF PGPLNDQDDE
DCINRHNVYI NGITYTPVSS TNEKDMYSFL EDMGLKAFTN SKIRKPKMCP QLQQYEMHGP EGLRVGFYES DVMGRGHARL
VHVEEPHTET VRKYFPETWI WDLVVVNSAG VAEVGVTVPD TITEWKAGAF CLSEDAGLGI SSTASLRAFQ PFFVELTMPY
SVIRGEAFTL KATVLNYLPK CIRVSVQLEA SPAFLAVPVE KEQAPHCICA NGRQTVSWAV TPKSLGNVNF TVSAEALESQ
ELCGTEVPSV PEHGRKDTVI KPLLVEPEGL EKETTFNSLL CPSGGEVSEE LSLKLPPNVV EESARASVSV LGDILGSAMQ
NTQNLLQMPY GCGEQNMVLF APNIYVLDYL NETQQLTPEV KSKAIGYLNT GYQRQLNYKH YDGSYSTFGE RYGRNQGNTW
LTAFVLKTFA QARAYIFIDE AHITQALIWL SQRQKDNGCF RSSGSLLNNA IKGGVEDEVT LSAYITIALL EIPLTVTHPV
VRNALFCLES AWKTAQEGDH GSHVYTKALL AYAFALAGNQ DKRKEVLKSL NEEAVKKDNS VHWERPQKPK APVGHFYEPQ
APSAEVEMTS YVLLAYLTAQ PAPTSEDLTS ATNIVKWITK QQNAQGGFSS TQDTVVALHA LSKYGAATFT RTGKAAQVTI
QSSGTFSSKF QVDNNNRLLL QQVSLPELPG EYSMKVTGEG CVYLQTSLKY NILPEKEEFP FALGVQTLPQ TCDEPKAHTS
FQISLSVSYT GSRSASNMAI VDVKMVSGFI PLKPTVKMLE RSNHVSRTEV SSNHVLIYLD KVSNQTLSLF FTVLQDVPVR
DLKPAIVKVY DYYETDEFAI AEYNAPCSKD LGNA

Figure 12 **Thiolester cleavage sequences from a2M.** The full length a2M precursor sequence is shown in both cases with the thiolester site, GCGEQ, shaded in yellow. Identified peptides are shown underlined for the a2M trains observed at (a) 135-141 kDa (green; uncleaved), (b) 111-123 kDa (red; high MWt fragment) and 61-62 kDa (blue; low MWt fragment). Potential *N*-glycosylation sites are shaded in pink.

a2M is able to inhibit proteases by binding to a 'bait region' in its sequence from aa 690-728. This binding event causes a major conformational change in a2M and cleavage at the thiolester site. Consequently a2M is no longer able to inhibit proteases (Bjork and Jornvall, 1986). The a2M-mediated inhibition of plasmin and elastase have been demonstrated and shown to result in this thiolester

cleavage (Roche and Pizzo, 1988). Plasmin activates MMPs resulting in ECM degradation and elastase breaks down elastin (see Section 2.1.2) and therefore this a2M-mediated inhibition of these preoteases would cause decreased ECM degradation and increased hepatic scarring. a2M has also been shown to inhibit MMPs and collagenase and therefore may also result in the same thiolester cleavage (Moshage, 1997; Truden and Boros, 1988). Although there is evidence to show that a2M is cleaved at the thiolester site after association with fibrolytic proteases possibly including MMPs, there are no studies outlining the relationship between proteases involved in hepatic fibrosis and the thiolester cleavage products of a2M. Based on our 2D-PAGE spot analysis and the studies already performed on a2M thiolester cleavage, we believe that cleavage of a2M increases with liver scarring. Although a2M is already established as an indicator of hepatic scarring in the FibroTest (Imbert-Bismut *et al.*, 2001), our results provide the first suggestion that additional analysis of the thiolester cleavage products may give a more reliable indication of fibrosis activity in the liver.

The plasmin-mediated conformational change of a2M has also been shown to allow binding of cytokines to the protease inhibitor including TGF-β1 and PDGF which may encourage HSC activation and promote hepatic scarring in the ECM (Tiggelman *et al.*, 1996). In addition to PDGF, the ECM also contains HSC synthesised hepatocyte growth factor (HGF) which can contribute to HSC activation and also increases the synthesis of a2M, further explaining the observed elevation in this acute phase protein (Guillen *et al.*, 1996).

Most of the spots for the three chains of a2M also contained peptides for the highly abundant protein serum albumin. However, the Mascot scores for albumin were significantly less than a2M signifying that the change in these spots are more likely to be due to a2M. Albumin has a similar pI to a2M and runs below the uncleaved and larger cleaved fragment and adjacent to the smaller cleaved fragment. We therefore believe that albumin peptides were present in the a2M spots as this highly abundant protein runs in close proximity to a2M.

One a2M spot at 62 kDa also contained β2 microglobulin, again with a lower Mascot score suggesting that the change in this feature is probably due to a2M. β2 microglobulin is the small subunit of MHC-1 and has been shown to increase in plasma of cirrhotic patients, although the mechanism of action is unknown (Amodio *et al.*, 1984). β2 microglobulin is an unreliable biomarker since it has never been described for the intermediate stages of fibrosis and also appears to correlate more closely to renal damage in cirrhotic patients rather than hepatic scarring (Gatta *et al.*, 1981).

2.3.8 Decrease in α1 antichymotrypsin may lead to HSC activation

The glycoprotein α1 antichymotrypsin was found to decrease in the serum from patients with liver cirrhosis in comparison to healthy controls by more than 2-fold (Figure 13). α1 antichymotrypsin is an inhibitor of the digestive protease, chymotrypsin and other chymotrypsin-like proteases (Kalsheker *et al.*, 2002). The protein was observed at 61 kDa, pI 4.7. The theoretical molecular weight and pI are 47 kDa, pI 5.4. However, this protein has three potential glycosylation sites (at

aa 70, 107 and 271) that could account for the higher molecular weight and more acidic pI due to negatively charged glycans, e.g. sialic acids.

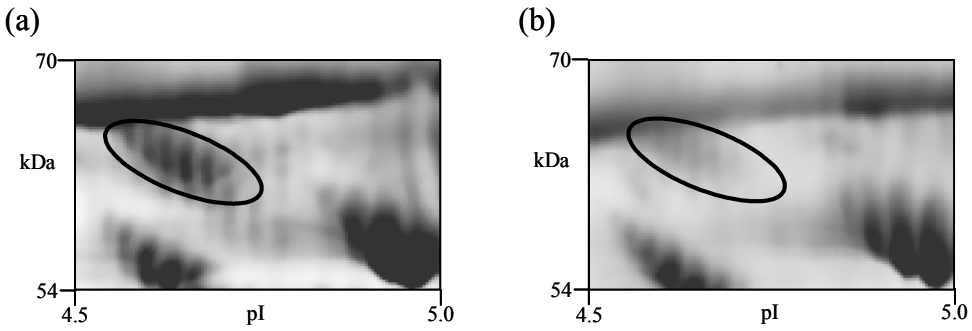

Figure 13 α1 antichymotrypsin decreases in cirrhosis. Magnified images of the region where the train of glycoprotein spots were found to change in expression for (a) control serum, and (b) cirrhosis serum.

Studies have shown that the levels of α1 antichymotrypsin, observed in globules within hepatocytes, decrease in HCV-related cirrhosis. The deficiency of this protease inhibitor appears to promote liver cirrhosis (Yoon *et al.*, 2002). However, a decrease of this enzyme inhibitor in hepatocytes does not reflect the levels observed in serum (Thomas *et al.*, 2000) and therefore α1 antichymotrypsin is a poor indicator for hepatic scarring.

It is unclear why α1 antichymotrypsin levels decrease in cirrhotic hepatocyte globules. One possibility is that HGF has been shown to decrease α1 antichymotrypsin; levels of this growth factor are elevated in the ECM in fibrosis (Guillen *et al.*, 1996). Another explanation for the reduced levels of this inhibitor is its association with the HSC activator angiotensin II. The renin substrate

angiotensinogen belongs to a family of proteins that also includes α1 antichymotrypsin (Sjoberg *et al.*, 1992). Renin converts angiotensinogen to angiotensin I which is then converted by ACE to angiotensin II. Chymotrypsin can also convert angiotensin I to angiotensin II (Owen and Campbell, 1998). The decreased levels of α1 antichymotrypsin in hepatic scarring will decrease the inhibition of chymotrypsin. As a result, there is an increased conversion of angiotensin I to angiotensin II. The increased levels of angiotensin II would activate HSC to stimulate ECM synthesis (Bataller and Brenner, 2005).

The gel spot containing this change in α1 antichymotrypsin also contained another protein, transcortin, identified with a lower Mascot score from only one peptide. It is therefore likely that the change observed in this spot intensity was due to α1 antichymotrypsin rather than transcortin, as transcortin appears to bear no relationship to hepatic scarring.

2.3.9 Haptoglobin decreases with fibrosis stage

Haptoglobin is a tetrameric protein composed of two α-chains and two β-chains. Expression levels of both chains were found to decrease with increasing hepatic scarring (Figure 14). The main role of haptoglobin is to bind to free plasma oxyhaemoglobin, preventing loss of iron through the kidneys. This protects the kidneys from damage by haemoglobin and makes the haemoglobin accessible for degradation by enzymes. The free haemoglobin comes from haemolysis, the lysis of red blood cells (RBC). Therefore haptoglobin levels can be measured to assess the rate of RBC destruction. Haptoglobin is synthesised in

the liver and the observed decrease in synthesis as fibrosis increases may be due to compromised hepatic function. Studies have also shown that HGF, expression of which is elevated in fibrosis, can decrease haptoglobin synthesis (Guillen *et al.*, 1996; Imbert-Bismut *et al.*, 2001). The mechanism by which HGF decreases haptoglobin synthesis is unknown.

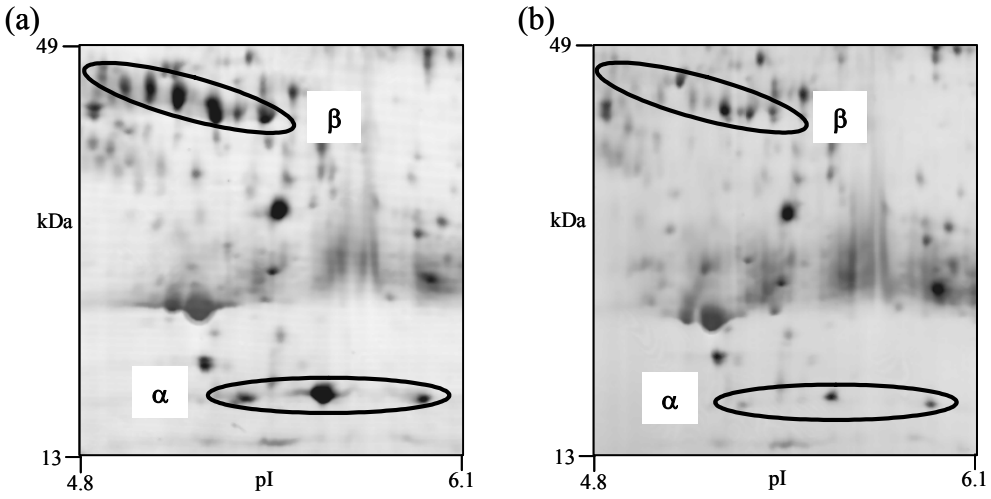

Figure 14 Haptoglobin decreases with increased hepatic scarring
Zoomed images of representative gels displaying the decrease in both chains of the acute phase glycoprotein. (a) control serum, and (b) cirrhosis serum.
α and β denote the α- and β-chains of haptoglobin, respectively.

The haptoglobin precursor consists of 406 aa. The α-chain spans aa 19 to 160 (theoretical molecular weight = 16 kDa, pI 5.6 with no *N*-glycosylation sites). In the low molecular weight region of the 2D-PAGE gels, haptoglobin spots observed at 13-17 kDa, pI 5.5-6.0 were found to be decreased in fibrosis with peptides spanning the region for the α-chain (Figure 15a). The observed molecular weight and pI range are consistent with the theoretical values for the α-

chain. The β-chain spans aa 162 to 406 (theoretical molecular weight = 27 kDa, pI 6.3 with four *N*-glycosylation sites at 184, 207, 211 and 241). Haptoglobin spots at 40-44 kDa, pI 4.8-6.0 were decreased with increasing fibrosis stage and had peptides spanning the range for the β-chain (Figure 15b). Glycosylation of the β-chain would account for the higher molecular weight and lower pI observed on the gel.

MSALGAVIAL LLWGQLFAVD SGNDVTDIAD DGCPKPPEIA HGYVEHSVRY QCKNYYKLRT EGDGVYTLND KKQWINKAVG
DKLPECEADD GCPKPPEIAH GYVEHSVRYQ CKNYYKLRTE GDGVYTLNNE KQWINKAVGD KLPECEAVCG KPKNPANPVQ
RILGGHLDAK GSFPWQAKMV SHHNLTTGAT LINEQWLLTT AKNLFLNHSE NATAKDIAPT LTLYVGKKQL VEIEKVVLHP
NYSQVDIGLI KLKQKVSVNE RVMPICLPSK DYAEVGRVGY VSGWGRNANF KFTDHLKYVM LPVADQDQCI RHYEGSTVPE
KKTPKSPVGV QPILNEHTFC AGMSKYQEDT CYGDAGSAFA VHDLEEDTWY ATGILSFDKS CAVAEYGVYV KVTSIQDWVQ
KTIAEN

Figure 15 The α- and β-chains of haptoglobin. The full length sequence of the haptoglobin precursor is shown with identified peptides underlined for the haptoglobin spots seen at 13 - 17 kDa (red) and 40 - 44 kDa (green). The α- and β-chains are shaded in blue and yellow, respectively. Potential *N*-glycosylation sites are shaded in pink.

In healthy individuals the 2D-PAGE gels show haptoglobin in high abundance as required to ensure that all free haemoglobin is bound. After haptoglobin binds to haemoglobin, the complex is taken to the liver for removal, where it is separated into iron, haem and amino acids; these components are recycled in the liver. This process destroys haptoglobin but a normal functioning liver continues to synthesise new haptoglobin and maintains levels in the circulation. When this balance is disrupted, RBC destruction increases and destruction of haptoglobin outpaces the rate of haptoglobin synthesis resulting in a decrease of the glycoprotein. This is seen not only in liver fibrosis but also in anaemia.

Levels of haemoglobin were found to be elevated in both mild fibrosis and cirrhosis compared to healthy controls. This observation is consistent with the observed decrease in haptoglobin expression. Haemoglobin only appears in serum in haemolysis. Haemoglobin may have also increased in moderate fibrosis but due to the fewer number of gels, the change was not considered to be statistically significant.

2.3.10 Perturbations in lipid metabolism leads to liver fibrosis

HCV core protein in infected hepatocytes causes disorder in lipid metabolism leading to steatosis and ultimately liver fibrosis (Schuppan *et al.*, 2003; Moriya *et al.*, 1997; Tilg and Diehl, 2000; see Section 2.1.6). 2D-PAGE analysis revealed that a few proteins associated with lipid metabolism were found to be differentially expressed in hepatic scarring.

2.3.10.1 Decreased hepatocyte uptake of chylomicrons and lipoproteins may elevate β2 glycoprotein

β2 glycoprotein I (β2GPI; also know as Activated protein C-binding protein) was found to be elevated in the serum samples from cirrhotic patients (Figures 16a and b). This change was observed adjacent to the highly abundant protein, albumin and so control serum was depleted of albumin and three other highly abundant proteins (transferrin, haptoglobin and IgG) using an immunoprecipitation technique (method not described). This improved the representation of features in this region, helping to confirm the apparent absence

of β2GPI in healthy contol serum (Figure 16c). β2GPI was observed at 58 kDa, pI 5.9. The theoretical values for this protein are 38 kDa and pI 8.3. However, the discrepancy is likely to be a consequence of the post-translational modifications of the protein; β2GPI has five glycosylation sites (*O*-linked at aa 149 and *N*-linked at aa 162, 183, 193 and 253), which would explain the larger and more acidic feature observed by 2D-PAGE. β2GPI is associated with chylomicrons and high-density lipoproteins, both of which are targeted to hepatocytes for uptake in normal lipid metabolism (Willems *et al.*, 1996).

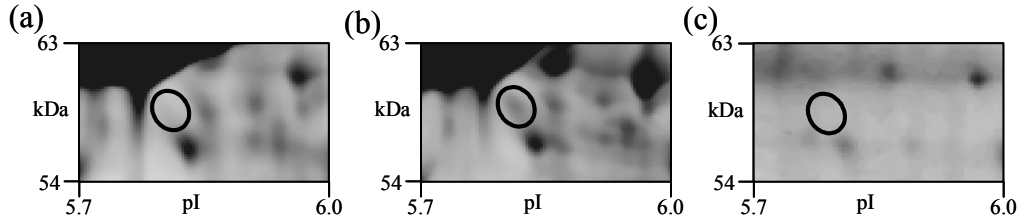

Figure 16 β2 glycoprotein increases in cirrhosis. Close up images of the region of gel where the glycoprotein was found to be increased in cirrhosis and appeared to be absent in healthy controls. (a) control serum, (b) cirrhosis serum, (c) control serum depleted of high abundance proteins.

In the normal liver, endothelial cells lining the sinusoids perform filtration functions due to the presence of small fenestrations that allow free diffusion of many substances between the blood and the hepatocyte surface (Kmiec, 2001). This "liver sieve" filters macromolecules of various sizes, allowing lipoproteins and cholesterol/retinol-rich chylomicron remnants to pass through and enter the space of Disse but preventing large parent chylomicrons (Fraser *et al.*, 1995; Le

Couteur *et al.*, 2002). In liver fibrosis, the porosity of the sieve is altered. The deposition of scar matrix widens the space of Disse resulting in the loss of endothelial fenestrations (Figure 3). This may affect the metabolism of lipoproteins, cholesterol and retinol. As β2GPI synthesis is increased in cirrhotic patients, it is possible that there is decreased entry of chylomicrons and lipoproteins into the space of Disse and uptake of these components into hepatocytes. This would result in an increase of β2GPI-bound chylomicrons and lipoproteins in the sinusoids which would ultimately be observed in the circulation. To our knowledge this is the first hypothesis to suggest that elevated levels of β2GPI may be related to fibrosis.

It is also likely that β2GPI/Activated protein C-binding protein is associated with the liver inflammation that usually accompanies cirrhosis. Activated protein C mediates anti-inflammatory properties and also up-regulates MMPs in skin to enhance wound healing (Jackson *et al.*, 2005). Therefore levels of the liver secreted β2GPI may be elevated in cirrhosis in a proportionate manner to its associated Activated protein C in the wound healing process and in an attempt to decrease liver inflammation.

Interestingly, β2GPI has already been shown to have an association with HBV infection. The glycoprotein can bind to hepatitis B surface antigen (HBsAg) and this association has been proposed as a way in which the HBV virus may attach and enter hepatocytes (Mehdi *et al.*, 1994). There does not appear to be any strong associations between β2GPI and HCV. β2GPI is also known as anticardiolipin cofactor and anticardiolipin antibodies have been shown to be elevated in HCV

infected patients. However, this study also showed that antibodies for its cofactor, β2GPI, are absent in HCV (Leroy *et al.*, 1998). The presence of anticardiolipin antibodies in HCV infected subjects has yet to be shown.

2.3.10.2 Apolipoprotein L1 is absent in hepatic cirrhosis

Apolipoprotein L1 (Apo L1) was present in the serum samples of healthy controls and the intermediate stages of fibrosis but appeared to be absent in cirrhotic patients (Figure 17). This protein was resolved at 34 kDa, pI 6.1 yet the theoretical values are 44 kDa and pI 5.8 suggesting that the protein was cleaved.

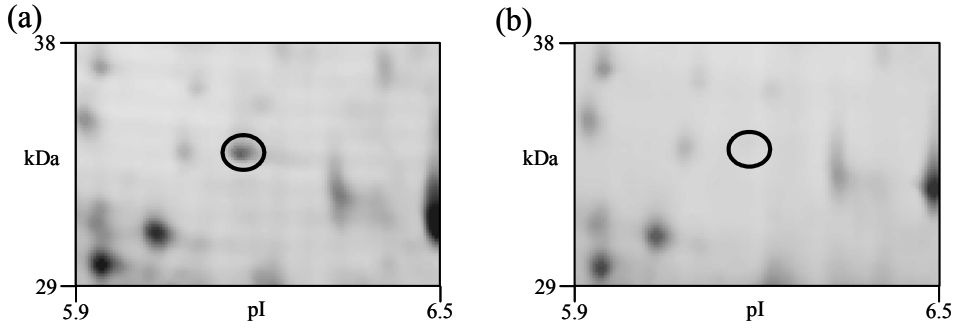

Figure 17 Apolipoprotein L1 appears to be absent in cirrhosis. Magnified regions of representative gels highlighting the relative position of the lipoprotein in (a) control serum, and (b) cirrhosis serum

There is limited data on this protein and to date there are no studies showing the relationship between Apo L1 and any form of scarring or hepatitis. The apolipoprotein L family was discovered using 2D-PAGE analysis of purified plasma and was later found to be secreted from various organs including the liver

(Duchateau *et al.*, 1997; Duchateau *et al.*, 2001). Apo L1 has been shown to be associated with high-density lipoproteins (HDL) that carry cholesterol in the circulation. The precise function of the apolipoprotein L family is uncertain and there is no homology with any other known protein. The apolipoprotein L family consists of six different proteins (Apo L1-VI) (Page *et al.*, 2001) and positively correlates with plasma triglyceride and cholesterol levels in normal individuals as well as in patients with aberrant lipid metabolism (e.g. hypertriglyceridemia, hypercholesterolemia) (Duchateau *et al.*, 2000). The liver is the most active site for cholesterol metabolism, therefore hepatic disease can lead to hypocholesterolemia, which has been described in viral mediated liver cirrhosis (D'Arienzo *et al.*, 1998). Hypocholesterolemia in hepatic cirrhosis would suggest a decrease in the apolipoprotein L family, consistent with the results described herein showing that Apo L1 levels are higher in serum from healthy controls compared with liver cirrhosis patients. HCV-induced aberrant lipid metabolism may be related to the apparent absence of Apo L1 in cirrhotic patients. This is the first time that Apo L1 has been described in any form of hepatic disease.

Other apolipoproteins may also be associated with liver scarring and Apo A1 has already been established in the hepatic FibroTest assay (Imbert-Bismut *et al.*, 2001). In a similar way to Apo L1, serum levels of Apo A1 decrease with increasing hepatic fibrosis. Studies have shown that Apo A1 mRNA in hepatocytes is down-regulated due to its interaction with the glycoprotein fibronectin, a major component of the ECM (Paradis *et al.*, 1996a). If Apo L1 is

associated with ECM components in a similar manner, this may provide a mechanism for how this apolipoprotein decreases with hepatic scarring.

HCV core has been shown to bind to apolipoprotein A2 (Apo A2) which may be related to the lipid metabolism disorder associated with this virally-mediated hepatic fibrosis (Sabile *et al.*, 1999). If Apo L1 also has the ability to associate with HCV core, this may explain the perturbations seen in lipid metabolism.

2.3.10.3 Paraoxonase/arylesterase 1 and possibly zinc-α2-glycoprotein decrease in cirrhosis

A 2D-PAGE gel spot at 44 kDa, pI 4.8 was higher in expression in serum from healthy controls compared with serum from cirrhotic patients (Figure 18). Three different proteins were identified in this spot (in descending order of Mascot score): Haptoglobin (see Section 2.3.9), Paraoxonase/arylesterase 1 (PON1) and Zinc-α2-glycoprotein (ZAG).

PON1 has a theoretical molecular weight of 40 kDa and pI 5.1. It has four potential *N*-glycosylation sites (at aa 226, 252, 296 and 323) which may account for the slightly higher molecular weight and lower pI observed on the gel. The decrease in expression of PON1 has long been known in cirrhosis and HCC (Lorentz *et al.*, 1979; Kawai *et al.*, 1991). The substrate for this enzyme is unknown but it is thought to degrade oxidised lipids in lipoproteins and cells and therefore may play an important role in the antioxidant systems within the liver (Aviram and Rosenblat, 2004). The activity of this enzyme has been shown to be reduced in chemically induced liver cirrhosis in rats and is inversely associated

with lipid peroxidation (Ferre *et al.*, 2001). However, 2D-PAGE based proteomics of rat serum has revealed that PON1 is also decreased in paracetamol induced hepatic injury (Amacher *et al.*, 2005) and therefore is not specific to liver scarring from lipid peroxidation.

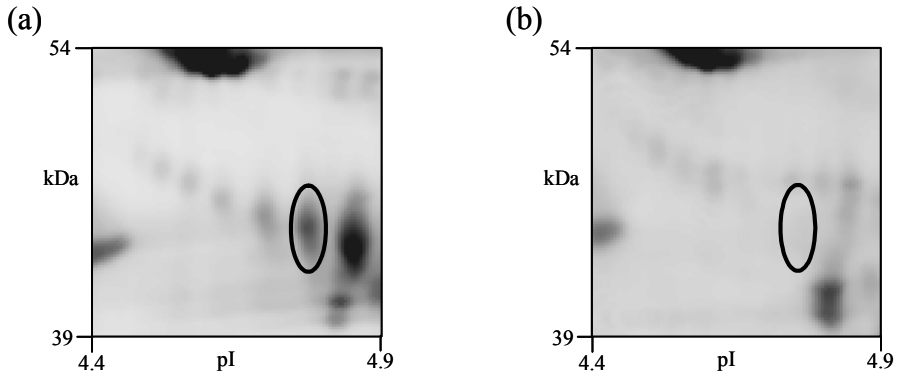

Figure 18 Differentially expressed feature identified containing ZAG, PON1 and haptoglobin. Representative magnified images showing the region of gel where the differentially expressed feature was found for (a) control serum, and (b) cirrhosis serum

ZAG has a theoretical molecular weight of 34 kDa and pI 5.6 but has three potential *N*-glycosylation sites (at aa 109, 125 and 256), occupation of these sites would account for the higher molecular weight and lower pI observed on the 2D-PAGE gel. There are no reports of ZAG being associated with liver scarring. However, there is evidence to show that this glycoprotein can bind to the F protein encoded by the open reading frame overlapping the core gene in the HCV genome (Huang *et al.*, 2005). Antibodies to this F protein have been found in HCV patients indicating that it is important in HCV infection but its function in the

virus life cycle remains unknown (Roussel *et al.*, 2003). The reason for a decrease in ZAG in hepatic cirrhosis is unclear but binding of this glycoprotein to the F protein within the infected liver may decrease its secretion into the circulation. Therefore such a decrease may be more likely to be associated with viral load rather than architectural hepatic damage from ECM accumulation.

The main function of ZAG is to stimulate lipolysis in adipocytes that can lead to fat losses associated with some cancers. For example, serum ZAG has been found to be elevated in prostate cancer (Hale *et al.*, 2001) but to our knowledge there is no reported association with HCC. The apparently decreased levels of ZAG in cirrhosis may therefore affect lipid metabolism in the liver.

This change in ZAG was observed in a single spot which also contained haptoglobin and Paraoxonase/arylesterase 1, both of which had greater protein scores than ZAG from the Mascot search. Therefore it is more likely that this change is due to haptoglobin and/or Paraoxonase/arylesterase 1 rather than ZAG. However, the possibility of ZAG being differentially expressed cannot be ruled out and requires further validation. Comunale *et al.*, 2004 have shown that ZAG can be better represented by de-*N*-glycosylating the serum sample prior to 2D-PAGE which results in ZAG being represented in a less crowded area of the gel thereby decreasing the possibility of multiple proteins in a single spot. This would affect all glycoproteins in serum and may help to simplify 2D-PAGE analysis by decreasing spot numbers.

2.3.11 Hypergammaglobulinemia in liver disease

An increase in serum immunoglobulins (hypergammaglobulinemia) is common in liver disease and has been observed, particularly for IgG and IgA, in both alcohol and HCV-mediated liver disease but it is not necessarily associated with hepatic fibrosis (Gonzalez-Quintela *et al.*, 2003a). Here, increased expression of IgG heavy constant chain and Ig κ/λ chain regions was observed with increasing fibrosis stage. Due to the high abundance of IgG, it was difficult to determine changes in its expression by computer aided spot volume analysis. Techniques such as nephelometry (Lotfy *et al.*, 2006) could be used to measure these changes.

Levels of the IgA heavy chain were also found to be elevated in serum samples from cirrhotic patients compared with those from healthy controls. This increase was not observed in the intermediate stages of fibrosis, an observation that is consistent with previous reports of IgA increasing usually only in liver cirrhosis (Gonzalez-Quintela *et al.*, 2003b). In this case of hepatic cirrhosis, IgA increase is due to increased production and decreased clearance and the resulting high levels of IgA can form deposits in the kidneys leading to nephropathy. Earlier studies have shown that IgA can also form deposits in the hepatic sinusoids and that IgA can trigger TNFα secretion, which has been shown to activate HSCs leading to fibrotic scarring (Deviere *et al.*, 1991). However, since IgA levels can increase in hepatic disease in the absence of liver scarring, this immunoglobulin is unreliable for assessing fibrosis. In the differential analysis, the change in IgA was found in a single spot which also contained a2M and albumin, both of which had higher protein scores than IgA from the Mascot database search. Although it is more

likely that this change is due to a2M and albumin rather than IgA, significance of this increase in IgA cannot be ruled out.

2.3.12 Compromised synthetic function decreases complement synthesis

Both liver synthesised complement C3 and C4 were decreased in the serum samples of patients with moderate fibrosis and cirrhosis compared with healthy controls (Figure 19). Complement C3 and C4 are large proteins with molecular weights of 188 kDa (1663 aa precursor) and 200 kDa (1744 aa precursor), respectively. These proteins work with (i.e. complement) antibody activity to eliminate pathogens and stimulate inflammation (Law and Dodds, 1997).

C3 is composed of a 75 kDa β-chain linked via an interchain disulphide bond to a 113 kDa α-chain. The α-chain of C3 is cleaved and activated by the protease C3 convertase (C4b2a) to form a small 9 kDa fragment, C3a, and the remaining 179 kDa cleaved α-chain and β-chain, C3b (Figure 20). The α-chain of C3b can then be cleaved further by other protease factors (Law and Dodds, 1997). The differentially expressed C3 fragment was found at approximately 45 kDa, pI 6.9 on the 2D-PAGE gel of healthy control serum. All peptides identified from this spot were from aa 722 to 1001 (data not shown). These peptides correspond to the α-chain of C3 (aa 672-1663) and span both the C3a (aa 672-748) and C3b (aa 749-1663) sequences suggesting that the protein is not proteolytically cleaved by C3 convertase. There is evidence showing that plasmin cleaves the α-chain at a thiolester site (Lachmann *et al.*, 1982) which would result in a fragment

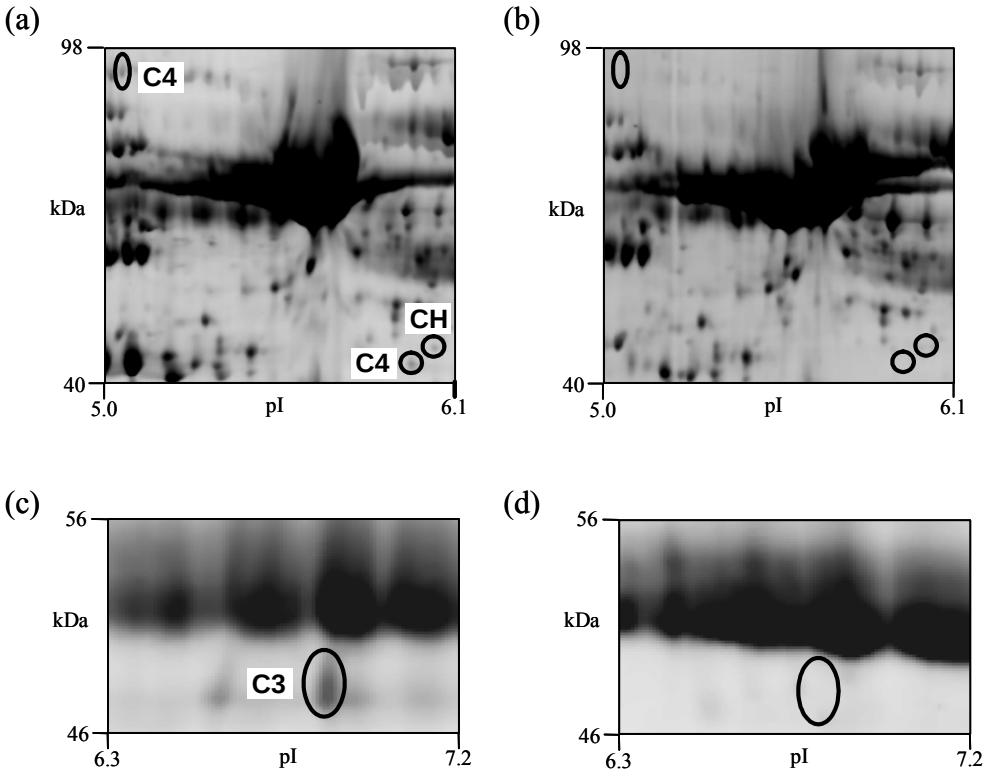

Figure 19 Hepatic synthesis of complement proteins decreases with hepatic scarring. Close up representative gel images showing the region where complement proteins were found to be differentially expressed.
C3 = complement C3, C4 = complement C4; CH = Complement factor H
(a) and (c) control serum, (b) cirrhosis serum, (d) moderate fibrosis serum

of approximately 39 kDa and pI 7. This fragment is of similar pI to the observed protein spot (49 kDa, pI 6.9) and all the peptides identified within this spot span this 39 kDa region of the α-chain. Complement C3 has a potential *N*-glycosylation site at aa 939 which may account for the slightly higher observed molecular weight. Since this fragment was decreased in expression in moderate fibrosis, it may indicate that there is less plasmin-mediated cleavage of the

Complement C3 α-chain. This is consistent with hepatic scarring since decreased plasmin activity would decrease MMP activation and therefore lead to ECM accumulation (see Section 2.1.2).

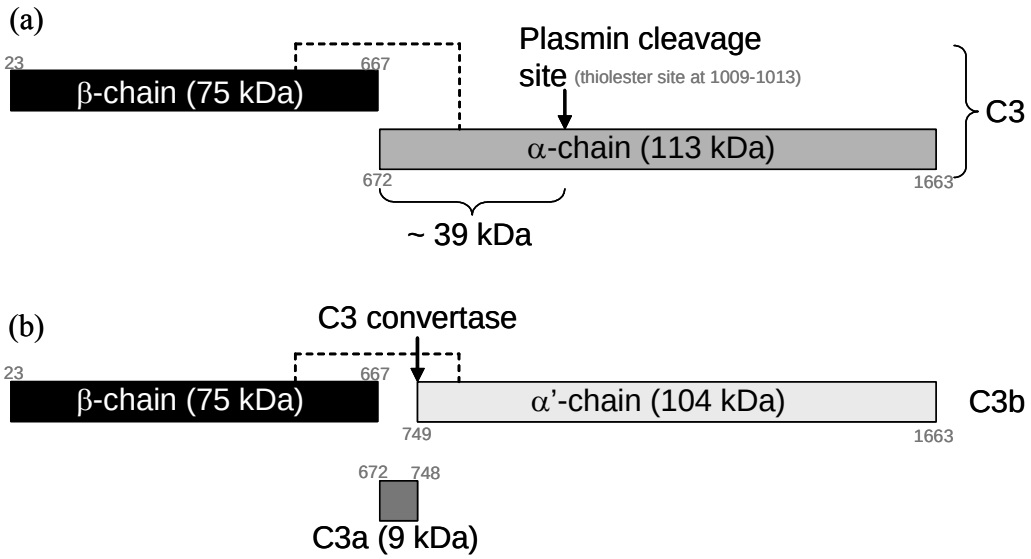

Figure 20 Structure of Complement C3 and its activation products.
(a) The uncleaved structure of C3. The 75 kDa β-chain is attached to the 113 kDa α-chain via one of the interchain disulphide bonds indicated by the dotted line. Plasmin has been shown to cleave the α-chain at a thiolester site approximately 39 kDa from its N-terminal end. Peptides identified for C3 spanned this region. This fragment was decreased in expression in serum samples from moderate fibrosis patients suggesting decreased plasmin mediated cleavage of C3.
(b) C3 is activated by the protease C3 convertase which cleaves the α-chain to form the 9 kDa C3a and 179 kDa C3b proteins. The peptides identified for the differentially expressed C3 spot spanned both the sequence of C3a and C3b suggesting that the α-chain was not cleaved by C3 convertase.
The numbers in grey indicate the amino acid position from the precursor.
Figure adapted from Law and Dodds, 1997.

C4 comprises a 75 kDa β-chain linked via an interchain disulphide bond to a 95 kDa α-chain which is linked via two interchain disulphide bonds to a 30 kDa γ-chain. The α-chain of C4 can be cleaved and activated by the protease C1s to form a 9 kDa fragment, C4a, and a 191 kDa protein, C4b (Figure 21). As with C3b, the α-chain of C4b can then be cleaved further by other protease factors (Law and Dodds, 1997). Differentially expressed C4 fragments were found at approximately 41 kDa, pI 6.0 and 92 kDa, pI 5.1 on 2D-PAGE gels of healthy control serum. Peptides identified for both of these spots were from the α-chain of C4 (data not shown). The α-chain of C4 is 95 kDa (aa 680-1446) with a charge of approximately pI 5 (Law and Dodds, 1997) which is consistent with the position observed for the higher molecular weight spot. The lower molecular weight spot is a fragment of the C4 α-chain.

Decreased levels of C3 and C4 have already been described in hepatic cirrhosis especially when related to alcohol intake (Calamita and Burini, 1995). Cirrhotic hepatic architectural damage compromises the liver's ability to synthesise these complement components resulting in reduced levels secreted into the circulation predisposing the individual to infection (Homann *et al.*, 1997). However, fragments of complement components do decrease in other cases of liver damage and are not specific to hepatic scarring, e.g. a decrease in C3 is seen in HBV-induced hepatitis and HCC but this observation is not always consistent (Steel *et al.*, 2003a).

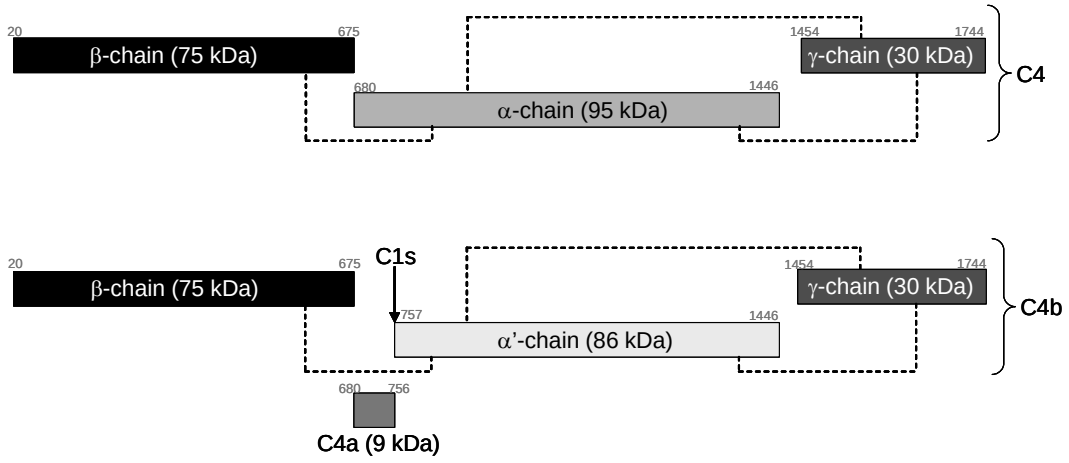

Figure 21 Structure of Complement C4 and its activation products.
(a) The uncleaved structure of C4. The 75 kDa β-chain is attached to the 95 kDa α-chain via an interchain disulphide bond indicated by the dotted line. This α-chain is attached to a 30 kDa γ-chain via two interchain disulphide bonds. Spots of C4 at 41 and 92 kDa were found to decrease in expression in serum samples from moderate fibrosis and cirrhosis patients. Peptides identified for both spots were from the α-chain. The higher molecular weight spot was consistent with the full length α-chain and the lower molecular weight spot was a fragment.
(b) C4 is activated by the protease C1s which cleaves the α-chain to form C4a (9 kDa) and C4b (191 kDa).
The numbers in grey indicate the amino acid position from the precursor.
Figure adapted from Law and Dodds, 1997.

Complement factor H-related protein 1 was found to decrease in the serum samples of patients with both mild fibrosis and cirrhosis compared with healthy controls (Figure 19). The same decrease was not detected by the image analysis software for moderate fibrosis, possibly due to the fewer samples analysed for this fibrosis stage and therefore was not considered to be statistically significant. This complement factor H-related protein has never been described in hepatic fibrosis or other liver diseases. There are a family of factor H-related proteins and they are

thought to associate with lipoproteins and may play a role in lipid metabolism (Skerka *et al.*, 1997). Therefore this protein may also disrupt lipid metabolism leading to hepatic scarring.

2.3.13 Albumin and prealbumin decrease with liver scarring

In a similar way to the complement components, the most abundant protein in serum, albumin, is also decreased in expression due to compromise in hepatic synthetic function (see Section 2.1.7). Spot peak intensity analysis for the main isoform of albumin revealed a general decrease in the serum samples from cirrhotic patients compared with healthy controls. However, spot volume analysis of the main isoform of albumin is unreliable due to its irregular shape and in many cases albumin is unable to successfully focus by IEF due to its high abundance and leaves a horizontal streak across the 2D-PAGE gel.

Prealbumin (transthyretin), observed at 32 kDa, was decreased in the serum of cirrhotic patients (Figure 22). This protein binds albumin and also acts as a carrier of vitamin A through association with retinol binding protein (RBP) (Filteau *et al.*, 2000). HSCs lose their ability to store vitamin A upon activation. The RBP-prealbumin complex may bind to this released vitamin A in the liver without being secreted into the circulation which may explain the decrease in prealbumin. If this were the case, RBP would decrease with fibrosis. RBP was located on the 2D-PAGE serum gels by coregistering with the online ExPASy 2D-PAGE serum database and confirming the spot identification by mass spectrometry. Analysis of the RBP spot by eye appeared to show a slight decrease in the serum from

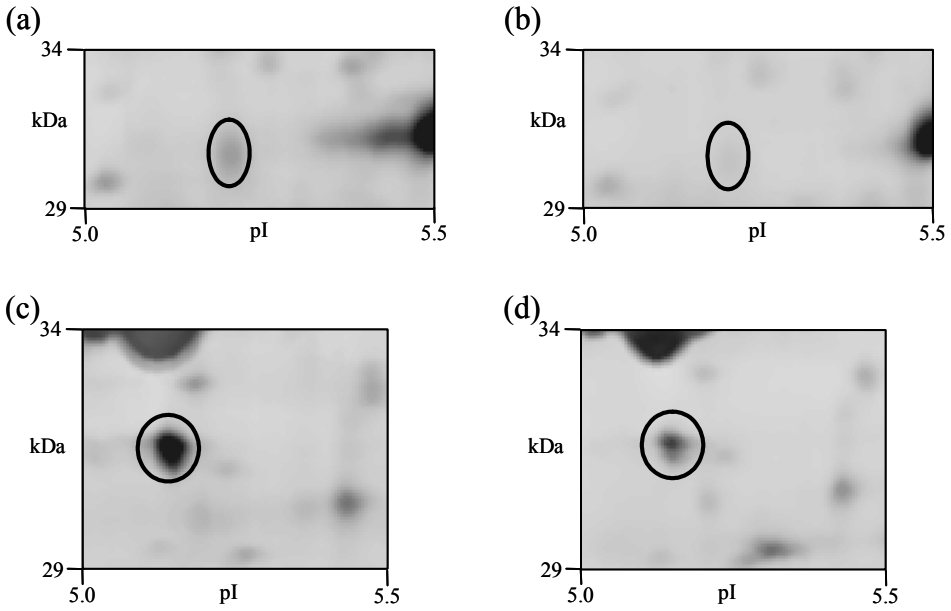

Figure 22 Prealbumin and possibly retinol binding protein (RBP) decrease in cirrhosis. Prealbumin was found to decrease in serum samples from cirrhotic patients by more than 2-fold. RBP, the binding partner of transthyretin, also appears to decrease in cirrhosis although by less than 2-fold. (a) Prealbumin in serum from controls, (b) Prealbumin in serum from cirrhosis patients, (c) RBP in serum from controls, and (d) RBP in serum from cirrhosis patients. Zoomed images of representative gels are shown for the region where these vitamin A-related proteins were found to be differentially expressed.

cirrhotic patients but was not different by more than 2-fold based on image analysis and therefore was not considered to be significant (Figure 22). However a greater than 2-fold change was observed for both prealbumin and RBP when analysing serum from another set of HCV-infected serum samples (data not shown). Others have also shown this decrease in prealbumin for cirrhotic patients and believe the reduction is due to poor nutritional status (Yovita *et al.*, 2004). However, earlier studies indicated that serum levels of RBP, vitamin A and prealbumin decrease in patients with liver cirrhosis and RBP increases in HSCs

suggesting that vitamin A deficiency is a consequence of its defective mobilisation from the liver (Nyberg *et al.*, 1988). As with albumin, prealbumin is a liver synthesised protein and therefore decreased levels in cirrhosis may also be a consequence of hepatic damage. In fibrosis, Kupffer cells secrete TNFα which activates HSCs (Section 2.1.11) and this cytokine has been shown to inhibit prealbumin synthesis and therefore decrease levels in serum (Reichel *et al.*, 2000). It is possible that prealbumin decreases due to a combination of the factors described and therefore may not accurately reflect hepatic scarring. Prealbumin also usually runs as a train of spots at 13 kDa but this region was close to the dye front of the gel and therefore it was difficult to perform reliable image analysis on these spots.

2.3.14 In-solution isoelectric focusing of serum prior to SDS-PAGE

High molecular weight proteins are poorly resolved by 2D-PAGE since they have difficulty in entering the second dimension gel matrix from the IEF strip (Oh-Ishi and Maeda, 2002). SDS-PAGE overcomes these issues with large proteins but is generally of lower resolution. In-solution pH fractionation of serum samples prior to SDS-PAGE therefore provides an option for increasing the visualisation of high molecular weight proteins.

Basic proteins are also poorly represented by 2D-PAGE due to their reduced solubility. The reducing agent, DTT, becomes negatively charged during IEF and migrates towards the anode thereby decreasing the concentration of DTT in the basic end of the strip. These unreduced basic proteins have decreased solubility

resulting in streaking in this region of the 2D-PAGE gel (Gorg *et al.*, 1995). To reduce these streaking effects in 2D-PAGE an additional reducing agent, TBP, which does not become charged during IEF, was used. Others have also improved the representation of features in the basic region by applying an extra wick soaked in 20 mM DTT at the cathodic end of the IPG strips (Gorg *et al.*, 1995). These approaches do not decrease spot streaking completely and it therefore remains a problem. These issues with basic proteins are not encountered with SDS-PAGE and a higher resolution analysis was achieved by fractionating the samples by pH prior to SDS-PAGE.

Serum samples from both healthy individuals and cirrhotic patients were separated in-solution into five different pH ranges (pH 3-4.6; pH 4.6-5.4; pH 5.4-6.2; pH 6.2-7; pH 7-10) using an IEF fractionator followed by SDS-PAGE analysis. The band profile seen by SDS-PAGE resembled that of a pH 3-10 2D-PAGE gel since these fractions also ranged from pH 3 to 10 (Figure 23a). SDS-PAGE analysis of unfractionated control and cirrhotic serum appeared to show no difference in differential band analysis due to the low resolution separation of this technique. However, by combining the in-solution IEF method with the SDS-PAGE approach, the proteins were separated to the extent that differences could be observed (Figure 23b). As with 2D-PAGE analysis, the following changes were observed in cirrhotic serum with respect to healthy control serum: a decrease in both α- and β-chains of haptoglobin, an increase in a2M, and an increase in IgG (both heavy and light chains). In addition to these proteins, changes were also observed in the high molecular weight basic fraction (pH 7-10). These changes

were not observed by 2D-PAGE analysis due to the issues with large proteins entering the polyacrylamide gel matrix and reduced solubility of basic proteins, demonstrating a major advantage of the combined in-solution IEF and SDS-PAGE approach over solely gel-based technologies.

Consistent with the 2D-PAGE results, other fragments of complement C3 and C4 were found to be higher in the serum of controls than cirrhotic patients. The differentially expressed band at approximately 75 kDa on the gel contained aa 22-512 of C4 and aa 291-530 of C3, which in both cases span their β-chains (aa 20-675 for C4 and aa 23-667 for C3). The theoretical pI of the β-chain for C4 is 8.7 which is consistent with the pH 7-10 range for this fraction. The theoretical pI of the β-chain for C3 is 6.8 which is marginally outside the range of this fraction but this was expected since in-house studies have shown that the IEF fractionator enriches proteins rather than providing a clear-cut fractionation for the pH range (data not shown). This is not an issue provided that proteins are enriched reproducibly. The differentially expressed band immediately below the 75 kDa also contained sequences within the β-chains of both C3 and C4 but these were clearly fragments since the band was at a lower molecular weight. Also consistent with the 2D-PAGE results, IgG fragments were found to be elevated in the serum from cirrhotic patients compared to healthy controls.

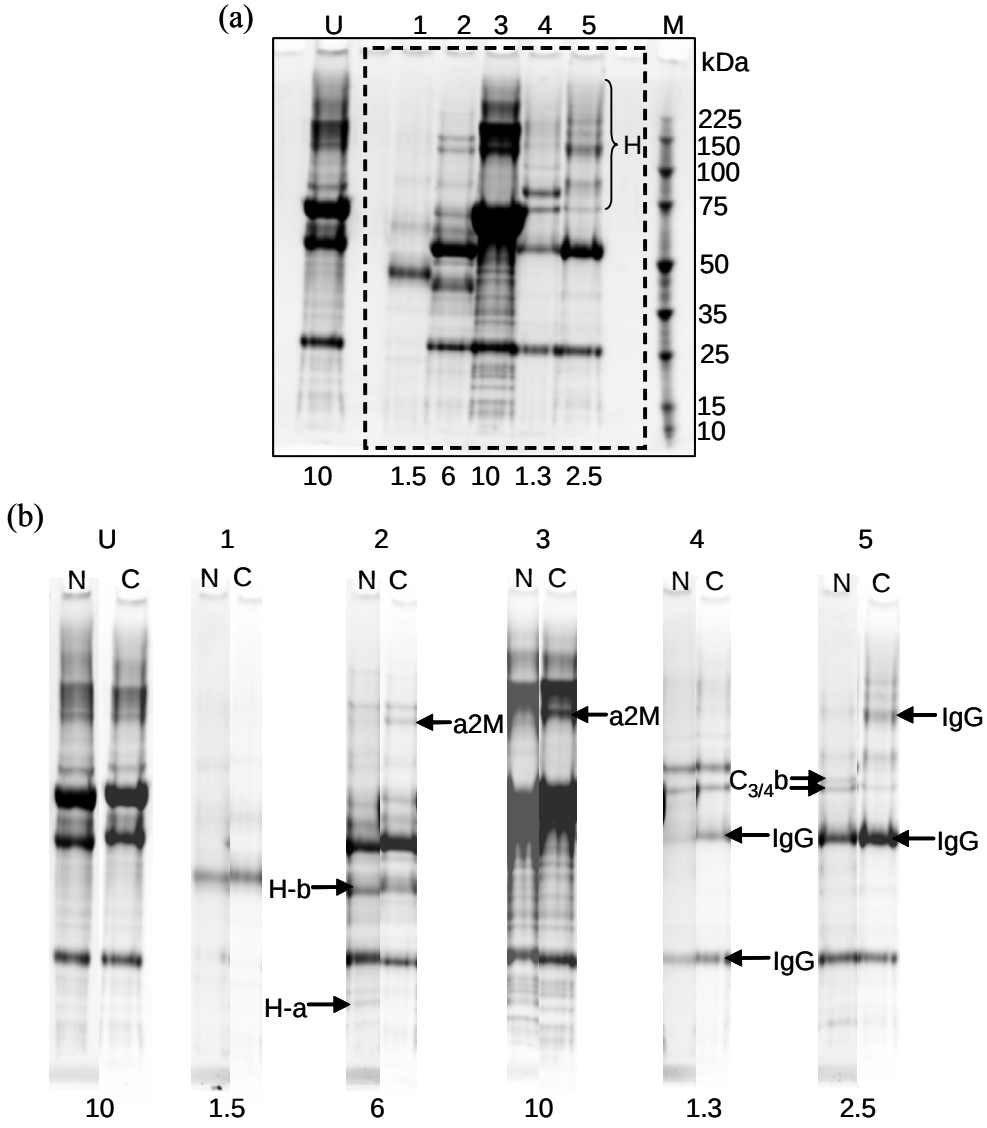

Figure 23 In-solution IEF combined with SDS-PAGE allows improved representation of high molecular weight basic proteins

Normal controls (N) and cirrhotic (C) serum samples were fractionated by in-solution IEF. The resulting five fractions from the IEF fractionator were then separated by 4-12% (w/v) SDS-PAGE alongside unfractionated serum.

(a) A typical profile observed for human serum. The dashed box region indicates the serum profile that is comparable to a pH 3-10 2D-PAGE gel.

H = high molecular weight basic proteins that are not as well represented by 2D-PAGE. (b) Differential analysis of the SDS-PAGE lanes comparing controls with cirrhotic serum for each of the fractions.

U = Unfractionated serum; 1 = pH 3-4.6; 2 = pH 4.6-5.4; 3 = pH 5.4-6.2; 4 = pH 6.2-7; 5 = pH 7-10; M = Molecular weight markers

H-b = Haptoglobin β-chain; H-a = Haptoglobin α-chain; a2M = α2 macroglobin; C3/4b = β-chains of complement C3 and C4

The values shown below each fraction indicate the total protein amounts, in μg, loaded in each lane.

2.4 Conclusion

HCV infection is one of the leading causes of hepatic fibrosis, a wound healing response observed in chronic liver disease, which can progress to liver cirrhosis if left untreated. There is an urgent need for reliable diagnosis of the early stages of fibrosis so that anti-fibrotic approaches could be applied to prevent scarring progression. Liver biopsy is currently the gold-standard tool for diagnosing and assessing hepatic fibrosis. However, as the technique has several well-documented disadvantages there is a requirement for a reliable, less invasive, serological diagnostic tool. Although some non-invasive diagnostic methods have been proposed, all appear to be unreliable to some extent.

Proteomics is a useful technique for elucidating serological biomarkers for disease and has been used successfully in some cases. Here, 2D-PAGE based proteomics has been used to identify serum markers for HCV-induced liver fibrosis. Serum from patients with varying stages of hepatic scarring (mild fibrosis, moderate fibrosis, and cirrhosis) were compared with normal healthy controls. Comparison of serum samples from cirrhotic patients with healthy controls revealed the most significant changes. The expression of inter-α-trypsin inhibitor heavy chain H4 fragments, α1 antichymotrypsin, Apo L1, prealbumin and albumin was decreased in cirrhotic serum, whereas CD5L and β2GPI increased. In general, a2M and immunoglobulin components increased with hepatic fibrosis whereas haptoglobin and complement components (C3, C4 and factor H-related protein 1) decreased.

Some of the identified proteins share similar function and can be grouped into categories related to hepatic scarring (Table 5). The inter-relationship between the proteins identified from the differential analysis of serum with the already established pathways for ECM synthesis and degradation is shown in Figure 24. Some of the changes identified are not specific to fibrosis and have been observed in other diseased states, e.g. the acute phase proteins, a2M and haptoglobin, change in exactly the same way in sickle cell anaemia (Bourantas *et al.*, 1998). Some patients with this disease are hypocholesterolemic (Rahimi *et al.*, 2006), which suggests that Apo L1 may also decrease. Also CD5L may correlate with viral infection rather than hepatic scarring. The proteins decreased due to compromise in hepatic synthetic function also decrease due to diseases or factors affecting the liver, e.g. complement components decrease due to hepatotoxic drugs (LeVier *et al.*, 1994) and albumin decreases in glomerulonephritis, extensive burns, ascites, malnutrition and malabsorption (Limdi and Hyde, 2003). RBP and prealbumin appear to have a significant link with fibrosis but since dietary factors can also affect these proteins, they may not be suitable as fibrosis biomarkers. However, some of the proteins identified from the differential analysis, or preferably a combination of proteins, may be useful as a biomarker in assessing hepatic fibrosis. The most promising novel candidates are β2GPI, the thiolester cleaved products of a2M and the fragments of inter-α-trypsin inhibitor heavy chain H4. These candidates have a close association with fibrosis and have not been reported to display similar expression changes in other diseased states. The reliability of these proteins as biomarkers for fibrosis can be validated by

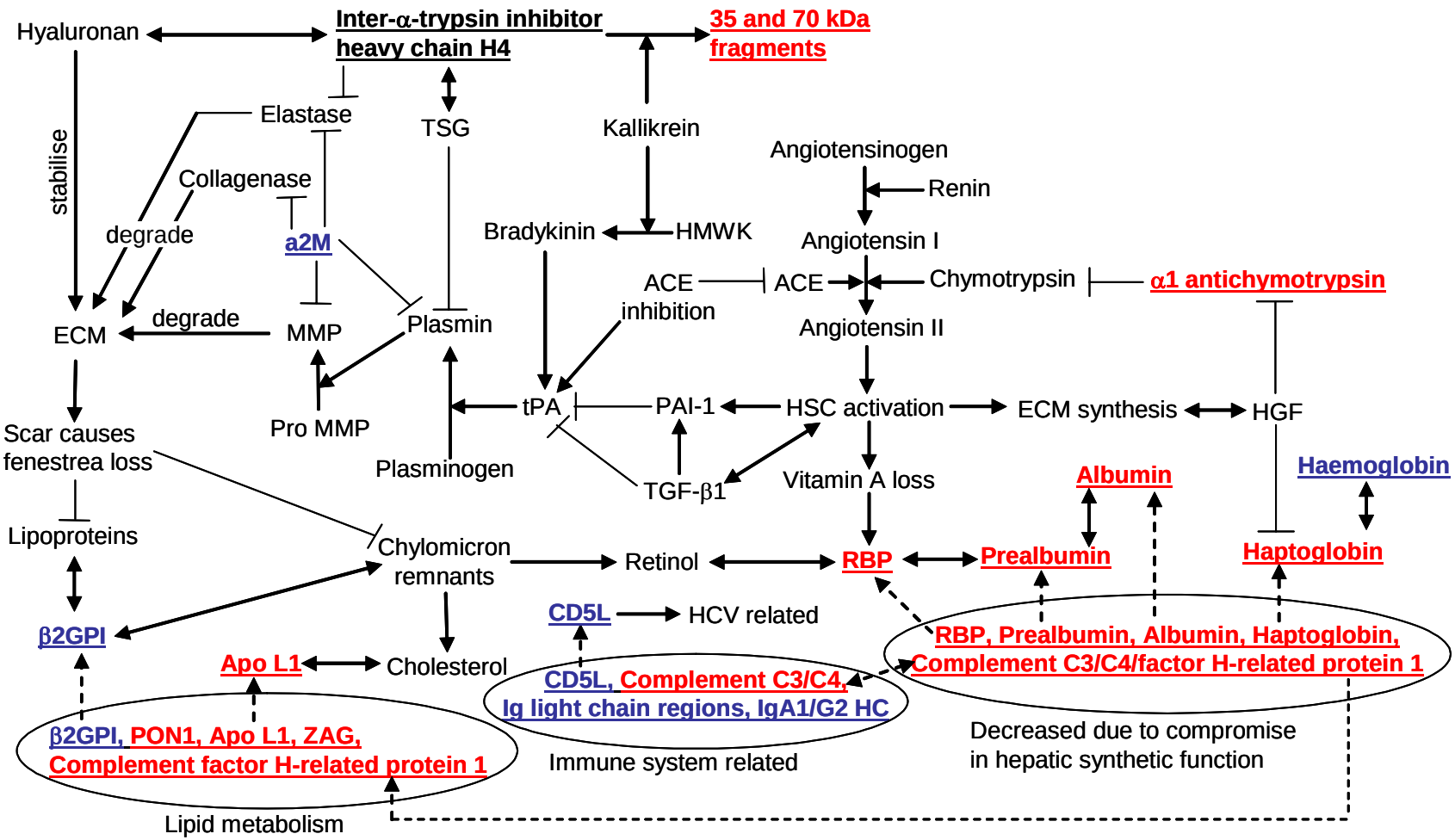

Figure 24 Inter-relationship between all the proteins identified in the differential analysis for serum from healthy controls versus hepatic scarring. Identified proteins are shown underlined and in bold. Proteins in red were decreased in hepatic scarring whereas proteins in blue were increased

Western blotting or ELISAs. These validation studies will be explored for further work using a greater number of serum samples from patients.

Biomarkers could also be identified by labelling serum proteins with stable isotope tags such as ICAT or iTRAQ prior to mass spectrometry. This approach provides both quantitative (relative protein expression) and qualitative (protein identification) results. However, due to the complexity of the serum proteome and because many of the potential biomarkers identified by 2D-PAGE were of low abundance, fractionation by multidimensional LC is required.

The dynamic concentration range of serum proteins spans over 10 orders of magnitude, far exceeding the measurement capability of current technologies (Guerrier *et al.*, 2005). Therefore fractionation of samples prior to analysis helps in biomarker discovery. In-solution fractionation with SDS-PAGE helped to resolve high molecular weight basic proteins, however the overall resolution was inferior to that of 2D-PAGE. A major issue with 2D-PAGE analysis of serum is the presence of high abundance proteins, in particular albumin and IgG which account for 55% and 15%, respectively, of the total serum proteome (Anderson and Anderson, 2002). These high abundance proteins limit the protein load on 2D-PAGE gels and therefore decrease the representation of low abundance proteins. Also, proteins running in the same relative position as these highly abundant proteins may be masked from visualisation. Depletion of high abundance proteins has been achieved using dye affinity and immunoprecipitation techniques, the latter presently being the more accepted way for serum prefractionation due to higher specificity (Steel *et al.*, 2003b). An immunoprecipitation technique

developed in-house using polyclonal antibodies against four highly abundant serum proteins (albumin, IgG, haptoglobin, and transferrin) in pooled healthy control serum improved the depiction of two of the differentially expressed proteins, CD5L and β2GPI (Figures 8c and 16c). The use of this depletion strategy on all serum samples in this study could have improved the representation of low abundance proteins and potentially increased the chances of identifying a fibrosis marker. This in-house depletion approach has been evaluated along with a commercially available serum partitioning kit from Beckman Coulter using IgY antibodies against twelve highly abundant proteins. Although both of these techniques do enhance the visualisation of low abundance features, recovery is poor and serum depletion is an exhaustive time-consuming procedure. Therefore, serum depletion is not feasible for multiple serum samples, as used in this study, unless automated chromatography approaches can be implemented. Alternatively, for this study serum samples from each fibrosis stage could be pooled, depleted manually and then compared. However, this approach would not be appropriate statistically or experimentally and would require validation by Western blotting or ELISAs for each individual sample. Due to time constraints, these serum depletion methods were not investigated and will be considered for further experimentation.

Narrow-range IPG strips have been shown to increase spot resolution (Gorg *et al.*, 2004) and therefore increase the likelihood of determining a fibrosis biomarker. Non-linear pH 3-5.6 IPG strips were used to separate serum proteins from normal controls and HCV-infected patients (data not shown). This IPG range

was outside the region where several high abundance proteins are observed (albumin, IgG, transferrin) allowing high protein load and increased representation of acidic serum proteins. The separation of serum using this pH range has not been reported previously. This approach revealed several new protein spots that to our knowledge have never been visualised by 2D-PAGE even after using serum depletion. Encouragingly many of these novel spot features corresponded to differentially expressed features. Clearly these narrow-range IPG strips greatly improve the visualisation of potential biomarker candidates but due to time restrictions this technique was not applied to the samples in the fibrosis study. This approach will be used in future studies.

In addition to the proteomics study, some initial glycan analysis studies were also performed (data not shown). Aberrant protein glycosylation is seen in several pathological states and glycan analysis may help to identify diagnostic biomarkers. Our preliminary results show that core fucosylation in serum increases in cirrhosis consistent with previous results (Morelle *et al.*, 2006). IgG, a2M and β2GPI are hyperfucosylated in HCC (Comunale *et al.*, 2006; Drake *et al.*, 2006) and therefore this increase in core fucosylation may be due to these elevated glycoproteins we identified in the 2D-PAGE differential analysis. We also found that core fucosylation appears to correlate with hepatic damage when assessing an individual during anti-viral therapy (data not shown). It is anticipated that these studies will form part of the future work on this project. We are also presently, in collaboration with Dr. Louise Royle and Dr. Pauline Rudd, optimising a method for analysing glycans from individual 2D-PAGE gel spots.

This technique will help to pinpoint which glycoproteins are responsible for this increase in core fucose. Also fucosylation of glycoproteins may be found to correlate better than protein levels in fibrosis since this has already been observed for GP73, which is hyperfucosylated in HCC development (Mehta, 2005). De-*N*-glycosylation of serum glycoproteins prior to 2D-PAGE analysis will also be considered since this approach simplifies the serum proteome and enhances spot resolution thereby aiding biomarker determination (Comunale *et al.*, 2004).

This thesis demonstrates that 2D-PAGE based proteomics has the potential to elucidate new serological biomarkers for diseased states. Although many of the changes highlighted in the 2D-PAGE analysis were only seen when comparing serum from controls with cirrhotic patients, it is possible that these changes are also present in the earlier stages of fibrosis but are below the detection limits of the fluorescent stain used. By assessing each of the identified differentially expressed proteins by Western blotting or ELISA over all fibrosis stages, a dependable biomarker that changes during the course of hepatic scarring may be revealed. Taking into consideration the suggested projects for further experimentation, these studies may reveal a protein, or combination of proteins, that for the first time can reliably be used to assess all stages of liver scarring. Ultimately such a biomarker would aid clinicians to diagnose the early stages of fibrosis. This would eliminate the need for liver biopsy and allow early treatment thereby preventing fibrosis progression.

CHAPTER 3

Differential protein expression analysis of Jurkat lipid raft proteins in the presence and absence of HIV Nef

3.1 Introduction

3.1.1 Human Immunodeficiency Virus (HIV)

HIV is a retrovirus responsible for the fatal illness acquired immunodeficiency syndrome (AIDS). This virus is passed from person to person via blood or sexual contact. In addition, infected pregnant women can pass HIV to their baby during pregnancy or delivery, as well as through breast-feeding. Some infected with HIV produce an immune response and remain asymptomatic, while others become progressively debilitated. The virus primarily infects vital components of the immune system (e.g. CD4+ T helper cells).

The HIV-1 genome contains nine genes, two of which code for structural proteins and the others for non-structural proteins (Figure 25a and b). The virus is composed of two single strands of RNA that, along with enzymes, are enclosed by a capsid which itself is surrounded by matrix and host-derived plasma membrane (Figure 25c). The virus is enveloped by the transmembrane glycoprotein, gp41, and the surface glycoprotein, gp120. To establish an infection, gp120 attaches to the CD4 receptor and a co-receptor on the surface of the host cell. After this interaction, the viral envelope and host cell membrane fuse resulting in entry of the virion into the host cell. Reverse transcriptase (RT) makes a double stranded DNA copy of the viral RNA that enters the nucleus and integrates with the host cell chromosome by the integrase (IN). In this state, it is called the provirus. Viral RNA synthesised from the provirus leaves the nucleus. Translation of the viral RNA yields enzymes and structural proteins some of which are cleaved by the viral protease (PR). The glycoproteins gp41 and gp120 insert into the host

(a)

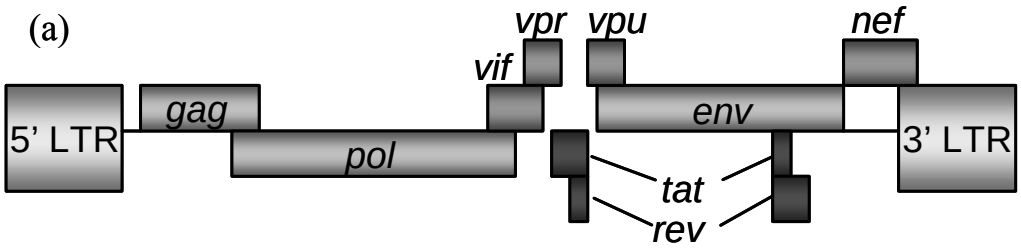

(b)

Gene	Codes for (+ function)
gag	p24(capsid); p17(matrix); p7(nucleocapsid)
pol	reverse transcriptase, integrase, and protease
env	gp120 and gp41 (envelope proteins from gp160)
tat	Tat (helps HIV reproduce)
rev	Rev (exports RNA from nucleus to cytoplasm)
nef	Nef (increases replication and pathogenicity)
vif	Vif (essential for replication)
vpr	Vpr (regulates nuclear preintegration import)
vpu	Vpu (involved in viral assembly and budding)

(c)

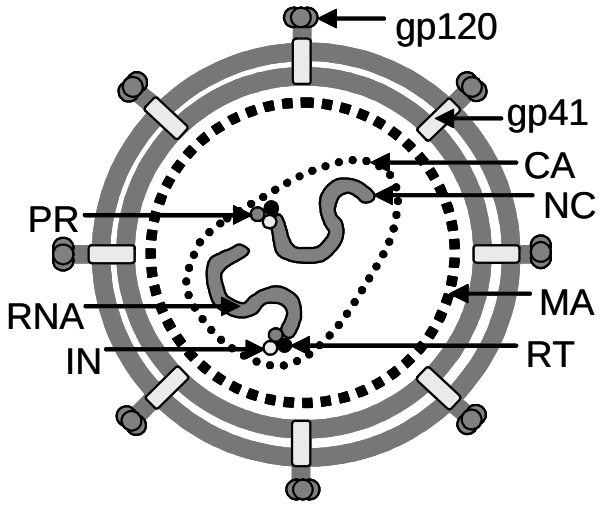

Figure 25 HIV structure and genome. (a) The HIV genome contains nine genes. Both *gag* and *env* encode for structural proteins and the others for non-structural proteins. At each end is a long terminal repeat (LTR) where the same sequence code is at each end. (b) Summary table showing the proteins expressed by each gene. (c) The HIV virion structure. CA, capsid; NC, nucleocapsid; MA; matrix; RT, reverse trasncriptase; PR, protease; IN, integrase. Figure adapted from Sierra *et al.*, 2005.

cell membrane and the viral proteins along with encapsidated RNA bud from the plasma membrane to release the virus. This HIV replication cycle is summarised in Figure 26. The viral Nef protein plays an important part in the HIV life cycle by increasing both replication and pathogenicity (Section 3.1.2).

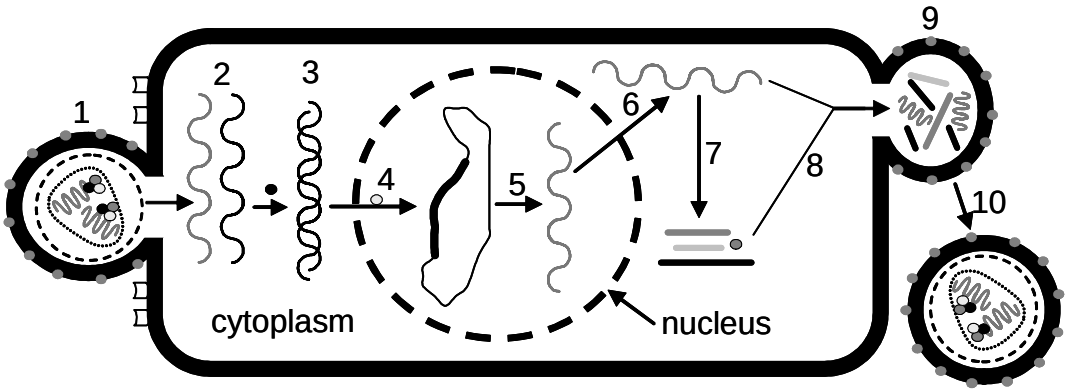

Figure 26 Simplified schematic diagram showing HIV replication.
1) The HIV virion binds to and fuses with the host cell membrane; 2) Reverse transcriptase produces single stranded DNA; 3) Double stranded copy of the viral RNA is produced by reverse transcriptase; 4) Viral DNA enters the nucleus and integrase enables integration with the cellular DNA; 5) mRNA transcription; 6) viral RNA leaves the nucleus; 7) translation forms polypeptides; 8) a protease cleaves polypeptides into functional HIV proteins that along with RNA are used to reconstrct the virion; 9) The HIV virion buds from the plasma membrane; 10) Maturation into fully infectious virions. Adapted from Sierra *et al.*, 2005.

3.1.2 Nef protein

The accessory gene *nef* encodes a phosphorylated, N-myristoylated membrane associated cytoplasmic protein that is 205 amino acids long and 27 kDa in size (Joseph *et al.*, 2005). Nef enhances viral replication and infectivity and is important for the progression of HIV and simian immunodeficiency virus (SIV) infections (Das and Jameel, 2005). Nef has several functional attributes including down-regulation of the antigen presenting cell surface molecule, MHC-1, to promote escape from the host's cellular immune response (Schwartz *et al.*, 1996; Collins *et al.*, 1998); alteration of host cell death pathways to prevent apoptosis of infected cells (Ameisen, 2001); and down-regulation of CD4, a cell surface glycoprotein that interacts with the envelope of budding HIV virions thereby inhibiting their release. Nef-induced CD4 down-regulation reverses this inhibition and therefore may facilitate the spread of HIV (Garcia and Miller, 1991; Ross *et al.*, 1999). The precise mechanisms of Nef action are not clearly understood but there is increasing evidence that it interacts with host cell signal transduction proteins. It has been shown that Nef induces a transcriptional program in T cells that is almost identical to that of anti-CD3 T cell activation (Simmons *et al.*, 2001).

3.1.3 Nef-mediated cell signalling in lipid rafts

Although the nature of Nef signalling in T cells is unclear, there is evidence for the involvement of lipid rafts (Alexander *et al.*, 2004, Wang *et al.*, 2000). Lipid rafts are liquid-ordered microdomains of the plasma membrane that are enriched

in sphingolipids and cholesterol and move within the fluid bilayer (Horejsi, 2005). These discrete microdomains act as platforms for conducting cellular functions such as vesicular trafficking and signal transduction (Simons and Ikonen, 1997).

The rafts recruit a specific set of proteins and exclude others. Some proteins are modified at their C-terminal end with a hydrophobic phosphatidyl inositol group linked through a carbohydrate linker. These glycosylphosphatidylinositol-anchored (GPI-anchored) proteins attach to the exoplasmic leaflet of the rafts and clusters of these proteins activate signalling pathways, possibly by interacting with signal-transduction proteins that in turn become activated. Alternatively, the GPI-anchors can be released by enzymes yielding phospho-oligosaccharides that may flip into the cell and act as second messengers. Other proteins associated with rafts include transmembrane proteins and doubly acylated tyrosine kinases binding to the cytoplasmic leaflet. Rafts may concentrate receptors in signalling processes to enable association with ligands on both sides of the membrane (Simons and Ikonen, 1997). In tyrosine kinase signalling, ligand activation results in the recruitment of enzymes and adaptor proteins to the cytoplasmic face of the raft. In receptor activation, recruitment of signalling complexes to rafts protects the signalling complex from non-raft enzymes which may alter signal transduction. However, enzymes located within rafts (e.g. kinases or phosphatases) can act on these signalling complexes to enhance downstream signalling (Simons and Toomre, 2000).

Nef is anchored onto lipid rafts and is associated with increased levels of tyrosine phosphorylated T cell signalling moieties in these rafts (Alexander *et al.*,

2004, Wang *et al.*, 2000). Nef is myristoylated which allows this raft association (Djordjevic *et al.*, 2004). Myristoylation, which is mediated by the enzyme *N*-myristoyltransferase (NMT), refers to the covalent attachment of myristate, a 14-carbon saturated fatty acid, to the N-terminal glycine of a protein. This N-terminal modification allows proteins to be anchored to the plasma membrane (Farazi *et al.*, 2001).

Nef is an example of a kinase activating protein that binds a subset of the Src family kinases via a polyproline motif (Craig *et al.*, 1999; Saksela *et al.*, 1995). The Src family tyrosine kinases contain a catalytic kinase and two protein binding domains called Src homology 2 (SH2) and Src homology 3 (SH3) (Alberts *et al.*, 2002). The SH3 domain prefers to bind to ligand sequences rich in proline and they can turn the kinase on by binding to an activating protein (Kay *et al.*, 2000).

Nef is associated with the activation and recruitment of activated p21-activated kinase (PAK), a downstream effector of Cdc42, to rafts (Krautkramer *et al.*, 2004). Cdc42 is one of the family of GTPases that switch between an active state when GTP is bound and an inactive state when GDP is bound. Activation of Cdc42 is probably responsible for PAK activation in Nef-expressing cells (Simmons *et al.*, 2005). HIV replicative capacity is induced when Nef binds to and activates Vav, a guanine nucleotide exchange factor (GEF). GEFs promote the exchange of bound nucleotide by stimulating the dissociation of GDP and the subsequent uptake of GTP from the cytosol. Vav binds to inactive Cdc42-GDP causing a conformational change in Cdc42 which releases GDP and allows GTP to bind, i.e. Nef leads to Cdc42 activation. However, the initial trigger for the Nef-

mediated activation of this Cdc42-dependent signalling pathway in rafts is unclear (Lu *et al.*, 1996; Krautkramer *et al.*, 2004).

3.1.4 Project objectives

By analysing proteins being recruited to or lost from rafts in the presence of Nef, other proteins involved in this signalling pathway may be elucidated thereby further aiding our understanding of HIV replication. In addition, identification of proteins changing in rafts of Nef-transfected cells may help to establish associations with the other major roles of Nef including pathogenicity, apoptosis and down-regulation of cell surface proteins to facilitate viral spreading and escape from the host's immune surveilance. Here, Nef signalling was investigated by analysing differential protein expression in CD4 T cell lipid rafts in the presence and absence of Nef. Proteins that were recruited to or lost from rafts after Nef expression were determined by using 2D-PAGE analysis and mass spectrometry. This project was carried out in collaboration with Dr. Alison Simmons and Prof. Andrew McMichael based at the Weatherall Institute of Molecular Medicine, John Radcliffe Hospital, Oxford and this chapter represents the author's contribution to the study.

3.2 Materials and Methods

3.2.1 Materials

Jurkat cells, a line of T lymphocyte cells from a leukaemia patient, were obtained from the American Type Culture Collection (ATCC) (Middlesex, UK). Cell culturing reagents and fluorescent conjugate secondary antibodies were purchased from Invitrogen (Paisley, UK). Anti-FLAG antibodies were provided by Sigma (Dorset, UK). Antibodies for Cbl, βPix and Cdc42 were from Santa Cruz (California, USA) and Chemicon (Hampshire, UK). UbcH7 antibodies were from Chemicon and Upstate Biotechnology (Hampshire, UK). Vav antibodies were from Upstate Biotechnology and Santa Cruz. Anti-ubiquitin antibodies were from Biomol (Exeter, UK). siRNAs were obtained from Qiagen (West Sussex, UK). Radiance 2000 laser scanning confocal and LaserSharp 2000 software were purchased from Bio-Rad (Hertfordshire, UK). Polyvinylidine difluoride (PVDF) membrane and Enhanced chemiluminescence (ECL) reagents were purchased from GE Healthcare (Buckinghamshire, UK). 10 kDa molecular weight cut-off (MWCO) 16 mm wide Spectra/Por® Biotech Regenerated Cellulose Dialysis Membrane Tubing was from Spectrum Laboratories (CA, USA). The Savant Modulyo freeze-drier was from Thermo Quest (MA, USA). The materials listed in Section 2.2.1 for 2D-PAGE and mass spectrometry were also used.

3.2.2 Jurkat raft samples

The methods described in this section were performed by Dr. Alison Simmons and coworkers.

Four replicate control and Nef-transfected lipid raft fractions were prepared from standard Jurkat cells derived from E6-1, a subclone with higher CD4 expression than normal Jurkat cells. Lipid raft samples were prepared by lysing 50 x 10^6 Jurkat cells at 4 °C in buffer containing 10 mM Tris-HCl (pH 7.5), 5 mM ethylene diamine tetra-acetate (EDTA), 1% (v/v) Triton X-100, protease inhibitors (pepstatin, leupeptin, aprotinin and PMSF) and phosphatase inhibitors (sodium fluoride and sodium orthovanadate) and floatation on sucrose density gradients as described previously (Cheng *et al.*, 1999). The supernatant was spun on a sucrose gradient (1 ml 85% (w/v) sucrose, 6 ml 30% (w/v) sucrose and 3.5 ml 0.5% (w/v) sucrose) in the lysis buffer but with 150 mM NaCl and without 1% (v/v) Triton X-100. Twelve fractions were collected; fractions 3 and 4 (the second to fifth millilitre of the gradient) contained rafts (as identified by Western blotting using GM1, the lipid raft marker, data not shown).

3.2.3 Preparation of samples for SDS-PAGE and 2D-PAGE

Prior to gel electrophoresis, it was necessary to remove both sucrose, to enable the determination of protein concentration, and sodium chloride, since salt concentrations above 10 mM can disturb isoelectric focusing and result in high strip conductivity thereby prolonging electrophoresis. Samples were dialysed overnight against water using 10 kDa MWCO dialysis tubing. The dialysis tubing

was pre-soaked for 30 min in Milli Q water and then stored in 0.1% (w/v) sodium azide (NaN_3) buffer at 4 °C. Samples were dialysed against Milli Q water with four changes of water over 24 h. Salt/sucrose depleted samples were recovered in fresh tubes and tightly sealed with Parafilm. Four small holes were pierced through the Parafilm cover to allow sample sublimation during freeze-drying. Freeze-drying was carried out overnight in a Savant Modulyo drier. The dried raft samples were resuspended in sample buffer and their concentrations determined using the Coomassie Plus protein assay kit (Section 2.2.3.2).

SDS-PAGE was performed as described in Section 2.2.5 with 10 μg of total protein per lane. Large format 2D-PAGE and mass spectrometry were also performed as described in Sections 2.2.4 to 2.2.10.3 but with 18 cm pH 3-10 linear IPG strips with 500 μg of raft sample for each gel. The four replicate control raft samples were compared against the four replicate Nef-transfected samples.

2.3.4 Analysis of Nef-mediated signalling

The methods described in this section were performed by Dr. Alison Simmons and co-workers.

For Western blot analysis, sucrose fractions, immunoprecipitates or whole cell lysates were resolved on SDS-PAGE, transferred to PVDF membrane, and detected with antibodies using the ECL system. When analysing the sucrose fractions, each fraction was also immunoblotted against GM1, a raft associated marker. Glutathione-S-transferase (GST) tagged p21 binding domain (PDB) was

immobilised on glutathione agarose to pull-down activated Cdc42 (GTP-Cdc42) which was analysed by Western blotting. To assess whether the myristoylation sequence of Nef is essential for certain signalling events, Nef was mutated at position 2 of the N-terminal myristoylation site where a glycine amino acid was converted to alanine (Nef-G2A). To determine whether an intact polyproline motif is required for certain signalling events, a mutant was created where aa 72-75 of the polyproline motif was mutated from FPVR to VRIT. siRNAs were used to knock down UbcH7 and βPix. Virus production was assayed by p24 ELISA and confocal analysis was carried out using a Radiance 2000 confocal and analysed with LaserSharp 2000 software.

3.3 Results and Discussion

3.3.1 Nef raft study: an overview

The HIV Nef protein is involved in a Cdc42 signalling pathway in lipid rafts (Krautkramer *et al.*, 2004). Nef activates Vav, which increases viral replication, and Vav activates Cdc42. However, the early stages of this pathway are unknown. Characterisation of this pathway and identification of other signalling protein associated with lipid rafts in Nef-expressing cells may increase understanding of Nef-mediated HIV replication. Here, 2D-PAGE and mass spectrometry were used to identify lipid raft associated proteins in T cells in the presence and absence of Nef.

3.3.2 Differentially expressed proteins

2D-PAGE analysis and mass spectrometry were used to identify proteins differentially expressed in lipid rafts of Jurkat CD4 T cells transfected with or without Nef (for complete gel images see Appendix). Four replicate 2D-PAGE gels (with a linear pI range of 3-10) were produced for both control and Nef-expressing lipid raft fractions to visualize changes in the lipid raft proteome in the presence of Nef. Image analysis revealed that each gel resolved approximately 1200 spots. Spots displaying an increase or decrease in expression post Nef transfection were selected for protein identification by mass spectrometry. In several examples, multiple spots represented the same protein with variations possibly due to post-translational modification. Using this methodology, 10 proteins were increased in expression in Nef-positive raft samples and 7 proteins

were decreased. A synthetic representative gel image highlighting all the valid changes is shown in Figure 27. Names of all identified proteins and their Swiss-Prot accession numbers theoretical molecular weight, pI, and function are listed in Table A3. Table 6 shows a summary of all differentially expressed proteins which have been classified according to their various functions.

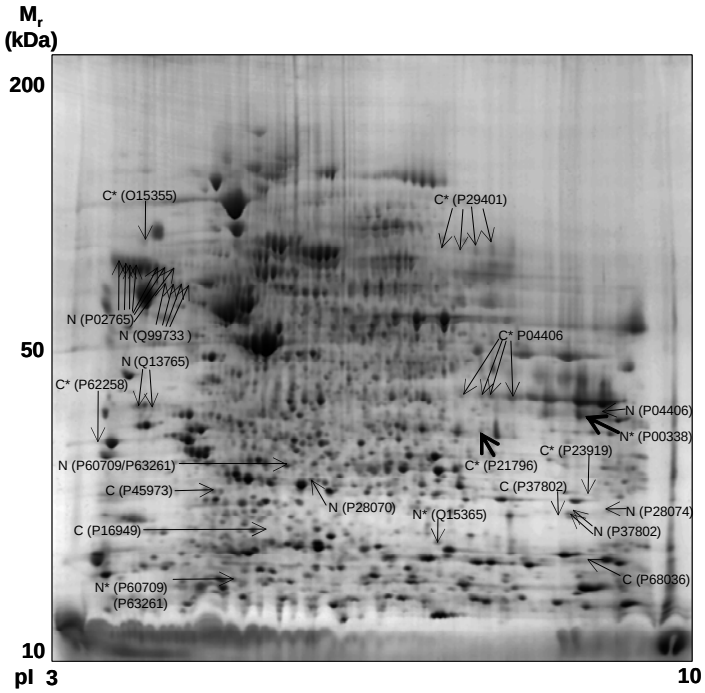

Figure 27 Synthetic 2D-PAGE image representing all protein spots present in the control versus Nef-transfected raft analysis. Differentially expressed features along with their Swiss-Prot accession number are highlighted. Gels were stained with the fluorescent dye OGT 1238. C, features present only in control rafts; N, features present only in Nef-transfected rafts; C*, features present in both control and Nef-transfected rafts but expressed to a higher extent in the control rafts; N*, features present in both control and Nef-transfected rafts but expressed to a higher extent in the Nef-transfected rafts. For complete gel figures, see Appendix.

Classification	Protein Name	Fold change	Protein function
Signal transduction	14-3-3 protein ε	C*	Binds to and reduces PI3K activity
	Glyceraldehyde 3-phosphate dehydrogenase	N, C*	Cytosolic glycolytic enzyme GA3P + Pi + NAD^+ ⇔ BPG +NADH
	L-lactate dehydrogenase A chain	N*	Enzyme in glycolysis. Expressed in activated lymphocytes
	Protein phosphatase 2C γ isoform	C*	Cytosolic enzyme - dephosphorylates phosphoproteins
	Thymidylate kinase	C*	Cytosolic enzyme: ATP + dTMP ⇔ ADP + dTDP
	Transketolase	C*	Cytosolic enzyme in pentose phosphate pathway
Cytoskeletal and related proteins	Actin (cytoplasmic)	N, N*	Cytoskeletal components necessary for cell surface shape and locomotion
	Stathmin	C	Destabilises microtubules by sequestering tubulin
	Transgelin 2	C, N	Mediates cross-linking of actin
Proteolysis	*Proteasome subunit β type 4*	N	Proteolysis (cytoplasm)
	Proteasome subunit β type 5	N	Proteolysis (cytoplasm)
Ubiquitination	Ubiquitin-conjugating enzyme E2 (UbcH7)	C	Cbl associated ubiquitination enzyme
mRNA processing and translation	*NASCENT polypeptide associated complex α subunit*	N	Nuclear/cytoplasmic mRNA processing
	Poly(rC)-binding protein 1 (hnRNP-E1)	N*	RNA binding protein involved in cell spreading
Nucleosome assembly	*Nucleosome assembly protein 1-like 4*	N	Located in nucleus and associated with nucleosome assembly
Ion channel	*Voltage-dependent anion-selective channel protein 1*	C*	Forms channels through mitochondrial membrane
Acute phase protein	*α2-HS-glycoprotein*	N	Acute phase protein usually found in plasma/serum

Table 6 Summary of differentially expressed proteins identified in control versus Nef-transfected rafts. Fold change refers to proteins that were differentially expressed by 2-fold or more when comparing serum gels from healthy controls with the different stages of hepatic fibrosis. C, feature only present in control rafts. N, feature only present in Nef-transfected rafts. C*, feature expressed to higher extent in control raft samples. N*, feature expressed to higher extent in Nef-transfected raft samples. The protein names in italics appeared to show no significance with Nef and/or are not raft proteins and therefore are not discussed.

3.3.2.1 Actin and transgelin 2 in Nef-mediated cytoskeletal dynamics

Nef-expressing lipid rafts exhibited an increase in fragments of actin (Figure 28) and post-translational modification of transgelin 2 (Figure 29). Polymers of the protein actin make up cytoskeletal actin filaments that determine cell surface shape and are necessary for cell locomotion (Carlier *et al.*, 2003). The changes in actin expression detected by 2D-PAGE may indicate that these actin filaments are recruited to Nef-expressing rafts. Cross-linking of actin has been shown to be mediated by transgelin. When transgelin is added to actin filaments, they are converted from a loose, random distribution into a tangled and cross-linked meshwork (Shapland *et al.*, 1993). The changes in both of these proteins are consistent with previous observations of Nef-driven cytoskeletal rearrangement caused by actin polymerisation (Fackler *et al.*, 1999).

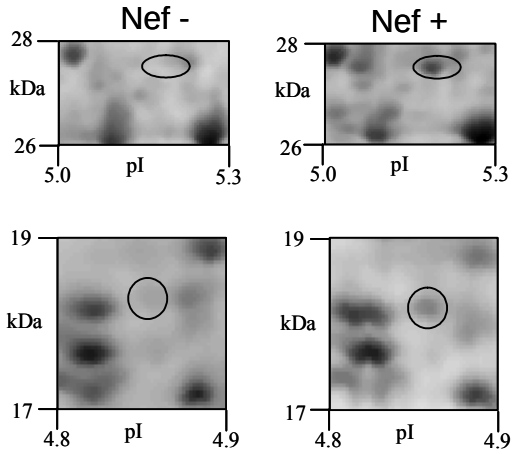

Figure 28 Nef-mediated increase in fragments of actin. Zoomed representative gel images of control (Nef -) and Nef-expressing (Nef +) rafts. Actin was found to be elevated in two regions of the gel, at approximately 28 and 18 kDa.

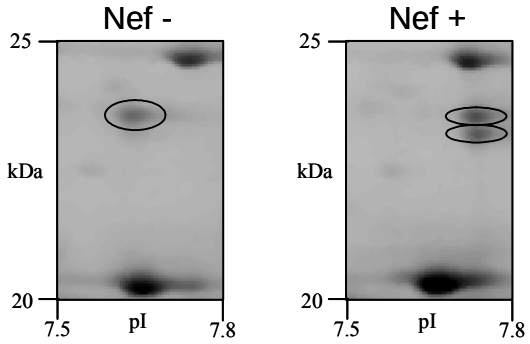

Figure 29 Post-translational modification of transgelin in rafts of Nef-tranfectants. Magnified images showing the region of gel where a shift in the basic direction was observed for this actin cross-linker.

3.3.2.2 Stathmin in Nef-mediated cellular trafficking

Nef-expressing rafts appeared to show an absence of stathmin (Figure 30), a protein that negatively regulates microtubule dynamics (Andersen, 2000). In a similar way to actin, microtubules are cytoskeletal components. Microtubules are composed of subunits of the protein tubulin. The tubulin subunit is a heterodimer comprising two globular proteins, α- and β-tubulin, that are non-covalently bound. The general function of these microtubules is to determine the positions of membrane-enclosed organelles and direct intracellular transport (Hunter and Wordeman, 2000). Microtubules can lengthen or shorten simply by the addition or removal of tubulin dimers at their ends, a process that is dependent on the surrounding free tubulin concentration. The phosphoprotein stathmin is able to sequester tubulin thereby decreasing the concentration of free heterodimers available for polymerisation (Belmont and Mitchison, 1996). In addition to this, stathmin induces catastrophe at microtubule tips for further destabilisation (Cassimeris, 2002). The apparent absence of stathmin in Nef-expressing rafts

suggests that less tubulin is sequestered and as a result microtubule organisation within the cell may be regulated to allow for increased vesicular transport. Although the reason for the absence of stathmin in rafts of Nef-transfectants is unclear, local microtubule stabilisation at the infected cell/uninfected cell interface may be associated with the formation of synapses to allow transport of virions, a phenomenon which has already been described (Jolly *et al.*, 2004; McDonald *et al.*, 2003).

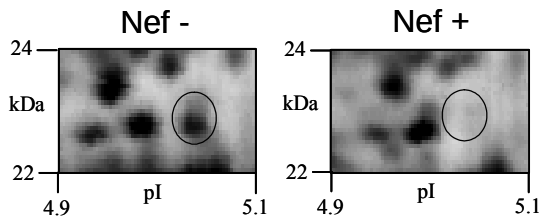

Figure 30 Microtubule stabilistation may increase in rafts of Nef-transfected cells. Close-up regions of the 2D-PAGE gel where stathmin was found to be absent in Nef-expressing rafts.

Nef-expressing rafts are associated with the activation and recruitment of PAK (Krautkramer *et al.*, 2004). It has been shown that this kinase can phosphorylate stathmin leading to its inactivation (Wittmann *et al.*, 2004). Usually phosphorylated proteins are observed to shift towards a more acidic pI on 2D-PAGE gels (García *et al.*, 2004b). Therefore the apparent absence of stathmin could be a result of it being present in its inactivated, phosphorylated form rather than decreased expression. However, computer-aided image analysis did not detect any spot displacement of this nature.

3.3.2.3 14-3-3ε in Nef-mediated T cell signalling

2D-PAGE analysis revealed that Nef-positive rafts lack the known negative regulator of signalling, 14-3-3ε (Figure 31).

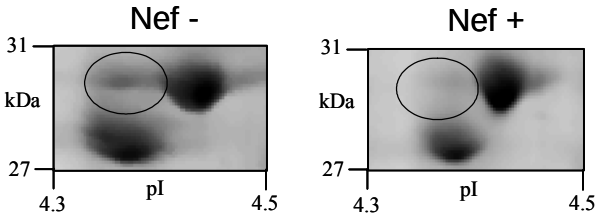

Figure 31 The adaptor protein, 14-3-3ε, is absent in Jurkat rafts in the presence of Nef. Zoomed gel regions indicating where 14-3-3ε was found to be differentially expressed.

14-3-3ε is an adaptor protein implicated in the regulation of a large spectrum of both general and specialised signalling pathways. 14-3-3ε binds to its partners usually by recognition of a phosphoserine or phosphothreonine motif. This binding generally results in alteration of the activity of the binding partner (Darling *et al.*, 2005). One such binding partner is the catalytic subunit of phosphatidylinositol 3-kinase (PI3K) (Bonnefoy-Berard *et al.*, 1995). PI3K is itself an adaptor protein that binds to activated phosphorylated protein-tyrosine kinases, mediating the association of the PI3K catalytic unit to the plasma membrane (Krasilnikov, 2000). PI3K is a heterodimer of one 110 kDa catalytic subunit and one 85 kDa regulatory subunit, called p110 and p85, respectively. It has been shown that isoforms of 14-3-3 expressed in T cells bind to the p110 catalytic subunit of activated PI3K (Bonnefoy-Berard *et al.*, 1995). This p110–14-

3-3 association reduces the enzymatic activity of PI3K. The decreased expression of 14-3-3ε in Nef-expressing rafts suggests that the activity of PI3K would not be reduced by as much as in control rafts. This is consistent with previous studies showing that Nef binds to and activates PI3K (Bonnefoy-Berard *et al.*, 1995; Wolf *et al.*, 2001); Nef-mediated PAK activation is PI3K dependent. Thus, Nef does not directly activate PAK (Linnemann *et al.*, 2002).

Nef down-regulates MHC-1 to promote escape of HIV-infected cells from the host's cytotoxic T lymphocyte (CTL) recognition and killing mechanism (Schwartz *et al.*, 1996; Collins *et al.*, 1998). Swann *et al.*, 2001 showed that Nef blocks transport of MHC-1 to the cell surface, a process that is dependent on PI3K activity. As a result, MHC-1 accumulates within the *trans*-Golgi network and is retained in this organelle (Larsen *et al.*, 2004). Others have shown that Nef-mediated PI3K activation indirectly leads to an ADP ribosylation factor 6 (ARF6) dependent increase in the rate of MHC-1 endocytosis from the cell surface (Blagoveshchenskaya *et al.*, 2002). Members of the ARF family, notably ARF1-3, play a role in vesicular budding and recruitment of clathrin / coatomer proteins. However ARF6, a small GTPase, does not recruit these coats and instead connects vesicle trafficking with actin cytoskeletal rearrangements (Chavrier and Goud, 1999). Recent live cell imaging has shown Nef- and ARF6-mediated internalisation of MHC-1 (Massol *et al.*, 2005). However, the exact means by which this internalisation occurs, and the proteins associated with ARF6 that are responsible for MHC-1 down-regulation remain unclear. In addition to the raft analysis of Nef-transfected cells described herein, a method for

immunoprecipitation of ARF6 followed by SDS-PAGE has been optimised (data not shown). This can be used to identify proteins binding to ARF6 in whole cell lysates of Nef-transfected Jurkat cells to further understand MHC-1 down-regulation and the proteins involved in its internalisation. This is being persued by Dr. Alison Simmons and co-workers.

In addition to PI3K, the class of 14-3-3 proteins also bind to the Cbl protein in activated T cells (Liu *et al.*, 1996). Cbl is thought to be an adaptor protein that functions as a T cell signalling attenuator. It is rapidly phosphorylated upon T cell activation and this phosphorylation increases according to its association with 14-3-3. Cbl can interact with several signalling molecules in T cells including PI3K and its association with 14-3-3 was detected both in intact T cells and *in vitro*. Liu *et al.*, 1996 hypothesise that 14-3-3 may enhance the association between PI3K and Cbl resulting in inhibition of PI3K activity. The 2D-PAGE data shows a decrease in 14-3-3 in Nef-expressing rafts. Based on this hypothesis, one would expect an increase in PI3K activity consistent with several reports described previously (Kim *et al.*, 1999; Wolf *et al.*, 2001; Blagoveshchenskaya *et al.*, 2002).

3.3.2.4 Nef and hnRNP E1 mediated cell spreading

Differential 2D-PAGE analysis revealed that Nef-expressing rafts were associated with recruitment of the RNA binding protein, hnRNP E1 (Figure 32). hnRNP E1 was first identified in a study to identify and quantify proteins interacting in an attachment-dependent manner with focal adhesion proteins. Focal adhesions are specialised attachment and signalling centres that form at sites

of cell-matrix contacts. Using a quantitative mass spectrometry-based method to identify interaction partners of key focal adhesion proteins, previously undescribed structures termed spreading initiation centres (SICs), were identified (de Hoog *et al.*, 2004). These SICs, visualised only in the early stages of cell spreading, appeared to be surrounded by actin, and contained focal adhesion markers and several RNA binding proteins including hnRNP E1. Interfering with the function of hnRNP E1 resulted in increased spreading. The increased expression of hnRNP E1 detected in Nef-expressing rafts and the suggested increased actin polymerisation (Section 3.3.2.1) may mediate cell spreading.

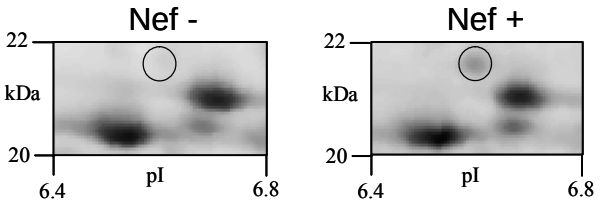

Figure 32 Increased levels of hnRNP E1 in Nef-expressing rafts may mediate cell spreading. Magnified images of the gel regions where hnRNP E1 was found to be elevated in rafts of Nef transfectants.

3.3.2.5 Lactate dehydrogenase-A signalling in Nef-mediated T cell activation

2D-PAGE analysis revealed that the expression of lactate dehydrogenase-A isoform (LDH-A) was elevated in Nef-expressing rafts (Figure 33). This enzyme converts lactate to pyruvate in the final step of glycolysis and although predominantly expressed in muscle, has also been characterised in lymphocytes.

The ‘A’ isoform of LDH is preferentially expressed in activated lymphocytes although the reason for this expression is unclear (Wollberg and Nelson, 1992). Detection of LDH-A in Nef-expressing rafts may be due to Nef-mediated T lymphocyte activation.

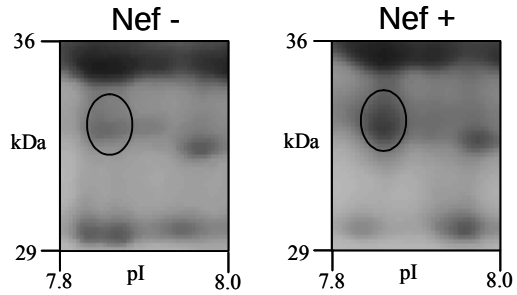

Figure 33 Elevation of the A isoform of lactate dehydrogenase in Nef-mediated T cell activation. Close-up images of representative gels highlighting the increase in lactate dehydrogenase-A isoform.

2.3.2.6 UbcH7 in Nef-mediated T cell signalling

Differential 2D-PAGE analysis revealed that UbcH7 was absent from lipid rafts of Nef-transfected Jurkat cells (Figure 34). UbcH7 is a member of the E2 ubiquitin-conjugating enzyme family (Zheng *et al.*, 2000). It mediates the transfer of activated ubiquitin to substrate proteins and is an essential component of the post-translational protein ubiquitination pathway.

The modification of proteins with ubiquitin is an important cellular mechanism for targeting abnormal or short-lived proteins for degradation (first described by Wollberg and Nelson, 1992). Ubiquitination involves three classes of enzymes: ubiquitin-activating enzymes (E1s), ubiquitin conjugating enzymes (E2s) and

ubiquitin-protein ligases (E3s). Ubiquitin is first activated by the E1 activating enzyme; activated ubiquitin is then transferred to the E2 conjugating enzyme and the E3 ligase facilitates the transfer of ubiquitin from E2 to the protein substrate. Finally, substrates marked with polyubiquitin chains are selectively targeted to proteasomal degradation (Alberts *et al.*, 2002).

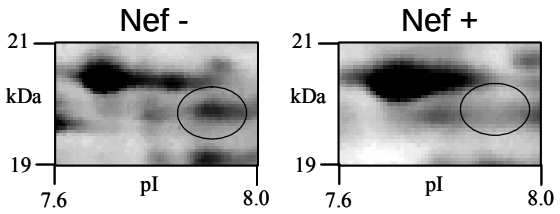

Figure 34 UbcH7 is absent in rafts of Nef-transfected Jurkat cells. Magnified representative gel images showing the absence of the E2 ubiquitin-conjugating enzyme in Nef-expressing rafts.

UbcH7 acts as the cognate E2 conjugating enzyme for Cbl family proteins and E3 ubiquitin ligases that mediate ubiquitination and down-regulation of activated T cell signalling molecules (Yokouchi *et al.*, 1999; Zheng *et al.*, 2000). Two family members of Cbl have been described: c-Cbl and Cbl-b (Thien and Langdon, 2005). Cbl can recruit components of the ubiquitin pathway and act as an ubiquitin–protein ligase (Joazeiro *et al.*, 1999). Cbl proteins have a small zinc-binding domain termed the RING finger domain. RING finger domains contain four pairs of ligand binding residues that attach to two zinc ions and interact with a diverse range of proteins. Several RING finger domains have E3 ligase activity, such as the one present in Cbl proteins, and promote conjugation of ubiquitin to

the target substrate. The Cbl RING finger has been shown to specifically recruit UbcH7 (Yokouchi *et al.*, 1999).

Among the identified proteins differentially expressed in lipid rafts in the presence of Nef, UbcH7 stands out as an attractive candidate for involvement in Nef signalling. Its absence may interfere with c-Cbl-mediated negative regulation of T cell signalling proteins and thus provide a means by which Nef might promote T cell signalling. Having identified UbcH7 as a candidate using the proteomics-based approach, the role of UbcH7 was further explored by Dr. Alison Simmons and co-workers. These data are discussed briefly in Sections 3.3.3 to 3.3.6 and a copy of the paper for this study can be found in the Appendix.

3.3.3 UbcH7 exclusion from Nef-expressing lipid rafts

Exclusion of UbcH7 from rafts of Nef-transfected cells (as detected by 2D-PAGE differential analysis) was confirmed using Western blotting performed by Dr. Alison Simmons and co-workers. All fractions obtained by sucrose density gradient centrifugation were probed with an anti-UbcH7 antibody. Each fraction was also immunoblotted against GM1 to indicate the presence of rafts. Figure 35a demonstrates the exclusion of UbcH7 from GM1 positive fractions of Nef-expressing cells by Western blot, validating the proteomics study.

By mutating the myristoylation sequence of Nef (Nef-G2A) it was shown that UbcH7 remains localised to the rafts (Figure 35a) suggesting that Nef must be physically associated with rafts for this exclusion. Dr. Alison Simmons and co-workers performed further mutagenesis experiments to investigate whether the

polyproline motif is needed for UbcH7 raft exclusion. Expression of this mutant (FPVR to VRIT; Nef-PxMu) abrogated the ability of Nef to exclude UbcH7 from lipid rafts fractions suggesting that an intact Nef SH3 binding domain is also essential for this exclusion (Figure 35a). Confocal studies were undertaken to further assess the redistribution of UbcH7. These confirmed the Western blot results (Figure 35a) since UbcH7 staining was down-regulated in lipid rafts of wild type Nef-transfected cells but co-localised with GM1 in control cells and cells transfected with both Nef mutants (Figure 35b).

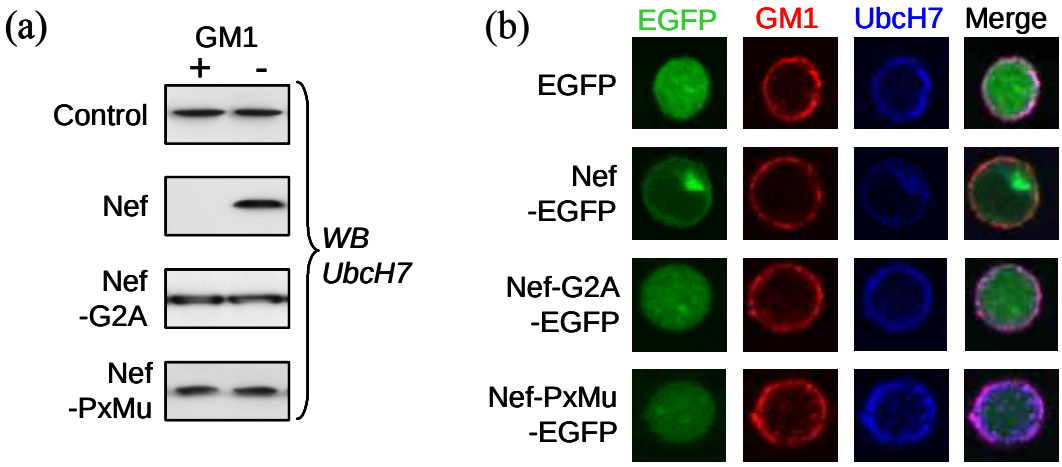

Figure 35 UbcH7 is selectively excluded from lipid rafts in the presence of Nef. (a) Representative Western blot images against UbcH7 for GM1 positive (raft) and negative (soluble) fractions for control, Nef, Nef-G2A, and Nef-PxMu transfected Jurkat cells. (b) Confocal images of EGFP (control), Nef-EGFP, Nef-G2A-EGFP, and Nef-PxMu-EGFP tranfected Jurkat cells. Texas red (red) was used to stain rafts, Alexa Fluor 674 (blue) for UbcH7 and EGFP (green) was expressed with each variant of Nef. Merging of blue and red results in magenta as seen in the rafts of EGFP control and mutants but is absent in Nef-EGFP suggesting exclusion of UbcH7 from rafts. These data were provided by Dr. Alison Simmons and are reproduced from Simmons *et al.*, 2005.

3.3.4 Failure of Vav ubiquitination in Nef-expressing CD4 T cells

The functional relevance of Nef-mediated exclusion of UbcH7 from lipid rafts was investigated by Dr. Alison Simmons and co-workers. UbcH7 has been shown to down-regulate the activated T cell signalling molecule Vav (Miura-Shimura *et al.*, 2003). Vav is activated by Nef leading to an increase in HIV replication (Krautkramer *et al.*, 2004). In T cell activation, Vav associates with c-Cbl (Marengere *et al.*, 1997) leading to its ubiquitination and proteasomal degradation (Miura-Shimura *et al.*, 2003). Since UbcH7 is absent in rafts in the presence of Nef, one would expect to see failure of ubiquitination of it substrate Vav. Western blot analysis revealed that Vav was hyperphosphorylated in the Nef positive raft fractions (Figure 36a). GTP-Cdc42 binds to PDB of PAK. GST-PDB was used to pull-down GTP-Cdc42. Consistent with previous studies, Vav was shown to activate Cdc42 (Figure 36b). Unlike conventional T cell activation, Nef-mediated T cell activation did not result in Vav ubiquitination or c-Cbl association (Figures 36c & d).

Small interfering RNAs (siRNAs) interfere with gene expression by binding to and degrading mRNA resulting in gene silencing (Valencia-Sanchez *et al.*, 2006). In further experiments by Dr. Alison Simmons and co-workers, siRNAs were used to knock down UbcH7 to confirm if this was responsible for the absence of Vav ubiquitination in the presence of Nef. UbcH7 knockdown increased activated Cdc42 (Figure 36f) and Vav ubiquitination was absent (Figure 36g). Collectively these results show that the exclusion of UbcH7 from rafts in Nef-expressing cells has functional consequences in Nef signalling.

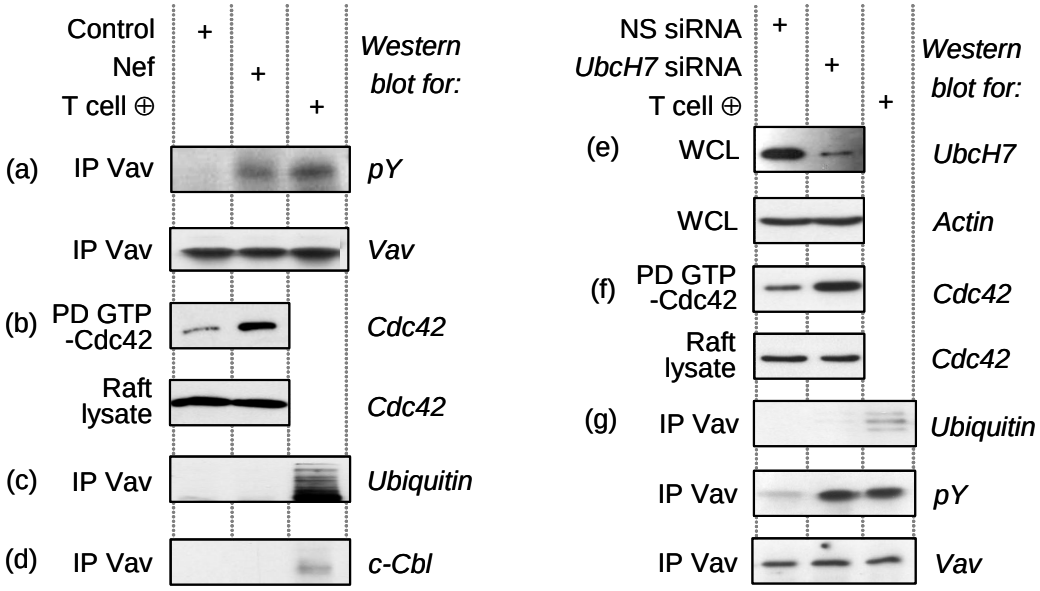

Figure 36 Failure of c-Cbl-mediated ubiquitination of Nef-activated Vav. (a-d) Western blot images for control, Nef-transfected, and anti-CD3/CD28 activated (conventional T cell activation, T cell ⊕) Jurkat cells. (a) Vav was immunoprecipitated from rafts and immunoblotted for anti-phosphotyrosine (pY) (upper panel) and Vav (lower panel). (b) GTP-Cdc42 was pulled down (PD) from rafts and GTP-Cdc42 levels were assessed (upper panel). The same raft samples were immunoblotted for Cdc42 (lower panel). (c) Vav was immunoprecipitated from rafts and immunoblotted for ubiquitin. (d) Vav was immunoprecipitated from rafts and immunoblotted for c-Cbl. (e-f) Western blot images for Jurkat cells transfected with non-silencing (NS) siRNA, UbcH7 siRNA, and cells activated with anti-CD3/CD28. (e) UbcH7 assessed in whole cell lysate (WCL) 48 h after transfection (upper panel). The lower panel shows an actin immunoblot from WCL. (f) Cdc42 immunoblot following PD of GTP-Cdc42 (upper panel). Cdc42 immunoblot from raft lysates (lower panel). (g) Vav was immunoprecipitated from rafts and blotted for ubiquitin (upper panel), pY (middle panel) and Vav (lower panel). These data were provided by Dr. Alison Simmons and are reproduced from Simmons *et al.*, 2005.

3.3.5 Cdc42 associates with βPix and c-Cbl in Nef-expressing cells

Cdc42 and c-Cbl form a ternary complex with PAK interacting exchange factor (βPix) when Cdc42 is constitutively active. This ternary complex inhibits c-Cbl-mediated ubiquitination (Wu *et al.*, 2003). Since Cdc42 activity is increased in

Nef-expressing cells, the formation of such a complex may be responsible for displacing UbcH7 from rafts. Unlike conventional T cell activation, in Nef-expressing cells, both βPix and c-Cbl coimmunoprecipitated with Cdc42 (Figure 37a) confirming that the hypothesised Cdc42-βPix-Cbl ternary complex does form in the presence of Nef. UbcH7 was found to be down-regulated in Jurkat rafts transfected with a Cdc42 mutant (F28L) capable of forming the ternary complex (Figure 37b) suggesting that the Cdc42-βPix-Cbl complex may be responsible for the absence of UbcH7.

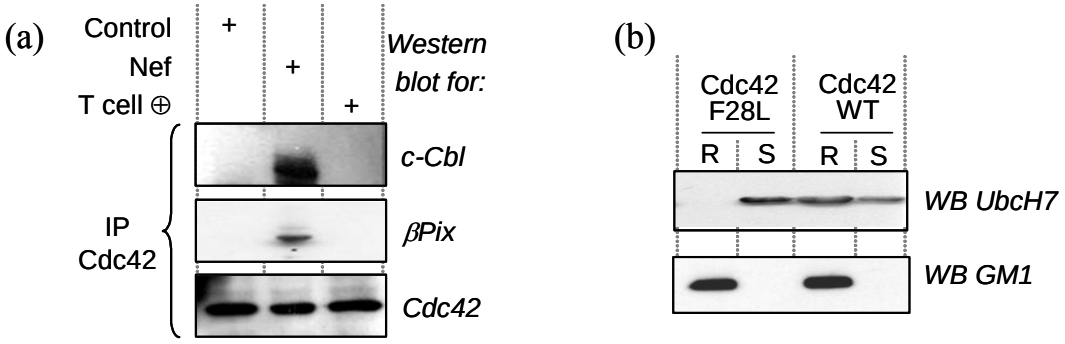

Figure 37 A Cdc42-βPix-Cbl ternary complex forms in the presence of Nef which requires constitutively active Cdc42. (a) Immunoprecipitates of Cdc42 were performed for control, Nef-transfected cells and cells activated with anti-CD3/CD28 (T cell ⊕). Immunoblots were performed for c-Cbl (upper panel), βPix (middel panel), and Cdc42 (lower panel). (b) Jurkat cells were transfected with Cdc42(F28L) and wild-type Cdc42 (Cdc42 WT) and UbcH7 was immunoblotted from GM1 positive raft (R) and GM1 negative soluble (S) fractions obtained from sucrose density gradient centrifugation. These data were provided by Dr. Alison Simmons and are reproduced from Simmons *et al.*, 2005.

3.3.6 βPix knockdown relocates UbcH7 to rafts, restores Vav ubiquitination and diminishes HIV replication

βPix was knocked down using siRNA and the elimination of βPix was confirmed by both Western blotting and confocal analysis (Figures 38a & b). βPix knockdown in Nef transfectants led to the relocalisation of UbcH7 to the rafts (Figure 38c), restoration of Vav ubiquitination (Figure 38d) and decrease in activated Cdc42 (Figure 38e). These results further suggest that the ternary complex displaces UbcH7 from rafts and prevents Vav ubiquitination. The effect of βPix knockdown on HIV replication was also investigated in HIV-transfected cells. HIV production was diminished compared to HIV-transfected cells without βPix knockdown (Figures 38f & g) suggesting that the Cdc42-βPix-Cbl ternary complex is imperative for HIV replication. One possibility is that the ternary complex may prevent UbcH7 from accessing the RING finger of Cbl due to steric interference. Figure 39 shows a possible mechanism of action for Nef-mediated T cell activation compared to conventional T cell activation.

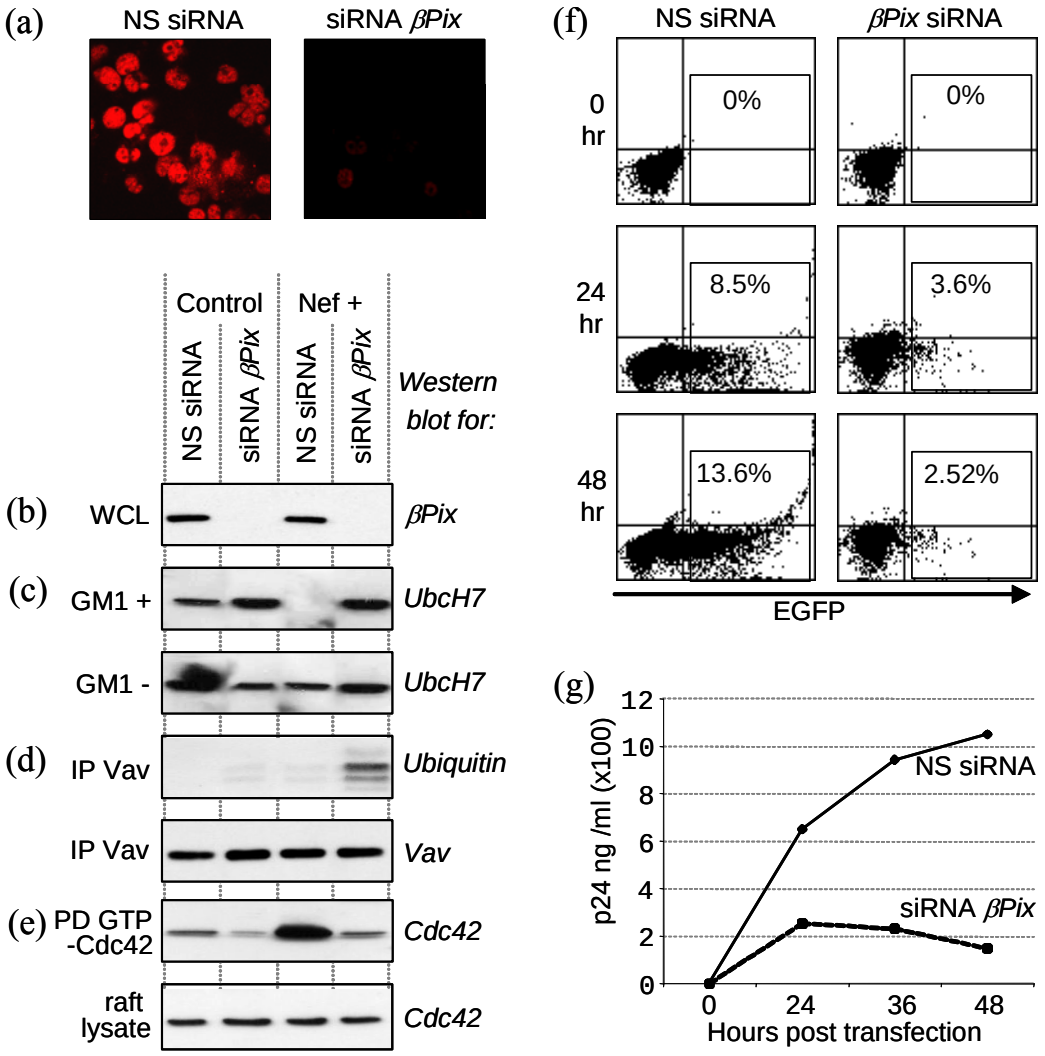

Figure 38 βPix knockdown restores UbcH7 raft localisation and Vav ubiquitination. (a) Confocal image of βPix expression in the presence of NS siRNA and siRNA *βPix* at 48 h post transfection. (b-e) Western blot analysis for control and Nef-transfected cells both in the presence of NS siRNA and siRNA *βPix*. (b) Confirmation of βPix knockdown in WCL. (c) GM1 positive, raft (upper panel) and negative, soluble (lower panel) fractions were immunoblotted for UbcH7. (d) Vav was immunoprecipitated from cells and blotted for ubiquitin (upper panel) and Vav (lower panel). (e) GTP-Cdc42 was pulled down (PD) from rafts and blotted for Cdc42 (upper panel). Cdc42 was also immunoblotted from rafts (lower panel). (f-g) Jurkat cells were transfected with EGFP expressing HIV virus with either NS siRNA and siRNA *βPix*. Levels of HIV production were assessed by both (f) FACS and (g) p24 ELISA, where values and error bars are representative of six separate experiments. These data were provided by Dr. Alison Simmons and are reproduced from Simmons *et al.*, 2005.

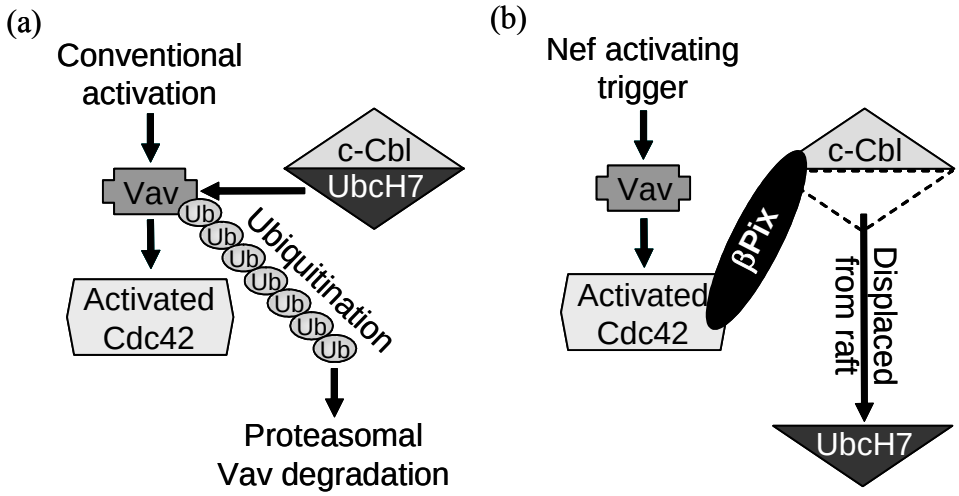

Figure 39 Model illustrating the inhibition of c-Cbl function by Nef
(a) In conventional T cell activation UbcH7 is present in lipid rafts associated with c-Cbl and is able to ubiquitinate Vav for proteasomal degradation.
(b) In the presence of Nef, the ternary complex Cdc42-βPix-Cbl is formed which causes UbcH7 to be displaced from the lipid raft. As a consequence, Vav is not ubquitinated. βPix knockdown disrupts the formation of this ternary complex and facilitates relocation of UbcH7 to lipid rafts restoring Vav ubiquitination.

3.4 Conclusion

The lipid raft-associated Nef protein increases HIV replication. Identification of raft-associated proteins in the presence of this accessory protein has helped to further understand the signalling events related to HIV. Here, 2D-PAGE-based proteomics was used, a technique that is advantageous for examining signalling within cells (Pelech, 2004), to identify differentially expressed raft-associated proteins by comparing T cells in the presence and absence of Nef. Of the changes characterised, increases in actin, LDH-A and hnRNP-E1, and decreases in 14-3-3ε, stathmin and UbcH7 in Nef-expressing rafts are of particular interest. Additionally, transgelin was found to be post-translationally modified. Possible reasons for the changes in these proteins are: cytoskeletal rearrangement from transgelin mediated actin polymerisation; microtubule stabilisation from decreased stathmin; LDH-A increase due to Nef-mediated T cell activation; and decreased 14-3-3ε to prevent PI3K inhibition, enabling both stathmin inactivation and the virus to escape the host's immune surveillance. The change of most interest was the absence of UbcH7 in Nef-expressing rafts. Dr. Alison Simmons and co-workers found that UbcH7 was displaced from lipid rafts due to the formation of a Cdc42-βPix-Cbl ternary complex. A summary of the proteins identified by 2D-PAGE and their inter-relationship with Nef is outlined in Figure 40.

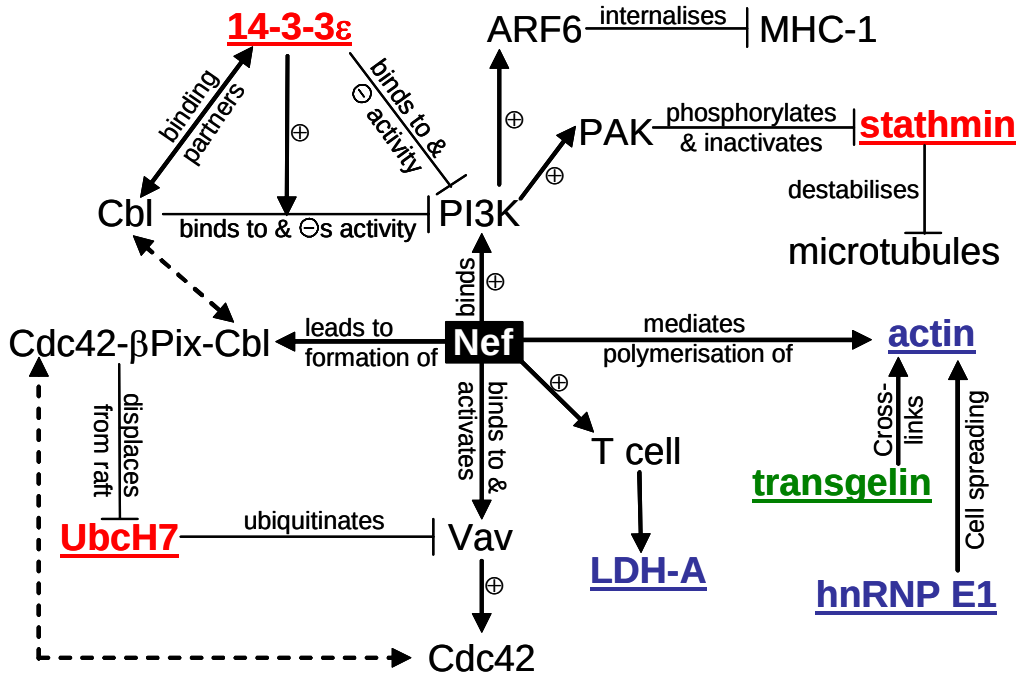

Figure 40 Inter-relationship between all the proteins identified in the differential analysis for control versus Nef-expressing rafts. Identified proteins are shown underlined and in bold. Proteins in red were decreased in Nef-expressing rafts whereas proteins in blue were increased. Proteins in green displayed a post-translational modification. + indicates activation and – inhibition

Although the gel-based proteomics method led to the successful identification of several interesting proteins, there were some practical issues with this approach. Suggestions to overcome these are discussed here. For all raft samples, the percentage recovery after dialysis was below 30%. Although this recovery was low, there was sufficient protein to load 500 μg per 2D-PAGE gel. The low recovery is probably due to proteins adhering to the dialysis membrane. Protein precipitation methods (e.g. TCA-acetone or methanol-chloroform as described in Section 2.2.11) could not be used as these are incompatible with the high levels of sucrose in the fractions. An alternative approach would be to spin the samples by

ultracentrifugation to pellet the raft proteins which could then be directly resuspended in rehydration sample buffer. This approach has been performed successfully for analysing rafts from platelets by SDS-PAGE (García *et al.*, 2004c; García *et al.*, 2005), where the authors comment that, due to their hydrophobic nature, these proteins are poorly represented by 2D-PAGE and a more complete protein profile might be obtained using SDS-PAGE followed by LC-MS/MS, or LC-MS/MS directly. Due to the unavailability of a suitable direct LC-MS/MS system, the raft samples for this study could not be analysed in this manner. The raft samples were however analysed by SDS-PAGE (data not shown) and there were no observable differences. Accurate protein quantitation is difficult using this low resolution separation. An approach currently being optimised for use in the Oxford Glycobiology Institute involves labelling proteins with ICAT reagent prior to SDS-PAGE. The resulting bands can be excised, digested and analysed by mass spectrometry to quantitatively determine protein differences directly from gel pieces. Such an approach may be a suitable option for hydrophobic raft proteins.

This analysis of Nef-expressing rafts is an excellent example where proteomics can assist in the investigation of signalling pathways within virally infected cells. Such an approach has the potential to aid in the analysis of signalling pathways in cells infected with other viruses. In this study we have analysed Nef to understand its involvement in enhancing viral replication and pathogenicity. The discovery of host proteins involved in the presence of Nef is vital for understanding how this accessory protein exerts pathogenicity and also in the rational design of drug

intervention strategies. The proteomics data, together with data from Dr. Alison Simmons and co-workers, show that the elimination of βPix in Nef-transfected cells restores a signalling pathway to what is observed in normal T cell activation and diminishes viral replication. These data provide a novel candidate target for inhibiting HIV replication that may offer a way of reducing the progression of the disease worldwide.

References

Aebersold R, Mann M, (2003), Mass spectrometry-based proteomics, *Nature*, **422**, 198-207

Agha S, Al-Gendy M, El-Fiky A, El-Emshaty W, (1999), Correlation of serum hepatitis C virus RNA titre with aminotransferases and liver histopathological findings in HCV-seropositive cases with end-stage chronic liver disease, *Microbes Infect*, **1**, 1091-4

Agnello V, Abel G, Elfahal M, Knight GB, Zhang QX, (1999), Hepatitis C virus and other flaviviridae viruses enter cells via low density lipoprotein receptor, *Proc Natl Acad Sci U S A*, **96**, 12766-71

Alberts B, Johnson A, Lewis J, Raff M, Roberts R, Walter P, (2002), Molecular Biology of the Cell, 4th Edition, *Garland Science*

Alexander M, Bor YC, Ravichandran KS, Hammarskjold ML, Rekosh D, (2004), Human immunodeficiency virus type 1 Nef associates with lipid rafts to downmodulate cell surface CD4 and class I major histocompatibility complex expression and to increase viral infectivity, *J Virol*, **78**, 1685-96

Alter H, (1999), Discovery of non-A, non-B hepatitis and identification of its etiology, *Am J Med*, **107**, 16S-20S

Amacher DE, Adler R, Herath A, Townsend RR, (2005), Use of proteomic methods to identify serum biomarkers associated with rat liver toxicity or hypertrophy, *Clin Chem*, **51**, 1796-803

Ameisen JC, (2001), Apoptosis subversion: HIV-Nef provides both armor and sword, *Nat Med*, **7**, 1181-2

Amess B, Tolkovsky AM, (1995), Programmed cell death in sympathetic neurons: a study by two-dimensional polyacrylamide gel electrophoresis using computer image analysis, *Electrophoresis*, **16**, 1255-67

Amodio P, Gatta A, Ruol A, (1984), Beta 2-microglobulin concentration in plasma and production in liver cirrhosis, *J Clin Chem Clin Biochem*, **22**, 147-51

Anatol P, Robert F, Danuta P, (2005), Effect of interferon alpha2b plus ribavirin treatment on selected growth factors in respect to inflammation and fibrosis in chronic hepatitis C, *World J Gastroenterol*, **11**, 1854-8

Andersen SS, (2000), Spindle assembly and the art of regulating microtubule dynamics by MAPs and Stathmin/Op18, *Trends Cell Biol*, **10**, 261-7

Anderson NL, Anderson NG, (2002), The human plasma proteome: history, character, and diagnostic prospects, *Mol Cell Proteomics*, **1**, 845-67

Aviram M, Rosenblat M, (2004), Paraoxonases 1, 2, and 3, oxidative stress, and macrophage foam cell formation during atherosclerosis development, *Free Radic Biol Med*, **37**, 1304-16

Bacon BR, (2002), Treatment of patients with hepatitis C and normal serum aminotransferase levels, *Hepatology*, **36**, S179-84

Bataller R, Brenner DA, (2005), Liver fibrosis, *J Clin Invest*, **115**, 209-18

Bataller R, Paik YH, Lindquist JN, Lemasters JJ, Brenner DA, (2004), Hepatitis C virus core and nonstructural proteins induce fibrogenic effects in hepatic stellate cells, *Gastroenterology*, **126**, 529-40

Bedossa P, Poynard T, (1996), An algorithm for the grading of activity in chronic hepatitis C. The METAVIR Cooperative Study Group, *Hepatology*, **24**, 289-93

Belmont LD, Mitchison TJ, (1996), Identification of a protein that interacts with tubulin dimers and increases the catastrophe rate of microtubules, *Cell*, **84**, 623-31

Berenguer M, Prieto M, Palau A, Rayon JM, Carrasco D, Juan FS, Lopez-Labrador FX, Moreno R, Mir J, Berenguer J, (2003), Severe recurrent hepatitis C after liver retransplantation for hepatitis C virus-related graft cirrhosis, *Liver Transpl*, **9**, 228-35

Berggren K, Steinberg TH, Lauber WM, Carroll JA, Lopez MF, Chernokalskaya E, Zieske L, Diwu Z, Haugland RP, Patton WF, (1999), A luminescent ruthenium complex for ultrasensitive detection of proteins immobilized on membrane supports, *Anal Biochem*, **276**, 129-43

Berne R, Levy M, (1998), Physiology, 4th Edition, *Mosby*

Beuselinck K, van Ranst M, van Eldere J, (2005), Automated extraction of viral-pathogen RNA and DNA for high-throughput quantitative real-time PCR, *J Clin Microbiol*, **43**, 5541-6

Bjellqvist B, Ek K, Righetti PG, Gianazza E, Gorg A, Westermeier R, Postel W, (1982), Isoelectric focusing in immobilized pH gradients: principle, methodology and some applications, *J Biochem Biophys Methods*, **6**, 317-39

Bjork I, Jornvall H, (1986), The structure around the thioester bond in bovine alpha 2-macroglobulin. Possible implications for the conformational stability of the inhibitor on thioester cleavage, *FEBS Lett*, **205**, 87-91

Blagoveshchenskaya AD, Thomas L, Feliciangeli SF, Hung CH, Thomas G, (2002), HIV-1 Nef downregulates MHC-I by a PACS-1- and PI3K-regulated ARF6 endocytic pathway, *Cell*, **111**, 853-66

Block TM, Comunale MA, Lowman M, Steel LF, Romano PR, Fimmel C, Tennant BC, London WT, Evans AA, Blumberg BS, Dwek RA, Mattu TS, Mehta AS, (2005), Use of targeted glycoproteomics to identify serum glycoproteins that correlate with liver cancer in woodchucks and humans, *Proc Natl Acad Sci U S A*, **102**, 779-84

Bonnefoy-Berard N, Liu YC, von Willebrand M, Sung A, Elly C, Mustelin T, Yoshida H, Ishizaka K, Altman A, (1995), Inhibition of phosphatidylinositol 3-kinase activity by association with 14-3-3 proteins in T cells, *Proc Natl Acad Sci U S A*, **92**, 10142-6

Borges LF, Taboga SR, Gutierrez PS, (2005), Simultaneous observation of collagen and elastin in normal and pathological tissues: analysis of Sirius-red-stained sections by fluorescence microscopy, *Cell Tissue Res*, **320**, 551-2

Bost F, Diarra-Mehrpour M, Martin JP, (1998), Inter-alpha-trypsin inhibitor proteoglycan family--a group of proteins binding and stabilizing the extracellular matrix, *Eur J Biochem*, **252**, 339-46

Bourantas KL, Dalekos GN, Makis A, Chaidos A, Tsiara S, Mavridis A, (1998), Acute phase proteins and interleukins in steady state sickle cell disease, *Eur J Haematol*, **61**, 49-54

Brewer GJ, (2003), Tetrathiomolybdate anticopper therapy for Wilson's disease inhibits angiogenesis, fibrosis and inflammation, *J Cell Mol Med*, **7**, 11-20

Bridle KR, Crawford DH, Fletcher LM, Smith JL, Powell LW, Ramm GA, (2003), Evidence for a sub-morphological inflammatory process in the liver in haemochromatosis, *J Hepatol*, **38**, 426-33

Brunt EM, (2000), Grading and staging the histopathological lesions of chronic hepatitis: the Knodell histology activity index and beyond, *Hepatology*, **31**, 241-6

Burlina A, Bugiardini R, (1978), Alkaline phosphatase isoenzymes in liver cirrhosis, *Enzyme*, **23**, 121-6

Cadranel JF, Mathurin P, (2002), Prothrombin index decrease: a useful and reliable marker of extensive fibrosis?, *Eur J Gastroenterol Hepatol*, **14**, 1057-9

Calamita Z, Burini RC, (1995), Immunologic changes in alcoholic liver cirrhosis, *Arq Gastroenterol*, **32**, 79-84

Callewaert N, Van Vlierberghe H, Van Hecke A, Laroy W, Delanghe J, Contreras R, (2004), Noninvasive diagnosis of liver cirrhosis using DNA sequencer-based total serum protein glycomics, *Nat Med*, **10**, 429-34

Carlier MF, Wiesner S, Le Clainche C, Pantaloni D, (2003), Actin-based motility as a self-organized system: mechanism and reconstitution in vitro, *C R Biol*, **326**, 161-70

Cassimeris L, (2002), The oncoprotein 18/stathmin family of microtubule destabilizers, *Curr Opin Cell Biol*, **14**, 18-24

Castera L, Foucher J, Bertet J, Couzigou P, de Ledinghen V, (2006), FibroScan and FibroTest to assess liver fibrosis in HCV with normal aminotransferases, *Hepatology*, **43**, 373-4; author reply 375-6

Castera L, Hartmann DJ, Chapel F, Guettier C, Mall F, Lons T, Richardet JP, Grimbert S, Morassi O, Beaugrand M, Trinchet JC, (2000), Serum laminin and type IV collagen are accurate markers of histologically severe alcoholic hepatitis in patients with cirrhosis, *J Hepatol*, **32**, 412-8

Castera L, Vergniol J, Foucher J, Le Bail B, Chanteloup E, Haaser M, Darriet M, Couzigou P, De Ledinghen V, (2005), Prospective comparison of transient elastography, Fibrotest, APRI, and liver biopsy for the assessment of fibrosis in chronic hepatitis C, *Gastroenterology*, **128**, 343-50

Chalmers RJ, Kirby B, Smith A, Burrows P, Little R, Horan M, Hextall JM, Smith CH, Klaber M, Rogers S, (2005), Replacement of routine liver biopsy by procollagen III aminopeptide for monitoring patients with psoriasis receiving long-term methotrexate: a multicentre audit and health economic analysis, *Br J Dermatol*, **152**, 444-50

Chavrier P, Goud B, (1999), The role of ARF and Rab GTPases in membrane transport, *Curr Opin Cell Biol*, **11**, 466-75

Cheng PC, Dykstra ML, Mitchell RN, Pierce SK, (1999), A role for lipid rafts in B cell antigen receptor signaling and antigen targeting, *J Exp Med*, **190**, 1549-60

Chevallet M, Santoni V, Poinas A, Rouquie D, Fuchs A, Kieffer S, Rossignol M, Lunardi J, Garin J, Rabilloud T, (1998), New zwitterionic detergents improve the analysis of membrane proteins by two-dimensional electrophoresis, *Electrophoresis*, **19**, 1901-9

Cho JJ, Hocher B, Herbst H, Jia JD, Ruehl M, Hahn EG, Riecken EO, Schuppan D, (2000), An oral endothelin-A receptor antagonist blocks collagen synthesis and deposition in advanced rat liver fibrosis, *Gastroenterology*, **118**, 1169-78

Colletta C, Smirne C, Fabris C, Toniutto P, Rapetti R, Minisini R, Pirisi M, (2005), Value of two noninvasive methods to detect progression of fibrosis among HCV carriers with normal aminotransferases, *Hepatology*, **42**, 838-45

Collins KL, Chen BK, Kalams SA, Walker BD, Baltimore D, (1998), HIV-1 Nef protein protects infected primary cells against killing by cytotoxic T lymphocytes, *Nature*, **391**, 397-401

Colombo M, Annoni G, Donato MF, Conte D, Martines D, Zaramella MG, Bianchi PA, Piperno A, Tiribelli C, (1985), Serum type III procollagen peptide in alcoholic liver disease and idiopathic hemochromatosis: its relationship to hepatic fibrosis, activity of the disease and iron overload, *Hepatology*, **5**, 475-9

Colombo M, Annoni G, Donato MF, Fargion S, Tiribelli C, Dioguardi N, (1983), Serum marker of type III procollagen in patients with idiopathic hemochromatosis and its relationship to hepatic fibrosis, *Am J Clin Pathol*, **80**, 499-502

Comunale MA, Lowman M, Long RE, Krakover J, Philip R, Seeholzer S, Evans AA, Hann HW, Block TM, Mehta AS, (2006), Proteomic analysis of serum associated fucosylated glycoproteins in the development of primary hepatocellular carcinoma, *J Proteome Res*, **5**, 308-15

Comunale MA, Mattu TS, Lowman MA, Evans AA, London WT, Semmes OJ, Ward M, Drake R, Romano PR, Steel LF, Block TM, Mehta A, (2004), Comparative proteomic analysis of de-N-glycosylated serum from hepatitis B carriers reveals polypeptides that correlate with disease status, *Proteomics*, **4**, 826-38

Cooper B, Eckert D, Andon NL, Yates JR, Haynes PA, (2003), Investigative proteomics: identification of an unknown plant virus from infected plants using mass spectrometry, *J Am Soc Mass Spectrom*, **14**, 736-41

Correale M, Giannuzzi V, Iacovazzi PA, Valenza MA, Lanzillotta S, Abbate I, Quaranta M, Caruso ML, Elba S, Manghisi OG, (1999), Serum 90K/MAC-2BP glycoprotein levels in hepatocellular carcinoma and cirrhosis, *Anticancer Res*, **19**, 3469-72

Courchesne PL, Patterson SD, (1999), Identification of proteins by matrix-assisted laser desorption/ionization mass spectrometry using peptide and fragment ion masses, *Methods Mol Biol*, **112**, 487-511

Craig HM, Pandori MW, Riggs NL, Richman DD, Guatelli JC, (1999), Analysis of the SH3-binding region of HIV-1 nef: partial functional defects introduced by mutations in the polyproline helix and the hydrophobic pocket, *Virology*, **262**, 55-63

Curry MP, Golden-Mason L, Nolan N, Parfrey NA, Hegarty JE, O'Farrelly C, (2000), Expansion of peripheral blood CD5+ B cells is associated with mild disease in chronic hepatitis C virus infection, *J Hepatol*, **32**, 121-5

Cutler P, Heald G, White IR, Ruan J, (2003), A novel approach to spot detection for two-dimensional gel electrophoresis images using pixel value collection, *Proteomics*, **3**, 392-401

Czaja AJ, Carpenter HA, (2004), Decreased fibrosis during corticosteroid therapy of autoimmune hepatitis, *J Hepatol*, **40**, 646-52

D'Arienzo A, Manguso F, Scaglione G, Vicinanza G, Bennato R, Mazzacca G, (1998), Prognostic value of progressive decrease in serum cholesterol in predicting survival in Child-Pugh C viral cirrhosis, *Scand J Gastroenterol*, **33**, 1213-8

Dalgic A, Karakayali H, Moray G, Emiroglu R, Sozen H, Torgay A, Haberal M, (2005), Liver transplantation and tacrolimus monotherapy for hepatocellular carcinoma with expanded criteria, *Transplant Proc*, **37**, 3154-6

Damoc E, Youhnovski N, Crettaz D, Tissot JD, Przybylski M, (2003), High resolution proteome analysis of cryoglobulins using Fourier transform-ion cyclotron resonance mass spectrometry, *Proteomics*, **3**, 1425-33

Darling DL, Yingling J, Wynshaw-Boris A, (2005), Role of 14-3-3 proteins in eukaryotic signaling and development, *Curr Top Dev Biol*, **68**, 281-315

Das SR, Jameel S, (2005), Biology of the HIV Nef protein, *Indian J Med Res*, **121**, 315-32

de Hoog CL, Foster LJ, Mann M, (2004), RNA and RNA binding proteins participate in early stages of cell spreading through spreading initiation centers, *Cell*, **117**, 649-62

Deviere J, Vaerman JP, Content J, Denys C, Schandene L, Vandenbussche P, Sibille Y, Dupont E, (1991), IgA triggers tumor necrosis factor alpha secretion by monocytes: a study in normal subjects and patients with alcoholic cirrhosis, *Hepatology*, **13**, 670-5

Di Bisceglie AM, Hoofnagle JH, (2002), Optimal therapy of hepatitis C, *Hepatology*, **36**, S121-7

Di Sario A, Bendia E, Taffetani S, Omenetti A, Candelaresi C, Marzioni M, De Minicis S, Benedetti A, (2005), Hepatoprotective and antifibrotic effect of a new silybin-phosphatidylcholine-Vitamin E complex in rats, *Dig Liver Dis*, **37**, 869-76

Diegelmann RF, Evans MC, (2004), Wound healing: an overview of acute, fibrotic and delayed healing, *Front Biosci*, **9**, 283-9

Djordjevic JT, Schibeci SD, Stewart GJ, Williamson P, (2004), HIV type 1 Nef increases the association of T cell receptor (TCR)-signaling molecules with T cell rafts and promotes activation-induced raft fusion, *AIDS Res Hum Retroviruses*, **20**, 547-55

Drake RR, Schwegler EE, Malik G, Diaz J, Block T, Mehta A, Semmes OJ, (2006), Lectin capture strategies combined with mass spectrometry for the discovery of serum glycoprotein biomarkers, *Mol Cell Proteomics*, **5**, 1957-67

Duchateau PN, Movsesyan I, Yamashita S, Sakai N, Hirano K, Schoenhaus SA, O'Connor-Kearns PM, Spencer SJ, Jaffe RB, Redberg RF, Ishida BY, Matsuzawa Y, Kane JP, Malloy MJ, (2000), Plasma apolipoprotein L concentrations correlate with plasma triglycerides and cholesterol levels in normolipidemic, hyperlipidemic, and diabetic subjects, *J Lipid Res*, **41**, 1231-6

Duchateau PN, Pullinger CR, Cho MH, Eng C, Kane JP, (2001), Apolipoprotein L gene family: tissue-specific expression, splicing, promoter regions; discovery of a new gene, *J Lipid Res*, **42**, 620-30

Duchateau PN, Pullinger CR, Orellana RE, Kunitake ST, Naya-Vigne J, O'Connor PM, Malloy MJ, Kane JP, (1997), Apolipoprotein L, a new human high density lipoprotein apolipoprotein expressed by the pancreas. Identification, cloning, characterization, and plasma distribution of apolipoprotein L, *J Biol Chem*, **272**, 25576-82

Faciullacci M, Galli P, Monetti MG, Pela I, Del Bianco PL, (1976), Prekallikein and kallikrein inhibitor in liver cirrhosis and hepatitis, *Adv Exp Med Biol*, **70**, 201-8

Fackler OT, Luo W, Geyer M, Alberts AS, Peterlin BM, (1999), Activation of Vav by Nef induces cytoskeletal rearrangements and downstream effector functions, *Mol Cell*, **3**, 729-39

Farazi TA, Waksman G, Gordon JI, (2001), The biology and enzymology of protein N-myristoylation, *J Biol Chem*, **276**, 39501-4

Ferre N, Camps J, Cabre M, Paul A, Joven J, (2001), Hepatic paraoxonase activity alterations and free radical production in rats with experimental cirrhosis, *Metabolism*, **50**, 997-1000

Filteau SM, Willumsen JF, Sullivan K, Simmank K, Gamble M, (2000), Use of the retinol-binding protein: transthyretin ratio for assessment of vitamin A status during the acute-phase response, *Br J Nutr*, **83**, 513-20

Fischer HP, Willsch E, Bierhoff E, Pfeifer U, (1996), Histopathologic findings in chronic hepatitis C, *J Hepatol*, **24**, 35-42

Foucher J, Chanteloup E, Vergniol J, Castera L, Le Bail B, Adhoute X, Bertet J, Couzigou P, de Ledinghen V, (2006), Diagnosis of cirrhosis by transient elastography (FibroScan): a prospective study, *Gut*, **55**, 403-8

Fraser R, Dobbs BR, Rogers GW, (1995), Lipoproteins and the liver sieve: the role of the fenestrated sinusoidal endothelium in lipoprotein metabolism, atherosclerosis, and cirrhosis, *Hepatology*, **21**, 863-74

Gabay C, Kushner I, (1999), Acute-phase proteins and other systemic responses to inflammation, *N Engl J Med*, **340**, 448-54

Gabrielli GB, Capra F, Casaril M, Squarzoni S, Tognella P, Dagradi R, De Maria E, Colombari R, Corrocher R, De Sandre G, (1997), Serum laminin and type III procollagen in chronic hepatitis C. Diagnostic value in the assessment of disease activity and fibrosis, *Clin Chim Acta*, **265**, 21-31

García A, Prabhakar S, Brock CJ, Pearce AC, Dwek RA, Watson SP, Hebestreit HF, Zitzmann N, (2004a), Extensive analysis of the human platelet proteome by two-dimensional gel electrophoresis and mass spectrometry, *Proteomics*, **4**, 656-68

García A, Prabhakar S, Hughan S, Anderson TW, Brock CJ, Pearce AC, Dwek RA, Watson SP, Hebestreit HF, Zitzmann N, (2004b), Differential proteome analysis of TRAP-activated platelets: involvement of DOK-2 and phosphorylation of RGS proteins, *Blood*, **103**, 2088-95

García A, Watson SP, Dwek RA, Zitzmann N, (2005), Applying proteomics technology to platelet research, *Mass Spectrom Rev*, **24**, 918-30

García A, Zitzmann N, Watson SP, (2004c), Analyzing the platelet proteome, *Semin Thromb Hemost*, **30**, 485-9

Garcia JV, Miller AD, (1991), Serine phosphorylation-independent downregulation of cell-surface CD4 by nef, *Nature*, **350**, 508-11

Gardner JP, Durso RJ, Arrigale RR, Donovan GP, Maddon PJ, Dragic T, Olson WC, (2003), L-SIGN (CD 209L) is a liver-specific capture receptor for hepatitis C virus, *Proc Natl Acad Sci U S A*, **100**, 4498-503

Garini G, Allegri L, Vaglio A, Buzio C, (2005), Hepatitis C virus-related cryoglobulinemia and glomerulonephritis: pathogenesis and therapeutic strategies, *Ann Ital Med Int*, **20**, 71-80

Gatta A, Amodio P, Frigo A, Merkel C, Milani L, Zuin R, Ruol A, (1981), Evaluation of renal tubular damage in liver cirrhosis by urinary enzymes and beta-2-microglobulin excretions, *Eur J Clin Invest*, **11**, 239-43

Geller SA, (2002), Hepatitis B and hepatitis C, *Clin Liver Dis*, **6**, 317-34, v

Giannini C, Brechot C, (2003), Hepatitis C virus biology, *Cell Death Differ*, **10 Suppl 1**, S27-38

Gnainsky Y, Spira G, Paizi M, Bruck R, Nagler A, Abu-Amara SN, Geiger B, Genina O, Monsonego-Ornan E, Pines M, (2004), Halofuginone, an inhibitor of collagen synthesis by rat stellate cells, stimulates insulin-like growth factor binding protein-1 synthesis by hepatocytes, *J Hepatol*, **40**, 269-77

Gonzalez-Quintela A, Alende MR, Gamallo R, Gonzalez-Gil P, Lopez-Ben S, Tome S, Otero E, Torre JA, (2003a), Serum immunoglobulins (IgG, IgA, IgM) in chronic hepatitis C. A comparison with non-cirrhotic alcoholic liver disease, *Hepatogastroenterology*, **50**, 2121-6

Gonzalez-Quintela A, Lopez-Ben S, Perez LF, Grana B, Varela M, Tome S, Varo E, (2003b), Time-course changes of serum immunoglobulins (IgA, IgG, IgM) after liver transplantation for alcoholic cirrhosis, *Transpl Immunol*, **11**, 73-7

Gonzalez Reimers E, Santolaria Fernandez F, Rodriguez Rodriguez E, Rodriguez Moreno F, Milena Abril A, Martinez-Riera A, Garcia-Castro C, (1996), Serum laminin in chronic alcoholic liver disease: its value in the estimation of the degree of fibrosis, *Rev Esp Enferm Dig*, **88**, 241-5

Gorg A, Boguth G, Obermaier C, Posch A, Weiss W, (1995), Two-dimensional polyacrylamide gel electrophoresis with immobilized pH gradients in the first dimension (IPG-Dalt): the state of the art and the controversy of vertical versus horizontal systems, *Electrophoresis*, **16**, 1079-86

Gorg A, Postel W, Gunther S, Weser J, (1985), Improved horizontal two-dimensional electrophoresis with hybrid isoelectric focusing in immobilized pH gradients in the first dimension and laying-on transfer to the second dimension, *Electrophoresis*, **6**, 599–604

Gorg A, Weiss W, (1999), Horizontal SDS-PAGE for IPG-Dalt, *Methods Mol Biol*, **112**, 235-44

Gorg A, Weiss W, Dunn MJ, (2004), Current two-dimensional electrophoresis technology for proteomics, *Proteomics*, **4**, 3665-85

Gravel P, Walzer C, Aubry C, Balant LP, Yersin B, Hochstrasser DF, Guimon J, (1996), New alterations of serum glycoproteins in alcoholic and cirrhotic patients revealed by high resolution two-dimensional gel electrophoresis, *Biochem Biophys Res Commun*, **220**, 78-85

Greenhalgh T, (2005), The Human Genome Project, *J R Soc Med*, **98**, 545

Gressner AM, Weiskirchen R, Breitkopf K, Dooley S, (2002), Roles of TGF-beta in hepatic fibrosis, *Front Biosci*, **7**, d793-807

Gretch DR, (1997), Diagnostic tests for hepatitis C, *Hepatology*, **26**, 43S-47S

Griesbacher T, Rainer I, Tiran B, Fink E, Lembeck F, Peskar BA, (2003), Mechanism of kinin release during experimental acute pancreatitis in rats: evidence for pro- as well as anti-inflammatory roles of oedema formation, *Br J Pharmacol*, **139**, 299-308

Griffiths WJ, (2000), Nanospray mass spectrometry in protein and peptide chemistry, *Exs*, **88**, 69-79

Guerrier L, Lomas L, Boschetti E, (2005), A simplified monobuffer multidimensional chromatography for high-throughput proteome fractionation, *J Chromatogr A*, **1073**, 25-33

Guido M, Rugge M, (2004), Liver biopsy sampling in chronic viral hepatitis, *Semin Liver Dis*, **24**, 89-97

Guillen MI, Gomez-Lechon MJ, Nakamura T, Castell JV, (1996), The hepatocyte growth factor regulates the synthesis of acute-phase proteins in human hepatocytes: divergent effect on interleukin-6-stimulated genes, *Hepatology*, **23**, 1345-52

Gygi SP, Rist B, Gerber SA, Turecek F, Gelb MH, Aebersold R, (1999), Quantitative analysis of complex protein mixtures using isotope-coded affinity tags, *Nat Biotechnol*, **17**, 994-9

Haber MM, West AB, Haber AD, Reuben A, (1995), Relationship of aminotransferases to liver histological status in chronic hepatitis C, *Am J Gastroenterol*, **90**, 1250-7

Hale LP, Price DT, Sanchez LM, Demark-Wahnefried W, Madden JF, (2001), Zinc alpha-2-glycoprotein is expressed by malignant prostatic epithelium and may serve as a potential serum marker for prostate cancer, *Clin Cancer Res*, **7**, 846-53

Halfon P, Imbert-Bismut F, Messous D, Antoniotti G, Benchetrit D, Cart-Lamy P, Delaporte G, Doutheau D, Klump T, Sala M, Thibaud D, Trepo E, Thabut D,

Myers RP, Poynard T, (2002), A prospective assessment of the inter-laboratory variability of biochemical markers of fibrosis (FibroTest) and activity (ActiTest) in patients with chronic liver disease, *Comp Hepatol*, **1**, 3

Hassner A, Birnbaum D, Loew LM, (1984), Charge-Shift Probes of Membrane Potential. Synthesis, *J Org Chem*, **49**, 2546-51

Hayden K, van Heyningen C, (2001), Measurement of total protein is a useful inclusion in liver function test profiles, *Clin Chem*, **47**, 793-4

He QY, Lau GK, Zhou Y, Yuen ST, Lin MC, Kung HF, Chiu JF, (2003), Serum biomarkers of hepatitis B virus infected liver inflammation: a proteomic study, *Proteomics*, **3**, 666-74

Herbert BR, Molloy MP, Gooley AA, Walsh BJ, Bryson WG, Williams KL, (1998), Improved protein solubility in two-dimensional electrophoresis using tributyl phosphine as reducing agent, *Electrophoresis*, **19**, 845-51

Hiramatsu S, Kojima J, Okada TT, Inai S, Ohmori K, (1976), The serum protein profile in chronic hepatitis, cirrhosis and liver cancer, *Acta Hepatogastroenterol (Stuttg)*, **23**, 177-82

Hirata M, Akbar SM, Horiike N, Onji M, (2001), Noninvasive diagnosis of the degree of hepatic fibrosis using ultrasonography in patients with chronic liver disease due to hepatitis C virus, *Eur J Clin Invest*, **31**, 528-35

Hochstrasser DF, Patchornik A, Merril CR, (1988), Development of polyacrylamide gels that improve the separation of proteins and their detection by silver staining, *Anal Biochem*, **173**, 412-23

Homann C, Varming K, Hogasen K, Mollnes TE, Graudal N, Thomsen AC, Garred P, (1997), Acquired C3 deficiency in patients with alcoholic cirrhosis predisposes to infection and increased mortality, *Gut*, **40**, 544-9

Hong WS, Hong SI, Park SY, Son Y, Lee YS, Chung YH, Yang SK, Suh DJ, Min YI, (1995), Elevation of serum type IV collagen in liver cancer as well as liver cirrhosis, *Anticancer Res*, **15**, 2777-80

Horejsi V, (2005), Lipid rafts and their roles in T-cell activation, *Microbes Infect*, **7**, 310-6

Houthaeve T, Gausepohl H, Ashman K, Nillson T, Mann M, (1997), Automated protein preparation techniques using a digest robot, *J Protein Chem*, **16**, 343-8

Huang YP, Cheng J, Zhang SL, Wang L, Guo J, Liu Y, Yang Y, Zhang LY, Bai GQ, Gao XS, Ji D, Lin SM, Shao Q, (2005), Screening of hepatocyte proteins

binding to F protein of hepatitis C virus by yeast two-hybrid system, *World J Gastroenterol*, **11**, 5659-65

Hunter AW, Wordeman L, (2000), How motor proteins influence microtubule polymerization dynamics, *J Cell Sci*, **113 Pt 24**, 4379-89

Hwang SJ, Luo JC, Lai CR, Chu CW, Tsay SH, Lu CL, Wu JC, Chang FY, Lee SD, (2000), Clinical, virologic and pathologic significance of elevated serum gamma-glutamyl transpeptidase in patients with chronic hepatitis C, *Zhonghua Yi Xue Za Zhi (Taipei)*, **63**, 527-35

Imbert-Bismut F, Ratziu V, Pieroni L, Charlotte F, Benhamou Y, Poynard T, (2001), Biochemical markers of liver fibrosis in patients with hepatitis C virus infection: a prospective study, *Lancet*, **357**, 1069-75

Ishak K, Baptista A, Bianchi L, Callea F, De Groote J, Gudat F, Denk H, Desmet V, Korb G, MacSween RN, et al., (1995), Histological grading and staging of chronic hepatitis, *J Hepatol*, **22**, 696-9

Jackson CJ, Xue M, Thompson P, Davey RA, Whitmont K, Smith S, Buisson-Legendre N, Sztynda T, Furphy LJ, Cooper A, Sambrook P, March L, (2005), Activated protein C prevents inflammation yet stimulates angiogenesis to promote cutaneous wound healing, *Wound Repair Regen*, **13**, 284-94

Jacobs JM, Adkins JN, Qian WJ, Liu T, Shen Y, Camp DG, 2nd, Smith RD, (2005), Utilizing human blood plasma for proteomic biomarker discovery, *J Proteome Res*, **4**, 1073-85

Jiang HQ, Zhang XL, Liu L, Yang CC, (2004), Relationship between focal adhesion kinase and hepatic stellate cell proliferation during rat hepatic fibrogenesis, *World J Gastroenterol*, **10**, 3001-5

Jiang XS, Tang LY, Dai J, Zhou H, Li SJ, Xia QC, Wu JR, Zeng R, (2005), Quantitative analysis of severe acute respiratory syndrome (SARS)-associated coronavirus-infected cells using proteomic approaches: implications for cellular responses to virus infection, *Mol Cell Proteomics*, **4**, 902-13

Joazeiro CA, Wing SS, Huang H, Leverson JD, Hunter T, Liu YC, (1999), The tyrosine kinase negative regulator c-Cbl as a RING-type, E2-dependent ubiquitin-protein ligase, *Science*, **286**, 309-12

Johansen JS, Christoffersen P, Moller S, Price PA, Henriksen JH, Garbarsch C, Bendtsen F, (2000), Serum YKL-40 is increased in patients with hepatic fibrosis, *J Hepatol*, **32**, 911-20

Jolly C, Kashefi K, Hollinshead M, Sattentau QJ, (2004), HIV-1 cell to cell transfer across an Env-induced, actin-dependent synapse, *J Exp Med*, **199**, 283-93

Joseph AM, Kumar M, Mitra D, (2005), Nef: "necessary and enforcing factor" in HIV infection, *Curr HIV Res*, **3**, 87-94

Josic D, Brown MK, Huang F, Lim YP, Rucevic M, Clifton JG, Hixson DC, (2006), Proteomic characterization of inter-alpha inhibitor proteins from human plasma, *Proteomics*,

Kalsheker N, Morley S, Morgan K, (2002), Gene regulation of the serine proteinase inhibitors alpha1-antitrypsin and alpha1-antichymotrypsin, *Biochem Soc Trans*, **30**, 93-8

Kasahara A, Hayashi N, Mochizuki K, Oshita M, Katayama K, Kato M, Masuzawa M, Yoshihara H, Naito M, Miyamoto T, Inoue A, Asai A, Hijioka T, Fusamoto H, Kamada T, (1997), Circulating matrix metalloproteinase-2 and tissue inhibitor of metalloproteinase-1 as serum markers of fibrosis in patients with chronic hepatitis C. Relationship to interferon response, *J Hepatol*, **26**, 574-83

Kawai H, Yomoda S, Inoue Y, (1991), ELISA using monoclonal antibody to human serum arylesterase, *Clin Chim Acta*, **202**, 219-25

Kawser CA, Iredale JP, Winwood PJ, Arthur MJ, (1998), Rat hepatic stellate cell expression of alpha2-macroglobulin is a feature of cellular activation: implications for matrix remodelling in hepatic fibrosis, *Clin Sci (Lond)*, **95**, 179-86

Kay BK, Williamson MP, Sudol M, (2000), The importance of being proline: the interaction of proline-rich motifs in signaling proteins with their cognate domains, *Faseb J*, **14**, 231-41

Kerenyi L, Gallyas F, (1972), A highly sensitive method for demonstrating proteins in electrophoretic, immunoelectrophoretic and immunodiffusion preparations, *Clin Chim Acta*, **38**, 465-7

Khundmiri SJ, Rane MJ, Lederer ED, (2003), Parathyroid hormone regulation of type II sodium-phosphate cotransporters is dependent on an A kinase anchoring protein, *J Biol Chem*, **278**, 10134-41

Kim W, Oe Lim S, Kim JS, Ryu YH, Byeon JY, Kim HJ, Kim YI, Heo JS, Park YM, Jung G, (2003), Comparison of proteome between hepatitis B virus- and hepatitis C virus-associated hepatocellular carcinoma, *Clin Cancer Res*, **9**, 5493-500

Kim YH, Chang SH, Kwon JH, Rhee SS, (1999), HIV-1 Nef plays an essential role in two independent processes in CD4 down-regulation: dissociation of the CD4-p56(lck) complex and targeting of CD4 to lysosomes, *Virology*, **257**, 208-19

Klose J, (1975), Protein mapping by combined isoelectric focusing and electrophoresis of mouse tissues. A novel approach to testing for induced point mutations in mammals, *Humangenetik*, **26**, 231-43

Kmiec Z, (2001), Cooperation of liver cells in health and disease, *Adv Anat Embryol Cell Biol*, **161**, III-XIII, 1-151

Knodell RG, Ishak KG, Black WC, Chen TS, Craig R, Kaplowitz N, Kiernan TW, Wollman J, (1981), Formulation and application of a numerical scoring system for assessing histological activity in asymptomatic chronic active hepatitis, *Hepatology*, **1**, 431-5

Krasilnikov MA, (2000), Phosphatidylinositol-3 kinase dependent pathways: the role in control of cell growth, survival, and malignant transformation, *Biochemistry (Mosc)*, **65**, 59-67

Krautkramer E, Giese SI, Gasteier JE, Muranyi W, Fackler OT, (2004), Human immunodeficiency virus type 1 Nef activates p21-activated kinase via recruitment into lipid rafts, *J Virol*, **78**, 4085-97

Lachmann PJ, Pangburn MK, Oldroyd RG, (1982), Breakdown of C3 after complement activation. Identification of a new fragment C3g, using monoclonal antibodies, *J Exp Med*, **156**, 205-16

Laemmli UK, (1970), Cleavage of structural proteins during the assembly of the head of bacteriophage T4, *Nature*, **227**, 680-5

Larsen JE, Massol RH, Nieland TJ, Kirchhausen T, (2004), HIV Nef-mediated major histocompatibility complex class I down-modulation is independent of Arf6 activity, *Mol Biol Cell*, **15**, 323-31

Lauer GM, Walker BD, (2001), Hepatitis C virus infection, *N Engl J Med*, **345**, 41-52

Law SK, Dodds AW, (1997), The internal thioester and the covalent binding properties of the complement proteins C3 and C4, *Protein Sci*, **6**, 263-74

Le Couteur DG, Fraser R, Cogger VC, McLean AJ, (2002), Hepatic pseudocapillarisation and atherosclerosis in ageing, *Lancet*, **359**, 1612-5

Leroy V, Arvieux J, Jacob MC, Maynard-Muet M, Baud M, Zarski JP, (1998), Prevalence and significance of anticardiolipin, anti-beta2 glycoprotein I and anti-prothrombin antibodies in chronic hepatitis C, *Br J Haematol*, **101**, 468-74

Leroy V, Monier F, Bottari S, Trocme C, Sturm N, Hilleret MN, Morel F, Zarski JP, (2004), Circulating matrix metalloproteinases 1, 2, 9 and their inhibitors TIMP-1 and TIMP-2 as serum markers of liver fibrosis in patients with chronic hepatitis C: comparison with PIIINP and hyaluronic acid, *Am J Gastroenterol*, **99**, 271-9

LeVier DG, McCay JA, Stern ML, Harris LS, Page D, Brown RD, Musgrove DL, Butterworth LF, White KL, Jr., Munson AE, (1994), Immunotoxicological profile of morphine sulfate in B6C3F1 female mice, *Fundam Appl Toxicol*, **22**, 525-42

Li C, Hong Y, Tan YX, Zhou H, Ai JH, Li SJ, Zhang L, Xia QC, Wu JR, Wang HY, Zeng R, (2004), Accurate qualitative and quantitative proteomic analysis of clinical hepatocellular carcinoma using laser capture microdissection coupled with isotope-coded affinity tag and two-dimensional liquid chromatography mass spectrometry, *Mol Cell Proteomics*, **3**, 399-409

Libra M, Gasparotto D, Gloghini A, Navolanic PM, De Re V, Carbone A, (2005), Hepatitis C virus (HCV) I hepatitis C virus (HCV) infection and lymphoproliferative disorders, *Front Biosci*, **10**, 2460-71

Lim SO, Park SJ, Kim W, Park SG, Kim HJ, Kim YI, Sohn TS, Noh JH, Jung G, (2002), Proteome analysis of hepatocellular carcinoma, *Biochem Biophys Res Commun*, **291**, 1031-7

Limdi JK, Hyde GM, (2003), Evaluation of abnormal liver function tests, *Postgrad Med J*, **79**, 307-12

Lin SD, Endo R, Kuroda H, Kondo K, Miura Y, Takikawa Y, Kato A, Suzuki K, (2004), Plasma and urine levels of urinary trypsin inhibitor in patients with chronic liver diseases and hepatocellular carcinoma, *J Gastroenterol Hepatol*, **19**, 327-32

Lindenbach BD, Rice CM, (2005), Unravelling hepatitis C virus replication from genome to function, *Nature*, **436**, 933-8

Linnemann T, Zheng YH, Mandic R, Peterlin BM, (2002), Interaction between Nef and phosphatidylinositol-3-kinase leads to activation of p21-activated kinase and increased production of HIV, *Virology*, **294**, 246-55

Liu YC, Elly C, Yoshida H, Bonnefoy-Berard N, Altman A, (1996), Activation-modulated association of 14-3-3 proteins with Cbl in T cells, *J Biol Chem*, **271**, 14591-5

Ljubimova JY, Petrovic LM, Wilson SE, Geller SA, Demetriou AA, (1997), Expression of HGF, its receptor c-met, c-myc, and albumin in cirrhotic and neoplastic human liver tissue, *J Histochem Cytochem*, **45**, 79-87

Lorentz K, Flatter B, Augustin E, (1979), Arylesterase in serum: elaboration and clinical application of a fixed-incubation method, *Clin Chem*, **25**, 1714-20

Lotfy M, El-Kady IM, Nasif WA, El-Kenawy AE, Badra G, (2006), Distinct serum immunoglobulins pattern in Egyptian patients with chronic HCV infection analyzed by nephelometry, *J Immunoassay Immunochem*, **27**, 103-14

Low TY, Leow CK, Salto-Tellez M, Chung MC, (2004), A proteomic analysis of thioacetamide-induced hepatotoxicity and cirrhosis in rat livers, *Proteomics*, **4**, 3960-74

Lu X, Wu X, Plemenitas A, Yu H, Sawai ET, Abo A, Peterlin BM, (1996), CDC42 and Rac1 are implicated in the activation of the Nef-associated kinase and replication of HIV-1, *Curr Biol*, **6**, 1677-84

Mackintosh JA, Choi HY, Bae SH, Veal DA, Bell PJ, Ferrari BC, Van Dyk DD, Verrills NM, Paik YK, Karuso P, (2003), A fluorescent natural product for ultra sensitive detection of proteins in one-dimensional and two-dimensional gel electrophoresis, *Proteomics*, **3**, 2273-88

MacSween R, Burt A, Portmann B, Ishak K, Scheuer P, Anthony P, (2002), Pathology of the Liver, 4th Edition, *Churchill Livingstone*

Mardini H, Record C, (2005), Detection assessment and monitoring of hepatic fibrosis: biochemistry or biopsy?, *Ann Clin Biochem*, **42**, 441-7

Marengere LE, Mirtsos C, Kozieradzki I, Veillette A, Mak TW, Penninger JM, (1997), Proto-oncoprotein Vav interacts with c-Cbl in activated thymocytes and peripheral T cells, *J Immunol*, **159**, 70-6

Markel A, Brook JG, Aviram M, (1985), Increased plasma triglycerides, cholesterol and apolipoprotein E during prolonged fasting in normal subjects, *Postgrad Med J*, **61**, 395-400

Massol RH, Larsen JE, Kirchhausen T, (2005), Possible role of deep tubular invaginations of the plasma membrane in MHC-I trafficking, *Exp Cell Res*, **306**, 142-9

McDonald D, Wu L, Bohks SM, KewalRamani VN, Unutmaz D, Hope TJ, (2003), Recruitment of HIV and its receptors to dendritic cell-T cell junctions, *Science*, **300**, 1295-7

McHutchison JG, Poynard T, (1999), Combination therapy with interferon plus ribavirin for the initial treatment of chronic hepatitis C, *Semin Liver Dis*, **19 Suppl 1**, 57-65

Mehdi H, Kaplan MJ, Anlar FY, Yang X, Bayer R, Sutherland K, Peeples ME, (1994), Hepatitis B virus surface antigen binds to apolipoprotein H, *J Virol*, **68**, 2415-24

Mehta A, (2005), Glycoproteomic tools for the discovery of biomarkers of primary hepatocellular carcinoma, *Glycobiology Institute Seminars,* University of Oxford

Meliconi R, Parracino O, Facchini A, Morselli-Labate AM, Bortolotti F, Tremolada F, Martuzzi M, Miglio F, Gasbarrini G, (1988), Acute phase proteins in chronic and malignant liver diseases, *Liver*, **8**, 65-74

Meyer TS, Lamberts BL, (1965), Use of coomassie brilliant blue R250 for the electrophoresis of microgram quantities of parotid saliva proteins on acrylamide-gel strips, *Biochim Biophys Acta*, **107**, 144-5

Miura-Shimura Y, Duan L, Rao NL, Reddi AL, Shimura H, Rottapel R, Druker BJ, Tsygankov A, Band V, Band H, (2003), Cbl-mediated ubiquitinylation and negative regulation of Vav, *J Biol Chem*, **278**, 38495-504

Mondelli MU, Cerino A, Cividini A, (2005), Acute hepatitis C: diagnosis and management, *J Hepatol*, **42 Suppl**, S108-14

Montazeri G, Estakhri A, Mohamadnejad M, Nouri N, Montazeri F, Mohammadkani A, Derakhshan MH, Zamani F, Samiee S, Malekzadeh R, (2005), Serum hyaluronate as a non-invasive marker of hepatic fibrosis and inflammation in HBeAg-negative chronic hepatitis B, *BMC Gastroenterol*, **5**, 32

Morelle W, Flahaut C, Michalski JC, Louvet A, Mathurin P, Klein A, (2006), Mass spectrometric approach for screening modifications of total serum N-glycome in human diseases: application to cirrhosis, *Glycobiology*, **16**, 281-93

Moriya K, Yotsuyanagi H, Shintani Y, Fujie H, Ishibashi K, Matsuura Y, Miyamura T, Koike K, (1997), Hepatitis C virus core protein induces hepatic steatosis in transgenic mice, *J Gen Virol*, **78 (Pt 7)**, 1527-31

Moshage H, (1997), Cytokines and the hepatic acute phase response, *J Pathol*, **181**, 257-66

Moustafellos E, Illueca M, Remotti HE, Auld PA, Hanauske-Abel HM, (2000), Objective ranking of fibrosis in standard histologic sections of human neonatal

liver: applicability to alpha1-antitrypsin deficiency, *J Pediatr Gastroenterol Nutr*, **30**, 503-8

Myers RP, De Torres M, Imbert-Bismut F, Ratziu V, Charlotte F, Poynard T, (2003), Biochemical markers of fibrosis in patients with chronic hepatitis C: a comparison with prothrombin time, platelet count, and age-platelet index, *Dig Dis Sci*, **48**, 146-53

Nagaoka MR, Kouyoumdjian M, Borges DR, (2003), Hepatic clearance of tissue-type plasminogen activator and plasma kallikrein in experimental liver fibrosis, *Liver Int*, **23**, 476-83

Naoumov NV, Chokshi S, Metivier E, Maertens G, Johnson PJ, Williams R, (1997), Hepatitis C virus infection in the development of hepatocellular carcinoma in cirrhosis, *J Hepatol*, **27**, 331-6

Naveau S, Poynard T, Benattar C, Bedossa P, Chaput JC, (1994), Alpha-2-macroglobulin and hepatic fibrosis. Diagnostic interest, *Dig Dis Sci*, **39**, 2426-32

Neuhoff V, Stamm R, Eibl H, (1985), Clear background and highly sensitive protein staining with Coomassie Blue dyes in polyacrylamide gels: A systematic analysis, *Electrophoresis*, **6**, 427–48

Nguyen MH, Keeffe EB, (2005), Prevalence and treatment of hepatitis C virus genotypes 4, 5, and 6, *Clin Gastroenterol Hepatol*, **3**, S97-S101

Nishimura H, Kakizaki I, Muta T, Sasaki N, Pu PX, Yamashita T, Nagasawa S, (1995), cDNA and deduced amino acid sequence of human PK-120, a plasma kallikrein-sensitive glycoprotein, *FEBS Lett*, **357**, 207-11

Nousbaum JB, Pol S, Nalpas B, Landais P, Berthelot P, Brechot C, (1995), Hepatitis C virus type 1b (II) infection in France and Italy. Collaborative Study Group, *Ann Intern Med*, **122**, 161-8

Nyberg A, Berne B, Nordlinder H, Busch C, Eriksson U, Loof L, Vahlquist A, (1988), Impaired release of vitamin A from liver in primary biliary cirrhosis, *Hepatology*, **8**, 136-41

O'Farrell PH, (1975), High resolution two-dimensional electrophoresis of proteins, *J Biol Chem*, **250**, 4007-21

Oh-Ishi M, Maeda T, (2002), Separation techniques for high-molecular-mass proteins, *J Chromatogr B Analyt Technol Biomed Life Sci*, **771**, 49-66

Okafor O, Ojo S, (2004), A comparative analysis of six current histological classification schemes and scoring systems used in chronic hepatitis reporting, *Rev Esp Patol*, **37**, 269-77

Ong SE, Blagoev B, Kratchmarova I, Kristensen DB, Steen H, Pandey A, Mann M, (2002), Stable isotope labeling by amino acids in cell culture, SILAC, as a simple and accurate approach to expression proteomics, *Mol Cell Proteomics*, **1**, 376-86

Ong TZ, Tan HJ, (2003), Ultrasonography is not reliable in diagnosing liver cirrhosis in clinical practice, *Singapore Med J*, **44**, 293-5

Owen CA, Campbell EJ, (1998), Angiotensin II generation at the cell surface of activated neutrophils: novel cathepsin G-mediated catalytic activity that is resistant to inhibition, *J Immunol*, **160**, 1436-43

Owens D, Jones EA, Carson ER, (1977), Studies on the kinetics of unconjugated [14C]bilirubin metabolism in normal subjects and patients with compensated cirrhosis, *Clin Sci Mol Med*, **52**, 555-70

Page NM, Butlin DJ, Lomthaisong K, Lowry PJ, (2001), The human apolipoprotein L gene cluster: identification, classification, and sites of distribution, *Genomics*, **74**, 71-8

Paradis V, (2005), Glycomics: a new taste of cirrhosis marker, *J Hepatol*, **43**, 913-4

Paradis V, Laurent A, Mathurin P, Poynard T, Vidaud D, Vidaud M, Bedossa P, (1996a), Role of liver extracellular matrix in transcriptional and post-transcriptional regulation of apolipoprotein A-I by hepatocytes, *Cell Mol Biol (Noisy-le-grand)*, **42**, 525-34

Paradis V, Mathurin P, Ratziu V, Poynard T, Bedossa P, (1996b), Binding of apolipoprotein A-I and acetaldehyde-modified apolipoprotein A-I to liver extracellular matrix, *Hepatology*, **23**, 1232-8

Pares A, Deulofeu R, Gimenez A, Caballeria L, Bruguera M, Caballeria J, Ballesta AM, Rodes J, (1996), Serum hyaluronate reflects hepatic fibrogenesis in alcoholic liver disease and is useful as a marker of fibrosis, *Hepatology*, **24**, 1399-403

Park GJ, Lin BP, Ngu MC, Jones DB, Katelaris PH, (2000), Aspartate aminotransferase: alanine aminotransferase ratio in chronic hepatitis C infection: is it a useful predictor of cirrhosis?, *J Gastroenterol Hepatol*, **15**, 386-90

Park SY, Kang KH, Park JH, Lee JH, Cho CM, Tak WY, Kweon YO, Kim SK, Choi YH, (2004), Clinical efficacy of AST/ALT ratio and platelet counts as predictors of degree of fibrosis in HBV infected patients without clinically evident liver cirrhosis, *Korean J Gastroenterol*, **43**, 246-51

Patel K, Lajoie A, Heaton S, Pianko S, Behling CA, Bylund D, Pockros PJ, Blatt LM, Conrad A, McHutchison JG, (2003), Clinical use of hyaluronic acid as a predictor of fibrosis change in hepatitis C, *J Gastroenterol Hepatol*, **18**, 253-7

Pavlović D, Neville DC, Argaud O, Blumberg B, Dwek RA, Fischer WB, Zitzmann N, (2003), The hepatitis C virus p7 protein forms an ion channel that is inhibited by long-alkyl-chain iminosugar derivatives, *Proc Natl Acad Sci U S A*, **100**, 6104-8

Peats S, (1984), Quantitation of protein and DNA in silver-stained agarose gels, *Anal Biochem*, **140**, 178-82

Pelech S, (2004), Tracking cell signaling protein expression and phosphorylation by innovative proteomic solutions, *Curr Pharm Biotechnol*, **5**, 69-77

Perdew GH, Schaup HW, Selivonchick DP, (1983), The use of a zwitterionic detergent in two-dimensional gel electrophoresis of trout liver microsomes, *Anal Biochem*, **135**, 453-5

Perkins DN, Pappin DJ, Creasy DM, Cottrell JS, (1999), Probability-based protein identification by searching sequence databases using mass spectrometry data, *Electrophoresis*, **20**, 3551-67

Perlemuter G, Sabile A, Letteron P, Vona G, Topilco A, Chretien Y, Koike K, Pessayre D, Chapman J, Barba G, Brechot C, (2002), Hepatitis C virus core protein inhibits microsomal triglyceride transfer protein activity and very low density lipoprotein secretion: a model of viral-related steatosis, *Faseb J*, **16**, 185-94

Petricoin EF, Liotta LA, (2003), Clinical applications of proteomics, *J Nutr*, **133**, 2476S-2484S

Pileri P, Uematsu Y, Campagnoli S, Galli G, Falugi F, Petracca R, Weiner AJ, Houghton M, Rosa D, Grandi G, Abrignani S, (1998), Binding of hepatitis C virus to CD81, *Science*, **282**, 938-41

Pol S, Poynard T, Bedossa P, Naveau S, Aubert A, Chaput JC, (1990), Diagnostic value of serum gamma-glutamyl-transferase activity and mean corpuscular volume in alcoholic patients with or without cirrhosis, *Alcohol Clin Exp Res*, **14**, 250-4

Poli G, (2000), Pathogenesis of liver fibrosis: role of oxidative stress, *Mol Aspects Med*, **21**, 49-98

Poon TC, Hui AY, Chan HL, Ang IL, Chow SM, Wong N, Sung JJ, (2005), Prediction of liver fibrosis and cirrhosis in chronic hepatitis B infection by serum proteomic fingerprinting: a pilot study, *Clin Chem*, **51**, 328-35

Poynard T, Bedossa P, (1997), Age and platelet count: a simple index for predicting the presence of histological lesions in patients with antibodies to hepatitis C virus. METAVIR and CLINIVIR Cooperative Study Groups, *J Viral Hepat*, **4**, 199-208

Poynard T, Imbert-Bismut F, Munteanu M, Messous D, Myers RP, Thabut D, Ratziu V, Mercadier A, Benhamou Y, Hainque B, (2004a), Overview of the diagnostic value of biochemical markers of liver fibrosis (FibroTest, HCV FibroSure) and necrosis (ActiTest) in patients with chronic hepatitis C, *Comp Hepatol*, **3**, 8

Poynard T, Munteanu M, Imbert-Bismut F, Charlotte F, Thabut D, Le Calvez S, Messous D, Thibault V, Benhamou Y, Moussalli J, Ratziu V, (2004b), Prospective analysis of discordant results between biochemical markers and biopsy in patients with chronic hepatitis C, *Clin Chem*, **50**, 1344-55

Pratt CW, Roche PA, Pizzo SV, (1987), The role of inter-alpha-trypsin inhibitor and other proteinase inhibitors in the plasma clearance of neutrophil elastase and plasmin, *Arch Biochem Biophys*, **258**, 591-9

Puoti C, (2003), HCV carriers with persistently normal aminotransferase levels: normal does not always mean healthy, *J Hepatol*, **38**, 529-32

Purcell R, (1997), The hepatitis C virus: overview, *Hepatology*, **26**, 11S-14S

Purohit V, Brenner DA, (2006), Mechanisms of alcohol-induced hepatic fibrosis: a summary of the Ron Thurman Symposium, *Hepatology*, **43**, 872-8

Qiu Y, Hoshida Y, Kato N, Moriyama M, Otsuka M, Taniguchi H, Kawabe T, Omata M, (2004), A simple combination of serum type IV collagen and prothrombin time to diagnose cirrhosis in patients with chronic active hepatitis C, *Hepatol Res*, **30**, 214-220

Quilliot D, Walters E, Guerci B, Fruchart JC, Duriez P, Drouin P, Ziegler O, (2001), Effect of the inflammation, chronic hyperglycemia, or malabsorption on the apolipoprotein A-IV concentration in type 1 diabetes mellitus and in diabetes secondary to chronic pancreatitis, *Metabolism*, **50**, 1019-24

Rabilloud T, (1998), Use of thiourea to increase the solubility of membrane proteins in two-dimensional electrophoresis, *Electrophoresis*, **19**, 758-60

Rachfal AW, Brigstock DR, (2003), Connective tissue growth factor (CTGF/CCN2) in hepatic fibrosis, *Hepatol Res*, **26**, 1-9

Rahimi Z, Merat A, Haghshenass M, Madani H, Rezaei M, Nagel RL, (2006), Plasma lipids in Iranians with sickle cell disease: hypocholesterolemia in sickle cell anemia and increase of HDL-cholesterol in sickle cell trait, *Clin Chim Acta*, **365**, 217-20

Reichel C, Sudhop T, Braun B, Kreuzer KA, Hahn C, Look MP, von Bergmann K, Sauerbruch T, Spengler U, (2000), Elevated soluble tumour necrosis factor receptor serum concentrations and short-term mortality in liver cirrhosis without acute infections, *Digestion*, **62**, 44-51

Ren FR, Lv QS, Zhuang H, Li JJ, Gong XY, Gao GJ, Liu CL, Wang JX, Yao FZ, Zheng YR, Zhu FM, Tiemuer MH, Bai XH, Shan H, (2005), Significance of the signal-to-cutoff ratios of anti-hepatitis C virus enzyme immunoassays in screening of Chinese blood donors, *Transfusion*, **45**, 1816-22

Rimola A, (2003), Beneficial effects of drugs interfering with the renin-angiotensin system on the development of fibrosis in hepatitis C recurrence after liver transplantation, *Am J Transplan*, **5**, 433

Roche PA, Pizzo SV, (1988), Analysis of thiolester bond cleavage-dependent conformational changes in binary alpha 2-macroglobulin-proteinase complexes, *Arch Biochem Biophys*, **267**, 285-93

Rosenthal-Allieri MA, Peritore ML, Tran A, Halfon P, Benzaken S, Bernard A, (2005), Analytical variability of the Fibrotest proteins, *Clin Biochem*, **38**, 473-8

Ross PL, Huang YN, Marchese JN, Williamson B, Parker K, Hattan S, Khainovski N, Pillai S, Dey S, Daniels S, Purkayastha S, Juhasz P, Martin S, Bartlet-Jones M, He F, Jacobson A, Pappin DJ, (2004), Multiplexed protein quantitation in Saccharomyces cerevisiae using amine-reactive isobaric tagging reagents, *Mol Cell Proteomics*, **3**, 1154-69

Ross TM, Oran AE, Cullen BR, (1999), Inhibition of HIV-1 progeny virion release by cell-surface CD4 is relieved by expression of the viral Nef protein, *Curr Biol*, **9**, 613-21

Rossi E, Adams L, Prins A, Bulsara M, de Boer B, Garas G, MacQuillan G, Speers D, Jeffrey G, (2003), Validation of the FibroTest biochemical markers score in assessing liver fibrosis in hepatitis C patients, *Clin Chem*, **49**, 450-4

Roussel J, Pillez A, Montpellier C, Duverlie G, Cahour A, Dubuisson J, Wychowski C, (2003), Characterization of the expression of the hepatitis C virus F protein, *J Gen Virol*, **84**, 1751-9

Russo MW, Firpi RJ, Nelson DR, Schoonhoven R, Shrestha R, Fried MW, (2005), Early hepatic stellate cell activation is associated with advanced fibrosis after liver transplantation in recipients with hepatitis C, *Liver Transpl*, **11**, 1235-41

Sabile A, Perlemuter G, Bono F, Kohara K, Demaugre F, Kohara M, Matsuura Y, Miyamura T, Brechot C, Barba G, (1999), Hepatitis C virus core protein binds to apolipoprotein AII and its secretion is modulated by fibrates, *Hepatology*, **30**, 1064-76

Sagnelli E, Coppola N, Marrocco C, Coviello G, Battaglia M, Messina V, Rossi G, Sagnelli C, Scolastico C, Filippini P, (2005), Diagnosis of hepatitis C virus related acute hepatitis by serial determination of IgM anti-HCV titres, *J Hepatol*, **42**, 646-51

Saksela K, Cheng G, Baltimore D, (1995), Proline-rich (PxxP) motifs in HIV-1 Nef bind to SH3 domains of a subset of Src kinases and are required for the enhanced growth of Nef+ viruses but not for down-regulation of CD4, *Embo J*, **14**, 484-91

Sanchez JC, Rouge V, Pisteur M, Ravier F, Tonella L, Moosmayer M, Wilkins MR, Hochstrasser DF, (1997), Improved and simplified in-gel sample application using reswelling of dry immobilized pH gradients, *Electrophoresis*, **18**, 324-7

Sandrin L, Fourquet B, Hasquenoph JM, Yon S, Fournier C, Mal F, Christidis C, Ziol M, Poulet B, Kazemi F, Beaugrand M, Palau R, (2003), Transient elastography: a new noninvasive method for assessment of hepatic fibrosis, *Ultrasound Med Biol*, **29**, 1705-13

Santos VN, Leite-Mor MM, Kondo M, Martins JR, Nader H, Lanzoni VP, Parise ER, (2005), Serum laminin, type IV collagen and hyaluronan as fibrosis markers in non-alcoholic fatty liver disease, *Braz J Med Biol Res*, **38**, 747-53

Savendahl L, Underwood LE, (1999), Fasting increases serum total cholesterol, LDL cholesterol and apolipoprotein B in healthy, nonobese humans, *J Nutr*, **129**, 2005-8

Scarselli E, Ansuini H, Cerino R, Roccasecca RM, Acali S, Filocamo G, Traboni C, Nicosia A, Cortese R, Vitelli A, (2002), The human scavenger receptor class B type I is a novel candidate receptor for the hepatitis C virus, *Embo J*, **21**, 5017-25

Schulenberg B, Patton WF, (2004), Combining microscale solution-phase isoelectric focusing with Multiplexed Proteomics dye staining to analyze protein post-translational modifications, *Electrophoresis*, **25**, 2539-44

Schuppan D, Krebs A, Bauer M, Hahn EG, (2003), Hepatitis C and liver fibrosis, *Cell Death Differ*, **10 Suppl 1**, S59-67

Schuppan D, Ruehl M, Somasundaram R, Hahn EG, (2001), Matrix as a modulator of hepatic fibrogenesis, *Semin Liver Dis*, **21**, 351-72

Schwartz O, Marechal V, Le Gall S, Lemonnier F, Heard JM, (1996), Endocytosis of major histocompatibility complex class I molecules is induced by the HIV-1 Nef protein, *Nat Med*, **2**, 338-42

Schwegler EE, Cazares L, Steel LF, Adam BL, Johnson DA, Semmes OJ, Block TM, Marrero JA, Drake RR, (2005), SELDI-TOF MS profiling of serum for detection of the progression of chronic hepatitis C to hepatocellular carcinoma, *Hepatology*, **41**, 634-42

Seibert V, Wiesner A, Buschmann T, Meuer J, (2004), Surface-enhanced laser desorption ionization time-of-flight mass spectrometry (SELDI TOF-MS) and ProteinChip technology in proteomics research, *Pathol Res Pract*, **200**, 83-94

Seow TK, Ong SE, Liang RC, Ren EC, Chan L, Ou K, Chung MC, (2000), Two-dimensional electrophoresis map of the human hepatocellular carcinoma cell line, HCC-M, and identification of the separated proteins by mass spectrometry, *Electrophoresis*, **21**, 1787-813

Shapland C, Hsuan JJ, Totty NF, Lawson D, (1993), Purification and properties of transgelin: a transformation and shape change sensitive actin-gelling protein, *J Cell Biol*, **121**, 1065-73

Shevchenko A, Wilm M, Vorm O, Mann M, (1996), Mass spectrometric sequencing of proteins silver-stained polyacrylamide gels, *Anal Chem*, **68**, 850-8

Shim JK, Lee YC, Chung TH, Kim CH, (2004), Elevated expression of bisecting N-acetylglucosaminyltransferase-III gene in a human fetal hepatocyte cell line by hepatitis B virus, *J Gastroenterol Hepatol*, **19**, 1374-87

Shimizu I, (2001), Antifibrogenic therapies in chronic HCV infection, *Curr Drug Targets Infect Disord*, **1**, 227-40

Shin JY, Hur W, Wang JS, Jang JW, Kim CW, Bae SH, Jang SK, Yang SH, Sung YC, Kwon OJ, Yoon SK, (2005), HCV core protein promotes liver fibrogenesis via up-regulation of CTGF with TGF-beta1, *Exp Mol Med*, **37**, 138-45

Siciliano M, De Candia E, Ballarin S, Vecchio FM, Servidei S, Annese R, Landolfi R, Rossi L, (2000), Hepatocellular carcinoma complicating liver cirrhosis in type IIIa glycogen storage disease, *J Clin Gastroenterol*, **31**, 80-2

Sidhaye A, (2005), Medical Encyclopedia entry for "Total protein"; U.S. National Library of Medicine and the National Institutes of Health, http://www.nlm.nih.gov/medlineplus/ency/article/003483.htm#Normal%20Values

Siegmund SV, Brenner DA, (2005), Molecular pathogenesis of alcohol-induced hepatic fibrosis, *Alcohol Clin Exp Res*, **29**, 102S-109S

Sierra S, Kupfer B, Kaiser R, (2005), Basics of the virology of HIV-1 and its replication, *J Clin Virol*, **34**, 233-44

Siller-Lopez F, Sandoval A, Salgado S, Salazar A, Bueno M, Garcia J, Vera J, Galvez J, Hernandez I, Ramos M, Aguilar-Cordova E, Armendariz-Borunda J, (2004), Treatment with human metalloproteinase-8 gene delivery ameliorates experimental rat liver cirrhosis, *Gastroenterology*, **126**, 1122-33; discussion 949

Silva IS, Ferraz ML, Perez RM, Lanzoni VP, Figueiredo VM, Silva AE, (2004), Role of gamma-glutamyl transferase activity in patients with chronic hepatitis C virus infection, *J Gastroenterol Hepatol*, **19**, 314-8

Simmons A, Aluvihare V, McMichael A, (2001), Nef triggers a transcriptional program in T cells imitating single-signal T cell activation and inducing HIV virulence mediators, *Immunity*, **14**, 763-77

Simmons A, Gangadharan B, Hodges A, Sharrocks K, Prabhakar S, Garcia A, Dwek R, Zitzmann N, McMichael A, (2005), Nef-mediated lipid raft exclusion of UbcH7 inhibits Cbl activity in T cells to positively regulate signaling, *Immunity*, **23**, 621-34

Simons K, Ikonen E, (1997), Functional rafts in cell membranes, *Nature*, **387**, 569-72

Simons K, Toomre D, (2000), Lipid rafts and signal transduction, *Nat Rev Mol Cell Biol*, **1**, 31-9

Sjoberg K, Alm R, Eriksson S, (1992), Angiotensinogen in chronic liver disease, *Scand J Clin Lab Invest*, **52**, 57-63

Skerka C, Hellwage J, Weber W, Tilkorn A, Buck F, Marti T, Kampen E, Beisiegel U, Zipfel PF, (1997), The human factor H-related protein 4 (FHR-4). A novel short consensus repeat-containing protein is associated with human triglyceride-rich lipoproteins, *J Biol Chem*, **272**, 5627-34

Smith PK, Krohn RI, Hermanson GT, Mallia AK, Gartner FH, Provenzano MD, Fujimoto EK, Goeke NM, Olson BJ, Klenk DC, (1985), Measurement of protein using bicinchoninic acid, *Anal Biochem*, **150**, 76-85

Stanosek J, Bojarski Z, Jahns K, Gregorczyk J, Modzelewska H, (1965), Gamma-glutamyl transpeptidase activity and serum bilirubin diglucuronide level in viral hepatitis and their comparison with other liver tests, *Pol Tyg Lek*, **20**, 1407-9

Steel LF, Mattu TS, Mehta A, Hebestreit H, Dwek R, Evans AA, London WT, Block T, (2001), A proteomic approach for the discovery of early detection markers of hepatocellular carcinoma, *Dis Markers*, **17**, 179-89

Steel LF, Shumpert D, Trotter M, Seeholzer SH, Evans AA, London WT, Dwek R, Block TM, (2003a), A strategy for the comparative analysis of serum proteomes for the discovery of biomarkers for hepatocellular carcinoma, *Proteomics*, **3**, 601-9

Steel LF, Trotter MG, Nakajima PB, Mattu TS, Gonye G, Block T, (2003b), Efficient and specific removal of albumin from human serum samples, *Mol Cell Proteomics*, **2**, 262-70

Sunayama T, Okada Y, Tsuji T, (1993), Elevated plasma levels of a carbohydrate antigen, sialyl Lewis X, in liver diseases, *J Hepatol*, **19**, 451-8

Surrenti C, Casini A, Milani S, Ambu S, Ceccatelli P, D'Agata A, (1987), Is determination of serum N-terminal procollagen type III peptide (sPIIIP) a marker of hepatic fibrosis?, *Dig Dis Sci*, **32**, 705-9

Swann SA, Williams M, Story CM, Bobbitt KR, Fleis R, Collins KL, (2001), HIV-1 Nef blocks transport of MHC class I molecules to the cell surface via a PI 3-kinase-dependent pathway, *Virology*, **282**, 267-77

Tabone M, Secreto P, Marini C, Bonardi R, Boero M, Taraglio S, Ercole E, Sallio Bruno F, Pera A, (1997), Pre-treatment levels of anti-HCV core IgM antibodies are closely associated with response to alpha interferon therapy in chronic hepatitis C patients, *Eur J Gastroenterol Hepatol*, **9**, 287-91

Tang HY, Speicher DW, (2005), Complex proteome prefractionation using microscale solution isoelectrofocusing, *Expert Rev Proteomics*, **2**, 295-306

Tarao K, Rino Y, Ohkawa S, Endo O, Miyakawa K, Tamai S, Hirokawa S, Masaki T, Nagaoka T, Okamoto N, Tanaka K, Tarao N, (2004), Sustained low alanine aminotransferase levels can predict the survival for 10 years without hepatocellular carcinoma development in patients with hepatitis C virus-associated liver cirrhosis of child stage A, *Intervirology*, **47**, 65-71

Tarao K, Rino Y, Ohkawa S, Shimizu A, Tamai S, Miyakawa K, Aoki H, Imada T, Shindo K, Okamoto N, Totsuka S, (1999), Association between high serum alanine aminotransferase levels and more rapid development and higher rate of incidence of hepatocellular carcinoma in patients with hepatitis C virus-associated cirrhosis, *Cancer*, **86**, 589-95

Thampanitchawong P, Piratvisuth T, (1999), Liver biopsy:complications and risk factors, *World J Gastroenterol*, **5**, 301-304

Thien CB, Langdon WY, (2005), c-Cbl and Cbl-b ubiquitin ligases: substrate diversity and the negative regulation of signalling responses, *Biochem J*, **391**, 153-66

Thomas RM, Schiano TD, Kueppers F, Black M, (2000), Alpha1-antichymotrypsin globules within hepatocytes in patients with chronic hepatitis C and cirrhosis, *Hum Pathol*, **31**, 575-7

Thuluvath PJ, Krok KL, (2005), Noninvasive markers of fibrosis for longitudinal assessment of fibrosis in chronic liver disease: are they ready for prime time?, *Am J Gastroenterol*, **100**, 1981-3

Tiggelman AM, Boers W, Moorman AF, de Boer PA, Van der Loos CM, Rotmans JP, Chamuleau RA, (1996), Localization of alpha 2-macroglobulin protein and messenger RNA in rat liver fibrosis: evidence for the synthesis of alpha 2-macroglobulin within Schistosoma mansoni egg granulomas, *Hepatology*, **23**, 1260-7

Tilg H, Diehl AM, (2000), Cytokines in alcoholic and nonalcoholic steatohepatitis, *N Engl J Med*, **343**, 1467-76

Tissot JD, Sanchez JC, Vuadens F, Scherl A, Schifferli JA, Hochstrasser DF, Schneider P, Duchosal MA, (2002), IgM are associated to Sp alpha (CD5 antigen-like), *Electrophoresis*, **23**, 1203-6

Tissot JD, Schifferli JA, Hochstrasser DF, Pasquali C, Spertini F, Clement F, Frutiger S, Paquet N, Hughes GJ, Schneider P, (1994), Two-dimensional polyacrylamide gel electrophoresis analysis of cryoglobulins and identification of an IgM-associated peptide, *J Immunol Methods*, **173**, 63-75

Tonella L, Walsh BJ, Sanchez JC, Ou K, Wilkins MR, Tyler M, Frutiger S, Gooley AA, Pescaru I, Appel RD, Yan JX, Bairoch A, Hoogland C, Morch FS, Hughes GJ, Williams KL, Hochstrasser DF, (1998), '98 Escherichia coli SWISS-2DPAGE database update, *Electrophoresis*, **19**, 1960-71

Truden JL, Boros DL, (1988), Detection of alpha 2-macroglobulin, alpha 1-protease inhibitor, and neutral protease-antiprotease complexes within liver granulomas of Schistosoma mansoni-infected mice, *Am J Pathol*, **130**, 281-8

Tsutsumi M, Takase S, Urashima S, Ueshima Y, Kawahara H, Takada A, (1996), Serum markers for hepatic fibrosis in alcoholic liver disease: which is the best marker, type III procollagen, type IV collagen, laminin, tissue inhibitor of metalloproteinase, or prolyl hydroxylase?, *Alcohol Clin Exp Res*, **20**, 1512-7

Ulrich D, Noah EM, Burchardt ER, Atkins D, Pallua N, (2002), Serum concentration of amino-terminal propeptide of type III procollagen (PIIINP) as a prognostic marker for skin fibrosis after scar correction in burned patients, *Burns*, **28**, 766-71

Ulrich D, Noah EM, von Heimburg D, Pallua N, (2003), TIMP-1, MMP-2, MMP-9, and PIIINP as serum markers for skin fibrosis in patients following severe burn trauma, *Plast Reconstr Surg*, **111**, 1423-31

Underwood J, (1996), General and Systematic Pathology, 2nd Edition, *Churchill Livingstone*

Valencia-Sanchez MA, Liu J, Hannon GJ, Parker R, (2006), Control of translation and mRNA degradation by miRNAs and siRNAs, *Genes Dev*, **20**, 515-24

Voisset C, Dubuisson J, (2004), Functional hepatitis C virus envelope glycoproteins, *Biol Cell*, **96**, 413-20

Wang JK, Kiyokawa E, Verdin E, Trono D, (2000), The Nef protein of HIV-1 associates with rafts and primes T cells for activation, *Proc Natl Acad Sci U S A*, **97**, 394-9

Ward DG, Cheng Y, N'Kontchou G, Thar TT, Barget N, Wei W, Billingham LJ, Martin A, Beaugrand M, Johnson PJ, (2006), Changes in the serum proteome associated with the development of hepatocellular carcinoma in hepatitis C-related cirrhosis, *Br J Cancer*, **94**, 287-92

Wasinger VC, Cordwell SJ, Cerpa-Poljak A, Yan JX, Gooley AA, Wilkins MR, Duncan MW, Harris R, Williams KL, Humphery-Smith I, (1995), Progress with gene-product mapping of the Mollicutes: Mycoplasma genitalium, *Electrophoresis*, **16**, 1090-4

Watts B, Burnett L, Chesher D, (2000), Measurement of total protein is not a useful inclusion in liver function test profiles, *Clin Chem*, **46**, 1022-3

Wessel D, Flugge UI, (1984), A method for the quantitative recovery of protein in dilute solution in the presence of detergents and lipids, *Anal Biochem*, **138**, 141-3

White IR, Pickford R, Wood J, Skehel JM, Gangadharan B, Cutler P, (2004), A statistical comparison of silver and SYPRO Ruby staining for proteomic analysis, *Electrophoresis*, **25**, 3048-54

Willems GM, Janssen MP, Pelsers MM, Comfurius P, Galli M, Zwaal RF, Bevers EM, (1996), Role of divalency in the high-affinity binding of anticardiolipin antibody-beta 2-glycoprotein I complexes to lipid membranes, *Biochemistry*, **35**, 13833-42

Williams AL, Hoofnagle JH, (1988), Ratio of serum aspartate to alanine aminotransferase in chronic hepatitis. Relationship to cirrhosis, *Gastroenterology*, **95**, 734-9

Wisniewski HG, Hua JC, Poppers DM, Naime D, Vilcek J, Cronstein BN, (1996), TNF/IL-1-inducible protein TSG-6 potentiates plasmin inhibition by inter-alpha-inhibitor and exerts a strong anti-inflammatory effect in vivo, *J Immunol*, **156**, 1609-15

Wittmann T, Bokoch GM, Waterman-Storer CM, (2004), Regulation of microtubule destabilizing activity of Op18/stathmin downstream of Rac1, *J Biol Chem*, **279**, 6196-203

Wolf D, (2005), Cirrhosis; Emedicine - Gastroenterology, http://www.emedicine.com/med/topic3183.htm

Wolf D, Witte V, Laffert B, Blume K, Stromer E, Trapp S, d'Aloja P, Schurmann A, Baur AS, (2001), HIV-1 Nef associated PAK and PI3-kinases stimulate Akt-independent Bad-phosphorylation to induce anti-apoptotic signals, *Nat Med*, **7**, 1217-24

Wollberg P, Nelson BD, (1992), Regulation of the expression of lactate dehydrogenase isozymes in human lymphocytes, *Mol Cell Biochem*, **110**, 161-4

Wong CS, Gibson PR, (1998), Effects of eating on plasma hyaluronan in patients with cirrhosis: its mechanism and influence on clinical interpretation, *J Gastroenterol Hepatol*, **13**, 1218-24

Wong VS, Hughes V, Trull A, Wight DG, Petrik J, Alexander GJ, (1998), Serum hyaluronic acid is a useful marker of liver fibrosis in chronic hepatitis C virus infection, *J Viral Hepat*, **5**, 187-92

Wu WJ, Tu S, Cerione RA, (2003), Activated Cdc42 sequesters c-Cbl and prevents EGF receptor degradation, *Cell*, **114**, 715-25

Xu XQ, Leow CK, Lu X, Zhang X, Liu JS, Wong WH, Asperger A, Deininger S, Eastwood Leung HC, (2004), Molecular classification of liver cirrhosis in a rat model by proteomics and bioinformatics, *Proteomics*, **4**, 3235-45

Yeh WC, Li PC, Jeng YM, Hsu HC, Kuo PL, Li ML, Yang PM, Lee PH, (2002), Elastic modulus measurements of human liver and correlation with pathology, *Ultrasound Med Biol*, **28**, 467-74

Yi YS, Park SG, Byeon SM, Kwon YG, Jung G, (2003), Hepatitis B virus X protein induces TNF-alpha expression via down-regulation of selenoprotein P in human hepatoma cell line, HepG2, *Biochim Biophys Acta*, **1638**, 249-56

Yokouchi M, Kondo T, Houghton A, Bartkiewicz M, Horne WC, Zhang H, Yoshimura A, Baron R, (1999), Ligand-induced ubiquitination of the epidermal growth factor receptor involves the interaction of the c-Cbl RING finger and UbcH7, *J Biol Chem*, **274**, 31707-12

Yokoyama Y, Kuramitsu Y, Takashima M, Iizuka N, Toda T, Terai S, Sakaida I, Oka M, Nakamura K, Okita K, (2004), Proteomic profiling of proteins decreased in hepatocellular carcinoma from patients infected with hepatitis C virus, *Proteomics*, **4**, 2111-6

Yoon D, Kueppers F, Genta RM, Klintmalm GB, Khaoustov VI, Yoffe B, (2002), Role of alpha-1-antichymotrypsin deficiency in promoting cirrhosis in two siblings with heterozygous alpha-1-antitrypsin deficiency phenotype SZ, *Gut*, **50**, 730-2

Yovita H, Djumhana A, Abdurachman SA, Saketi JR, (2004), Correlation between anthropometrics measurements, prealbumin level and transferin serum with Child-Pugh classification in evaluating nutritional status of liver cirrhosis patient, *Acta Med Indones*, **36**, 197-201

Zheng M, Cai WM, Zhao JK, Zhu SM, Liu RH, (2005), Determination of serum levels of YKL-40 and hyaluronic acid in patients with hepatic fibrosis due to schistosomiasis japonica and appraisal of their clinical value, *Acta Trop*, **96**, 148-52

Zheng N, Wang P, Jeffrey PD, Pavletich NP, (2000), Structure of a c-Cbl-UbcH7 complex: RING domain function in ubiquitin-protein ligases, *Cell*, **102**, 533-9

Zuckerman E, Kessel A, Slobodin G, Sabo E, Yeshurun D, Toubi E, (2003), Antiviral treatment down-regulates peripheral B-cell CD81 expression and CD5 expansion in chronic hepatitis C virus infection, *J Virol*, **77**, 10432-6

Zuckerman E, Slobodin G, Kessel A, Sabo E, Yeshurun D, Halas K, Toubi E, (2002), Peripheral B-cell CD5 expansion and CD81 overexpression and their

association with disease severity and autoimmune markers in chronic hepatitis C virus infection, *Clin Exp Immunol*, **128**, 353-8

Appendix

Fibrosis stage	Sample	Age when sample was taken	Sex	HCV PCR	ALT (IU/l)	Genotype	Ishak fibrosis score (out of 6)	Necroinflam-matory index (out of 18)	Total serum protein (g/l)
Normal healthy controls	N1	33	Male	-	N	-	0	0	76.2
	N2	34	Male	-	N	-	0	0	65.0
	N3	35	Male	-	N	-	0	0	83.8
	N4	35	Male	-	N	-	0	0	65.4
Mild fibrosis	L1	38	Female	+	28	1b	1	4	53.8
	L2	52	Male	+	104	1b	1	3	72.6
	L3	45	Female	+	27	1a	1	4	82.7
	L4	46	Female	+	38	1b	1	N	58.2
Moderate fibrosis	M1	55	Male	+	142	1	3	2	61.4
	M2	45	Male	+	21	1	3	3	69.9
	M3	77	Male	+	32	1	3	4	59.9
Cirrhosis	C1	52	Male	+	111	3a	6	N	85.8
	C2	N	N	+	N	N	6	N	67.9
	C3	N	N	+	N	N	6	N	77.0
	C4	N	N	+	N	N	6	N	68.6

Table A1 Clinical data for the serum samples analysed. All values were provided by the clinician except for total protein which was determined using the BCA assay (Section 2.2.3.1). Biopsies were taken for all patients except for the healthy controls who were assumed to have zero values for fibrosis and necroinflammation.
N = not known or not provided by clinician.

Protein Name [AN]	M_r, kDa	pI	Fold change	No. of MS/MS peptide matches	% sequence coverage	Protein function
Albumin [P02768]	134.6 135.9 135.4 115.1 114.7 61.6 123.3 121.7 140.8 137.6	5.74 5.62 5.70 5.74 5.80 5.90 5.74 5.68 5.67 5.60	C(2.17) C(2.17) C(2.30) C C C(3.36) M M L(3.84) L(2.67)	5 1 3 1 4 4 6 5 4 9	15.27 1.97 8.37 1.97 9.85 8.70 11.65 15.59 8.70 23.31	synthesised by liver, most abundant protein of serum; regulates blood pressure
Alpha 1 antichymotrypsin [P01011]	60.7	4.65	N(C)(2.02)	3	11.34	physiological function unclear; inhibits chymotrypsin and other similar proteases; inhibits conversion of angiotensin I to II
Alpha 2 macroglobulin [P01023]	134.6 135.9 135.4 115.4 115.8 115.1 114.7 113.7 112.6 111.2 110.6 110.9 61.6 60.7 123.3 121.7 119.3 140.8 137.6	5.74 5.62 5.70 5.72 5.69 5.74 5.80 5.35 5.39 5.42 5.45 5.49 5.90 6.01 5.74 5.68 5.63 5.67 5.60	C(2.17) C(2.17) C(2.30) C C C C C(2.50) C(2.79) C(2.36) C(2.14) C(2.10) C(3.36) C(2.38) M M M L(3.84) L(2.67)	28 23 20 10 21 23 17 14 21 27 14 27 14 16 19 22 14 2 25	25.44 20.82 18.99 10.17 21.37 22.38 15.40 13.02 17.57 25.44 13.90 26.86 12.95 14.51 16.96 22.79 13.50 1.56 27.88	protease inhibitor; inhibits plasmin and MMP; binding to proteases (e.g. plasmin) causes a conformational change which causes cleavage at the thiolester site
Apolipoprotein L1 [O14791]	34.2	6.12	N(C)	1	3.76	precise function unknown; levels correlate with triglycerides and cholesterol
Beta 2 glycoprotein I (APC inhibitor) [P02749]	58.4	5.85	C	8	37.68	binds to chylomicrons and high-density lipoproteins; binds to activated protein C
Beta 2 microglobulin [Q9UP60]	61.6	5.90	C(3.36)	9	43.22	small subunit of MHC1, SNC73
CD5 antigen-like [O43866]	41.1	5.25	C	3	16.13	may play a role in immune system regulation; IgM associated protein
Complement C3 [P01024]	44.6	6.93	N(M)(2.88)	10	7.45	liver synthesised proteins;

Protein Name [AN]	M_r, kDa	pI	Fold change	No. of MS/MS peptide matches	% sequence coverage	Protein function
Complement C4 [P0C0L4 / P0C0L5]	41.4 41.4 92.3	6.04 6.04 5.09	N(M)(2.12) N(C) N(C)(2.03)	2 2 2	1.37 1.37 1.43	involved in the complement cascade for eliminating pathogens and stimulating inflammation
Complement factor H-related protein 1 [Q03591]	43.2 43.2	6.10 6.10	N(L) N(C)(2.21)	2 2	9.39 9.39	liver synthesised protein; might be involved in complement regulation; associates with lipoproteins & may play role in lipid metabolism
Haptoglobin [P00738]	12.9 43.9 41.9 42.2 41.4 39.9 39.8 16.8	5.53 4.81 5.02 4.91 5.15 5.45 5.64 5.97	N(C) N(C)(2.48) N(C)(2.49) N(C)(2.23) N(C)(2.19) N(C)(2.38) N(C) N(L)(2.10)	2 7 12 13 13 14 6 5	7.14 16.25 28.32 29.80 29.31 29.80 16.50 20.44	liver synthesised glycoprotein thought to be regulated by hepatocyte growth factor; combines with free oxyhaemoglobin and prevents iron loss through kidneys - this protects the kidneys from damage by haemoglobin
Haemoglobin alpha chain [P69905]	9.7 9.8	7.93 8.11	C(2.03) L	10 4	78.72 36.87	involved in oxygen transport from the lung to the various peripheral tissues
Haemoglobin beta chain [P69971]	10.5 9.7	7.04 7.93	C(2.73) C(2.03)	16 1	97.26 15.06	
Immunoglobulin alpha 1 chain C region [P01876]	61.6	5.90	C(3.36)	9	47.02	constant region of heavy chain of IgA1
Immunoglobulin gamma-2 chain C region [P01859]	49.0	6.07	C	2	7.97	constant region of heavy chain of IgG2
Immuno-globulin kappa or lambda chain regions [P01834] [P01625] [P01842]	29.9	5.67	C	4 2 2	54.71 23.68 36.19	immunoglobulin light chain regions
[P01842] [P01714] [P01834] [P01717]	28.4	5.63	C	3 1 3 1	46.66 16.66 39.62 17.75	
[P01834] [P01842]	27.9	6.50	C	5 4	73.58 50.47	
[P01834]	27.0	6.43	C(2.03)	3	48.11	
[P01834] [P01842] [P01625]	27.0	5.62	C	5 4 1	73.58 68.57 15.78	
[P01842] [P01616]	26.0	5.91	C	1 1	21.90 11.60	
[P01834] [P01842]	23.9	6.06	C	5 3	80.18 46.66	
[P01620] [P01593] [P01842]	25.7	5.46	M	3 1 1	30.27 14.81 14.28	

Protein Name [AN]	M_r, kDa	pI	Fold change	No. of MS/MS peptide matches	% sequence coverage	Protein function
[P04433] [P01604]				1 1	7.82 14.81	
Inter-alpha-trypsin inhibitor heavy chain H4 (Plasma kallikrein sensitive glycoprotein 120) [Q14624]	83.9 36.3 35.7	4.85 5.06 5.29	N(C)(3.32) N(C) N(C)	3 5 5	4.19 4.73 4.73	a trypsin inhibitor; can be cleaved by kallikrein;
Paraoxonase / arylesterase 1 (PON 1) (K-45) (Aromatic esterase 1) (aryldialkylphosphatase 1) [P27169]	43.9	4.81	N(C)(2.48)	2	7.34	degrades oxidised lipids in lipoproteins and cells and therefore may play a role in antioxidant systems
Prealbumin (Transthyretin) [P02766]	31.6	5.29	N(C)(2.17)	2	17.68	liver synthesised protein; carries vitamin A through retinol binding protein association
Transcortin [P08185]	60.7	4.65	N(2.02)	1	2.46	major transport protein for glucocorticoids and progestins
Zinc-alpha2-glycoprotein [P25311]	43.9	4.81	N(C)(2.48)	2	8.13	stimulates lipolysis in adipocytes & causes fat loss in some cancers

Table A2 Differentially expressed proteins identified in serum samples of healthy controls versus the different stages of hepatic scarring.

AN, Swiss-Prot accession number;

pI, isoelectric point on gel as determined by MELANIE using calibrated landmarks;

M_r, relative molecular mass on gel as determined by MELANIE using calibrated landmarks;

The number of MS/MS peptide matches and percentage sequence coverage were determined by the Mascot Daemon search sengine.

Fold change refers to proteins that were differentially expressed by 2-fold or more when comparing serum gels from healthy controls with the different stages of hepatic fibrosis. The numerical values shown in parentheses for fold change indicates features that were present in both controls and hepatic scarring but expressed to a higher extent in the indicated stage. For cases where no numerical value is shown for fold change, the feature was only present in the indicated stage.

N, features present in serum from healthy controls (with respect to the stage of hepatic scarring shown in parentheses)

L, features present in serum from mild fibrosis patients

M, features present in serum from moderate fibrosis patients

C, features present in serum from cirrhosis patients

Protein functions have been adapted from the ExPASy website

N1

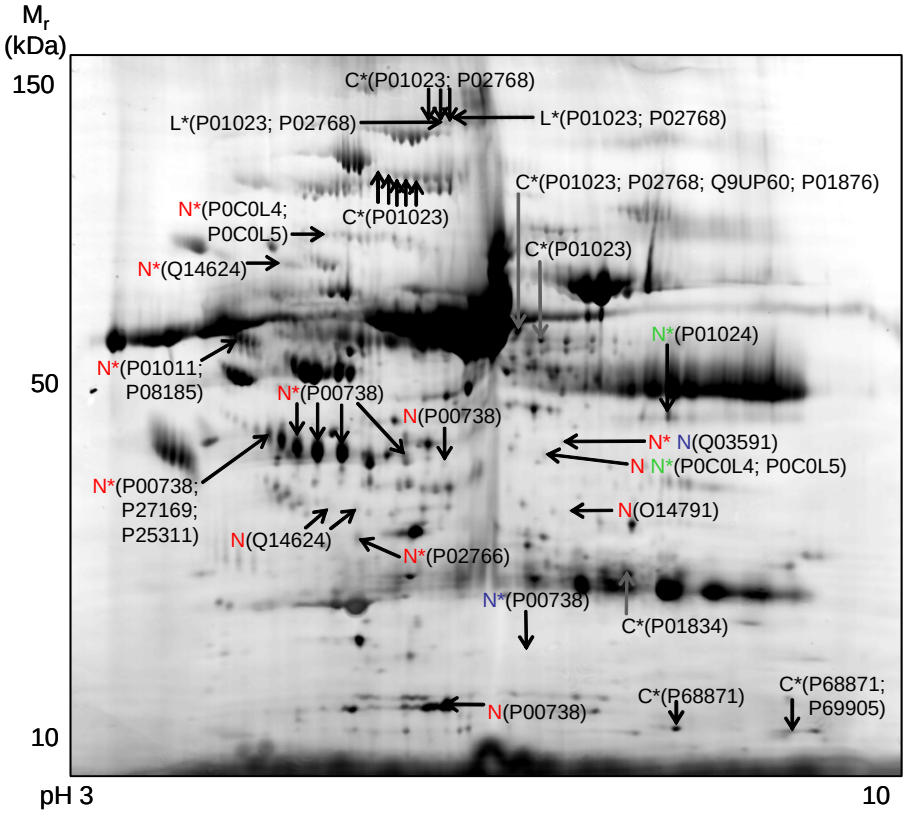
Mr (kDa)
150
50
10
pH 3
10
C*(P01023; P02768)
L*(P01023; P02768)
L*(P01023; P02768)
C*(P01023; P02768; Q9UP60; P01876)
N*(P0C0L4; P0C0L5)
C*(P01023)
N*(Q14624)
C*(P01023)
N*(P01024)
N*(P01011; P08185)
N*(P00738)
N(P00738)
N* N(Q03591)
N N*(P0C0L4; P0C0L5)
N*(P00738; P27169; P25311)
N(O14791)
N(Q14624)
N*(P02766)
N*(P00738)
C*(P01834)
C*(P68871)
C*(P68871; P69905)
N(P00738)

N2

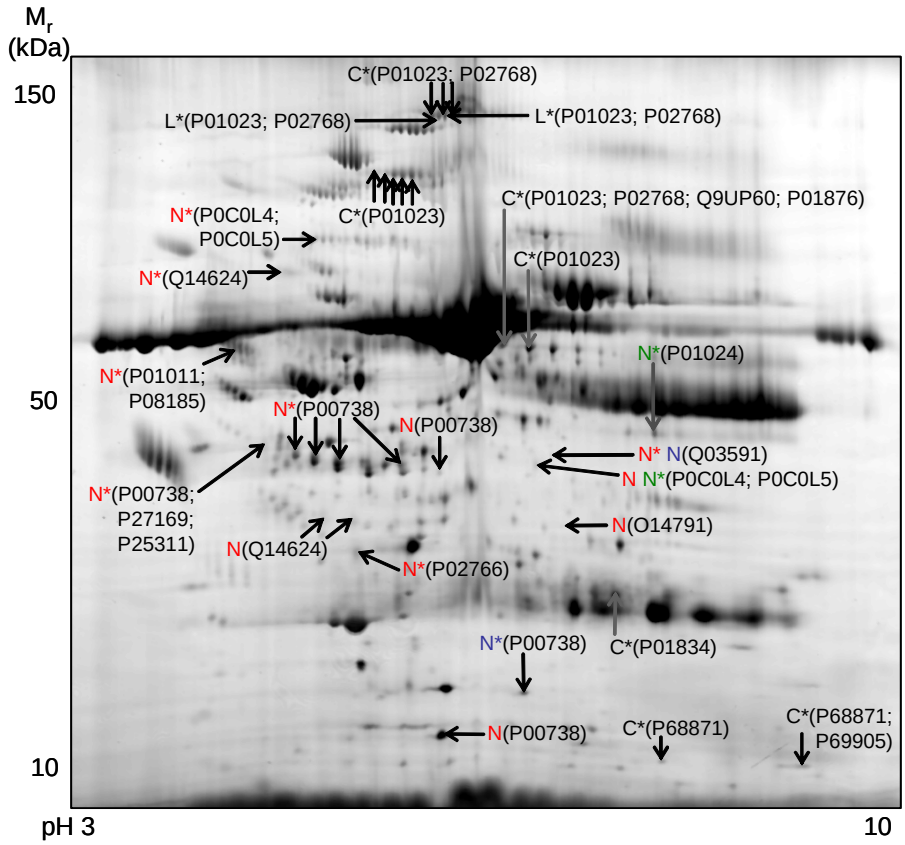
Mr (kDa)
150
50
10
pH 3
10
C*(P01023; P02768)
L*(P01023; P02768)
L*(P01023; P02768)
C*(P01023; P02768; Q9UP60; P01876)
N*(P0C0L4; P0C0L5)
C*(P01023)
N*(Q14624)
C*(P01023)
N*(P01024)
N*(P01011; P08185)
N*(P00738)
N(P00738)
N* N(Q03591)
N N*(P0C0L4; P0C0L5)
N*(P00738; P27169; P25311)
N(O14791)
N(Q14624)
N*(P02766)
N*(P00738)
C*(P01834)
C*(P68871)
C*(P68871; P69905)
N(P00738)

N3

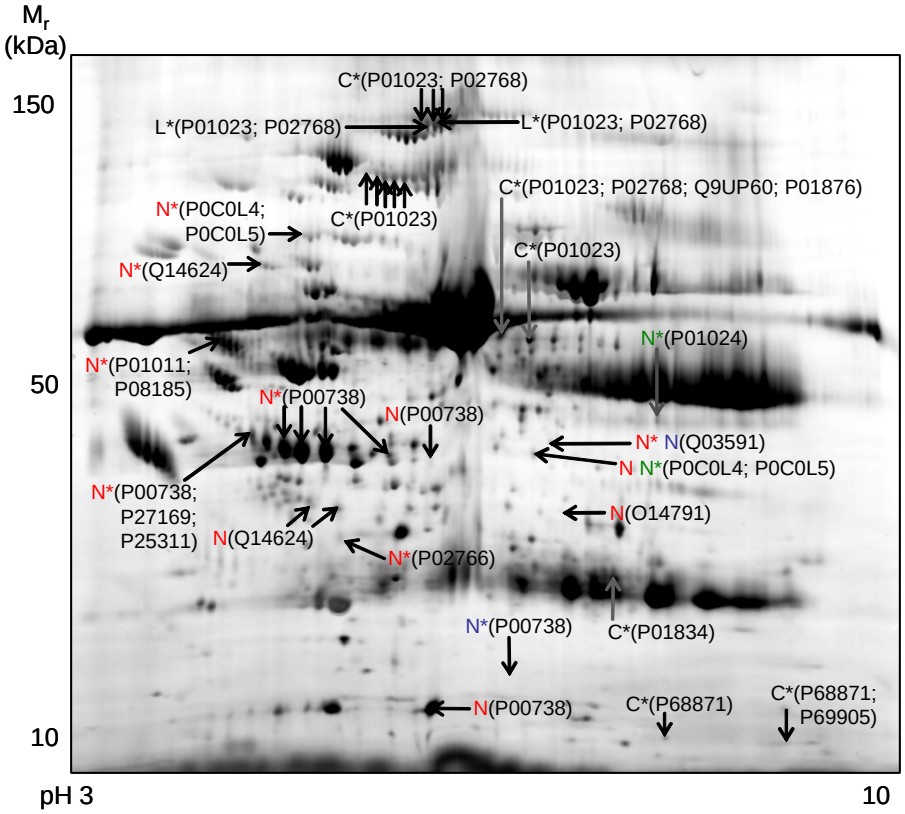
M$_r$ (kDa)
150
50
10
pH 3
10
C*(P01023; P02768)
L*(P01023; P02768)
L*(P01023; P02768)
C*(P01023; P02768; Q9UP60; P01876)
N*(P0C0L4; P0C0L5)
C*(P01023)
N*(Q14624)
C*(P01023)
N*(P01024)
N*(P01011; P08185)
N*(P00738)
N(P00738)
N* N(Q03591)
N N*(P0C0L4; P0C0L5)
N*(P00738; P27169; P25311)
N(Q14624)
N(O14791)
N*(P02766)
N*(P00738)
C*(P01834)
N(P00738)
C*(P68871)
C*(P68871; P69905)

N4

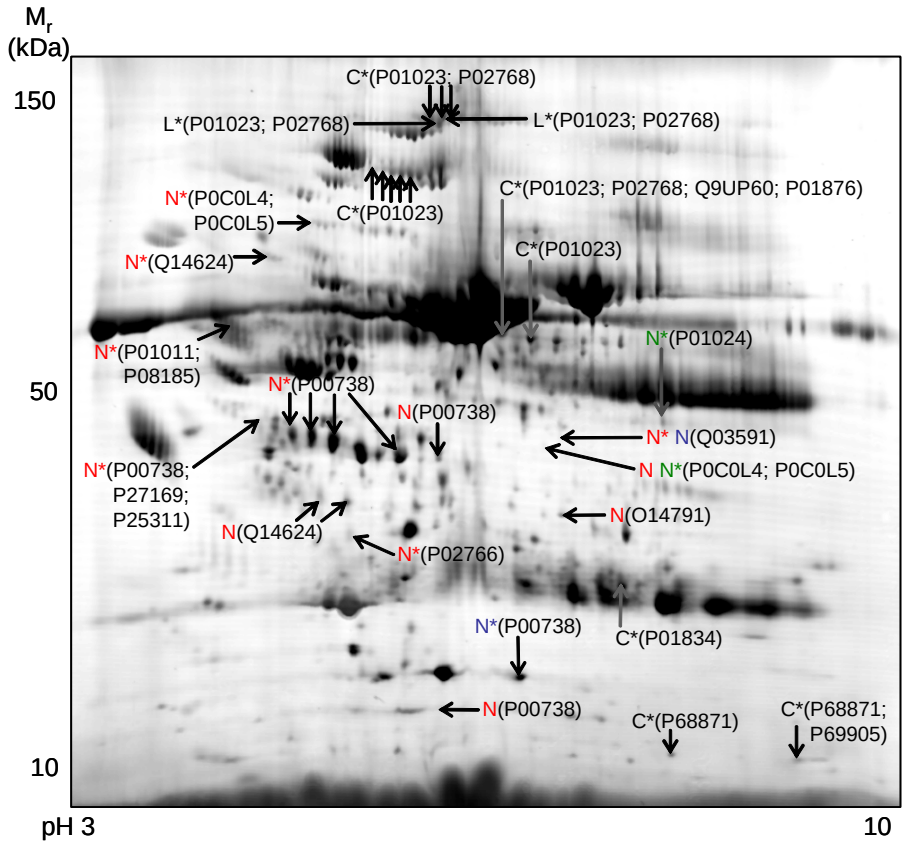
M$_r$ (kDa)
150
50
10
pH 3
10
C*(P01023; P02768)
L*(P01023; P02768)
L*(P01023; P02768)
C*(P01023; P02768; Q9UP60; P01876)
N*(P0C0L4; P0C0L5)
C*(P01023)
N*(Q14624)
C*(P01023)
N*(P01024)
N*(P01011; P08185)
N*(P00738)
N(P00738)
N* N(Q03591)
N N*(P0C0L4; P0C0L5)
N*(P00738; P27169; P25311)
N(Q14624)
N(O14791)
N*(P02766)
N*(P00738)
C*(P01834)
N(P00738)
C*(P68871)
C*(P68871; P69905)

L1

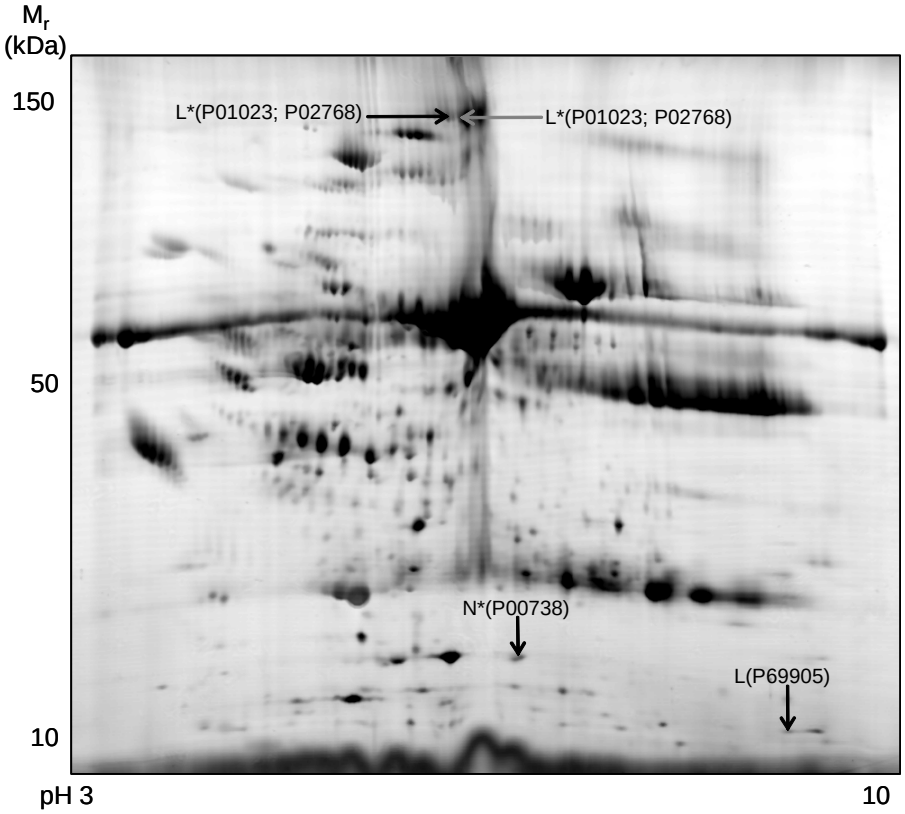
Mr
(kDa)
150
50
10
L*(P01023; P02768)
L*(P01023; P02768)
N*(P00738)
L(P69905)
pH 3
10

L2

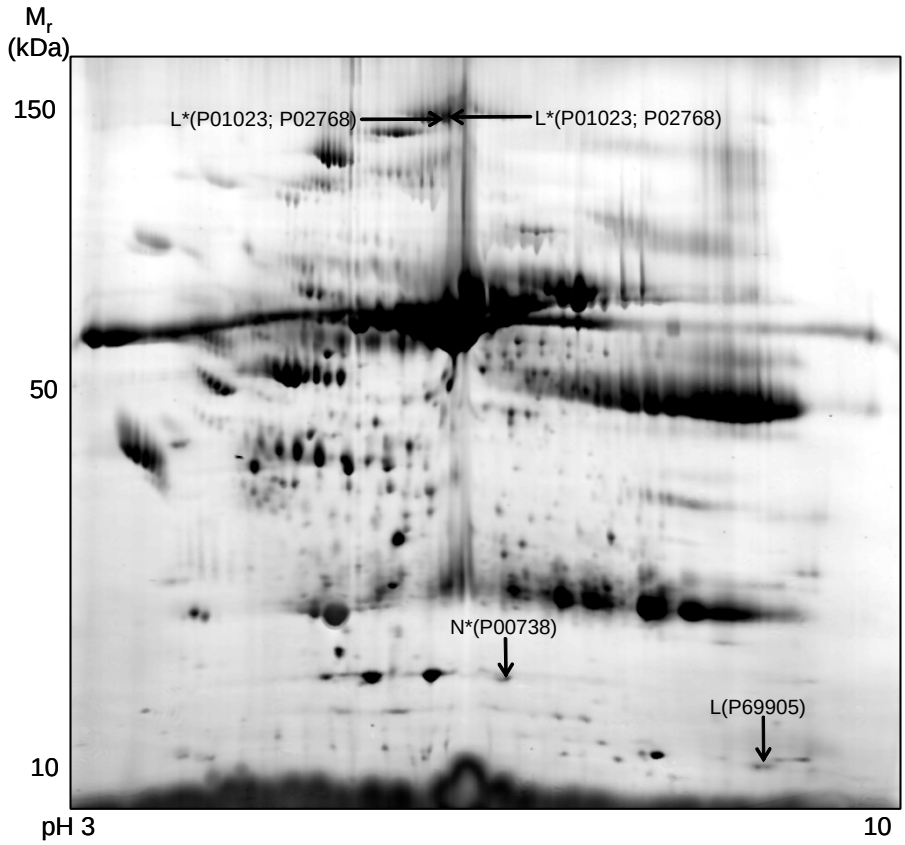
Mr
(kDa)
150
50
10
L*(P01023; P02768)
L*(P01023; P02768)
N*(P00738)
L(P69905)
pH 3
10

L3

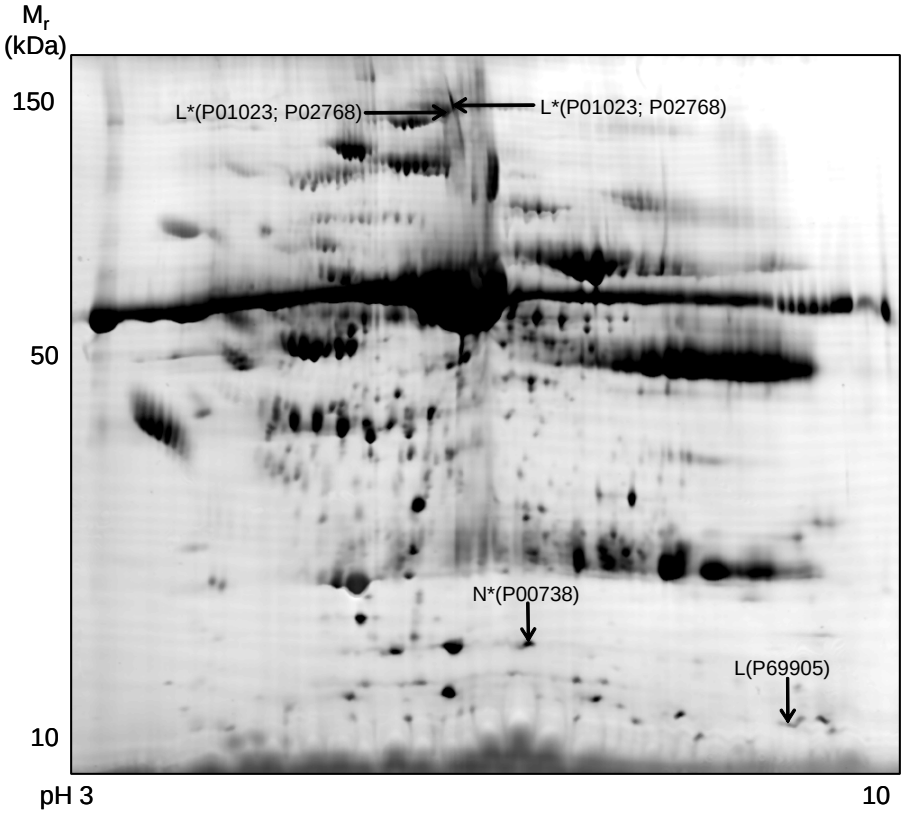
M_r
(kDa)
150
50
10
L*(P01023; P02768)
L*(P01023; P02768)
N*(P00738)
L(P69905)
pH 3
10

L4

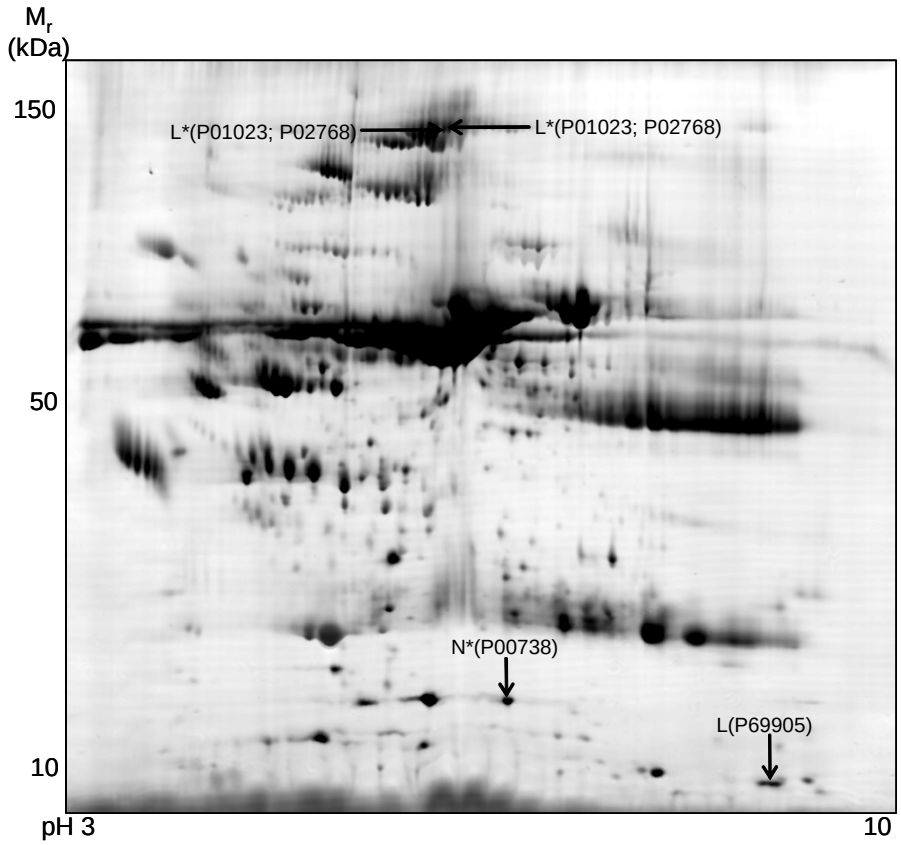
M_r
(kDa)
150
50
10
L*(P01023; P02768)
L*(P01023; P02768)
N*(P00738)
L(P69905)
pH 3
10

M1

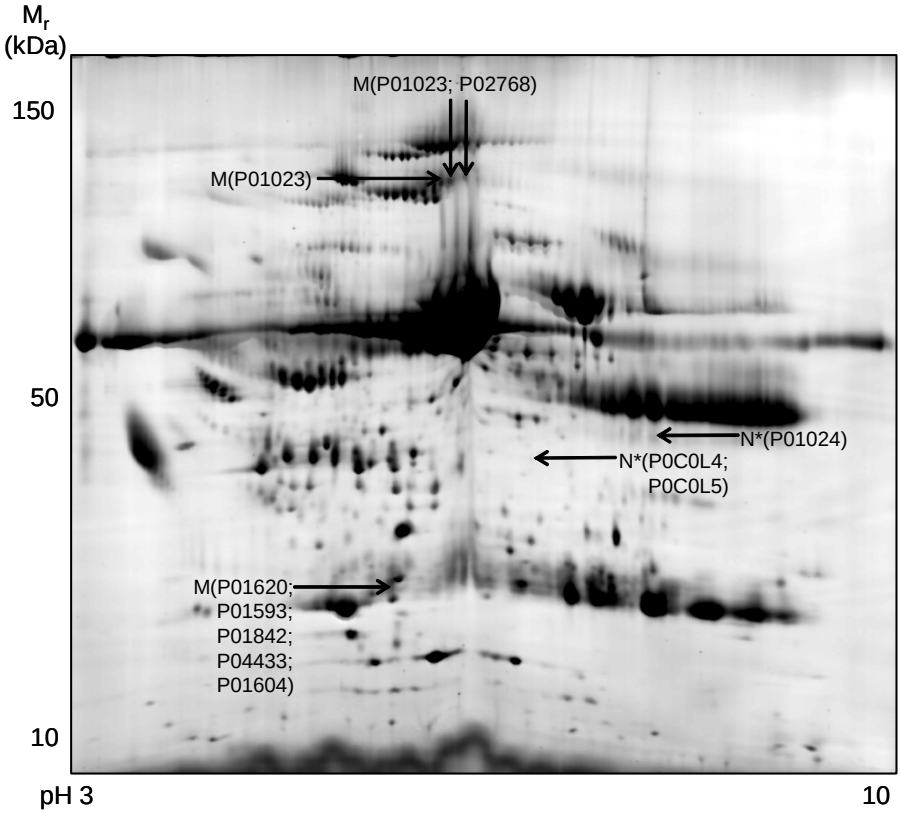
Mr
(kDa)
150
50
10
M(P01023; P02768)
M(P01023)
N*(P01024)
N*(P0C0L4;
P0C0L5)
M(P01620;
P01593;
P01842;
P04433;
P01604)
pH 3
10

M2

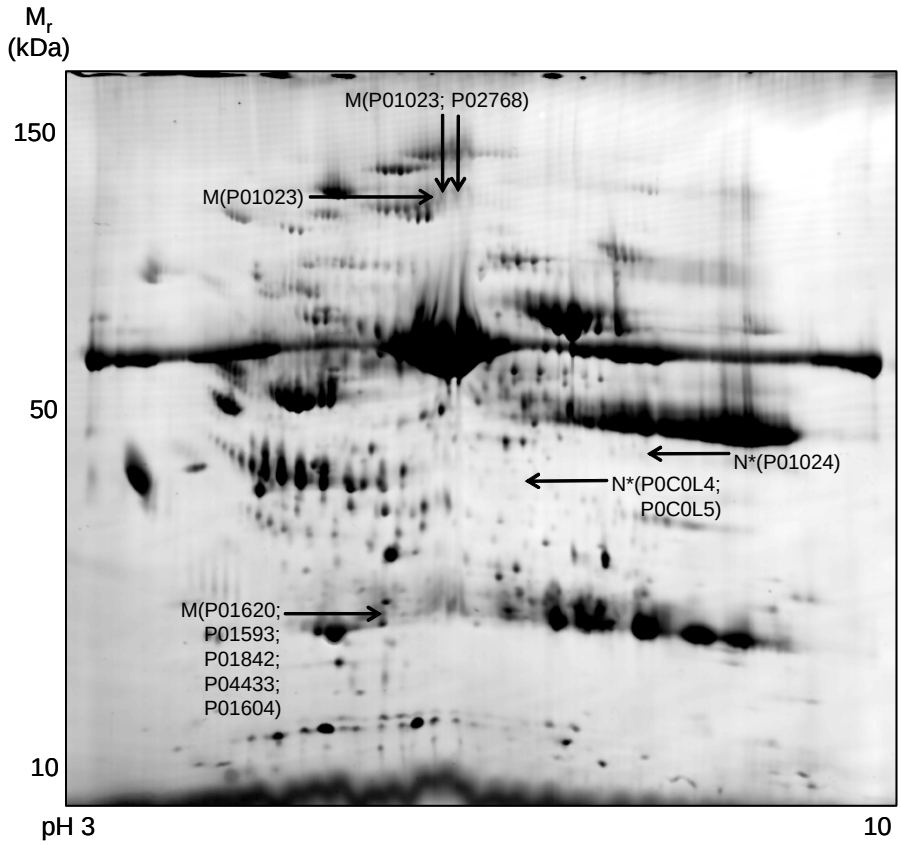
Mr
(kDa)
150
50
10
M(P01023; P02768)
M(P01023)
N*(P01024)
N*(P0C0L4;
P0C0L5)
M(P01620;
P01593;
P01842;
P04433;
P01604)
pH 3
10

M3

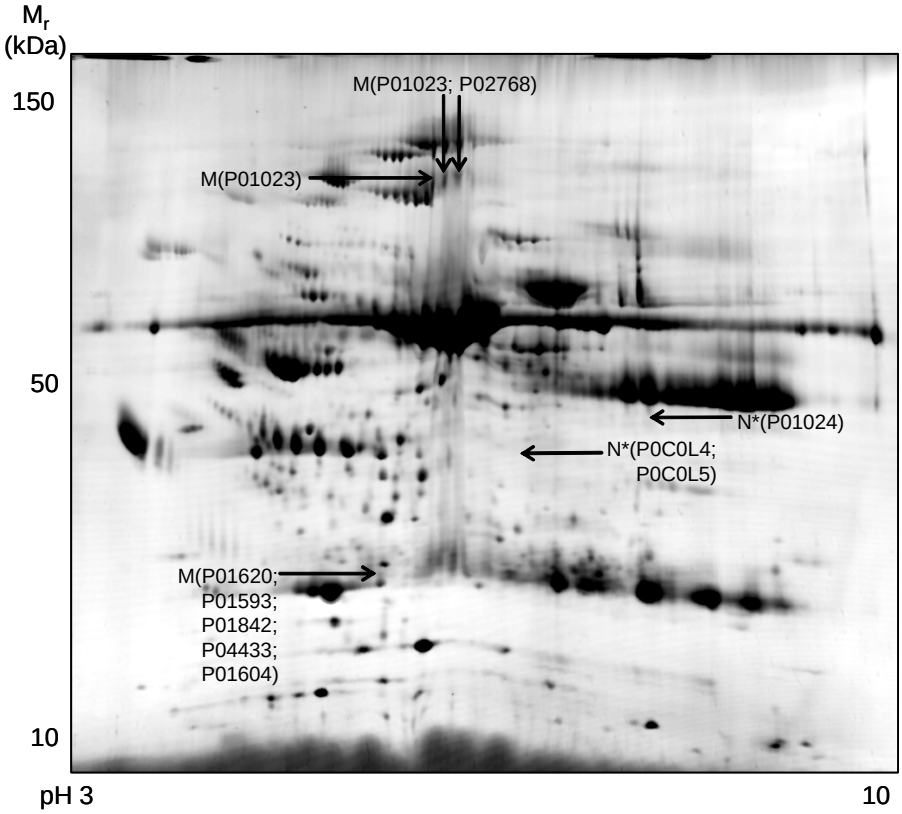
Mr
(kDa)
150
50
10
pH 3
10
M(P01023; P02768)
M(P01023)
N*(P01024)
N*(P0C0L4;
P0C0L5)
M(P01620;
P01593;
P01842;
P04433;
P01604)

C1

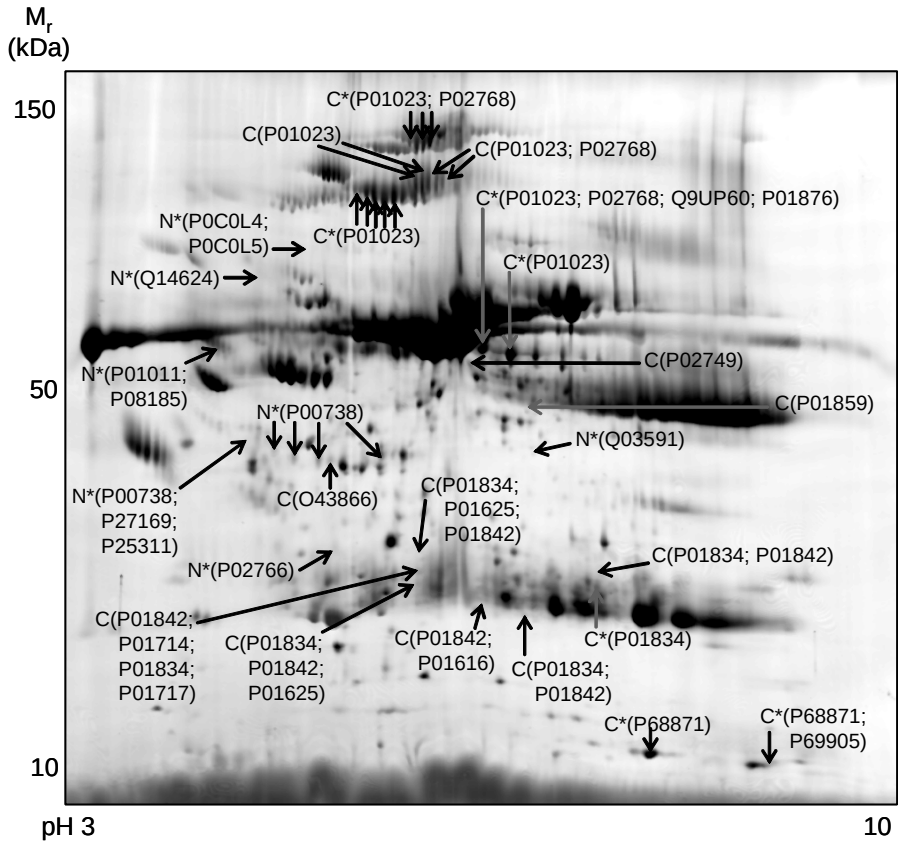
Mr
(kDa)
150
50
10
pH 3
10
C*(P01023; P02768)
C(P01023)
C(P01023; P02768)
C*(P01023; P02768; Q9UP60; P01876)
N*(P0C0L4;
P0C0L5)
C*(P01023)
C*(P01023)
N*(Q14624)
C(P02749)
N*(P01011;
P08185)
C(P01859)
N*(P00738)
N*(Q03591)
N*(P00738;
P27169;
P25311)
C(O43866)
C(P01834;
P01625;
P01842)
C(P01834; P01842)
N*(P02766)
C(P01842;
P01714;
P01834;
P01717)
C(P01834;
P01842;
P01625)
C(P01842;
P01616)
C*(P01834)
C(P01834;
P01842)
C*(P68871)
C*(P68871;
P69905)

C2

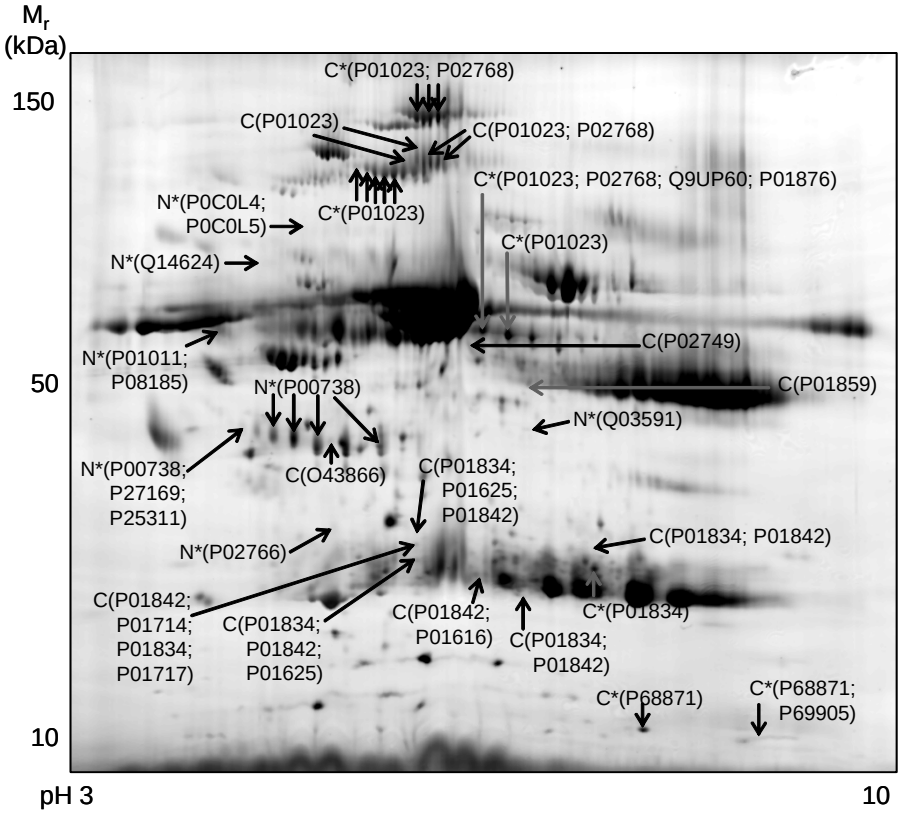
Mr
(kDa)
150
50
10
pH 3
10
C*(P01023; P02768)
C(P01023)
C(P01023; P02768)
C*(P01023; P02768; Q9UP60; P01876)
N*(P0C0L4;
P0C0L5)
C*(P01023)
C*(P01023)
N*(Q14624)
C(P02749)
N*(P01011;
P08185)
N*(P00738)
C(P01859)
N*(Q03591)
N*(P00738;
P27169;
P25311)
C(O43866)
C(P01834;
P01625;
P01842)
C(P01834; P01842)
N*(P02766)
C(P01842;
P01714;
P01834;
P01717)
C(P01834;
P01842;
P01625)
C(P01842;
P01616)
C*(P01834)
C(P01834;
P01842)
C*(P68871)
C*(P68871;
P69905)

C3

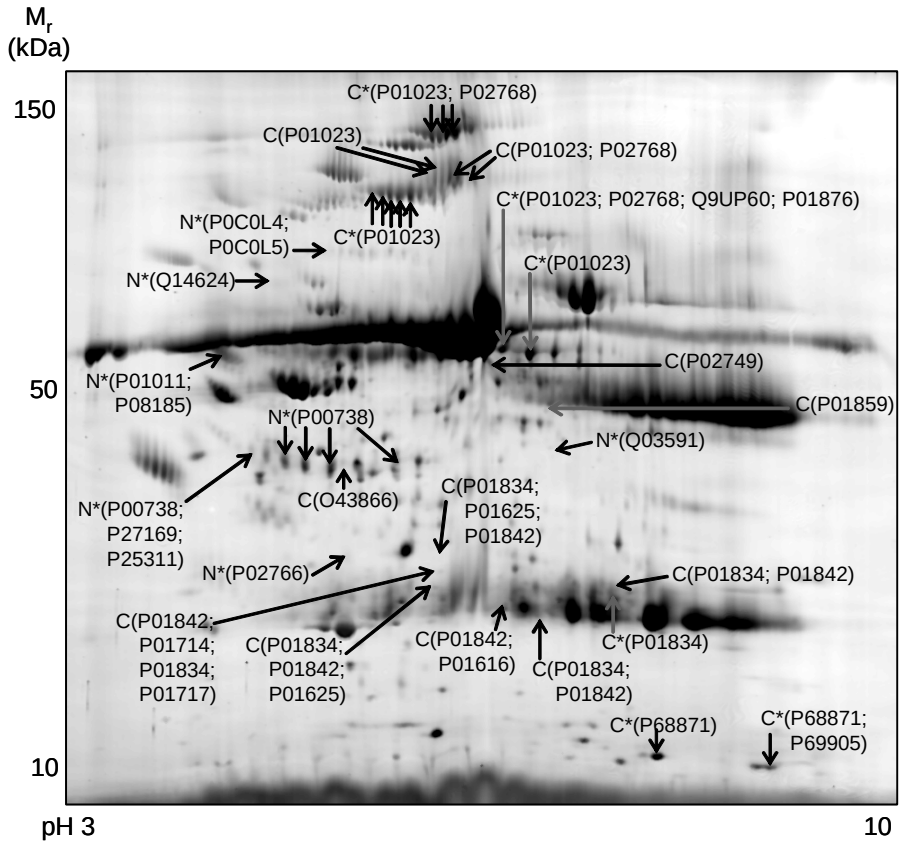
Mr
(kDa)
150
50
10
pH 3
10
C*(P01023; P02768)
C(P01023)
C(P01023; P02768)
C*(P01023; P02768; Q9UP60; P01876)
N*(P0C0L4;
P0C0L5)
C*(P01023)
C*(P01023)
N*(Q14624)
C(P02749)
N*(P01011;
P08185)
N*(P00738)
C(P01859)
N*(Q03591)
N*(P00738;
P27169;
P25311)
C(O43866)
C(P01834;
P01625;
P01842)
C(P01834; P01842)
N*(P02766)
C(P01842;
P01714;
P01834;
P01717)
C(P01834;
P01842;
P01625)
C(P01842;
P01616)
C*(P01834)
C(P01834;
P01842)
C*(P68871)
C*(P68871;
P69905)

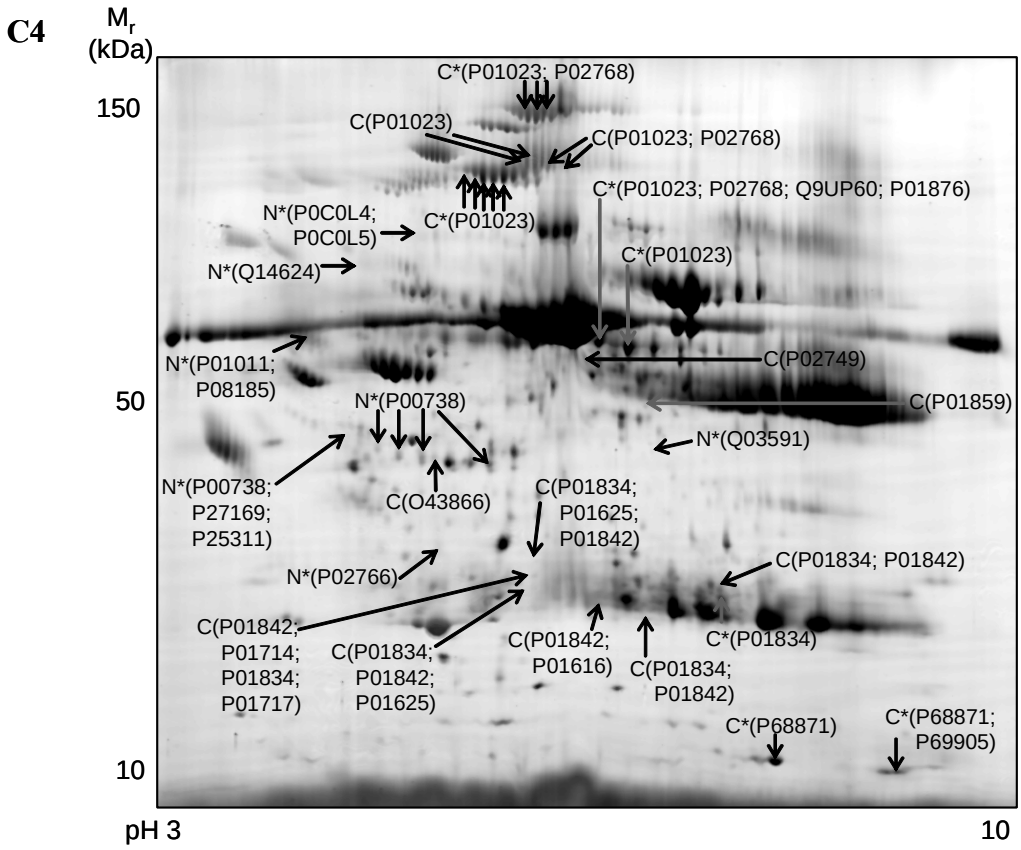

Figure A1 500 µg of serum was separated by 9-16% 2D-PAGE (pH3-10 NL) for serum samples from healthy controls (N1-N4), mild fibrosis (L1-L4), moderate fibrosis (M1-M3), and cirrhosis (C1-C4) patients. Gels were stained with the fluorescent dye OGT 1238. Differentially expressed features along with their Swiss-Prot accession numbers are highlighted.
N, features present only in serum from healthy controls
L, features present only in serum from mild fibrosis patients
M, features present only in serum from moderate fibrosis patients
C, features present only in serum from cirrhosis patients
, features present in serum from both control and heptic scarring but expressed to a higher extent in asterisked stage of hepatic scarring (e.g. L for mild, M* for moderate, C* for cirrhosis) or control (N*)
For images N1-N4 the colours blue, green and red indicate a greater expression in healthy controls compared with mild fibrosis, moderate fibrosis and cirrhosis, respectively.

Protein Name	AN	M_r, Da	pI	Fold change	Protein function
14-3-3 protein ε	P62258	29100	4.35	C*	Binds to and reduces PI3K activity
Actin cytoplasmic 1 (β-actin) or Actin cytoplasmic 2 (γ-actin)	P60709 or P63261	18900 27000	4.82 5.20	N* N	Cytoskeletal components necessary for cell surface shape and locomotion
α2-HS-glycoprotein	P02765	66500 67000 67300 68100 68200 68500 69200	4.59 4.57 4.55 4.47 4.45 4.43 4.41	N N N N N N N	Acute phase protein usually found in plasma/serum
Glyceraldehyde 3-phosphate dehydrogenase	P04406	33300 37500 38100 38100 38200	8.17 7.23 7.03 6.94 6.76	N C* C* C* C*	Cytosolic glycolytic enzyme GA3P + Pi + NAD^+ ⇔ BPG +NADH
L-lactate dehydrogenase A chain (EC 1.1.1.27)	P00338	33100	7.86	N*	Enzyme in glycolysis. Expressed in activated lymphocytes
NASCENT polypeptide associated complex α subunit	Q13765	34700 34800	4.53 4.49	N N	Nuclear/cytoplasmic mRNA processing
Nucleosome assembly protein 1-like 4	Q99733	61500 62200 62600 63600	4.66 4.64 4.62 4.55	N N N N	Located in nucleus and associated with nucleosome assembly
Proteasome subunit β type 4	P28070	25800	5.40	N	Proteolysis (cytoplasm)
Proteasome subunit β type 5	P28074	23600	8.25	N	Proteolysis (cytoplasm)
Protein phosphatase 2C γ isoform	O15355	76200	4.51	C*	Dephosphorylates phosphoproteins
Stathmin (Oncoprotein 18)	P16949	22000	4.97	C	Destabilises microtubules by sequestering tubulin
Thymidylate kinase	P23919	24700	7.93	C*	Cytosolic enzyme: ATP+dTMP⇔ADP+dTDP
Transgelin 2	P37802	23300 23100 23400	7.64 7.77 7.79	C N N	Mediates cross-linking of actin
Transketolase	P29401	72800 72900 73000 74100	6.89 7.04 6.74 6.58	C* C* C* C*	Cytosolic enzyme in pentose phosphate pathway
Ubiquitin-conjugating enzyme E2 (UbcH7)	P68036	19800	7.92	C	Cbl associated ubiquitination enzyme
Voltage-dependent anion-selective channel protein 1	P21796	30600	6.94	C*	Forms channels through mitochondrial membrane

Table A3 List of differentially expressed proteins identified in control versus Nef-transfected rafts. AN indicates Swiss-Prot accession number. M_r, relative molecular mass on gel. pI, isoelectric point on gel. Fold change refers to proteins that were differentially expressed by 2-fold or more when comparing serum gels from healthy controls with the different stages of hepatic fibrosis. C, feature only present in control rafts. N, feature only present in Nef-transfected rafts. C*, feature expressed to higher extent in control raft samples. N*, feature expressed to higher extent in Nef-transfected raft samples.

Immunity, Vol. 23, 621–634, December, 2005, Copyright ©2005 by Elsevier Inc. DOI 10.1016/j.immuni.2005.11.003

Nef-Mediated Lipid Raft Exclusion of UbcH7 Inhibits Cbl Activity in T Cells to Positively Regulate Signaling

Alison Simmons,[1,*] Bevin Gangadharan,[2] Ashleigh Hodges,[1] Katherine Sharrocks,[1] Sripadi Prabhakar,[2] Angel García,[2] Raymond Dwek,[2] Nicole Zitzmann,[2] and Andrew McMichael[1]

[1] MRC Human Immunology Unit
Weatherall Institute of Molecular Medicine
John Radcliffe Hospital
Headington
Oxford OX3 9DS
United Kingdom

[2] Oxford Glycobiology Institute
Department of Biochemistry
University of Oxford
South Parks Road
Oxford OX1 3QU
United Kingdom

Summary

Lentiviral Nef increases T cell signaling activity, but the molecular nature of the stimulus involved is incompletely described. We explored CD4 T cell lipid raft composition in the presence and absence of Nef. Here, the E2 ubiquitin-conjugating enzyme UbcH7, which acts in conjunction with c-Cbl, is absent from lipid rafts. This Nef-mediated exclusion is associated with failure of ubiquitination of activated Vav. In the presence of Nef, lipid raft Cdc42 is activated and forms a ternary complex between the c-Cbl-interacting protein p85Cool-1/βPix and c-Cbl, displacing UbcH7 from rafts. Suppression of p85Cool-1/βPix expression restores UbcH7 raft localization and Vav ubiquitination and diminishes Cdc42 activity. Moreover, p85Cool-1/βPix knockdown attenuates HIV replication. Thresholds for activation of signaling involve the intricate balance of positive and negative regulators. Here we provide evidence for Nef disruption of a negative regulator of T cell signaling in promoting HIV replication.

Introduction

The Nef gene of HIV is important for pathogenicity, increasing viral infectivity and replicative capacity. Several functional attributes have been ascribed to Nef, including the downregulation of MHC class 1 A and B alleles to promote escape from the cellular immune response, downregulation of cell-surface CD4 to enhance virion release from the infected cell surface, and alteration of host cell death pathways to prevent apoptosis of infected cells while promoting death of activated bystander CD8 T cells (for reviews, see Doms and Trono, 2000; Fackler and Baur, 2002). In addition, Nef alters cell signaling to induce an activating stimulus in CD4 T cells (Fackler and Baur, 2002). The principal function and exact molecular mechanism involved in Nef alteration of signaling in the viral life cycle are not fully defined but are likely to contribute to pathogenicity. A key motif required for Nef signaling is the SH3 binding domain, essential for optimal spread of HIV in primary cells (Fackler et al., 2001; Manninen et al., 1998; Saksela et al., 1995). This domain also mediates association with a variety of signaling proteins including the Src family kinases, PAK2, Protein kinase C theta, Erk-1, Raf1, TCRζ, and Vav (for review, see Renkema and Saksela, 2000).

The molecular event facilitating Nef alteration of cell signaling has engendered much interest, and evidence has accumulated for a role at the plasma membrane. Nef is detectable in lipid rafts in T cells (Alexander et al., 2004; Wang et al., 2000) and is associated with the recruitment of activated p21-activated kinase (PAK) to these domains (Krautkramer et al., 2004). Nef activates the GTPases Cdc42 and Rac via the guanine nucleotide exchange factors (GEF) Vav and DOCK2/ELMO1 (Fackler et al., 1999; Janardhan et al., 2004; Lu et al., 1996). PAK is a downstream effector of Cdc42 and Rac; activation of these GTPases by Nef is probably responsible for the consistent observation of PAK activation in Nef-expressing cells. Despite evidence that Nef activates a Cdc42-dependent signaling path in lipid rafts, the initial trigger remains unclear.

To shed further light on the nature of Nef signaling in T cells, we undertook an analysis of differential protein expression in CD4 T cell lipid rafts in the presence and absence of Nef. We investigated proteins recruited or lost from rafts after Nef expression by 2D-PAGE analysis and mass spectrometry. Among proteins absent from Nef-expressing rafts was the E2 ubiquitin-conjugating enzyme UbcH7, which is implicated in the c-Cbl-mediated ubiquitination and negative regulation of T cell signaling molecules such as Lck, Vav, and TCRζ (Rao et al., 2002; Miura-Shimura et al., 2003; Wang et al., 2001). This raft loss of UbcH7 has functional consequences. In the presence of Nef, activated Vav fails to undergo ubiquitination, resulting in the accumulation of tyrosine-phosphorylated Vav in lipid rafts and increased Cdc42 activity. This effect of Nef was recapitulated by UbcH7 knockdown and did not occur after conventional T cell activation. Expression of Nef in signaling-defective Jurkat T cell lines revealed a requirement for Lck but not TCRζ in inhibiting c-Cbl function. We established that in the presence of Nef, a ternary complex forms between activated Cdc42, the PAK interactive exchange factor p85Cool-1/βPix (hereafter referred to as βPix), and c-Cbl that displaces UbcH7 from the c-Cbl RING finger and lipid rafts. This ternary complex has been shown previously to occur after expression of constitutively active Cdc42, resulting in failure of EGFR ubiquitination (Wu et al., 2003). The complex is likely to be responsible for UbcH7 raft displacement, as expression of a constitutively active Cdc42 mutant in Jurkat led to diminished expression of UbcH7 in lipid rafts. Destruction of the complex by knockdown of βPix by short hairpin-interfering RNAs (siRNA) resulted in UbcH7 relocation to lipid rafts in Nef-positive cells and diminished Nef-induced Cdc42 activity. We found that Cbl was

*Correspondence: alison.simmons@molecular-medicine.oxford.ac.uk

required for constitutive localization of UbcH7 in lipid rafts, and it is likely that the Cdc42-βPix-c-Cbl interaction displaces UbcH7 from the Cbl RING finger by steric hindrance. The relevance of these observations to the HIV life cycle was explored by βPix knockdown in infected CD4 T cells, which led to attenuation of HIV replication. These findings indicate that at least part of Nef's signaling activity in T cells derives from inhibition of a negative regulator of T cell signaling.

Results

Changes in the Protein Content of CD4 T Cell Lipid Rafts in the Presence of Nef

Plasma membrane lipid rafts are cholesterol- and sphingolipid-rich plasma membrane domains thought to contribute to compartmentalizing signal transduction events in different regions of the plasma membrane (Harder, 2004). Evidence exists for Nef commandeering T cell signaling machinery high in the T cell signaling pathway and probably within lipid rafts themselves. Nef targeting to lipid rafts in CD4 T cells is dependent on its myristoylated N terminus (Wang et al., 2000). Flag-tagged Nef expression vectors were used to demonstrate the presence of Nef in Jurkat CD4 T cell lipid rafts. Figure 1A compares the raft localization of wild-type SF2 Nef with a mutant (glycine to alanine) at position 2, the myristoylation site (Nef-G2A). Western blotting illustrates cofractionation of the lipid raft marker GM1 with Nef but not Nef-G2A. 2D-PAGE analysis and mass spectrometry were used to sequence proteins differentially expressed in lipid rafts of Jurkat CD4 T cells transfected with either Nef or Flag (pCMV-Tag4A) control vector (for complete gel images, see Figure S1 in the Supplemental Data available with this article online). Cells were harvested at 24 hr posttransfection for sucrose density gradient centrifugation and lipid raft isolation. Four replicate 2D-PAGE gels (with a linear pI range of 3–10) were obtained for both control and Nef-expressing lipid raft fractions to visualize changes in the lipid raft proteome in the presence of Nef. Each gel resolved around 1200 spots, and differentially expressed proteins were selected for protein identification after image analysis. In-gel digestion with trypsin and peptide extraction were carried out by an automated workstation. Tryptic peptides were desalted on an LC system and eluted into a tandem mass spectrometer. The database search was performed with a protein search tool by Swiss-Prot. In several examples, multiple spots represented the same protein, with variations due to posttranslational modification or alternative splicing (Figure S1). Names of the identified proteins and their Swiss-Prot accession numbers are listed in Table 1. Information about sequence coverage and peptide sequence is given in Table S1. By using this methodology, we identified ten proteins that showed increased expression or were exclusively present in Nef-expressing rafts and seven proteins that were decreased in expression or were absent from Nef-expressing rafts.

In the presence of Nef, the E2 ubiquitin-conjugating enzyme UbcH7 was absent from lipid rafts (Figure 1C). UbcH7 has been shown to act as the cognate E2-conjugating enzyme for Cbl family proteins, E3 ubiquitin ligases that mediate ubiquitination, and downregulation of activated T cell signaling molecules (Yokouchi et al., 1999; Zheng et al., 2000). Among the identified proteins differentially expressed in lipid rafts in the presence of Nef, UbcH7 stands out as an attractive candidate for involvement in Nef signaling. This absence may interfere with c-Cbl-mediated negative regulation of T cell signaling proteins and thus provide a means by which Nef might promote T cell signaling.

In addition to UbcH7, several other notable changes in lipid raft protein composition were detected (Figure 1C; Table 1; Figure S1). Nef-expressing lipid rafts exhibited recruitment of components of the actin cytoskeleton and posttranslational modification of transgelin 2, consistent with previous observations of Nef-driven actin polymerization (Fackler et al., 1999). Nef-expressing rafts lack stathmin, which is phosphorylated and consequently inactivated by PAK. Stathmin negatively regulates microtubule dynamics (Andersen, 2000) by sequestering tubulin, by decreasing the concentration of free heterodimers available for polymerization (Belmont and Mitchison, 1996), or by inducing catastrophe at microtubule tips (Cassimeris, 2002). The raft analysis revealed that Nef is associated with recruitment of the RNA binding protein hnRNP E1 that localizes to spreading initiation centers present in the early stages of cell spreading prior to the formation of focal adhesions (de Hoog et al., 2004). Signaling proteins recruited to rafts in the presence of Nef include lactate dehydrogenase-A isoform that is preferentially expressed in activated lymphocytes (Wollberg and Nelson, 1992). Finally, Nef-positive rafts lack a known negative regulator of signaling, 14-3-3ε. Isoforms of 14-3-3 expressed in T cells bind the catalytic subunit of activated PI3K (p110), reducing its enzymatic activity (Bonnefoy-Berard et al., 1995), and the key T cell signaling attenuator c-Cbl after TCR stimulation (Liu et al., 1996).

UbcH7 Is Excluded from Nef-Expressing Lipid Rafts

To confirm the results obtained by 2D-PAGE, Jurkat CD4 T cells were transfected with Nef and Flag vectors and lipid raft fractions were obtained by sucrose density gradient centrifugation. Figure 2A demonstrates exclusion of UbcH7 from the lipid raft fractions of Nef-expressing cells. Comparison of UbcH7 raft localization after expression of Nef-G2A revealed that Nef must be physically present in lipid rafts for UbcH7 raft exclusion to occur (Figure 2A). The majority of signaling functions described for Nef require an intact polyproline motif. To establish whether this Nef domain is needed for UbcH7 lipid raft exclusion, a mutant Flag expression construct was created in which the FPVR motif of Nef (aa 72–75) was mutated to VRIT (Nef-Px-Mu). Expression of this mutant also abrogated the ability of Nef to exclude UbcH7 from lipid raft fractions (Figure 2A).

Confocal studies were then undertaken to further assess the redistribution of UbcH7 observed after 2D-PAGE analysis. Nef-EGFP fusion vectors were created expressing wild-type Nef, Nef-G2A, and Nef-Px-Mu and used to transfect Jurkat. 24 hr posttransfection, lipid rafts were patched by anti-cholera toxin antibody. As observed for Western blots of T cell lipid raft fractions, UbcH7 staining is downregulated in lipid rafts in Nef-EGFP-expressing cells but colocalized with GM1 after expression of the empty EGFP vector, Nef-G2A-EGFP

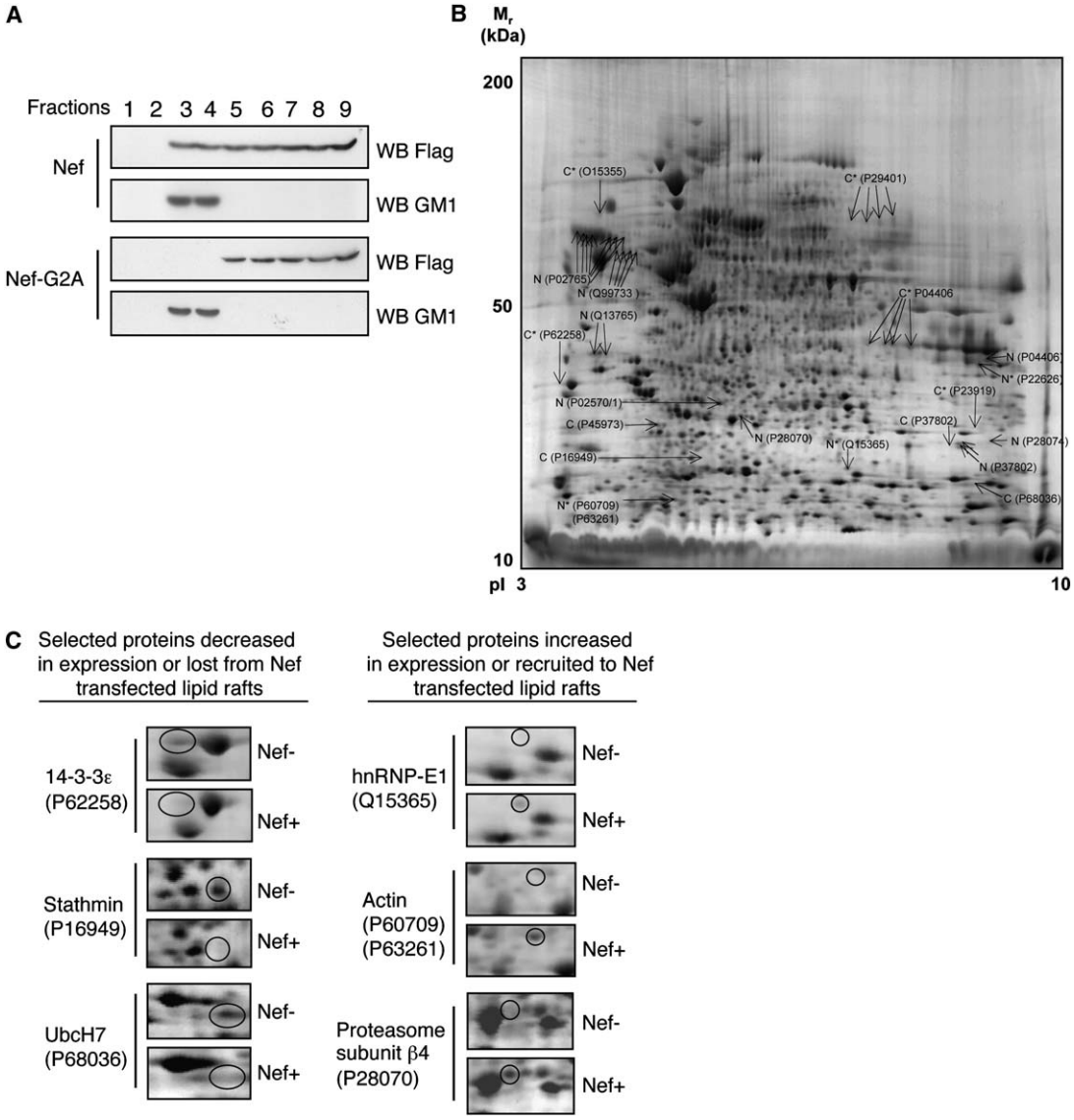

Figure 1. Identification of Proteins Differentially Expressed in Jurkat Lipid Rafts in the Presence of Nef

(A) Western blot of Nef- or Nef-G2A-expressing Jurkat lysate fractions obtained after sucrose density gradient centrifugation. Fractions were immunoblotted to identify Nef with anti-Flag antibody and GM1 with cholera-toxin HRP.

(B) Synthetic 2D-PAGE image representing all protein spots present in the control versus Nef-transfected raft analysis highlighting the differentially expressed features along with their Swiss-Prot accession number. C, features present only in control rafts; N, features present only in Nef-transfected rafts; C*, features present in both control and Nef-transfected rafts but expressed to a higher extent in the control rafts; N*, features present in both control and Nef-transfected rafts but expressed to a higher extent in the Nef-transfected rafts. For complete gel figures and analysis, see Supplemental Data.

(C) Selected close-up examples of representative 2D-PAGE images showing changes in protein expression in Nef-transfected rafts.

and Nef-Px-Mu-EGFP (Figure 2B). Thus, Nef is associated with exit of UbcH7 from lipid rafts and this function requires both the Nef N-terminal myristoylation site and an intact Nef SH3 binding domain.

Failure of Vav Ubiquitination in Nef-Expressing CD4 T Cells

The functional relevance of Nef-mediated exclusion of UbcH7 from lipid rafts was investigated. Nef-interacting proteins known to be substrates for c-Cbl-mediated negative regulation after T cell activation stimuli include Lck, Vav, and TCRζ (Rao et al., 2002; Miura-Shimura et al., 2003; Wang et al., 2001). We focused on characterizing Vav activity in the presence of Nef, as this has been directly linked to PAK activation, a highly conserved function of Nef. Vav GEF activity is important for HIV replication, as dominant-negative Vav suppresses HIV replication when expressed in infected cells (Fackler et al., 1999). In the normal immune response, Vav plays a crucial role in TCR signaling events, including Ca^{2+} flux and cytoskeletal reorganization (Cantrell, 2003). In turn, c-Cbl participates in turning off Vav activity through ubiquitination. After CD4 T cell activation, phosphorylated Vav undergoes c-Cbl association (Marengère et al., 1997), ubiquitination, and degradation (Miura-Shimura et al., 2003). We reasoned that if the exclusion

Table 1. Summary of Differentially Expressed Lipid Raft Proteins and Functional Roles

Functional Category	Increased in Expression or Exclusively Present in Nef-Expressing CD4 T Cell Lipid Rafts	Decreased in Expression or Absent from Nef-Expressing CD4 T Cell Lipid Rafts
Signal transduction	(P00338) L-lactate dehydrogenase A chain (EC 1.1.1.27) (LDH-A) (LDH muscle subunit) (LDH-M)	(O15355) protein phosphatase 2C γ isoform
	(P04406) glyceraldehyde 3-phosphate dehydrogenase (EC 1.2.1.12) (GAPDH)[a]	(P62258) 14-3-3 protein ε
		(P29401) transketolase
		(P23919) thymidylate kinase
Cytoskeletal and microtubule-organizing center regulation	(P37802) transgelin 2[a]	(P16949) stathmin (Oncoprotein 18)
	(P60709) (P63261) actin[a]	
Proteolysis	(P28070) proteasome subunit beta type 4 precursor	
	(P28074) proteasome subunit beta type 5 precursor	
Ubiquitination		(P68036) ubiquitin-conjugating enzyme E2-18 kDa UbcH7
mRNA processing and translation	(Q15365) poly(rC)-binding protein 1 (hnRNP-E1)	
	(Q13765) NASCENT polypeptide associated complex alpha subunit	
Nucleosome assembly	(Q99733) nucleosome assembly protein 1-like 4	
Ion channel		(P21796) voltage-dependent anion-selective channel protein 1 (VDAC-1)
Acute phase protein	(P02765) alpha-2-HS-glycoprotein precursor[a]	

Identified proteins are specified by Swiss-Prot accession number. Further information about sequence coverage and peptide sequences can be obtained from the Supplemental Data.
[a] Posttranslational modification detected by 2D-PAGE after Nef expression.

of UbcH7 from lipid rafts by Nef has functional relevance for Nef signaling, then it should be possible to demonstrate failure of ubiquitination of Nef-activated c-Cbl substrates.

Nef-mediated Vav activation was first confirmed after transfection of Jurkat with Flag or Nef vectors. Similar to the scenario occurring after anti-CD3/CD28 triggering, Nef expression resulted in Vav hyperphosphorylation in lipid raft fractions, as shown on Western blots from Nef-expressing versus control lysates (Figure 3A). The level of Vav GEF activity was then assessed with a Cdc42 activation assay. Here, active GTP bound Cdc42 binds to the p21 binding domains (PBD) of PAKs so GST-PBD can be used to pull down Cdc42-GTP. Levels of GTP bound Cdc42 in lipid rafts were assessed by glutathione agarose bound GST-PBD, and the fraction of PBD bound Cdc42 were assayed by immunoblotting (Figure 3B). This demonstrated that Nef increased the level of GTP-Cdc42 in lipid rafts, consistent with previous reports (Krautkramer et al., 2004). We next examined whether Vav becomes ubiquitinated in Nef-expressing CD4 T cell lipid rafts. c-Cbl has been implicated directly in the ubiquitination and negative regulation of Vav after T cell activation or conditions that promote both c-Cbl and Vav phosphorylation (Miura-Shimura et al., 2003). Figure 3C shows Western blots for ubiquitin after Vav immunoprecipitation from lipid rafts of Nef and control transfectants and T cells activated via ligation of CD3 and CD28. While Nef expression was associated with increased Vav GEF activity and phosphorylation, no ubiquitination of Vav could be detected in Nef-expressing CD4 T cell lipid rafts. In contrast, activation of Jurkat via plate bound anti-CD3/CD28 resulted in detectable Vav ubiquitination. In addition, after TCR stimulation of Jurkat, Vav could be coimmunoprecipitated with c-Cbl as would be expected for a Cbl substrate (Marengère et al., 1997). However, in Nef-expressing cells, no such association could be demonstrated (Figure 3D).

To examine whether accessibility to UbcH7 might be responsible for failure of Vav ubiquitination in the presence of Nef, an siRNA targeting UbcH7 was used to diminish UbcH7 expression (Verma et al., 2004). Jurkat were transfected with this *UbcH7* siRNA and a nonsilencing (NS) siRNA, whose sequence did not match any known human gene (Figure 3E). A comparison of the effect of UbcH7 knockdown on Vav activation with that occurring after antigen receptor triggering was undertaken. Similar to the results obtained after Nef expression, levels of GTP bound Cdc42 increased after UbcH7 knockdown (Figure 3F), and Vav tyrosine phosphorylation increases to levels comparable with conventional T cell activation (Figure 3G). In addition, we were unable to detect significant levels of Vav ubiquitination after UbcH7 knockdown (Figure 3G). These observations indicate that CD4 T cell c-Cbl-mediated negative regulatory activity is defective in Nef-expressing cells and suggest that the exclusion of UbcH7 away from raft-localized c-Cbl has functional consequences for Nef signaling.

Lck but Not TCRζ Is Required for Nef-Mediated UbcH7 Lipid Raft Exclusion

To establish whether UbcH7 lipid raft exclusion is idiosyncratic to the Nef T cell activation stimulus, the effect of antigen receptor triggering on UbcH7 raft location was studied. Jurkat were stimulated with plate bound anti-CD3/CD28 over a time course extending to 24 hr. It was not possible to demonstrate changes in expression of UbcH7 between raft and nonraft compartments either by Western blot (Figure 4A) or confocal microscopy (Figure 4B) throughout.

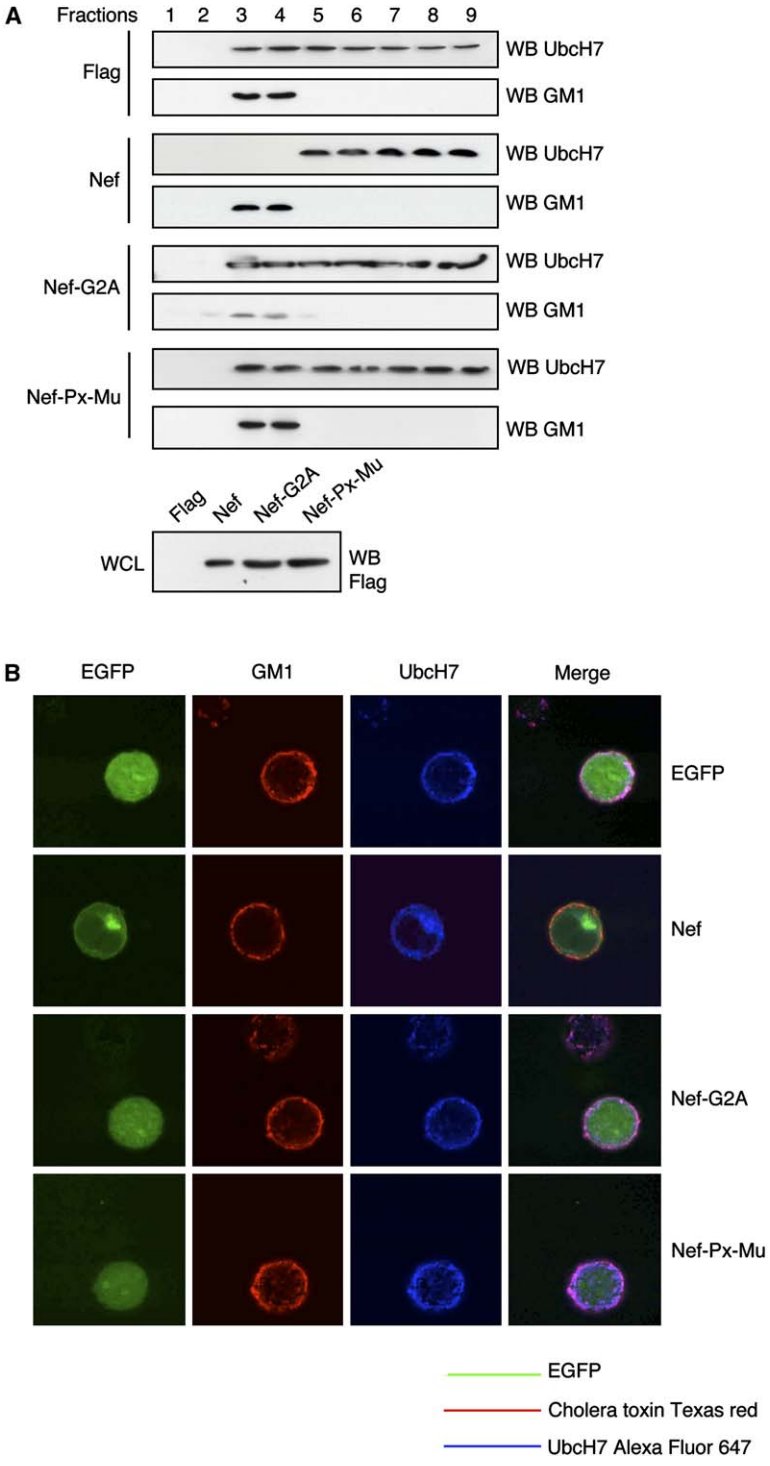

Figure 2. UbcH7 Is Selectively Excluded from Lipid Rafts in the Presence of Nef

(A) Fractions obtained after sucrose density gradient centrifugation from Jurkat transfected with Flag, Nef, Nef-G2A, or Nef-PX-Mu were immunoblotted for UbcH7 (top) and GM1 (middle). The lower panel indicates presence of Nef after Flag Western blot of whole-cell lysates (WCL) from the corresponding transfectants.

(B) Confocal images of Jurkat transfected with EGFP or Nef-EGFP, Nef-G2A-EGFP, and Nef-PX-Mu-EGFP. 24 hr posttransfection, cells were stained with cholera toxin Texas red, lipid rafts were patched with anti-cholera toxin, and UbcH7 was stained with anti-UbcH7 Alexa Fluor 647.

The requirement for upstream T cell signaling molecules in Nef-mediated downregulation of lipid raft UbcH7 was investigated with mutant Jurkat T cell lines defective in key T cell signaling molecules. JCaM1.6, genetically deficient in Lck (Straus and Weiss, 1992), and J.RT3-T3.5, functionally deficient in TCRζ (Ohashi et al., 1985), were transfected with Nef or Flag vectors and lipid raft fractions were prepared. Western blotting of GM1-positive fractions of Nef-transfected rafts revealed the absence of UbcH7 in J.RT3-T3.5 but not JCaM1.6, thus indicating a requirement for Lck but not TCRζ in UbcH7 raft exclusion (Figure 4C). These results were confirmed by confocal analysis of J.RT3-T3.5 and JCaM1.6 transfected with EGFP and Nef-EGFP (Figure 4D). Next, Lck expression in JCaM1.6 was restored by either wild-type Lck or a kinase-dead mutant Lck-R273A (Rao et al., 2002), and localization of UbcH7 was examined. Interestingly, both Lck constructs restored the ability of Nef to downregulate UbcH7 expression in lipid rafts (Figures 4E and 4F), indicating that while Lck

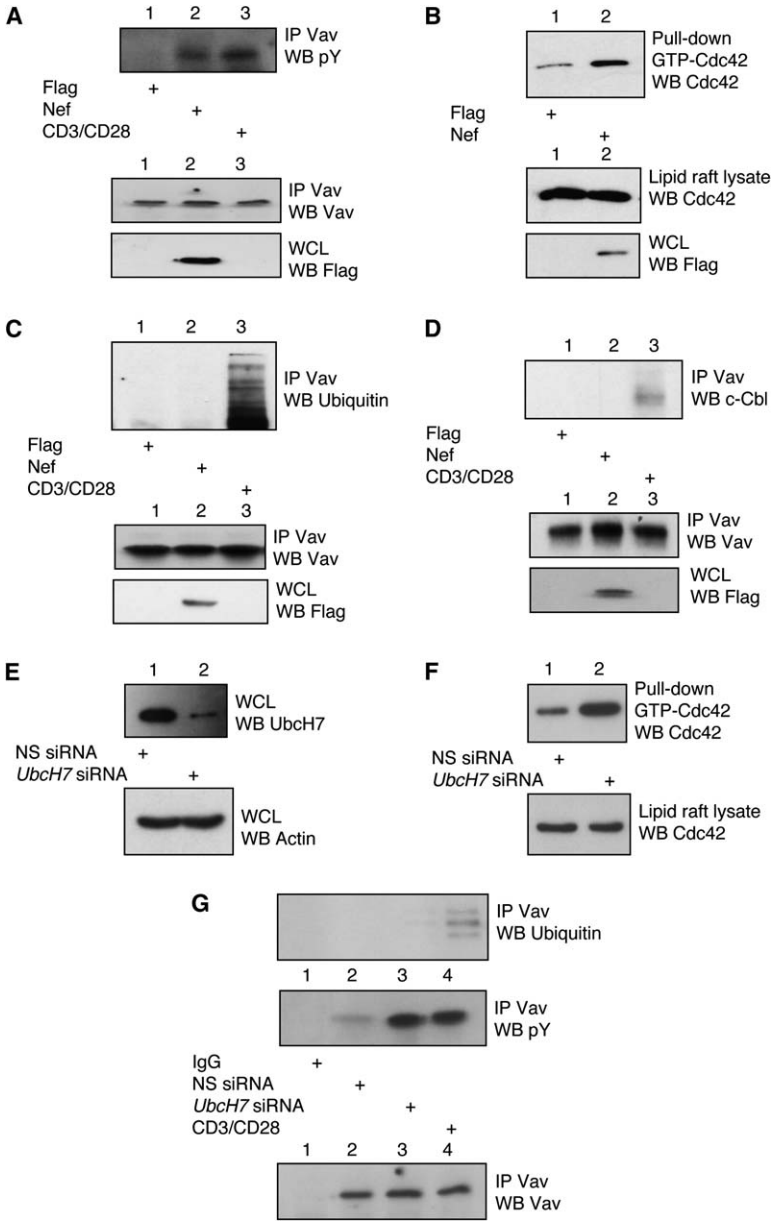

Figure 3. Failure of c-Cbl-Mediated Ubiquitination of Nef-Activated Vav

(A) Vav was immunoprecipitated from lipid rafts of Flag or Nef transfectants or Jurkat activated with anti-CD3/CD28, and anti-phosphotyrosine (pY) immunoblot was performed as shown in the top panel and Vav immunoblot below. Flag Western blot of WCL is in the lower panel.

(B) PBD-agarose was used to pull down GTP bound Cdc42 from lipid rafts of Flag- or Nef-transfected cells, and levels of GTP-Cdc42 were assessed by Western blot. The middle panel shows Cdc42 immunoblot from the same lipid raft samples. The bottom panel shows Flag immunoblot of WCL.

(C) Vav was immunoprecipitated from lipid rafts of Flag or Nef transfectants or Jurkat activated with anti-CD3/CD28. Immunoblot for ubiquitin is shown in the top panel and for Vav below. Flag immunoblot of WCL is in the lower panel.

(D) Jurkat were transfected with Flag or Nef vectors or activated with anti-CD3/CD28. Vav immunoprecipitate and c-Cbl Western blot is shown above and Vav Western blot from the corresponding immunoprecipitates below. The lower panel shows Flag immunoblot of the corresponding WCL.

(E) Jurkat were transfected with NS siRNA or *Ubch7* siRNA and UbcH7 protein level assessed at 48 hr by Western blot, with actin immunoblot below.

(F) Cdc42 immunoblot following pull-down of GTP-Cdc42 with PBD-agarose from cells treated as in (E) with Cdc42 immunoblot from lipid raft lysates shown below.

(G) Vav was immunoprecipitated from NS, or *Ubch7* siRNA transfected, and from CD3/CD28 activated Jurkat and Western blotted with anti-phosphotyrosine. Below is the corresponding anti-Vav immunoblot. The top panel illustrates ubiquitin immunoblot of the same Vav immunoprecipitates.

is required for this function of Nef, the kinase activity of Lck is dispensable.

Cdc42 Associates with βPix and c-Cbl in Nef-Expressing Cells

The mechanism by which Nef mediates exclusion of UbcH7 from lipid rafts and inhibition of Cbl-mediated ubiquitination was investigated. Crystallographic studies have established that UbcH7 interacts with Cbl via a weak association with the Cbl RING finger domain (Zheng et al., 2000). A known inhibitor of Cbl activity is Human Sprouty 2 (hSpry2). hSpry2 directly interacts with the c-Cbl RING finger domain, displacing UbcH7 from its binding site on the E3 ligase, thus abrogating epidermal growth factor receptor (EGFR) ubiquitination and endocytosis (Wong et al., 2002). We hypothesized that Nef might facilitate displacement of UbcH7 in such a manner by precipitating the interaction of an inhibitory protein with Cbl in an area at or in proximity to the RING finger. It has been demonstrated in conditions where Cdc42 activity is increased that a ternary complex can form between Cdc42 and c-Cbl, mediated by the PAK-interacting exchange factor βPix (Wu et al., 2003). Formation of this complex after expression of constitutively active Cdc42 mutants inhibits c-Cbl-mediated ubiquitination and degradation of EGFR. βPix proteins are binding partners of PAK (Bagrodia et al., 1999; Manser et al., 1998), Cbl-b (Flanders et al., 2003), and c-Cbl (Wu et al., 2003). The binding of c-Cbl to βPix is mediated via the βPix SH3 domain (Wu et al., 2003), and the Cbl family protein SH3 binding domain lies directly adjacent to the RING finger. We hypothesized that lipid raft Nef-activated Cdc42 might facilitate the formation of such a ternary complex of βPix, Cdc42, and c-Cbl that would displace UbcH7 from its binding site on the c-Cbl RING finger. To test this, we transfected Jurkat CD4 T cells

with either Flag or Nef vectors and immunoprecipitated Cdc42. It was possible to demonstrate coimmunoprecipitation of both βPix and c-Cbl with Cdc42 in the Nef-expressing T cell lysates (Figure 5A). In contrast, coimmunoprecipitation experiments carried out after T cell activation did not reveal formation of this ternary complex (Figure 5A). The requirement for Lck in inducing this ternary interaction complex in the presence of Nef was assessed by expressing Nef in JCaM1.6 alone, or together with Lck or Lck-R273A expression vectors. Figure 5B shows that the Nef-mediated interaction of Cdc42 with Cbl and βPix is not detectable in the absence of Lck but does not require the enzymatic activity of Lck to occur. These data indicate that Nef does indeed induce formation of a lipid raft Cdc42-βPix-Cbl complex in an Lck-dependent manner, which might be responsible for inhibition of c-Cbl activity by directly displacing the c-Cbl E2 UbcH7 away from its active site on the c-Cbl RING finger.

Expression of a Constitutively Active Cdc42 Mutant Is Associated with UbcH7 Raft Loss while βPix Knockdown Results in Relocation of UbcH7 to Lipid Rafts and Restores Ubiquitination of Nef-Activated Vav

To test this hypothesis further, the requirement for Cbl in facilitating UbcH7 entry to lipid rafts was examined after knockdown of c-Cbl and Cbl-b with siRNAs. Figure 6A illustrates the reduction in Cbl protein levels obtained after transfection of Cbl but not NS siRNA. Figure 6B demonstrates a reduction in level of UbcH7 detectable in lipid rafts after Cbl knockdown. We examined whether steric hindrance induced by association of activated Cdc42 and βPix with Cbl might explain the exit of UbcH7 from lipid rafts observed after Nef expression. A constitutively active Cdc42 mutant capable of constitutive GDP-GTP exchange, Cdc42(F28L), shown previously to induce Cdc42-βPix-Cbl formation (Wu et al., 2003), was transfected in Jurkat. UbcH7 lipid raft localization was assessed by Western blot (Figure 6C). Downregulation of UbcH7 raft expression was observed, suggesting formation of a Cdc42-βPix-Cbl complex that may prevent UbcH7 binding to the Cbl RING finger, probably via steric hindrance effects.

To investigate further whether the Nef-mediated Cdc42-βPix-Cbl complex formation was responsible for UbcH7 lipid raft displacement and failure of Vav homeostasis in Nef-expressing cells, we inhibited βPix expression. To do so, we chose several sequences in the human *βPix* gene and designed siRNA directed against βPix. These were tested for their ability to knock down βPix expression in Jurkat. Transfection of 20 μM *βPix* siRNA1 efficiently diminished expression of βPix when assessed by Western blot (Figure 6D, i) and confocal analysis (Figure 6D, ii) in comparison with NS siRNA. The effect of βPix knockdown on the subcellular distribution of UbcH7 was investigated in the presence of Nef. *βPix* siRNA1 and control NS siRNA were cotransfected with either control Flag or Nef expression vectors; lipid rafts were extracted and Western blotted for the presence of UbcH7. Figure 6E demonstrates that while UbcH7 remains excluded from raft fractions in Nef and NS siRNA transfectants, raft localization returns when βPix protein expression is diminished. We next addressed whether βPix knockdown could restore Nef-activated Vav ubiquitination. Jurkat were transfected with Nef or Flag plasmids together with either *βPix* siRNA1 or NS siRNA. Vav was immunoprecipitated from lipid raft fractions obtained from these transfectants, and levels of ubiquitination were assessed by Western blotting. As predicted after βPix knockdown in Nef-expressing cells, Vav becomes detectably ubiquitinated in lipid rafts (Figure 6F). In addition, detection of Cdc42 activity in the same transfectants demonstrates that, after expression of *βPix* siRNA1, Nef-mediated Cdc42 activity is reversed (Figure 6G). Therefore, it appears that the formation of a ternary complex between Cdc42, βPix, and c-Cbl occurring in the presence of Nef results in lipid raft displacement of UbcH7 and failure of c-Cbl-mediated ubiquitination activity.

βPix Knockdown and HIV Replication

βPix siRNA1 was used to examine whether Nef interference with c-Cbl-mediated ubiquitination influences its function in enhancement of HIV replication. Figure 7A demonstrates the kinetics of βPix knockdown after transfection of βPix siRNA1 in Jurkat. Reporter EGFP-expressing HIV virus HIV NL-GI, where EGFP replaces Nef in HIV NL4-3 and Nef is replaced downstream of an IRES (Cohen et al., 1999), was then transfected with either *βPix* siRNA1 or NS siRNA. Viral production was compared for 48 hr posttransfection. Figure 7B shows βPix levels in the HIV-transfected cells. After introduction of NL-GI into βPix knockdown cells, HIV production was significantly diminished, as assessed by FACS analysis of EGFP expression (Figure 7C) and ELISA analysis of p24 production (Figure 7D). The data shown are representative of six replicate experiments. These results indicate that Nef-mediated Cdc42-βPix-Cbl association is important for HIV replication in CD4 T cells.

Discussion

The precise nature of the activation stimulus that Nef delivers to CD4 T cells has remained elusive. Signal transduction by T cells is through the translocation and activation of protein tyrosine kinases and the formation of a network of adaptor molecules (Kane et al., 2000). Nef has been proposed to act as an adaptor bringing signaling substrates into proximity to initiate signaling. While multiple interacting partners have been described, and several of these have been shown to change in activity in the presence of Nef, definition of a unifying single molecular unit involved has not been forthcoming.

In this study, we conducted a proteomic analysis of lipid rafts that revealed loss of UbcH7, hinting at a role for Nef in disruption of Cbl activity. We demonstrate that Cbl-mediated ubiquitination in lipid rafts of at least one of the Nef activated proteins, Vav, is diminished, leading to enhanced Cdc42 activity. This process requires an upstream Src kinase, Lck, but not TCRζ, and results in the formation of a ternary complex between Cdc42, βPix, and c-Cbl. The complex appears to be responsible for raft loss of UbcH7, as diminishing expression of βPix leads to relocation of UbcH7 to lipid rafts and ubiquitination of Nef-activated Vav. The Cdc42-βPix-Cbl-ternary complex formation has been described previously following expression of constitutively active

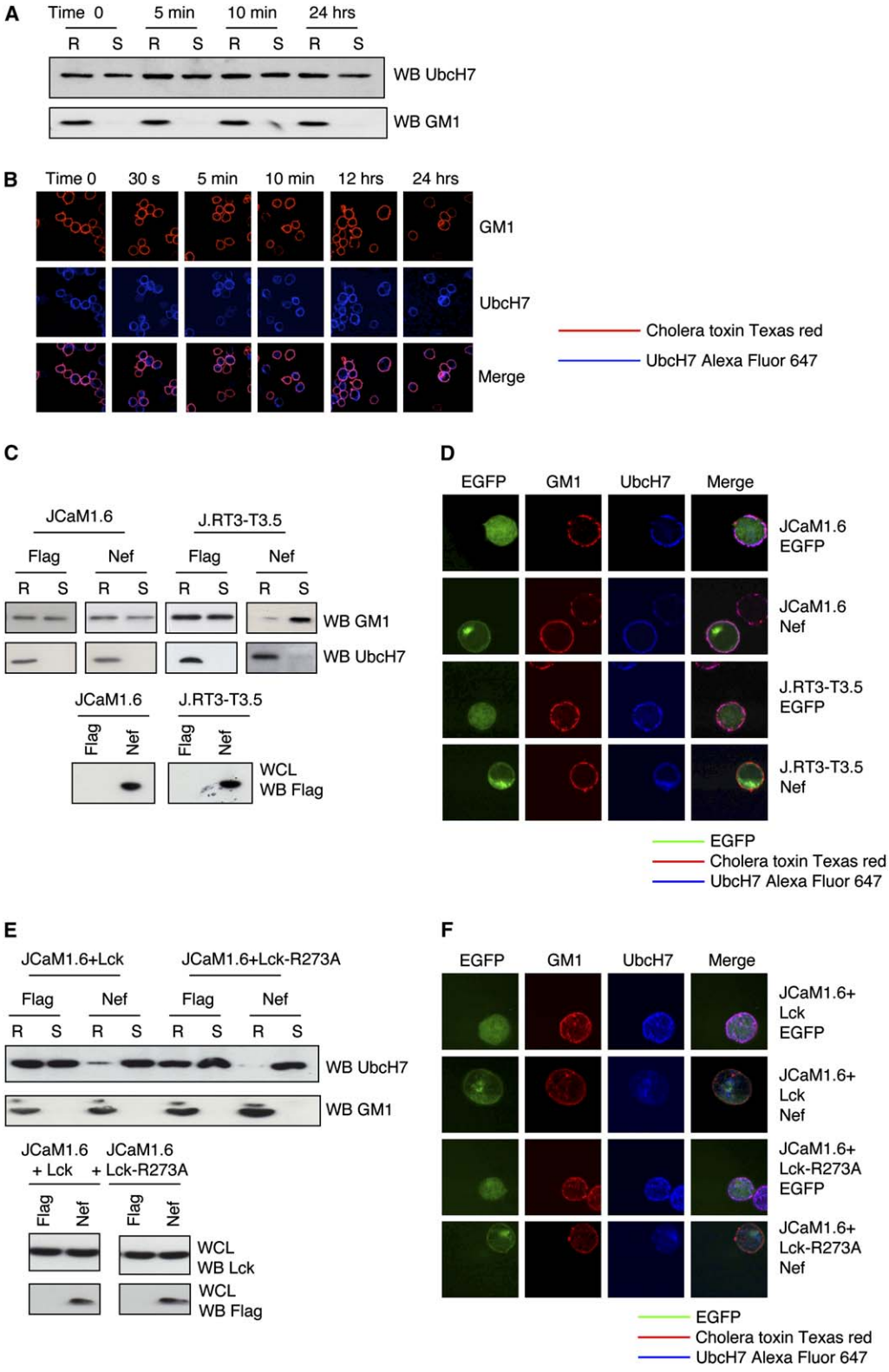

Figure 4. UbcH7 Raft Exclusion Is Distinct to the Nef Activation Stimulus and Is Reliant on Lck

(A) Western blot of UbcH7 in lipid raft (R) and nonraft (S) fractions of Jurkat stimulated with CD3/CD28 over a period of 24 hr. UbcH7 Western blot is in the top panel and GM1 below.

(B) Jurkat were stimulated with plate bound anti-CD3/CD28, harvested, and stained for GM1 with cholera toxin Texas red and UbcH7 Alexa Fluor 647 over a time course of 24 hr.

(C) JCaM1.6 and J.RT3-T3.5 cells were transfected with Flag or Nef vectors. Western blot for UbcH7 in lipid raft and nonraft lysates is shown in the top panel, with GM1 immunoblot below with cholera toxin. Flag Western blot of WCL is shown in the lower panel.

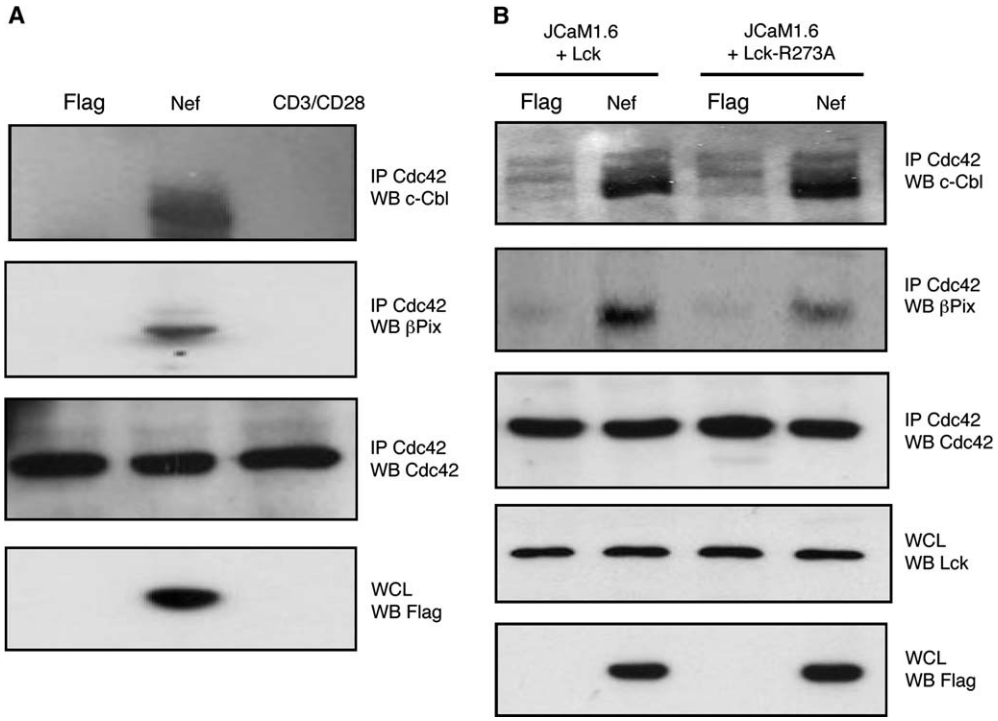

Figure 5. Cdc42 Associates with c-Cbl and βPix in the Presence of Nef

(A) Jurkat CD4 T cells were transfected with Flag or Nef or were activated with anti-CD3/CD28, and immunoprecipitates were performed with anti-Cdc42. The top panel shows Western blot for c-Cbl, the middle panel for βPix, and the lower panel for Cdc42. Flag expression in WCL is shown below.

(B) JCaM1.6 were transfected with Flag or Nef vectors and either Lck or Lck-R273A. Cdc42 was immunoprecipitated and Western blot for c-Cbl (top), βPix (middle), or Cdc42 (lower) was performed. Lck and Flag expression in WCL is shown below.

Cdc42 mutants, leading to failure of ubiquitination of EGFR, with resultant accumulation of surface EGFR and cellular transformation. The binding of activated Cdc42 to a βPix-Cbl complex here was thought to sterically interfere with the binding of Cbl to the EGF receptor, thus preventing E3 ligase activity. We found that expression of the mutant Cdc42, Cdc42(F28L), that is capable of constitutive GDP-GTP exchange, results in downregulation of lipid raft UbcH7 expression. It is likely that Cdc42-βPix-Cbl ternary complex formation also prevents the ubiquitin-charged E2 from gaining access to the Cbl RING finger by steric interference. Interestingly, diminishing Cbl expression with siRNAs resulted in loss of UbcH7 from lipid rafts, suggesting that interaction with Cbl is required for constitutive UbcH7 lipid raft localization in T cells.

Why Nef induces UbcH7 exit from lipid rafts but TCR stimulation fails to do so remains unclear. As a viral protein, Nef is not subject to the same negative regulatory constraints as endogenous T cell signaling mediators, which may lead to sustained imbalance in Cdc42 activity in lipid rafts and forward feed signaling. It might be expected that Nef should lead to transformation in cells in which it is expressed. Nef has been shown to be transforming in certain cell types including fibroblasts (Briggs et al., 1997) and neurons in an SH3-dependent manner (Kramer-Hammerle et al., 2001). However, in the case of whole HIV infection, active viral replication leads to cellular cytopathicity, which likely overrides any transforming effect.

A paradigm exists for the control of ubiquitination by spatial localization of an E2 ubiquitin-conjugating enzyme, as UbcM2 is localized to the nucleus via importin-11 after ubiquitin charging (Plafker et al., 2004). It is possible that Nef parodies a yet undiscovered conventional physiological stimulus to interfere with c-Cbl function via control of the cellular localization of UbcH7. Nef has previously been shown to mimic integrin signaling by inducing the relocalization of the Eed transcriptional repressor to the plasma membrane in T cells (Witte et al., 2004). Lipid rafts have been implicated in the proper organization of integrin signaling (Palazzo et al., 2004; del Pozo et al., 2005). Nef-mediated recruitment of hnRNP E1 to lipid rafts is supportive of an integrin-type trigger. hnRNP E1 localizes to spreading initiation centers present in the early stages of cell spreading prior to the

(D) JCaM1.6 and J.RT3-T3.5 cells were transfected with EGFP or Nef-EGFP, stained for GM1 with cholera toxin Texas red and rafts patched with anti-cholera toxin antibody. UbcH7 was stained with UbcH7 Alexa Fluor 647.

(E) JCaM1.6 were transfected with Lck or Lck-R273A and Flag or Nef vectors before Western blot for UbcH7 and GM1 in raft and nonraft fractions. The lower panels show Western blot for Lck and Flag in WCL.

(F) JCaM1.6 were transfected with Lck or Lck-R273A and EGFP or Nef-EGFP before staining for GM1 with cholera toxin Texas red, raft patching, and subsequent UbcH7 Alexa Fluor 647 staining.

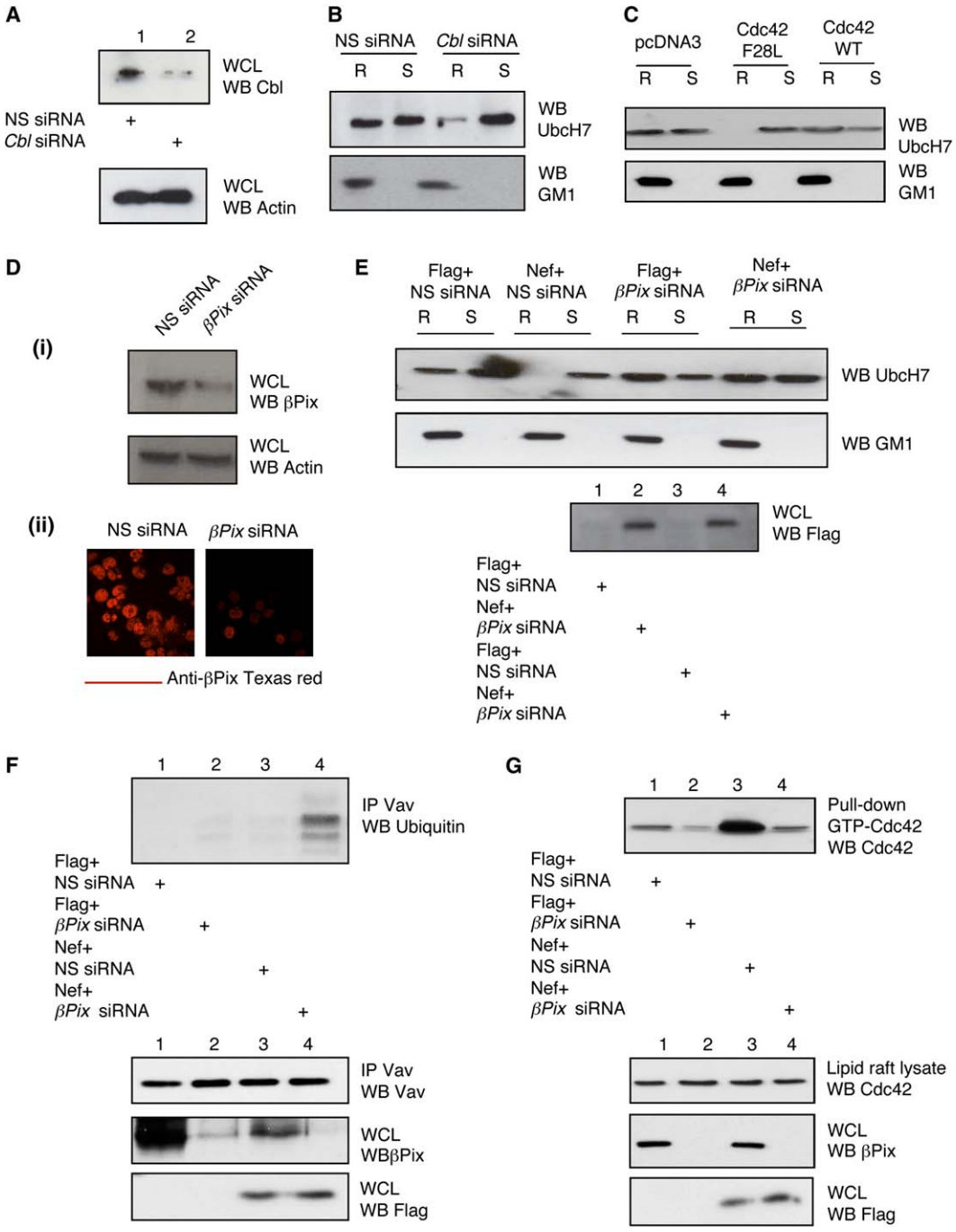

Figure 6. Cbl Is Required for UbcH7 Raft Localization, Expression of Cdc42(F28L) Displaces UbcH7 from Rafts, while βPix Knockdown Restores UbcH7 Raft Localization

(A) Jurkat were transfected with either NS siRNA or Cbl siRNA and Western blot for Cbl protein levels performed at 48 hr.

(B) The effect of Cbl knockdown on UbcH7 raft localization. The top panel shows UbcH7 protein levels in lipid raft fractions of Jurkat transfected with either NS siRNA or Cbl siRNA, and the lower panel shows GM1 Western blot.

(C) Jurkat were transfected with EGFP+empty vector (pcDNA3), Cdc42(F28L), or Cdc42WT, and Western blot for UbcH7 was performed on lipid raft (R) and soluble (S) fractions obtained after sucrose density gradient centrifugation. GM1 immunoblot is shown below. Transfection efficiency was comparable in all three transfections as assessed by EGFP expression on FACS analysis (data not shown).

(D) Western blot (i) and confocal (ii) images of βPix expression in the presence of NS siRNA and *βPix* siRNA1 at 48 hr post transfection.

(E) Lipid raft fractions obtained from cells transfected with Flag or Nef together with either NS siRNA or *βPix* siRNA. Fractions were Western blotted for UbcH7 and GM1 and WCL for Flag (bottom).

(F) Vav was immunoprecipitated from CD4 T cells transfected with Flag or Nef and either NS siRNA or *βPix* siRNA1. Western blot with anti-ubiquitin is shown in the top panel. The lower panel shows Vav Western blot from the same immunoprecipitates.

(G) Jurkat were transfected as in (C), lipid rafts were obtained, and Cdc42-GTP pull-down was conducted with PBD-agarose. Bound Cdc42 is shown in the top panel, lipid raft Cdc42 in the middle panel, and Flag immunoblot below.

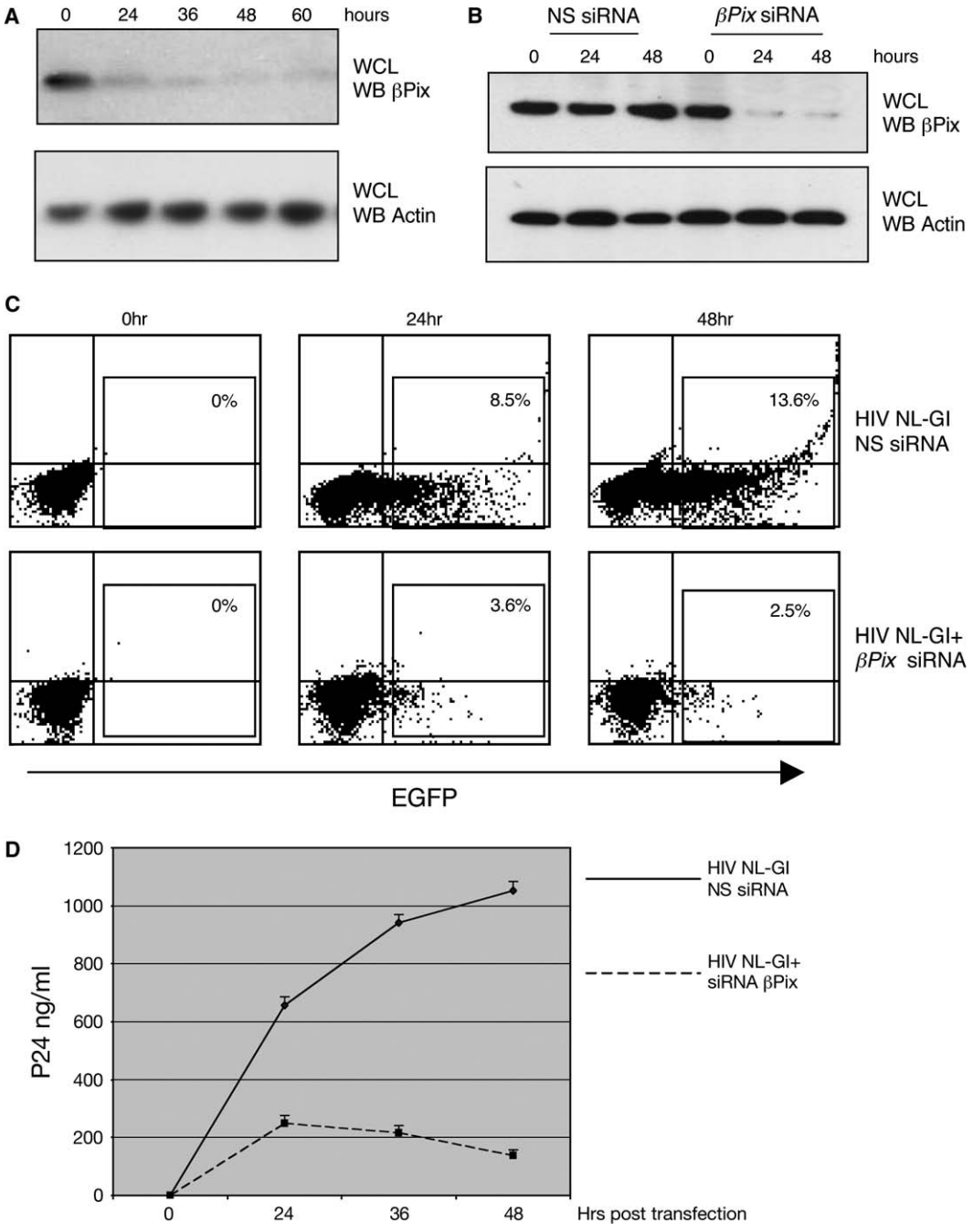

Figure 7. βPix Is Required for HIV Replication

(A) Time course demonstrating βPix knockdown after transfection of βPix siRNA1.

(B) Jurkat CD4 T cells were transfected with NL-GI HIV virus and either 20 μM *βPix* siRNA1 or NS siRNA, and the degree of βPix knockdown was assessed by Western blot.

(C and D) Levels of HIV production were documented by FACS analysis of EGFP expression (C) and by p24 ELISA, where values shown are averages ± SD from six separate experiments (D).

formation of focal adhesions that are induced by integrin triggering (de Hoog et al., 2004). Indeed, the requirement for Lck in inducing UbcH7 raft exit would also support such a stimulus, as Lck has been shown to be necessary for integrin activation in T cells (Fagerholm et al., 2002). It was interesting that the kinase domain of Lck was dispensable, hinting at an adaptor function for Lck in Nef-mediated UbcH7 raft downregulation. A previous study has also implicated Lck in alteration of c-Cbl phenotype (in this case phosphorylation) in the presence of Nef and in the context of HIV infection of primary CD4 T cells (Yang and Henderson, 2005).

A consequence of Nef inhibition of c-Cbl-mediated ubiquitination is the maintenance of self-sustaining populations of GTP bound Cdc42 at the plasma membrane and in lipid rafts. How this dysregulation of signaling

functions to propagate virions is unclear. Cdc42 has been implicated in diverse cellular processes such as control of the actin cytoskeleton to help establish cell polarity, intracellular trafficking, and regulation of cell growth (reviewed by Cerione, 2004). It is possible that these roles may be usurped by Nef to govern aspects of the HIV life cycle. Localized plasma membrane Cdc42 activity may be required for virological synapse formation. Infected cells form a synapse with uninfected target cells that facilitates efficient cell-cell transfer of virions (Jolly et al., 2004; McDonald et al., 2003). It may be that Nef plays a role in the formation of this synapse by promoting local microtubule stabilization at the cell/cell interface via Cdc42 and PAK activation. The observed exit of the microtubule destabilizer stathmin from Nef-expressing lipid rafts is supportive of this hypothesis. Analogies have been made between the immunological and virological synapse, and interestingly in T lymphocytes, dominant-negative Cdc42 has been shown to block polarization toward antigen-presenting cells (Stowers et al., 1995). Ultimately, achieving heightened Cdc42 activity may be important in the HIV life cycle to direct HIV budding. HIV buds via the multivesicular body in a manner requiring TSG101 (tumor susceptibility gene 101 protein) and ESCRT-1 (endosomal sorting complex required for transport) (von Schwedler et al., 2003). The multivesicular body is specifically localized to sites of active exocytosis and enables secretory vesicle targeting and plasma membrane docking. Cdc42 has been shown to direct activity of the exocyst in yeast by binding Sec3p in its GTP bound form. Sec3p is an exocyst component that acts as a spatial landmark for polarized exocytosis. Cdc42 coordinates the vesicle docking machinery and the actin cytoskeleton for polarized secretion (Zhang et al., 2001). Most simply the inhibition of c-Cbl by Nef may serve to direct new gene expression akin to a weak form of T cell activation that has been proposed to provide a transcriptional environment favorable for completion of the HIV life cycle.

Ever since Nef was demonstrated to be essential for maintenance of high viral loads and progression to simian AIDS in adult rhesus macaques (Kestler et al., 1991), its primary function in achieving this effect has been under investigation. Identification of the principal host cell molecules involved is crucial to understanding how Nef exerts pathogenicity and in the rational design of intervention strategies. Our work demonstrates a role for Nef in interfering with an intrinsic negative feedback loop of T cell signaling. This inhibition of Cbl by Nef provides new candidate targets for inhibition of HIV replication.

Experimental Procedures

Cell Culture, Stimulation, Plasmids, Transfections, and p24 ELISA

Jurkat E6-1, JCaM1.6, and J.RT3-T3.5 cells were obtained from ATCC and were cultured in RPMI 1640 media (GIBCO-BRL) supplemented with 10% fetal calf serum, penicillin, streptomycin, and glutamine (GIBCO-BRL). For stimulation of Jurkat with anti-CD3/CD28, 30 μl of 10 μg/ml OKT3 and anti-CD28 were added to 96-well plates and incubated at 37ºC for 90 min. The wells were washed with PBS three times and 2×10^5 cells were added to each well in 0.2 ml media. Cells were incubated at 37ºC and harvested at 24 hr. Anti-CD28 antibody (clone CD28.2) was obtained from Pharmingen. Flag-tagged Nef constructs were generated by cloning SF2 *nef* from pWT-IRES-EGFP (Simmons et al., 2001) into the pCMV-Tag-4A vector from Invitrogen. For the mutant G2A, the forward primer CGC GGA TCC GCG ACC ATG GCG GGC AAG TGG TCA AAA was used to amplify *nef* before insertion into pCMV-Tag-4A. The mutant Nef-PX-Mu was created by cloning PX-Mu-*nef* from the vector CN.94PXmu/Nef.Pxmu (Xu et al., 1999) before insertion to pCMV-Tag-4A. Nef-EGFP fusion expression vectors were created by cloning wild-type *nef* and mutants into the vector pEGFP-N3 from Clontech. Wild-type and kinase-dead Lck expression vectors PAlterMAX2-Lck and PAlterMAX2-R273A were obtained from Hamid Band, and the wild-type and constitutively active Cdc42 expression vectors, Cdc42(F28L), were from Richard Cerione. Transient transfection of Jurkat was carried out with AMAXA cell line nucleofector kit. Virus production was assayed by p24 ELISA; EGFP expression in HIV-infected cells was analyzed by FACSCalibur (Becton Dickinson).

Antibodies, Cdc42 Activation Assay, and siRNAs

The anti-Flag M2, anti-β Actin antibodies, and cholera-toxin HRP were obtained from Sigma. Antibodies to Cbl, βPix, and Cdc42 were obtained from Santa Cruz and Chemicon. Anti-cholera toxin antibodies were obtained from Sigma. Antibodies to UbcH7 were obtained from Upstate Biotechnology and Chemicon, and Vav and Lck antibodies were from Upstate Biotechnology and Santa Cruz. Anti-ubiquitin antibody was from Affiniti. Fluorescent conjugate secondary antibodies were obtained from Molecular Probes. Cdc42 activation assays were performed with the Cdc42 activation assay kit from Chemicon. Custom high performance purity (HPP) grade siRNAs were obtained from Qiagen. The target DNA sequence used to construct *βPix* siRNA1 was 5′-AAG AGCTCGAGAGACACATGG-3′, for *UbcH7* siRNA 5′- AAATGTGGGATGAAAAACTTC-3′, and the nonsilencing target sequence 5′-AAT TCT CCG AAC GTG TCA CGT-3′. *c-Cbl* and *Cbl-b* siRNA sequences are available from Qiagen.

Lipid Raft Extraction, Immunoprecipitation, and Western Blots

Lipid rafts were isolated from cell lysates of 50×10^6 cells in Triton X-100 and floatation on sucrose density gradients as described previously (Cheng et al., 1999). Among 12 fractions collected from the top of the gradient, fractions 3 and 4 were confirmed as rafts by detection of GM1 by Western blot analysis. For immunoprecipitations, the lipid raft fraction 4 was mixed with 60 mM octyl β-D-glucopyranoside (Sigma), and solubilized fractions were incubated with the corresponding antibody and either Protein A or G-agarose. For Western blot analysis, immunoprecipitates or WCL were resolved on SDS-PAGE, transferred to PVDF membrane (Amersham Biosciences), and detected by the indicated antibodies by ECL system (Amersham Biosciences).

Confocal Analysis

For confocal analysis, cells were stained with cholera toxin to detect GM1, and lipid rafts were patched with anti-cholera toxin antibody. For intracellular staining with antibodies against UbcH7 or βPix, cells were fixed with 4% v/v paraformaldehyde and permeabilized with 1% v/v Triton X-100. Confocal microscopy was performed with a Bio-Rad Radiance 2000 laser scanning confocal and analyzed with LaserSharp 2000 software (Bio-Rad). All images were acquired in sequential scanning mode.

Two-Dimensional Gel Electrophoresis and Mass Spectrometric Analysis

See Supplemental Data.

Supplemental Data

Supplemental Data include eight figures, one table, and Supplemental Experimental Procedures and can be found with this article online at http://www.immunity.com/cgi/content/full/23/6/621/DC1/.

Acknowledgments

This work was supported by the Medical Research Council (MRC). A.S. is the recipient of a Department of Health MRC Clinician Scientist award, B.G. of an MRC Research Studentship and CASE award from Oxford GlycoSciences, K.S. of an MRC Research Studentship, and N.Z. of a Dorothy Hodgkin Fellowship. We would like to thank Hamid Band, Andreas Baur, Richard Cerione, and George Cohen

for providing reagents and Jo O'Leary for critical reading of the manuscript.

Received: October 19, 2004
Revised: September 9, 2005
Accepted: November 9, 2005
Published: December 13, 2005

References

Alexander, M., Bor, Y.C., Ravichandran, K.S., Hammarskjold, M.L., and Rekosh, D. (2004). Human immunodeficiency virus type 1 Nef associates with lipid rafts to downmodulate cell surface CD4 and class I major histocompatibility complex expression and to increase viral infectivity. J. Virol. *78*, 1685–1696.

Andersen, S.S. (2000). Spindle assembly and the art of regulating microtubule dynamics by MAPs and Stathmin/Op18. Trends Cell Biol. *10*, 261–267.

Bagrodia, S., Bailey, D., Lenard, Z., Hart, M., Guan, J.L., Premont, R.T., Taylor, S.J., and Cerione, R.A. (1999). A tyrosine-phosphorylated protein that binds to an important regulatory region on the cool family of p21-activated kinase-binding proteins. J. Biol. Chem. *274*, 22393–22400.

Belmont, L.D., and Mitchison, T.J. (1996). Identification of a protein that interacts with tubulin dimers and increases the catastrophe rate of microtubules. Cell *84*, 623–631.

Bonnefoy-Berard, N., Liu, Y.C., von Willebrand, M., Sung, A., Elly, C., Mustelin, T., Yoshida, H., Ishizaka, K., and Altman, A. (1995). Inhibition of phosphatidylinositol 3-kinase activity by association with 14–3-3 proteins in T cells. Proc. Natl. Acad. Sci. USA *92*, 10142–10146.

Briggs, S.D., Sharkey, M., Stevenson, M., and Smithgall, T.E. (1997). SH3-mediated Hck tyrosine kinase activation and fibroblast transformation by the Nef protein of HIV-1. J. Biol. Chem. *272*, 17899–17902.

Cantrell, D. (2003). Commentary: Vav-1 and T cells. Eur. J. Immunol. *33*, 1070–1072.

Cassimeris, L. (2002). The oncoprotein 18/stathmin family of microtubule destabilizers. Curr. Opin. Cell Biol. *14*, 18–24.

Cerione, R.A. (2004). Cdc42: new roads to travel. Trends Cell Biol. *14*, 127–132.

Cheng, P.C., Dykstra, M.L., Mitchell, R.N., and Pierce, S.K. (1999). A role for lipid rafts in B cell antigen receptor signaling and antigen targeting. J. Exp. Med. *190*, 1549–1560.

Cohen, G.B., Gandhi, R.T., Davis, D.M., Mandelboim, O., Chen, B.K., Strominger, J.L., and Baltimore, D. (1999). The selective downregulation of class I major histocompatibility complex proteins by HIV-1 protects HIV-infected cells from NK cells. Immunity *10*, 661–671.

de Hoog, C.L., Foster, L.J., and Mann, M. (2004). RNA and RNA binding proteins participate in early stages of cell spreading through spreading initiation centers. Cell *117*, 649–662.

del Pozo, M.A., Balasubramanian, N., Alderson, N.B., Kiosses, W.B., Grande-Garcia, A., Anderson, R.G., and Schwartz, M.A. (2005). Phospho-caveolin-1 mediates integrin-regulated membrane domain internalization. Nat. Cell Biol. *7*, 901–908.

Doms, R.W., and Trono, D. (2000). The plasma membrane as a combat zone in the HIV battlefield. Genes Dev. *14*, 2677–2688.

Fackler, O.T., and Baur, A.S. (2002). Live and let die: Nef functions beyond HIV replication. Immunity *16*, 493–497.

Fackler, O.T., Luo, W., Geyer, M., Alberts, A.S., and Peterlin, B.M. (1999). Activation of Vav by Nef induces cytoskeletal rearrangements and downstream effector functions. Mol. Cell *3*, 729–739.

Fackler, O.T., Wolf, D., Weber, H.O., Laffert, B., D'Aloja, P., Schuler-Thurner, B., Geffin, R., Saksela, K., Geyer, M., Peterlin, B.M., et al. (2001). A natural variability in the proline-rich motif of Nef modulates HIV-1 replication in primary T cells. Curr. Biol. *11*, 1294–1299.

Fagerholm, S., Hilden, T.J., and Gahmberg, C.G. (2002). Lck tyrosine kinase is important for activation of the CD11a/CD18-integrins in human T lymphocytes. Eur. J. Immunol. *32*, 1670–1678.

Flanders, J.A., Feng, Q., Bagrodia, S., Laux, M.T., Singavarapu, A., and Cerione, R.A. (2003). The Cbl proteins are binding partners for the Cool/Pix family of p21-activated kinase-binding proteins. FEBS Lett. *550*, 119–123.

Harder, T. (2004). Lipid raft domains and protein networks in T-cell receptor signal transduction. Curr. Opin. Immunol. *16*, 353–359.

Janardhan, A., Swigut, T., Hill, B., Myers, M.P., and Skowronski, J. (2004). HIV-1 Nef binds the DOCK2-ELMO1 complex to activate rac and inhibit lymphocyte chemotaxis. PLoS Biol. *2*, e6. 10.371/journal.pbio.0020006.

Jolly, C., Kashefi, K., Hollinshead, M., and Sattentau, Q.J. (2004). HIV-1 cell to cell transfer across an Env-induced, actin-dependent synapse. J. Exp. Med. *199*, 283–293.

Kane, L.P., Lin, J., and Weiss, A. (2000). Signal transduction by the TCR for antigen. Curr. Opin. Immunol. *12*, 242–249.

Kestler, H.W., 3rd, Ringler, D.J., Mori, K., Panicali, D.L., Sehgal, P.K., Daniel, M.D., and Desrosiers, R.C. (1991). Importance of the nef gene for maintenance of high virus loads and for development of AIDS. Cell *65*, 651–662.

Kramer-Hammerle, S., Kohleisen, B., Hohenadl, C., Shumay, E., Becker, I., Erfle, V., and Schmidt, J. (2001). HIV type 1 Nef promotes neoplastic transformation of immortalized neural cells. AIDS Res. Hum. Retroviruses *17*, 597–602.

Krautkramer, E., Giese, S.I., Gasteier, J.E., Muranyi, W., and Fackler, O.T. (2004). Human immunodeficiency virus type 1 Nef activates p21-activated kinase via recruitment into lipid rafts. J. Virol. *78*, 4085–4097.

Liu, Y.C., Elly, C., Yoshida, H., Bonnefoy-Berard, N., and Altman, A. (1996). Activation-modulated association of 14–3-3 proteins with Cbl in T cells. J. Biol. Chem. *271*, 14591–14595.

Lu, X., Wu, X., Plemenitas, A., Yu, H., Sawai, E.T., Abo, A., and Peterlin, B.M. (1996). CDC42 and Rac1 are implicated in the activation of the Nef-associated kinase and replication of HIV-1. Curr. Biol. *6*, 1677–1684.

Manninen, A., Hiipakka, M., Vihinen, M., Lu, W., Mayer, B.J., and Saksela, K. (1998). SH3-domain binding function of HIV-1 Nef is required for association with a PAK-related kinase. Virology *250*, 273–282.

Manser, E., Loo, T.H., Koh, C.G., Zhao, Z.S., Chen, X.Q., Tan, L., Tan, I., Leung, T., and Lim, L. (1998). PAK kinases are directly coupled to the PIX family of nucleotide exchange factors. Mol. Cell *1*, 183–192.

Marengère, L.E., Mirtsos, C., Kozieradzki, I., Veillette, A., Mak, T.W., and Penninger, J.M. (1997). Proto-oncoprotein Vav interacts with c-Cbl in activated thymocytes and peripheral T cells. J. Immunol. *159*, 70–76.

McDonald, D., Wu, L., Bohks, S.M., KewalRamani, V.N., Unutmaz, D., and Hope, T.J. (2003). Recruitment of HIV and its receptors to dendritic cell-T cell junctions. Science. *300*, 1295–1297.

Miura-Shimura, Y., Duan, L., Rao, N.L., Reddi, A.L., Shimura, H., Rottapel, R., Druker, B.J., Tsygankov, A., Band, V., and Band, H. (2003). Cbl-mediated ubiquitinylation and negative regulation of Vav. J. Biol. Chem. *278*, 38495–38504.

Ohashi, P.S., Mak, T.W., Van den Elsen, P., Yanagi, Y., Yoshikai, Y., Calman, A.F., Terhorst, C., Stobo, J.D., and Weiss, A. (1985). Reconstitution of an active surface T3/T-cell antigen receptor by DNA transfer. Nature *316*, 606–609.

Palazzo, A.F., Eng, C.H., Schlaepfer, D.D., Marcantonio, E.E., and Gundersen, G.G. (2004). Localized stabilization of microtubules by integrin- and FAK-facilitated Rho signaling. Science *303*, 836–839.

Plafker, S.M., Plafker, K.S., Weissman, A.M., and Macara, I.G. (2004). Ubiquitin charging of human class III ubiquitin-conjugating enzymes triggers their nuclear import. J. Cell Biol. *167*, 649–659.

Rao, N., Miyake, S., Reddi, A.L., Douillard, P., Ghosh, A.K., Dodge, I.L., Zhou, P., Fernandes, N.D., and Band, H. (2002). Negative regulation of Lck by Cbl ubiquitin ligase. Proc. Natl. Acad. Sci. USA *99*, 3794–3799.

Renkema, G.H., and Saksela, K. (2000). Interactions of HIV-1 NEF with cellular signal transducing proteins. Front. Biosci. *5*, D268–D283.

Saksela, K., Cheng, G., and Baltimore, D. (1995). Proline rich (PxxP) motifs in HIV-1 Nef bind to SH3 domains of a subset of Src kinases

and are required for the enhanced growth of Nef+ viruses but not for down-regulation of CD4. EMBO J. *14*, 484–491.

Simmons, A., Aluvihare, V., and McMichael, A. (2001). Nef triggers a transcriptional program in T cells imitating single-signal T cell activation and inducing HIV virulence mediators. Immunity *14*, 763–777.

Stowers, L., Yelon, D., Berg, L.J., and Chant, J. (1995). Regulation of the polarization of T cells toward antigen-presenting cells by Ras-related GTPase CDC42. Proc. Natl. Acad. Sci. USA *92*, 5027–5031.

Straus, D.B., and Weiss, A. (1992). Genetic evidence for the involvement of the lck tyrosine kinase in signal transduction through the T cell antigen receptor. Cell *70*, 585–593.

Verma, S., Ismail, A., Gao, X., Fu, G., Li, X., O'Malley, B.W., and Nawaz, Z. (2004). The ubiquitin-conjugating enzyme UBCH7 acts as a coactivator for steroid hormone receptors. Mol. Cell. Biol. *24*, 8716–8726.

von Schwedler, U.K., Stuchell, M., Muller, B., Ward, D.M., Chung, H.Y., Morita, E., Wang, H.E., Davis, T., He, G.P., Cimbora, D.M., et al. (2003). The protein network of HIV budding. Cell *114*, 701–713.

Wang, J.K., Kiyokawa, E., Verdin, E., and Trono, D. (2000). The Nef protein of HIV-1 associates with rafts and primes T cells for activation. Proc. Natl. Acad. Sci. USA *97*, 394–399.

Wang, H.Y., Altman, Y., Fang, D., Elly, C., Dai, Y., Shao, Y., and Liu, Y.C. (2001). Cbl promotes ubiquitination of the T cell receptor zeta through an adaptor function of Zap-70. J. Biol. Chem. *276*, 26004–26011.

Witte, V., Laffert, B., Rosorius, O., Lischka, P., Blume, K., Galler, G., Stilper, A., Willbold, D., D'Aloja, P., Sixt, M., et al. (2004). HIV-1 Nef mimics an integrin receptor signal that recruits the polycomb group protein Eed to the plasma membrane. Mol. Cell *13*, 179–190.

Wollberg, P., and Nelson, B.D. (1992). Regulation of the expression of lactate dehydrogenase isozymes in human lymphocytes. Mol. Cell. Biochem. *110*, 161–164.

Wong, E.S., Fong, C.W., Lim, J., Yusoff, P., Low, B.C., Langdon, W.Y., and Guy, G.R. (2002). Sprouty2 attenuates epidermal growth factor receptor ubiquitylation and endocytosis, and consequently enhances Ras/ERK signalling. EMBO J. *21*, 4796–4808.

Wu, W.J., Tu, S., and Cerione, R.A. (2003). Activated Cdc42 sequesters c-Cbl and prevents EGF receptor degradation. Cell *114*, 715–725.

Xu, X.N., Laffert, B., Screaton, G.R., Kraft, M., Wolf, D., Kolanus, W., Mongkolsapay, J., McMichael, A.J., and Baur, A.S. (1999). Induction of Fas ligand expression by HIV involves the interaction of Nef with the T cell receptor zeta chain. J. Exp. Med. *189*, 1489–1496.

Yang, P., and Henderson, A.J. (2005). Nef enhances c-Cbl phosphorylation in HIV-infected CD4+ T lymphocytes. Virology *336*, 219–228.

Yokouchi, M., Kondo, T., Houghton, A., Bartkiewicz, M., Horne, W.C., Zhang, H., Yoshimura, A., and Baron, R. (1999). Ligand-induced ubiquitination of the epidermal growth factor receptor involves the interaction of the c-Cbl RING finger and UbcH7. J. Biol. Chem. *274*, 31707–31712.

Zhang, X., Bi, E., Novick, P., Du, L., Kozminski, K.G., Lipschutz, J.H., and Guo, W. (2001). Cdc42 interacts with the exocyst and regulates polarized secretion. J. Biol. Chem. *276*, 46745–46750.

Zheng, N., Wang, P., Jeffrey, P.D., and Pavletich, N.P. (2000). Structure of a c-Cbl-UbcH7 complex: RING domain function in ubiquitin-protein ligases. Cell *102*, 533–539.

Supplemental Data

Nef-Mediated Lipid Raft Exclusion of UbcH7

Inhibits Cbl Activity in T Cells

to Positively Regulate Signaling

Alison Simmons, Bevin Gangadharan, Ashleigh Hodges, Katherine Sharrocks, Sripadi Prabhakar, Angel García, Raymond Dwek, Nicole Zitzmann, and Andrew McMichael

Supplemental Experimental Procedures

Two-Dimensional Gel Electrophoresis and Mass Spectrometric Analysis

For each 2D-PAGE gel, lipid raft fractions were obtained from 5×10^8 cells by identification of GM1-positive fractions. Samples were dialyzed to remove sucrose and freeze dried before resuspension in sample buffer. 500 μg of each lipid raft sample was separated by 2D-PAGE essentially as described by García et al. (2004a). After electrophoresis, gels were fixed in 40% v/v ethanol: 10% v/v acetic acid, stained with the fluorescent dye OGT 1238 (Oxford GlycoSciences, Abingdon, UK), and scanned with an Apollo linear fluorescence scanner (Oxford GlycoSciences). Scanned images were processed with a custom version of Melanie II (Biorad) as described by García et al. (2004b). An automated robotic cutter (Oxford Glycosciences) was used to excise gel protein features that were differentially expressed. Differential expression of a protein present in both the raft control and raft transfected gels was considered significant when fold change was at least 1.5. After drying the gel pieces in a Speed-Vac, in-gel digestion was performed in the automated DigestPro workstation (ABiMED, Langenfeld, Germany) with the trypsin digestion procedure as described previously (Shevchenko et al., 1996). Mass spectrometry was performed by a Q-Tof (Micromass, Manchester, UK) coupled to CapLC (Waters, Milford, MA). Tryptic peptides were loaded and desalted on a 300 μm internal diameter/5 mm length C18 PepMap column (LC Packings, San Francisco, CA). Elution of the peptide mixture was carried out with 80% to 95% v/v acetonitrile containing 0.1% v/v formic acid over 20 min at a flow rate of 200 nl/min. Mass data acquisitions were piloted by Mass Lynx software (Micromass) with automated switching between MS and coupled tandem mass spectrometry (MS/MS) modes. Acquisition of the survey scan (1 s) took place over the mass range of m/z 300 to 1200 in the positive ion mode with a cone voltage of 40 V. When the signal achieved a user-defined threshold of >10 counts/s, peptide precursor ions were selected for MS/MS scan (2 s) over the mass range m/z 50-2000. Argon was used to perform fragmentation with a collision energy profile (20-40 eV) optimized for various mass ranges of precursor ions. The selected precursor ions were placed automatically in the exclusion list. Database searches were performed with the MASCOT search tool (Matrix Science, London, UK) screening Swiss-Prot and TrEMBL restricted to human taxonomy.

Supplemental References

García, A., Prabhakar, S., Brock, C.J., Pearce, A.C., Dwek, R.A., Watson, S.P., Hebestreit, H.F., and Zitzmann, N. (2004a). Extensive analysis of the human platelet proteome by two-dimensional gel electrophoresis and mass spectrometry. Proteomics *4*, 656–668.

García, A., Prabhakar, S., Hughan, S., Anderson, T.W., Brock, C.J., Pearce, A.C., Dwek, R.A., Watson, S.P., Hebestreit, H.F., and Zitzmann, N. (2004b). Differential proteome analysis of TRAP-activated platelets: involvement of DOK-2 and phosphorylation of RGS proteins. Blood *103*, 2088–2095.

Shevchenko, A., Wilm, M., Vorm, O., and Mann, M. (1996). Mass spectrometric sequencing of proteins silver-stained polyacrylamide gels. Anal. Chem. *68*, 850–858.

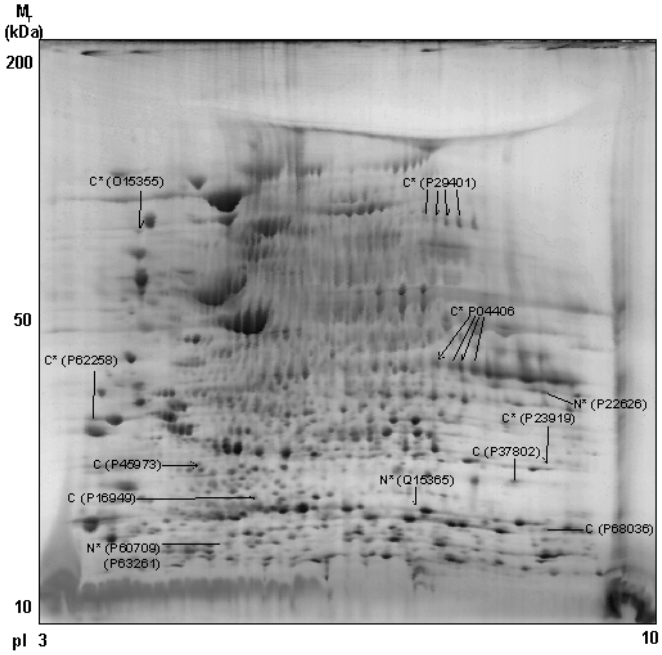

Figure S1. Complete Lipid Raft 2D-PAGE Gel Images

Four replicate 9%–16% 2D-PAGE gels (linear pI range 3-10) for control (pCMV-Tag4A) (Figures S1-S4) and Nef (Nef-Flag) (Figures S5-S8) expressing samples. Gels were stained with the fluorescent dye OGT 1238 (Oxford GlycoSciences). Spots were selected for protein identification after image analysis with a custom version of Melanie II on the basis of demonstrating an increased or decreased expression post Nef transfection. All gels were internally calibrated for pI and molecular weight with the *E. coli* proteome as a standard.

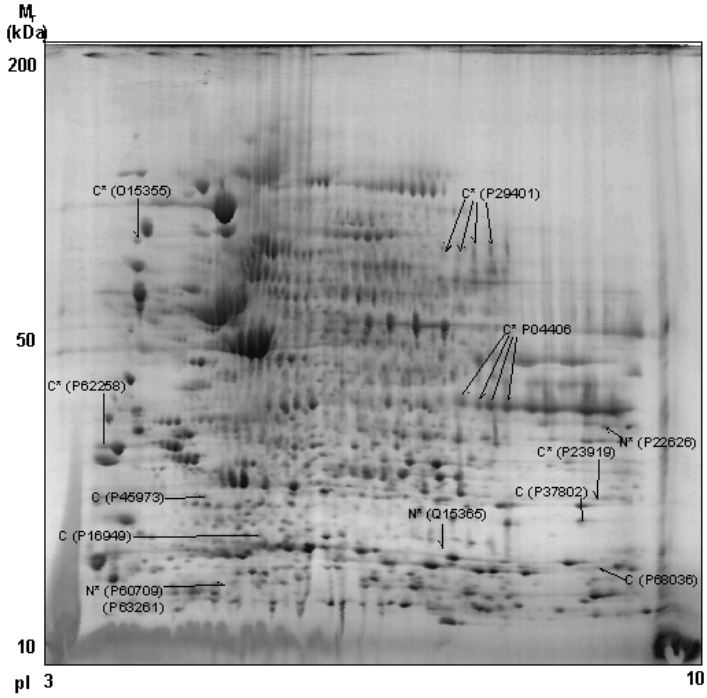

Figure S2. Complete Lipid Raft 2D-PAGE Gel Images

See Figure S1 for details.

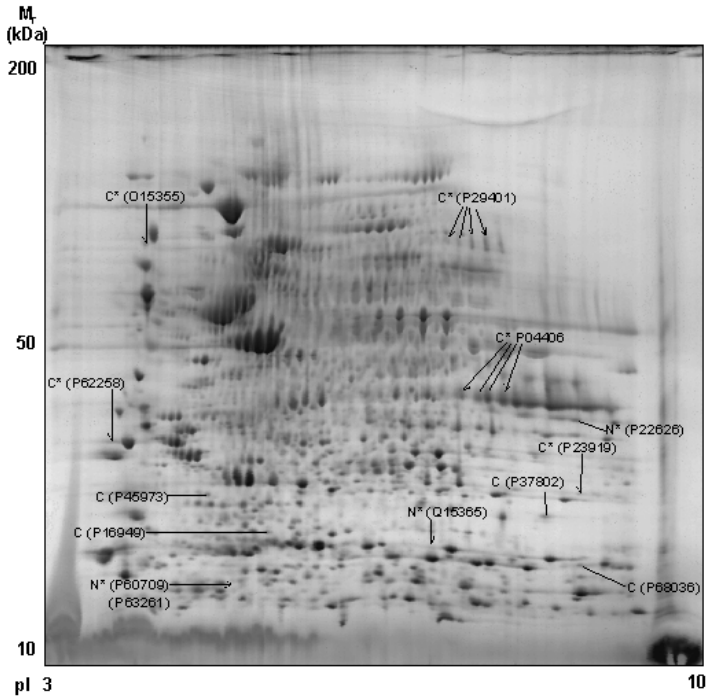

Figure S3. Complete Lipid Raft 2D-PAGE Gel Images

See Figure S1 for details.

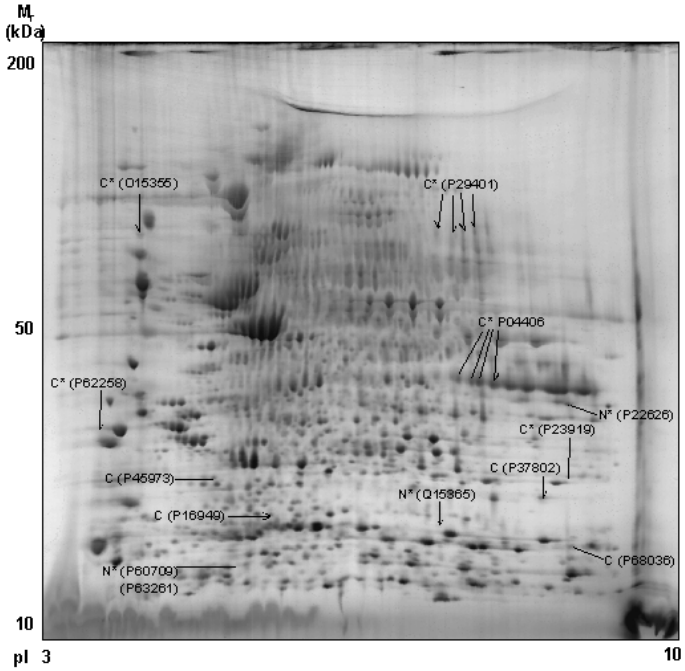

Figure S4. Complete Lipid Raft 2D-PAGE Gel Images

See Figure S1 for details.

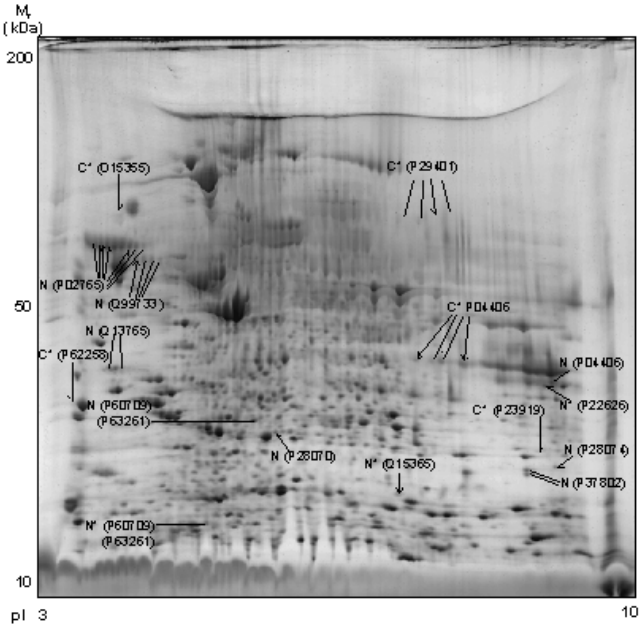

Figure S5. Complete Lipid Raft 2D-PAGE Gel Images
See Figure S1 for details.

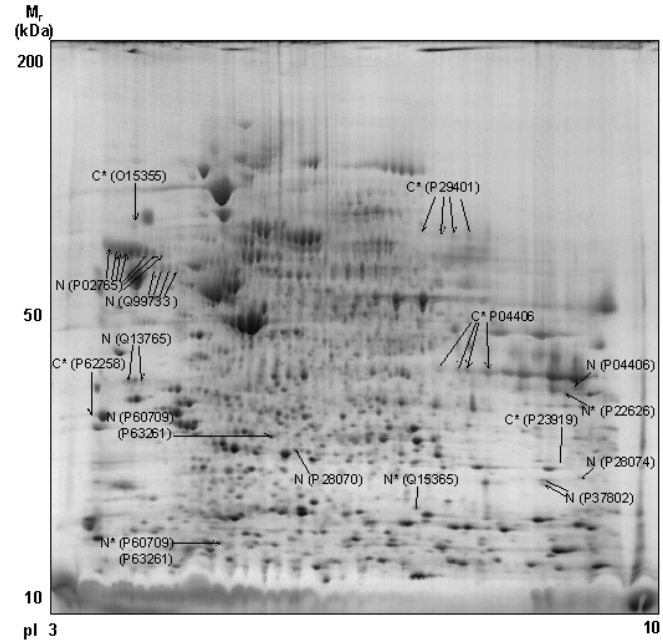

Figure S6. Complete Lipid Raft 2D-PAGE Gel Images
See Figure S1 for details.

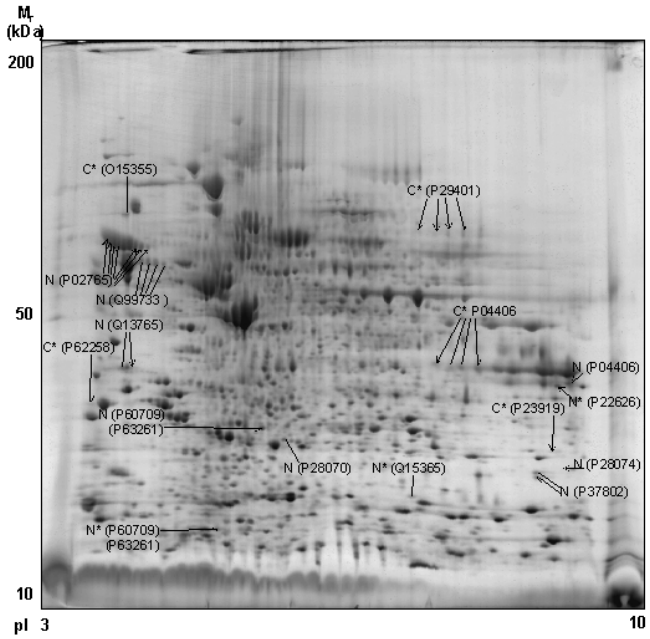

Figure S7. Complete Lipid Raft 2D-PAGE Gel Images
See Figure S1 for details.

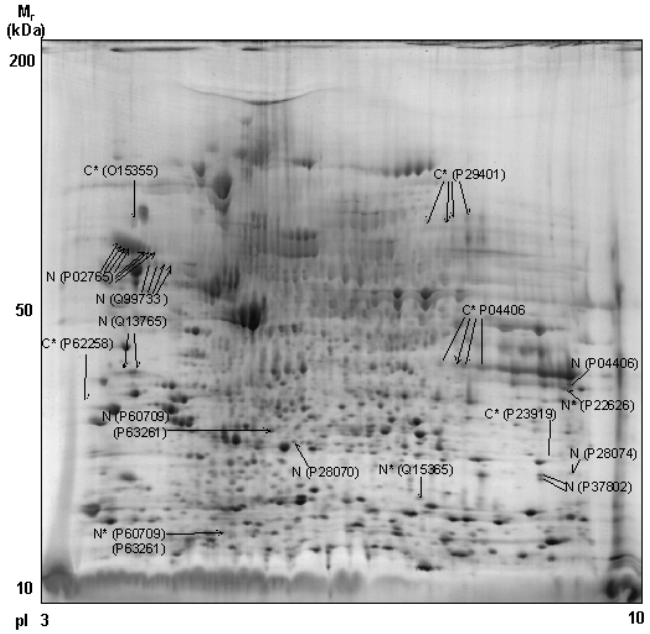

Figure S8. Complete Lipid Raft 2D-PAGE Gel Images
See Figure S1 for details.

Table S1. List of Differentially Expressed Proteins Identified in Control versus Nef-Transfected Rafts

Protein Name	AN	M_r, Da	pI	Fold[a]	Protein Function
Protein phosphatase 2C γ isoform	O15355	76241	4.51	-1.59	signal transduction
Alpha-2-HS-glycoprotein precursor	P02765	66543 66969 67319 68091 68218 68501 69179	4.59 4.57 4.55 4.47 4.45 4.43 4.41	N N N N N N N	acute phase protein
Glyceraldehyde 3-phosphate dehydrogenase	P04406	33322 37515 38081 38142 38196	8.17 7.23 7.03 6.94 6.76	N -1.68 -2.09 -2.30 -1.98	signal transduction
Stathmin (Oncoprotein 18)	P16949	21962	4.97	C	cytoskeletal and microtubule organizing centre regulation
Thymidylate kinase	P23919	24715	7.93	-2.61	signal transduction
Proteasome subunit beta type 4 precursor	P28070	25777	5.40	N	proteolysis
Proteasome subunit beta type 5 precursor	P28074	23553	8.25	N	proteolysis
Transketolase	P29401	72802 72931 72975 74115	6.89 7.04 6.74 6.58	-1.88 -1.60 -2.66 -2.84	signal transduction
Transgelin 2	P37802	23274 23073 23359	7.64 7.77 7.79	C N N	cytoskeletal and microtubule organizing centre regulation
Actin, cytoplasmic 1 (β-actin) or Actin, cytoplasmic 2 (γ-actin)	P60709 or P63261	18930 26955	4.82 5.20	1.74 N	cytoskeletal and microtubule organizing centre regulation
14-3-3 protein ε	P62258	29062	4.35	-2.98	signal transduction
Ubiquitin-conjugating enzyme E2-18 kDa UbcH7	P68036	19809	7.92	C	ubiquitination
NASCENT polypeptide associated complex alpha subunit	Q13765	34749 34766	4.53 4.49	N N	mRNA processing and translation
Poly(rC)-binding protein 1 (hnRNP-E1)	Q15365	21410	6.53	2.61	mRNA processing and translation
Nucleosome assembly protein 1-like 4	Q99733	61505 62179 62632 63560	4.66 4.64 4.62 4.55	N N N N	nucleosome assembly

AN, Swiss-Prot accession number; pI, isoelectric point on gel; M_r, relative molecular mass on gel; C, protein feature only present in control rafts; N, protein feature only present in Nef-transfected rafts.

[a]Fold change (control versus Nef-transfected rafts); a negative value indicates that the feature is expressed to a higher extent in control raft samples.